UNIVERSITÉ DE SHERBROOKE

Faculté de génie

Département de génie civil

The effect of fish baffles on the hydraulic capacity of HDPE slipline insert culverts

L'impact des chicanes à poisson sur la capacité hydraulique des ponceaux réhabilités par insertion d'une conduite en PEHD

Mémoire de maîtrise

Spécialité : génie civil

Jason DUGUAY

Jury : Jay Lacey (directeur)

Bertrand Côté

Hubert Cabana

Sherbrooke (Québec) Canada avril 2014

UNIVERSITÉ DE SHERBROOKE

Faculty of Engineering

Departement of Civil Engineering

The effect of fish baffles on the hydraulic capacity of HDPE slipline insert culverts

In partial fulfillment of the requirements for Master's thesis

Civil Engineering

Jason DUGUAY

Jury : Jay Lacey (supervisor)

Bertrand Côté

Hubert Cabana

Sherbrooke (Québec) Canada January 2014

Acknowledgment

Special appreciation goes to my supervisor, Jay Lacey for his guidance on all things hydraulic ; to the members of the jury, Hubert Cabana and Bertrand Côté, for their efforts in improving the quality of the manuscript ; to Nicolas Simard for his humor and help in the laboratory ; to Normand Bergeron for his ingenious insight on how to fix the baffles in place ; to the camaraderie, advice and endless debating spirit of those who dwelled at rue Prunier, you know who you are ; to all the members of my family who have supported me morally through this endeavor and to Sylvie, who was always there for support during the worst of times and to share in my joy during the best of times.

Université de Sherbrooke, March 2014

Abstract

The use of fish baffles in HDPE slipliners is growing in popularity to improve hydraulic conditions for fish passage, yet little is known on how baffles affect the outlet controlled discharge capacity of these types of culverts. First, an analytical study was undertaken to determine the variation of velocity and depth between a parent corrugated steel culvert and an HDPE slipliner for a fixed flow rate. It was found that velocities will increase between 65% and 260% and depth will decrease between -58% and -27% depending on the actual roughness values of the parent and HDPE culverts. These findings justify mesures to improve fish passage through culverts such as the installation of fish baffles. To this end, roughness coefficients (Manning's n and friction factor f values) were experimentally determined for weir baffle, slotted weir baffle and spoiler baffle configurations at four baffle spacings ($\lambda = 0.6$D, 1.2D, 1.8D, 2.4D) and three baffle heights ($h = 0.15$D, 0.10D, 0.05D), where D is the nominal diameter of the culvert. Roughness height was found to be the determinant geometric parameter affecting hydraulic roughness. Roughness spacing was found to play a secondary role. An analytical model was developed and analyzed to determine the effects of roughness reduction ($\alpha = \mathrm{n}/\mathrm{n}_f$), radial reduction ($\beta$), barrel length ($L$) and inlet treatments ($k_e$) on the hydraulic capacity of corrugated steel culverts after being sliplined with baffled HDPE culverts. Results demonstrate that many HDPE slipliner culverts can house baffles with α values in the range of 0.5 to 0.9, showing promise that a wide range of rehabilitated culverts can house baffles to improve fish passage an still respect discharge requirements. Design recommendations for the use of baffles in short and long HDPE slipline culverts are discussed.

Key-words : Culverts, Design, Fish Management, Hydraulic Roughness, Culvert roughness, Baffled culverts, Culvert Rehabilitation, Fish Passage, Manning's roughness, Slip-lined HDPE culverts

Résumé

L'utilisation de chicanes dans les ponceaux de type insertion en polyéthylène de haute densité (PEHD) est devenu une pratique de plus en plus courante afin d'améliorer les conditions hydrauliques pour le passage des poissons. Cependant, on sait peu sur la façon dont les chicanes affectent la capacité hydraulique des ponceaux. Tout d'abord, une étude comparative a été menée afin de déterminer la variation de la vitesse et de la profondeur entre un ponceau en acier ondulé et un ponceau de type insertion en PEHD pour un débit fixe. Il a été constaté que la vitesse augmentera entre 65% et 260% et la profondeur diminuera entre -58% et -27% selon les valeurs de rugosité réels du ponceau en tôle ondulé et du ponceau en PEHD. Ces résultats justifient des mesures pour améliorer le passage des poissons, comme par exemple l'installation de chicanes. À cette fin, les coefficients de rugosité n de Manning et f de Darcy ont été déterminés expérimentalement pour les chicanes de type déversoir, les chicanes de type fente et les chicanes de type spoiler pour quatre espacements ($\lambda = 0.6$D , 1.2D, 1.8D, 2.4D) et trois hauteurs ($h = 0.15$D, 0.10D, 0.05D), où D est le diamètre nominal du ponceau. La hauteur des chicanes est ressortie comme étant le paramètre géométrique déterminant affectant la rugosité hydraulique. L'espacement se trouve à jouer un rôle secondaire. Un modèle analytique a été développé et analysé afin de déterminer les effets de la réduction de la rugosité ($\alpha = n/n_f$), la réduction radiale ($\beta = \mathrm{D}/\mathrm{D}_o$), la longueur du ponceau (L) et les traitements d'entrée (k_e) sur la capacité hydraulique des ponceaux en tôle ondulée après avoir été réhabilité par insertion d'un ponceaux en PEHD. Les résultats montrent que de nombreux ponceaux en PEHD peuvent accueillir des configurations de chicanes ayant des valeurs de α se situant entre 0,5 à 0,9 et continuer de respecter la capacité hydraulique réquise. Des recommandations de conception pour l'utilisation de chicanes dans des courts et longs ponceaux en PEHD sont discutées.

Mots-clés : ponceaux, conception, aménagement des poissons, rugosité hydraulique, déversoirs, refection des ponceaux, passage des poissons, rugosité de Manning, ponceaux en polyéthène de haute densité

Contents

Contents ix

List of Figures xiii

List of Tables xv

Chapter 1 Introduction 1

1.1 Research Context . . . 3
1.2 Research Questions . . . 6
1.3 Impacts . . . 7
1.4 Resources . . . 8

Chapter 2 Background 9

2.1 Introduction . . . 11
2.2 Hydraulic parameters affecting fish passage in culverts . . . 11
2.2.1 Velocity . . . 11
2.2.2 Turbulence . . . 16
2.2.3 Depth . . . 20
2.3 Variation of Manning's roughness coefficients . . . 21
2.3.1 Corrugated Steel Pipe . . . 22
2.3.2 HDPE roughness coefficients at low relative depths . . . 24
2.3.3 A word on the ASCE hydraulic-elements graph for circular sewers . . . 26
2.4 Common Baffle Forms . . . 28
2.4.1 Weir and Slotted-Weir Baffles . . . 29
2.4.2 Spoiler baffles . . . 32

2.5 Hydraulic design of Culverts . . . 35
2.5.1 The culvert design process . . . 35
Inlet control . . . 36
Outlet control . . . 36
2.5.2 The energy equation applied to culverts . . . 38
2.5.3 The effect of HDPE Sliplining on Hydraulic Capacity . . . 40
2.5.4 The effect of baffles on hydraulic capacity . . . 41
2.5.5 Inlet and Outlet coefficients . . . 44
2.6 Flow regime . . . 47

Chapter 3 Effects of Sliplining on Depth and Velocity **51**
3.1 Introduction . . . 53
3.2 Methodology . . . 54
3.2.1 Theory . . . 54
3.2.2 Testing . . . 56
3.3 Results . . . 57
3.4 Analysis and discussion . . . 60
3.4.1 Effect on velocity and depth . . . 60
3.4.2 Effect on the Froude number . . . 62
3.4.3 A word on radial reductions . . . 62
3.5 Conclusion . . . 63
3.5.1 Future work . . . 64

Chapter 4 The Effects of Fish Baffles on the Hydraulic Capacity of Slipline Rehabilitated Culverts **65**

Avant-propos **67**
4.1 Introduction . . . 71
4.1.1 Baffles . . . 72
4.1.2 Hydraulic Capacity . . . 74
Partially Full Flow . . . 74
Full Flow . . . 74

4.1.3 Objectives . . . 75
4.2 Experimental setup . . . 76
4.3 Methodology . . . 79
4.4 Theory . . . 79
4.5 Results and Analysis . . . 80
4.5.1 Baffle roughness . . . 80
4.6 Discussion . . . 83
4.6.1 Flow regime and Reynold's independence . . . 83
4.6.2 Comparison with previous work . . . 85
4.6.3 Retrofit effect on discharge . . . 85
4.6.4 Baffle choice for outlet controlled culverts . . . 88
Recommendations for baffle use in short and long culverts . . . 88
Short culverts outlet control . . . 89
Long culverts outlet control . . . 90
Comments on Spoiler baffle height and spacing . . . 90
Can baffles be excluded? . . . 90
4.7 Conclusions and Recommendations . . . 91
4.8 Acknowledgements . . . 93
4.9 Notation . . . 93

Chapter 5 Additional Spoiler Baffle Testing **95**
5.1 Introduction . . . 97
5.1.1 Tested Spoiler Baffle Configurations . . . 97
5.2 Results and Analysis . . . 98
5.3 Analysis and discussion . . . 101
5.3.1 Reynolds independence . . . 104
5.3.2 Discussion on the experimental design . . . 104
5.4 Conclusions and Further Research . . . 104

Chapter 6 Conclusion **107**
6.1 Introduction . . . 109

6.1.1 How does HDPE sliplining affect depth and velocities? 109
6.1.2 How does a baffle configuration's geometric parameters affect energy losses? 110
6.1.3 Can baffles be used in HDPE slipliner rehabilitaitons? 110
6.1.4 How can practitioners optimize hydraulic capacity and fish passage in HDPE slipliners? 111
6.1.5 Concluding Remarks 112
6.2 Conclusion version française 112
6.2.1 Introduction 112
6.2.2 Qu'arrive- t-il aux vitesses et profondeurs après qu'un ponceau en tôle ondulée soit réfectionné par un ponceau en PEHD? 112
6.2.3 Qu'est-ce que la relation entre les paramètres géométriques des chicanes à poisson et les pertes d'énergie engendrées dans le système? 113
6.2.4 L'utilisation des déversoirs dans les ponceaux en PEHD 114
6.2.5 Comment optimiser la capacité hydraulique et le passage des poissons dans les ponceaux en PHED utilisé pour réfectionner les ponceaux défaillants? 115
6.2.6 Mot final 116

Appendices **117**

Appendix A Experimental Data **119**

Appendix B Letter from the Journal of Hydraulic Engineering **143**

Bibliography **147**

List of Figures

1.1 Sliplined culvert 4

2.1 Adult fish swimming speeds (from Olsen and Tullis, 2013). 12
2.2 Variation of f with Reynolds number in corrugated steel pipes 14
2.3 Ichthyomechanics Database processed data from Katopodis and Gervais (2012) . . . 15
2.4 Ichthyomechanics Database processed data legend (Katopodis and Gervais, 2012) . 16
2.5 Schematic showing the effect of eddy orientation on fish swimming behaviour. . . . 18
2.6 Vertically averaged centerline TKE values for the sloped-weir baffle 19
2.7 Latral TI values for sloped-weir baffle 19
2.8 Fish passage success versus EDF 20
2.9 Manning's roughness values for corrugated steel 23
2.10 Manning's roughness versus relative depth in corrugated steel pipe 24
2.11 Manning's roughness HDPE versus relative depth 25
2.12 Manning's roughness versus relative depth in a HDPE pipe of 0.604 m diameter . . 26
2.13 Hydraulic elements graph of circular sewers 28
2.14 Standard baffle geometries 29
2.15 Example dimensionless discharge curve 31
2.16 Spoiler Baffles studied by MacDonald and Davies and passage results 34
2.17 Outlet control scenearios 37
2.18 Example figure of depth variation versus dimensionless discharge 43
2.19 Entrance loss coefficients as a function of headwater depth 45
2.20 Sketch of the the three principle flow types 48
2.21 Variation of f with Reynolds number in corrugated steel pipes 49

2.22 Descending f-**R** curve from Olsen's data 50

3.1 Schematic of y as a function of r and θ 55

4.1 Baffle Forms 73
4.2 Laboratory setup 77
4.3 Schematic of the laboratory setup 78
4.4 Averaged Roughness Coefficients 81
4.5 Averaged Roughness Coefficients 82
4.6 Comparison of the effects of HDPE sliplining on a 10 m and 80 m culvert 88

5.1 Supplementary spoiler baffle configurations 98
5.2 Spoiler Baffle Roughness data 99
5.3 Series averaged roughness values for additional spoiler baffle configurations 99

List of Tables

2.10 Exit loss test conditions and data from Tullis et al. (2008) 46
2.11 Exit loss coefficient comparison Tullis et al. (2008) 47

3.1 Assumed Manning's roughnesses and y/D for tested scenarios 57
3.2 Initial velocities, flow rates, depths and Froude number in the corrugated steel culvert scenarios 1, 2 and 3(n=0.024) 58
3.3 Initial velocities, flow rates, depths and Froude number in the corrugated steel culvert scenarios 4, 5 and 6 (n=0.028) 58
3.4 Velocity and depth variation results 59
3.5 Velocity and depth variation results 59
3.6 Velocity and depth change coefficients 60
3.7 Velocity and depth change coefficients 60

4.1 Dimensions and areas of tested baffles 79
4.2 Tabluated f and n roughness coefficients 83
4.3 Regression coefficients 83
4.4 α values for the tested baffle configurations 89

5.1 Series averaged roughness values for additional spoiler baffle configurations 100
5.2 Results from the ordinary least squares analysis performed on the series averaged roughness data versus λ 101
5.3 Alpha values of the tested spoiler baffle configurations 103

Chapter 1

Introduction

1.1 Research Context

It is widely known that road culverts act as barriers for aquatic organism migration (Warren and Pardew, 1998; Macpherson et al., 2012). There are a number of problems inherent to road culverts which contribute to varying extents at making the culvert a partial or a complete barrier to upstream fish passage. First, a culvert's entrance is substantially narrower compared to the natural width of the waterway. This has the effect of constricting the flow and increasing the mean water velocities in the culvert. The higher velocities may surpass the swimming capacity of native fish species, effectively blocking their access to suitable upstream habitats. Secondly, the length of a culvert is an influential parameter which can adversely affect fish passage. Culverts of excessive length, especially those lacking appropriate resting areas (which can be created with the addition of fish baffles), demand prolonged periods of physical exertion for weaker fish species migrating upstream. Nearing the exit of the culvert, fish lack the necessary stamina to complete their ascent and are consequently washed downstream when they can no longer resist the flow (Macdonald and Davies, 2007). Inadequate flow depths may also impede upstream fish passage. A final barrier condition is created by the flow conditions at the culvert's exit (downstream). If an improper bedding substrate is placed at the downstream end of the culvert, excessive scour may occur resulting in a perched entrance. Perched culverts, depending on the height of the drop and the velocity of the flow, often pose complete barriers for many fish species. The problems identified above apply to both conventional corrugated steel culverts as well as rehabilitated slip-line culverts. The combined effects of high barrel velocities, excessive length,, reduced depths and perched end conditions all contribute to limiting fish passage success rates at culverts.

In order to remedy these problems, many interest groups (e.g., Departement of Fisheries and Oceans, Washington Departement of Fish and Wildlife) promote the practice of natural stream bed culverts. This form of culvert calls for the placement of natural river substrate as bedding material over a culvert width comparable to that of the natural stream width. Although not completely exempt of problems, this method does have the advantages of keeping velocities to a minimum, providing an adequate number of resting areas and eliminating the negative effects of perched entrances. New culverts should be designed to provide optimal conditions for fish passage such as is developed by a natural stream bed culvert. Older culverts, however,

Figure 1.1: Sliplined culvert (www.culvert-rehab.com)

installed throughout North America under roadway and railines during the post World War II decades are beginning to succumb to the elements. Many require immediate repair or replacement to ensure the stability of the infrastructure which they were designed to support. The need to repair failing culverts in a timely and economic fashion, while limiting impact on traffic flow and freight routes has attracted many engineers to trenchless high density polyethylene (HDPE) slipline culvert rehabilitation technologies (see Fig. 1.1 for an illustration of a slipliner installation). Addressing these existing culverts with updated culvert designs which take fish passage into account is an expensive endeavor and in many situations transport ministries will opt for the expedient HDPE slipliner option.

The installation of an HDPE slipliner is performed often within a time frame of one or two days by a small team of workers equipped with light machinery. A smaller diameter HDPE culvert is inserted inside the larger diameter parent culvert and permanently secured in place with grout. Many different commercial slipline products are available on the market and they all generally respect the following installation method. First the culvert is assessed if it can be rehabilitated with a slipline insert or if it is beyond rehabilitation and instead should be removed and replaced. If sliplining is deemed as an appropriate option, the parent culvert is cleaned and minor repairs and corrections to the wall are performed. Grouting tubes are then fitted on the upper side of the existing culvert which later serve to evenly distribute a grout to fill the inter-annular space and the cavities which may have developed at the exterior of rusted

sections of the existing culvert. The slipline culvert is then pushed into place with the bucket of a small excavator. The slipliner culvert may be a continuous length of HDPE pipe or smaller sections of equal length fitted together with notched couplings. Once the slipliner is in place, the grout is then pumped to fill the inter-annular void.

Regarding hydraulic conveyance, the smooth interior surface of the HDPE slipline culvert is *thought* to compensate for the loss in discharge capacity ensuing from the inevitable restriction in available flow area. The low roughness values of HDPE pipes is what makes sliplining a feasible option. Though ideal for maintaining adequate discharge, the smooth interior surface of the pipe develops high velocities and decreases depths which are known to develop barriers to fish passage (Mangin et al., 2010; Olsen and Tullis, 2013). In order to mitigate the problems that HDPE slipline culverts pose to fish passage, manufacturers often install fish baffles within the slipliner culvert (e.g., Snap-Tite). Although the addition of baffles does promote fish passage by reducing velocities, creating resting zones and developing depth (Macdonald and Davies, 2007; Olsen, 2011) they also present a considerable risk to compromising the hydraulic capacity of the culvert.

Sliplining failing corrugated steel culverts with a *baffled* HDPE culvert presents three risks which can significantly reduce the hydraulic capacity of the culvert: (1) an increase in Manning's n roughness values, (2) a reduction in available flow area, and (3) an amplified risk of debris blockage (Tullis et al., 2008; Webb and Hotchkiss, 2009). To illustrate the effect of sliplining on available flow area it is useful to remember that the area of a circle is proportional to the second power of its diameter. Therefore, inserting a slipline culvert with a diameter 10% smaller than that of the parent culvert reduces the available flow area by 19%. Moreover, the addition of baffles further reduces the available flow area and the additional turbulent energy dissipation associated with flow impinging on the baffles increases friction losses, further reducing the hydraulic capacity of the culvert. Furthermore, the reduced inlet area and the abrupt edges of the baffles increase the likelihood of debris blockage. If a baffled slipline culvert is used in an inappropriate application, an inadequate flow rate may result. Consequently, the headwater level during a storm event would elevate beyond the acceptable limit and the erosive forces of water over the bedding adjacent to the culvert may compromise its structural integrity resulting in a blown out culvert placing the public at risk.

Thus the installation of a baffles in HDPE slipliners may be beneficial for fish passage, yet

it also places the culvert's discharge capacity at risk. Advocates of the recent trend towards using fish friendly buried culverts discourage the continued use of HDPE slipline culverts, and their concerns can be fully justified for the reasons stated above. However, the many practical considerations (i.e., time, budgetary constraints, inconvenience to the public) implicated in culvert repair and replacement suggest that HDPE sliplining technologies will continue to play an important role in the industry for the foreseeable future. Consequently, research directed towards finding compromising solutions between the issues of hydraulic capacity and fish passage at HDPE slipliners is merited. The present thesis intends to provide practitioners with the necessary tools to pursue this endeavor.

1.2 Research Questions

The current thesis investigates four pressing research questions. For which obtaining satisfactory answers to will further our understanding of how to address fish passage issues at HDPE slipliner culverts. **The first question is: (1)** to what extent does sliplining with HDPE culverts affect barrel depth and velocity compared to those originally found in the parent culvert? Very few studies have attempted to tackle this first question. Researchers know that velocities increase and depths decrease after sliplining, however the extent to which these parameters vary has not yet been clearly quantified. A discussion on the matter is necessary to shed light on the problems that HDPE sliplining pose to fish passage. **The second question: (2)** Can baffles be used in *outlet controlled* slipliner rehabilitation applications? Outlet control is emphasized here since the hydraulic capacity of outlet controlled culverts is known to be heavily influenced by barrel roughness (Chanson, 2004), or for that matter, by the addition of baffles which act as isolated roughness elements. In contrast, inlet control is not influenced by additional barrel roughness. **The third question: (3)** Which parameters amongst (λ) baffle spacing, (h) baffle height, baffle type or spatial complexity (for the case of spoiler baffles), are the most influential on hydraulic capacity? **Finally: (4)** How can practitioners optimize baffle designs and the practice of HDPE sliplining to ensure adequate hydraulic capacity and reasonably provide for fish passage?

This thesis is organized to follow the progression of the four research questions mentioned above. Chapter 2 presents a literature review of a selection of scientific articles and technical reports relevant to the present research. The literature review is further divided into three sub-

sections. The first of which summarizes research efforts which have investigated the roughness coefficients of HDPE and corrugated steel pipe. The second subsection presents literature published on the hydraulic roughness of fish baffles and their effects on hydraulic capacity. The third subsection details the method used for determining the hydraulic capacity of an outlet controlled culvert. Chapter 3 details the approach used to respond to the first research above (the effects of sliplining on depth and velocity). The analysis and discussion of the findings of the study are also elaborated in chapter 3. Chapter 4 presents a study which addresses the research questions 2, 3 and 4 written in article format. The article details an experimental study performed to obtain full flow roughness coefficients of a variety of weir, slotted-weir and spoiler baffles. An analytical model is proposed and discussed in the context of the previously determined roughness findings. This model serves to predict the effects of baffles on the hydraulic capacity of HDPE culverts. The final section of the article provides baffle design recommendations intended to optimize hydraulic capacity and improve fish passage in HDPE slipliners. Chapter 5 concludes with the presentation, analysis and discussion of supplementary experimental roughness findings stemming from laboratory testing of a number of spoiler baffle configurations of varying height and spatial complexity.

Finally, chapter 6 synthesizes the major findings and implications of this master's thesis in the context of the four research questions. Suggestions for future research are also provided, which seasoned fish passage researchers may find of interest, or to those beginning research in this field, may be used as a starting point.

1.3 Impacts

The experimental and analytical efforts directed towards answering research question 1 produced a number of insights of notable interest to fishery managers and hydraulic engineers involved in the field of fish passage. First, HDPE slipliners are shown to drastically reduce depths and significantly increase velocities compared to those present in a standard corrugated steel parent culvert. This finding can be cited by environmental regulatory bodies to place pressure on industry to reserve HDPE slipliner use only to situations where other more appropriate options have been ruled out and no other practical option remains. Alternatively, this finding can be used to promote the use of baffles which are known to slow velocities and increase depths and have been shown in the present thesis to be a feasible option for a large number

of common slipline scenarios (both under inlet control and outlet control). Furthermore, the analytical discharge prediction model presented in chapter 4 can be used by engineers and slipline manufacturers to better tailor baffle configuration designs to site specific constraints. Finally, revelations from the discussion in chapter 5 demonstrate that smaller spoiler baffles are likely the most appropriate baffle type for application in HDPE culverts, since they are shown to develop low roughness coefficients and are known from other research efforts to improve fish passage compared to other baffle forms.

1.4 Resources

The hydraulics department at the Université de Sherbrooke is staffed by an experienced and knowledgeable personnel (Bertrand Côté, ing., M.Sc.; Robert Leconte ing., Ph.D.; Jay Lacey ing., Ph. D.) and were of invaluable assistance over the course of this project. The hydraulic laboratory is overseen by Nicolas Simard, a seasoned technician whose skills proved of immense utility during the laboratory experiments.

This project is funded primarily by a grant from the Natural Science and Engineering Research Council of Canada. Partial funding is also provided through an interuniversity collaboration research stimulus grant provided by the *Groupe de recherche interuniversitaire en limnologie et en environnement aquatique* (GRIL).

Chapter 2

Background

2.1 Introduction

This chapter covers the current state of fish passage research as it relates to HDPE slipine culverts. The chapter is divided into five sections. The first section examines studies which have investigated the effects of velocity, turbulence and depth on fish passage through culverts and gives the reader a general understanding of the importance of these parameters. The second section summarizes research efforts pertaining to how HDPE sliplining affects velocities and depth. The third section presents the findings of past research of interest to understanding how sliplining and baffles affect hydraulic capacity.The fourth section presents a brief overview of the process and theory used to design culverts for hydraulic capacity. The five and final section presents a brief overview of the three predominante flow regimes that occur over isolated roughness elements.

2.2 Hydraulic parameters affecting fish passage in culverts

There are many factors which limit the passage of fish through anthropogenic structures such as HDPE slipliner culverts. Besides any physical barriers which many prevent the fish from entering the culvert (e.g., perched entrances, boulders, branches or debris), elevated values of certain hydraulic parameters in the flow field present within the culvert may also considerably reduce its passibility. Two important hydraulic parameters influencing fish passage success rates through culverts are the velocity and the magnitudes of certain turbulence parameters. Insufficient depths also significantly restrict the movement of fish; especially in non baffle HDPE slipliner culverts where supercritical flow depths commonly occur. Velocity barriers, turbulence and water depth are treated separately in the three subsections that follow by calling on the results and discussions of articles having the objective to understand the effects of these phenomena on fish passage.

2.2.1 Velocity

The effect of velocity on fish passage has been perhaps the most rigorously investigated of the three hydraulic parameters stated above. A number of studies have examined the subject of velocity for a diverse selection of commercially and socially important fish species (Enders et al., 2003; Kemp and Williams, 2008; Davis and Davis, 2011; Poplar-Jeffers et al., 2009). In fact, one account (Katopodis and Gervais, 2012) stated that at least 1900 studies have been

performed to determine swimming velocities of fish.

It is generally accepted that each species of fish has three fundamental swimming speeds (Clay, 1995). The fastest, a fish's burst-speed, is normally applied in nature only to evade predators and to swim through much higher than average water velocities. Burst-speed can only be maintained for very brief periods and a recuperation period is needed after its use. Sustained speeds are those which can be held for a duration of a few of minutes. Fish use a sustained speed to make it through quick reaches of a river, over a small set of rapids or to overcome low level cascades. Cruising speeds (or sometimes *prolonged*) are maintainable for a long period of time and are used while feeding or moving over slower reaches of water (Clay, 1995). Figure 2.1 shows the characteristic swim speed ranges for a number of adult fish species.

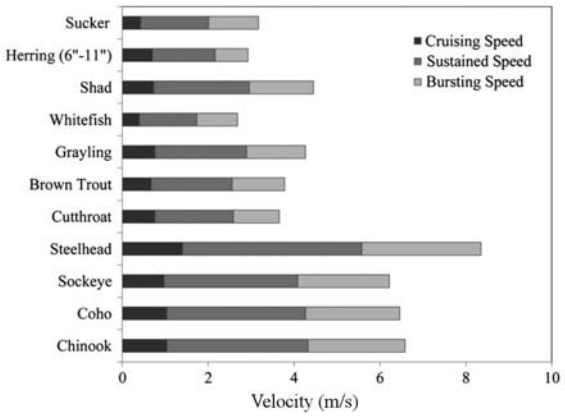

Figure 2.1: Adult fish swimming speeds (from Olsen and Tullis, 2013).

Among these three characteristic speeds, the burst-speed of the target species is of particular importance for the design of baffle configurations. If the mean velocity over a critical section surpasses the burst speed of the target fish, then the culvert risks to severely limit the successful passage rate for this particular species. The same result would occur for fish exposed to prolonged reaches of flow exhibiting velocity means higher than their sustained swimming speeds, which can generally only be maintained for a duration of a few minutes. Therefore, a model capable of predicting flow velocities through critical sections of a baffle configuration is an essential tool for engineers concerned in the design of culvert fishway. Rajaratnam et al. (1989) and Rajaratnam and Katopodis (1990) empirically developed velocity profile equations for both the slotted-weir and weir baffle systems. The authors defined a dimensionless velocity scale formula (Eq. 2.1) which can be used in conjunction with eq. 2.2 as a means to determine

the barrier velocity (U_b) at the baffle. The coefficients (C) were obtained by performing linear regression on the plotted points of dimensionless velocity scale versus (y/h) (see Fig. 2.2 for an example).

$$U^+ = C\left(\frac{y}{h}\right) \tag{2.1}$$

$$U^+ = \frac{U_b}{\sqrt{gDS_o}} \tag{2.2}$$

Where:

D = culvert diameter (m)
U^+ = dimensionless velocity
U_b = barrier velocity (m/s)
S_o = culvert slope expressed in decimal form
y = water depth (m)
h = baffle height (m)

Rajaratnam et al. (1990), also produced figures similar to Fig. 2.2 and the coefficient C for Eq. 2.1 which can be applied to estimate the velocity barrier over the top of the weir for the weir baffle configuration.

Another regression model was proposed by Katopodis and Gervais (2012) to predict critical swimming speeds and maximum endurance times for a variety of fish species. Katopodis and Gervais (2012) performed the operation of reducing nearly 1900 references to a grouping of only 126 dependable sources. Using analysis with dimensionless quantities, the authors determined regression constants for dimensionless fatigue curves produced from the retained data for a large number of fish species (e.g., salmon, trout, sturgeon and eels). The data that they obtained is presented in Fig. 2.3. A legend of the symbols used in Fig. 2.3 is found in Fig. 2.4. The Eqs. 2.3 and 2.4 can be applied with the regression constants for any target fish species from the exhaustive list available in their publication. Notable species pertinent to the present study include; Brook trout ($k = 1.920$), Brown trout ($k = 3.297$), Walleye ($k = 11.235$), among many other possible species important to the waterways of North America. For the Eqs. 2.3 and Eqs. 2.4, (U_S) represents the fish's swimming velocity.

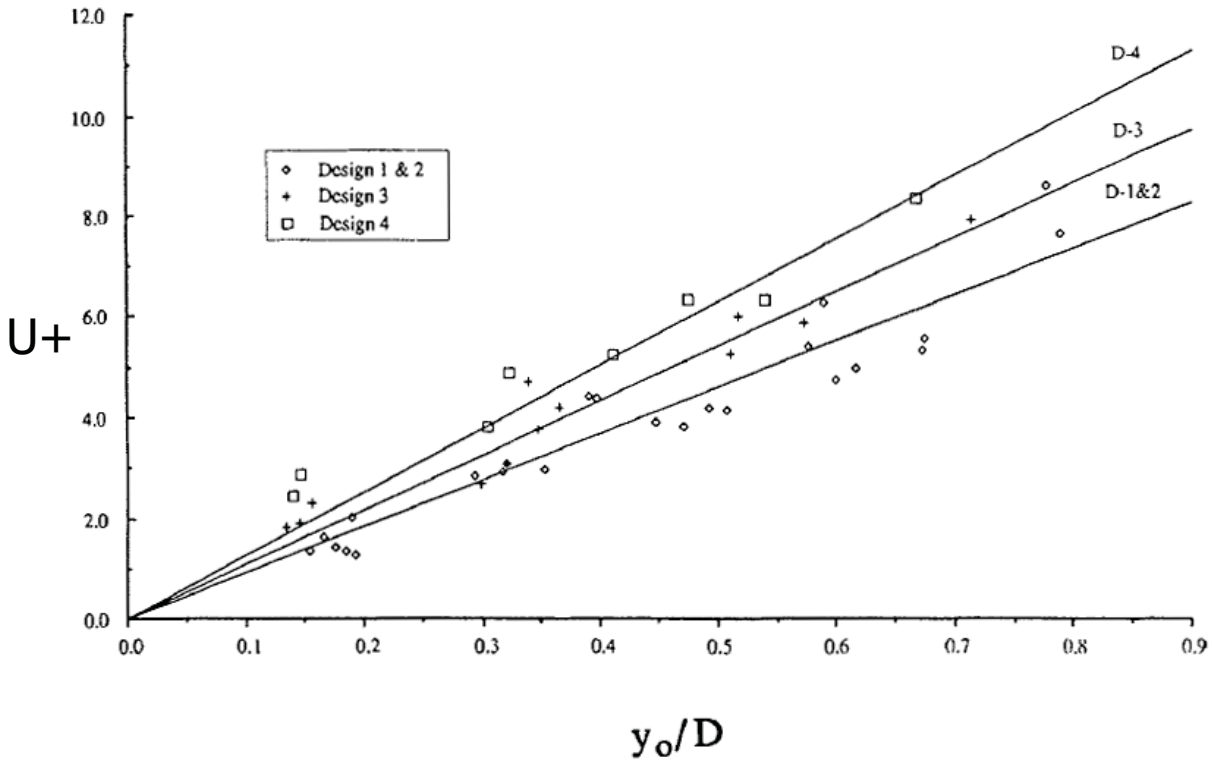

Figure 2.2: Variation of U^+ versus y/D for the weir baffle system Rajaratnam and Katopodis (1990). The designs D1, D2, D3 and D4 are slotted weir baffles with h=0.15D and $\lambda = 0.6$, 0.3, 1.2 and 2.4, respectively.

$$U^* = K t_*^{\eta} \tag{2.3}$$

The dimensionless swimming velocity is defined as:

$$U^* = \frac{U_S}{\sqrt{gL}} \tag{2.4}$$

The dimensionless swim time is defined as:

$$t_* = \frac{t}{\sqrt{\frac{l}{g}}} \tag{2.5}$$

Where:

K = species dependent regression coefficient
U^* = dimensionless velocity (not to be confused with shear velocity)
U_s = fish swim velocity (m/s)
η = species dependent coefficient

t^* = dimensionless sustained swimming time
t = sustained swimming time
l = body length (m)

The fatigue curves were plotted with dimensionless swimming speed (U^*) against dimensionless sustained swimming time (t^*) and are a useful source of data for determining if a given velocity surpasses the swimming capabilities of a target fish species.

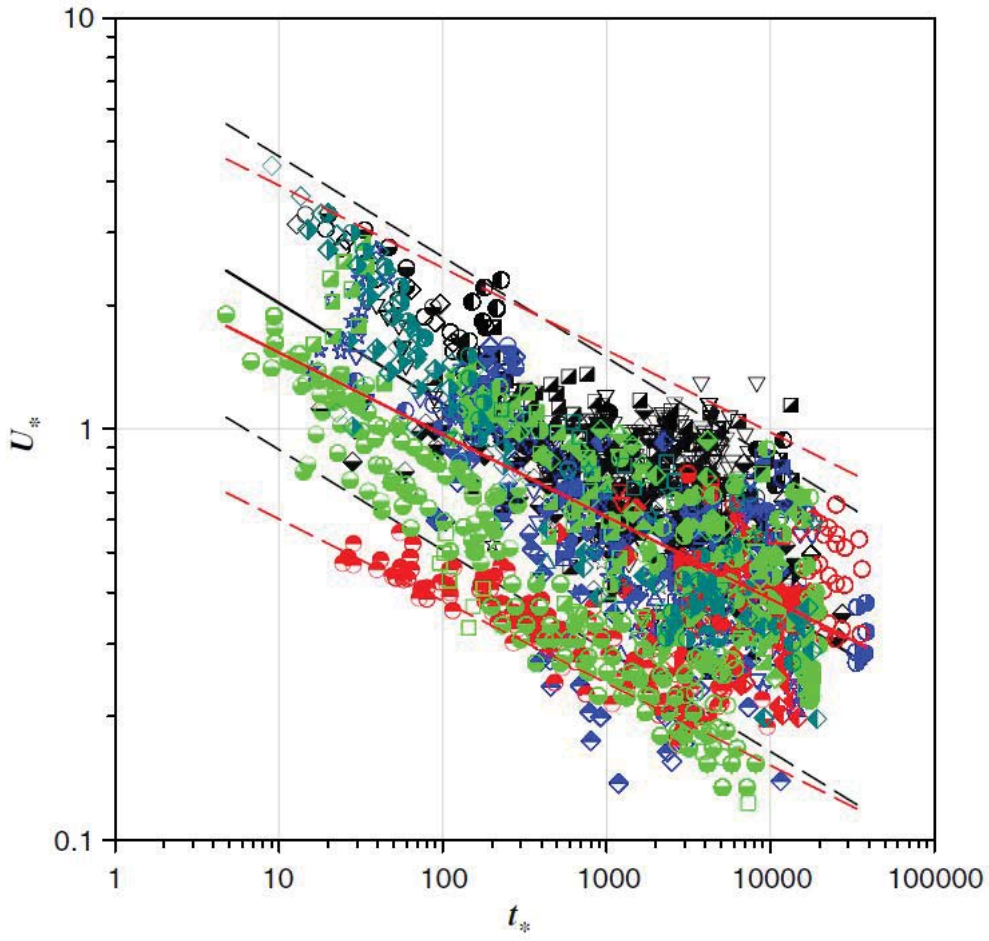

Figure 2.3: Ichthyomechanics Database processed data (weighted and not weighted) for fish speed versus time (≤30min) using dimensionless variables (U* versus t*) by species. Graph includes the regression lines and the 95% prediction intervals for weighted (black lines) and nonweighted (red lines) data. (caption adapted from Katopodis and Gervais (2012).

The majority of studies directed towards determining fatigue times assume constant flow and fish swimming velocities. This model is an effective simplification useful for many common applications; however, these assumptions are rarely exhibited in nature or in anthropogenic

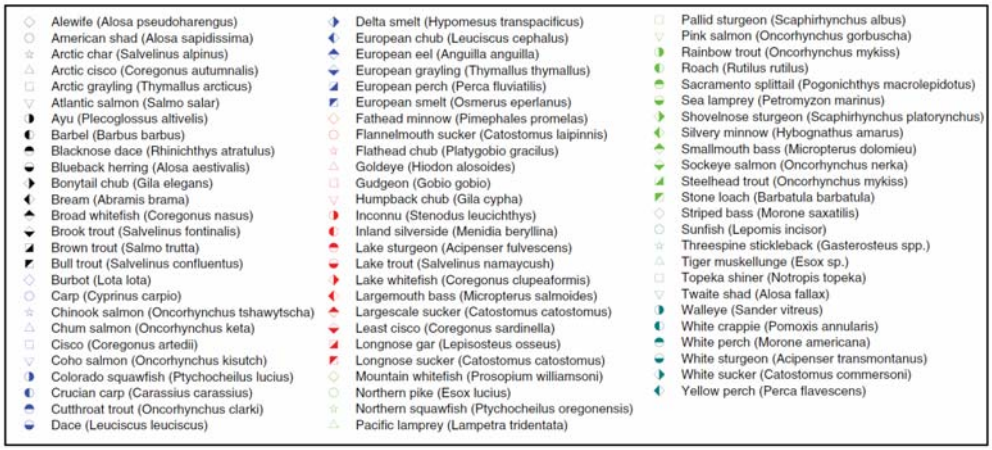

Figure 2.4: Legend for use with Fig. 2.3 (Caption adapted from Katopodis and Gervais (2012).

structures (ex. culverts and fishway). In an attempt to improve on this simplified model by introducing variable swimming speeds and flow velocities, Castro-Santos (2006) proposes a novel mathematical model (Eq. 2.6) to predict the maximum ascent distance (D_{max}) in a dynamically varying velocity stream. The method first involves the determination of the fatigue time (T^*) which is dependent on the species and size of fish as well as characteristics of the velocity field before determining the maximum distance of ascent (D_{max}) using Eq. 2.6. The variable U_s (m/s) represents the swimming speed of the target fish while U_f (m/s) indicates the flow velocity. This model may be of use to predict if complex flow fields of a baffled HDPE culverts would present a velocity barrier for a given target species. The interested reader is directed towards Castro-Santos (2005) and Castro-Santos (2006) for a detailed explanation of the model and how it can be applied for a number of important fish species (e.g., American Shad, Walleye, White Sucker).

$$D_{max} = 100 \int_{t=0}^{T^*} \left(U_s - U_f\right) dt \tag{2.6}$$

2.2.2 Turbulence

Turbulence is thought to have a major influence on the swimming performance of fish, their habitat selection and their choice for resting positions (Liao, 2007; Tritico, 2009; Webb and Cotel, 2010; Lacey et al., 2012). Turbulence has also been studied extensively in the context of corrugated steel culverts and it is now apparent that it is an important fish passage design

parameter (Ead et al., 2002; Richmond et al., 2007; Clark and Kehler, 2011). Turbulence in a flow field is generally accepted to be characterized by the velocity and vorticity fluctuations of all three axial components about a statistically steady mean (Lacey et al., 2012). Turbulent structures are further defined as intermittent coherent motions in a flow field, which can be decomposed into smaller scale eddies and larger scale wedges (Lacey et al., 2012). Across the many studies which have looked at the influence of turbulence on fish passage many metrics have been applied to quantify turbulence. For example, Lacey et al. (2012) have listed 12 turbulent metrics which have been widely applied to the study of turbulence. Given this over-abundance of metrics and the need for researchers to be able to contrast and compare results, a simplified turbulent assessment model was proposed by Lacey et al. (2012), based solely on four important turbulent characteristics: turbulence Intensity, Periodicity, Orientation and Scale (IPOS). These are the four proposed metrics which should be used to investigate turbulence in hydraulic studies related to fish science.

A study was carried out at an earlier date by Tritico and Cotel (2010) who investigated the effects of turbulent eddy diameter (scale), vorticity and orientation on the 2 min critical swimming speed and stability of creek chub (*Semotilus atromaculatus*). The specimens were subjected to two turbulent flow fields, each dominated either by horizontal or vertical spinning eddies. Eddy diameter was varied as a percentage of body length (eddy scale) over a number of trials. One of the principal objectives was to determine at what eddy scale postural spills became frequent. A spill was defined as a loss in postural control in the fish followed by a downstream translation in the fish's position. Spills were found to be 230% more frequent in turbulent flow fields with horizontal eddies (with the axis of rotation lies in the horizontal plane) than in those dominated by vertical eddies (who's axis of rotation lies in the vertical plane). This suggests that turbulent flows dominated by horizontal eddies may possibly be more difficult for fish to navigate than flows dominated by vertical eddies. Vertical eddies induce forces along the flexible vertical plane of the fish as shown in Fig. 2.5, whereas horizontal eddies act along the much less flexible horizontal axis, where forces are not easily absorbed by natural fish movements such as the Kármán gait.

Turbulence, unfortunately, has not received considerable attention as it applies to the study of fish passage through culverts (HDPE or otherwise). There are, nonetheless, a few studies which have. Of particular interest is the Morrison et al. (2008) study on the turbulent flow

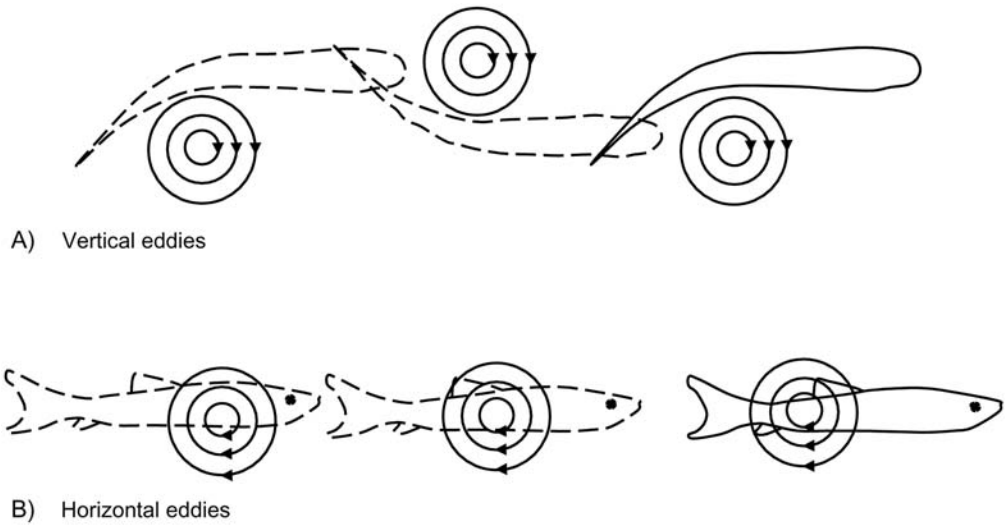

Figure 2.5: Schematic showing the effect of eddy orientation on fish swimming behaviour. A) Plan view vertically oriented eddies. B) Side view horizontal eddies. Lacey et al. (2012)

field of slanted weir baffles in corrugated culverts. The principal objective of Morrison et al. (2008) was to compare the turbulent flow structure of a corrugated steel baffle fitted culvert with the turbulent flow structure of a non-baffle fitted culvert. Despite the fact that Morrison et al. (2008) examined only corrugated steel culverts, their results are still of interest in view of the relatively few articles which have looked at turbulence in culverts. The experimental setup consisted of two full scale corrugated steel culverts (1.83 m diameter and 12.2 m length) on a 1.14% slope. Turbulence characteristics (turbulent intensity - *TI*, and turbulent kinetic energy - *TKE*) were tested for four different flow rates and various configurations for both slotted-weir and slopped weir baffle configurations. Figures 2.6 and 2.7 present examples of the authors' findings. As can be seen in Fig. 2.6, higher *TKE* values (0.84 m^2/s^2) were measured closer to the baffle and Fig. 2.7 depicts a general trend for slightly higher *TI* values towards the centerline of the culvert. They found slightly higher vertically average streamwise turbulent intensities for the slopped-weir baffle (0.35 cm/s) compared to the slotted-weir baffle (0.30 cm/s) close to the baffles. The authors also provide insights into improving their experimental method which would be of use for studies of turbulence in proximity to baffles.

A second study performed by Olsen (2011) investigated turbulence around corner-baffle and sloped-weir baffle systems placed within a 164 foot slip-line culvert in a laboratory setting. One of the studies objectives, was to quantify the turbulent flow field through the use of four different turbulent metrics (TI, TKE, average vector method and also by using the energy

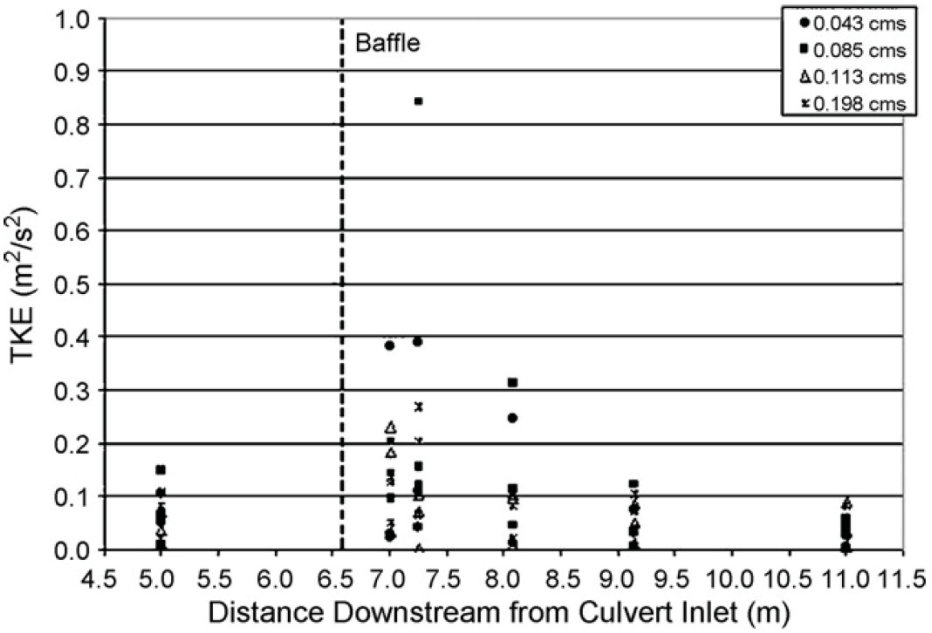

Figure 2.6: Vertically averaged centerline TKE values for the sloped-weir baffle at four flow rates (Morrison et al., 2008)

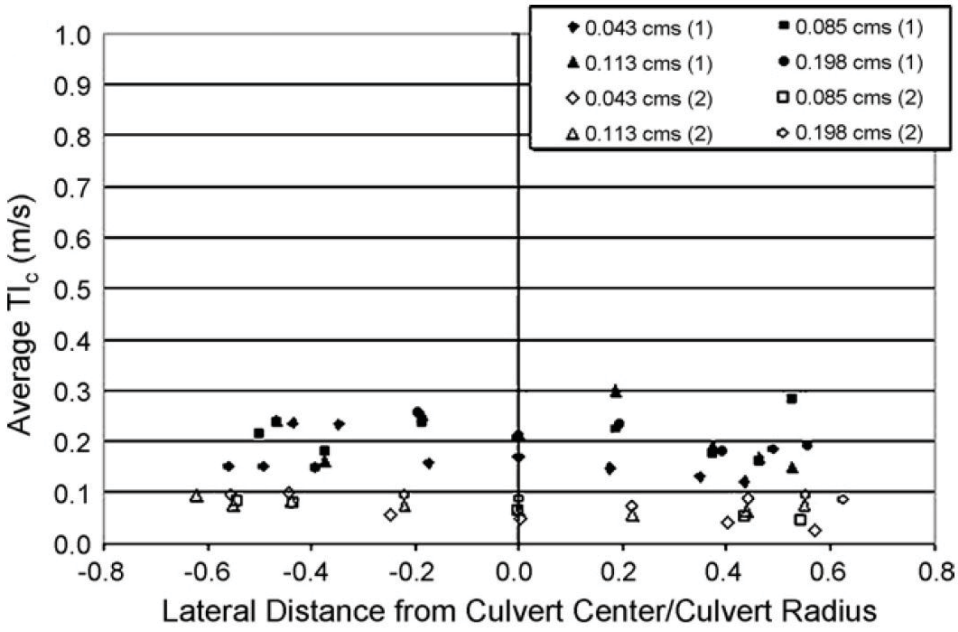

Figure 2.7: Lateral TI values at 0.31 m (1) and 4.32 m (2) downstream from the sloped-weir baffle (Morrison et al., 2008)

dissipation factor). For each of the four metrics studied, the results were correlated with fish passage success. It was found that the energy dissipation factor (EDF) was the metric presenting the highest positive correlation with fish passage success (Fig. 2.8). The authors proposed that future studies involving fish passage through culverts focus on evaluating the turbulent flow field through the use of EDF.

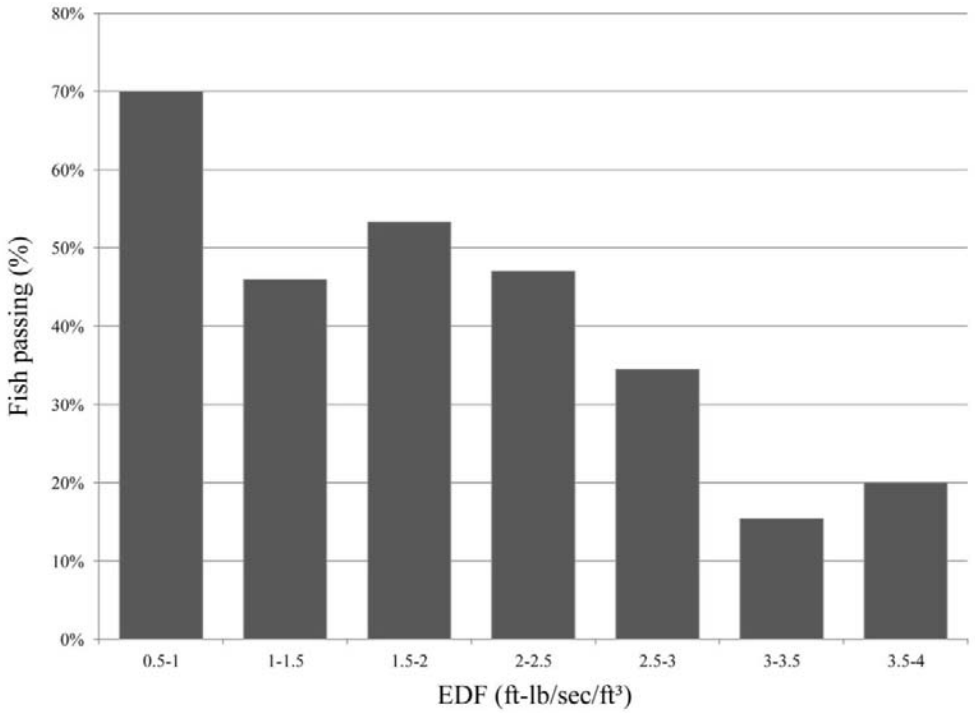

Figure 2.8: Fish passage success versus average EDF values for the corner-baffle and sloped-weir baffle culvert (Olsen, 2011)

2.2.3 Depth

There are a number of studies which have lightly touched on the subject of depth and fish passage. Most literature comes from technical design manuals published by governmental regulatory bodies. For example, The Washington Departement of Fish and Wildlife recommend that subcritical flow should be present throughout the length of the culvert (Bates et al., 2003). They also recommend a minimum depth of 0.23 m for adult trout, pink salmon and chum salmon. They recommend a slightly higher value of 0.30 m for adult chinook, coho and sockeye salmon. The Departement of Fisheries and Oceans recommend a depth of 0.350 m and do not specify fish species (Savoie and Haché, 2002). However, it is generally accepted that depths in culverts be as high as practically possible since fish attain their maximum swim capacity when

fully submerged.

2.3 Variation of Manning's roughness coefficients

The following sections synthesizes the research findings relevant to understanding how partially full Manning's roughness coefficients vary in corrugated steel and HDPE culverts. The ultimate goal is to obtain a complete understanding of how Manning's roughness coefficients (n) vary with depth for these two culvert materials and determine the lowest and highest possible n values. Roughness values will be acquired from published works or calculated using raw depth and discharge data using Manning's open channel equation. Knowledge of the range of n values for corrugated steel and HDPE culverts is invaluable for estimating the effects of a slipliner on depth and velocity which is the central theme of chapter 3.

Much research has been performed on partially full flow in corrugated steel and HDPE culverts. While some of these research efforts had the explicit objective of determining partially full roughness coefficients, many others were interested in a wide variety of other subjects. The focus by the industry towards determining full flow roughness coefficients has left little attention towards improving our knowledge of how roughness varies with partial depth in culverts. Consequently, we are lacking a clear understanding of how roughness varies with depth in culverts. Fortunately, many of these studies also published raw depth and discharge data which can be used to calculate partially full roughness coefficients which can serve to complete our knowledge of how roughness varies with depth in culverts.

A thorough literature review revealed very few studies which have investigated partially full roughness coefficients in corrugated steel culverts. Similarily, a literature review on partially full roughness coefficients in HDPE culverts returned only a meager selection of articles. Fortunately, a study performed by Devkota et al. (2012) produced a nearly complete picture of how n varies with depth in HDPE culverts. Despite the short supply of experimental data available, it can be argued that enough data does exist to sufficiently estimate the maximum and minimum Manning's n values for corrugated steel and HDPE culverts. In the following subsections roughness coefficients (whether obtained directly from the cited sources or calculated with the Manning's open channel equation) are synthesized and presented for both corrugated steel and HDPE culverts.

2.3.1 Corrugated Steel Pipe

Beginning with corrugated steel pipe, Straub and Morris (1951) studied 18 inch (0.457 m), 24 inch (0.609 m) and 36 inch (0.914 m) corrugated steel culverts at slopes near 0.2% with discharges ranging from 0.0215 m^3/s (0.76 cfs) to 0.490 m^3/s (17.32 cfs). The three culverts studied had corrugations with an amplitude of 0.038 m. The wavelength (distance from crest to crest) was not given. In another study Richmond et al. (2007) studied mean flow and turbulence conditions in a full scale corrugated steel culvert with a diameter of 1.83 m and corrugations crest to crest of 0.076 m and an amplitude of 0.025 m. Besides the numerous insights into the structure of the flow field in corrugated steel culverts, their work also provided flow depth data for various discharges at a single bed slope of 1.14% for a range of discharges from 0.028 m^3/s to 0.453 m^3/s. Clark and Kehler (2011) studied turbulent flow characteristics of a circular corrugated steel culverts; except with an emphasis on milder slopes (0.0028%, 0.11%, 0.27%). They employed a 0.8 m diameter culvert with corrugations 0.068 m crest to crest and an amplitude of 0.013 m and published five flow depth/discharge data pairs. Ead et al. (2000) investigated the velocity field in a corrugated steel culvert with diameter of 0.622 m at three slopes 0.55%, 1.14% and 2.55% and published 17 depth - discharge data pairs. The interested reader will find the details of these data pairs in the respective articles.

Figure 2.9 below shows the n/n_f values calculated from the experimental data from the four studies mentioned above. The full flow roughness (n_f) (Manning coefficient) was assumed to be equal to 0.024, which is the commonly accepted value for corrugated steel and all types of corrugations. Figure 2.10 presents the same data as in Fig. 2.9, however, n is shown versus y/D. A popular open channel hydraulic calculator was employed to determine the respective roughness coefficients using the culvert dimensions, depth and discharge data listed in the respective studies. The results of Richmond et al. (2007) were from a full scale culvert (1.63 m in diameter) and are representative of a typical field installation. It is worthy to note the elevated roughness coefficients (e.g., 0.028 to 0.034) that were determined for the lowest relative depths (<10%) studied by Richmond et al. (2007). The lowest roughness values near 0.020 were obtained from trails performed on a very low slope of 0.55% which may help explain their substantial deviance from the rest of the group. Manning's n values near 0.020 for corrugated steel culverts are unlikely, therefore these data are probably erroneous. If the large discrepan-

cies in n mentioned above are ignored for the time being, it can be seen from Fig. 2.9 that n values vary generally between 0.028 and 0.023. However, the high roughness values obtained at low relative depths are still important given the need for fish to navigate through culverts at low flow rates producing shallow depths, a common situation during the summer months. Further investigation into the evolution of n at low relative depths in culverts is needed to improve the prediction of depths and velocities for fish passage purposes in corrugated steel culverts.

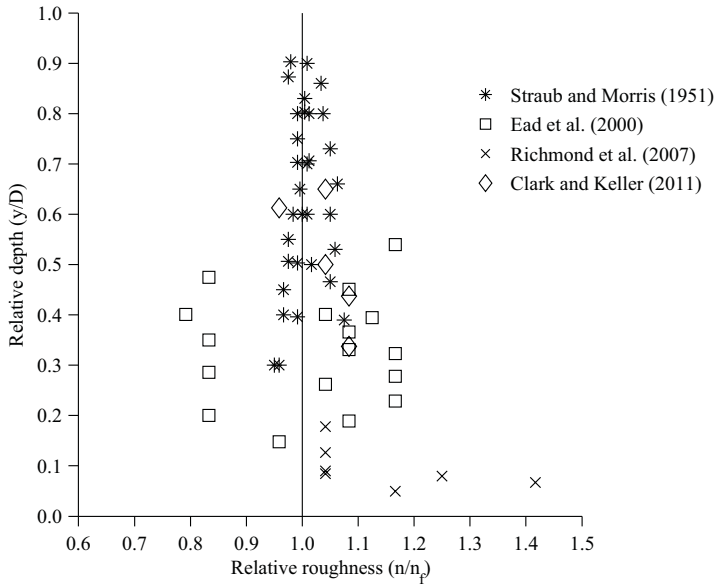

Figure 2.9: Relative roughness (n/n_f) of corrugated steel pipe from various researches as a function of relative depth (y/D).

The mean value of the roughness values presented in 2.10 is 0.0246 with a standard deviation of 0.0024. The mean n value of 0.0246 is in close accordance with the value of 0.024 that is typically used for calculations of depth and velocity in corrugated steel culverts. The small standard deviation demonstrates that the use of $n = 0.024$ is a valid approximation for estimating depth and velocity profiles in corrugated steel culverts. For very low relative depths ($y/D < 0.10$) the use of a higher value near 0.028 will likely provide a more realistic estimation for the actual depth and velocity conditions in a culvert. For the purpose of the study performed in chapter 3, a value of 0.024 will be used for the estimation of the original depths and velocities in the corrugates steel culverts.

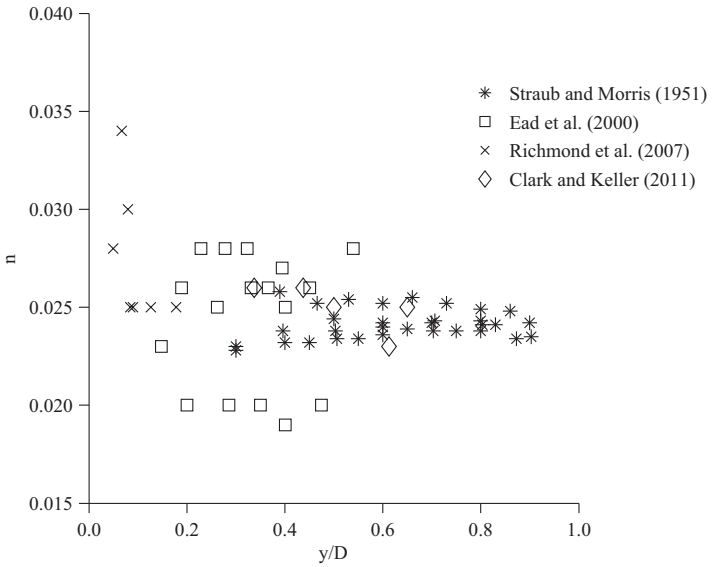

Figure 2.10: Back calculated roughness coefficients for various corrugated steel culverts.

2.3.2 HDPE roughness coefficients at low relative depths

Devkota et al. (2012) performed a thorough study including some 11 000 depth value data points taken in a laboratory setting on a 0.305 m, a 0.610 m and a 1.07 m diameter culvert at flow rates ranging from 0.0056 m^3/s to 0.292 m^3/s at two different slopes (0.2% and 2%). The roughness data obtained in terms of n/n_f (where n_f=0.009) versus y/D are presented in Fig. 2.11. From the allure of the data cloud in Fig. 2.11 it can be assumed that the lowest roughness coefficients for HDPE culverts occur for relative depths < 0.1. For y/D in the range of $0.1 < y/D < 0.3$ no true roughness value can be confidently ascertained. Relative roughness values fluctuate between 0.9 and slightly over 1.2. After $y/D > 0.4$ a substantial decrease in roughness ranging from $n/n_f = 1$ to approximately $n/n_f = 0.7$ is seen to occur. This is likely due to a lack of experimental points in the specified region of the curve, since theoretically the curve should rise to attain $n/n_f = 1$ at higher values of relative roughness. Maximum roughness develops at y/D in the range of $0.2 < y/D < 0.35$ and is roughly a factor of 1.2 greater than full flow roughness. At low relative depths a number of the curves for the trials performed have their lowest roughness's occurring at $y/D < 0.1$ with relative roughness values $n/n_f \cong 0.4$ or $n = 0.0036$.

Olsen (2011) performed a series of partially full flow depth measurements for a 0.609 m diameter HDPE culvert at three slopes (0%, 0.5%=0.005, 1%=0.01). Flow rates ranged

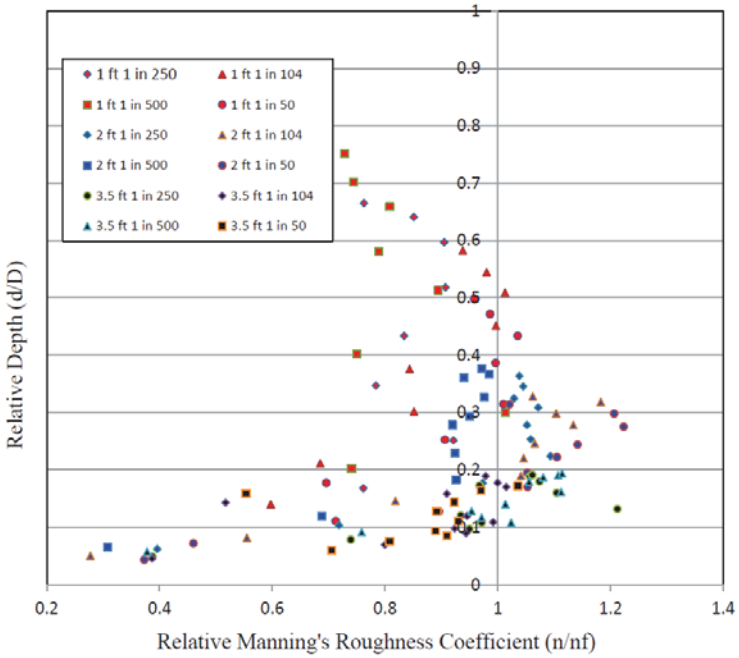

Figure 2.11: Relative depth presented as a function of relative roughness for an HDPE culvert ($n_f = 0.009$) (Devkota et al., 2012). Note - The first number (XX ft) in each legend entry refers to the culvert diameter in feet whereas the second and third numbers (XX in XX) refer to the slope of the culvert.

from 0.0283 m^3/s to 0.1302 m^3/s. A 0.0001 slope was assumed for energy grade line for the calculations of the horizontal pipe since the Manning's formula requires a slope as shown in 3.1 introduced further on in section 3.2.1. The roughness values calculated from depth and discharge from the open channel experiments are shown in Fig. 2.12. Relative depths were below 0.25 for all the trials studied and n values range from 0.005 to 0.014. The lowest roughness value ($n = 0.005$) was found for the horizontal slope at the lowest tested flow rate. The highest roughness value ($n = 0.014$) was obtained for the 0.5% slope and the lowest flow rate.

Even though no conclusive trends with y/D can be taken from Olsen's work, Olsen's values compliment the work of Devkota et al. (2012) and strengthen the fact that roughness is highly variable in HDPE culverts. The work presented in chapter 3 references the work presented in this last section. The reader is directed towards chapter 3 for a detailed analysis into how HDPE sliplining affects depth and velocity.

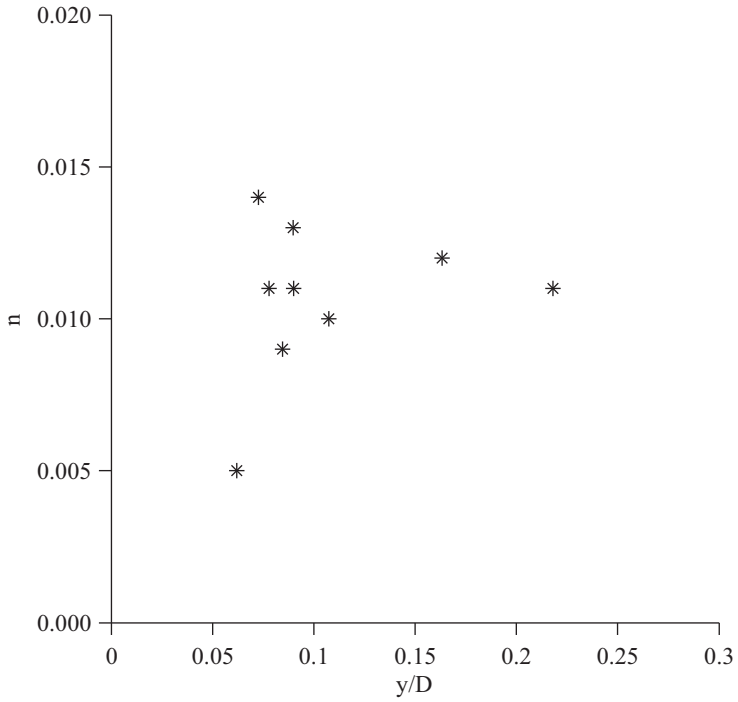

Figure 2.12: Manning's roughness versus relative depth in a HDPE pipe of 0.604 m diameter (Olsen 2013).

2.3.3 A word on the ASCE hydraulic-elements graph for circular sewers

Figure 2.13 is a popular tool for the determination of the partial full roughness coefficients for circular pipes and was first presented in an ASCE publication on the construction of sanitary storm sewers (Langworthy and Bargman, 1967). The variable Manning's *n* curve near the left axis of the figure is constructed from the averages of experimental roughness data obtained from a number of studies performed by independent and government laboratories on various pipe materials. It is intended to give an approximate roughness value at a relative depth of interest when the full flow roughness coefficient is known. Langworthy and Bargman (1967) note that the experimental roughness data often varies widely from their group averages (used to fit the curve) at a specific relative depth. They further note that the decision to use a variable *n* instead of the full flow roughness coefficient should be left to the judgment of the designer in light of the inherent limitations of the data.

Contemporary design theory suggests that the maximum Manning's roughness coefficient is exhibited between 0.2 and 0.4 y/D for partial flows in circular channels. Upon examination of the variation of roughness with relative depth from many of the authors whose data was

used in the construction of Fig. 2.13 (a comprehensive literature review is given in Mangin (2010) which includes many of the underlying studies), the author is of opinion that indeed the maximum roughness does occur in the stated range of relative depth. However, the raw roughness data shows large variations from the mean roughness value of approximately $n/n_f = 1.3$ shown in Fig. 2.13. Therefore, a margin of safety should be taken into consideration. On a further note, the data used in the construction of the variable roughness curve at low relative depths (i.e., y/D <0.3) was taken from a very limited data set and therefore its accuracy is questionable. The interested reader is recommended to read Langworthy and Bargman (1967), which presents an in-depth review of the limitations of the data used in the construction of the variable n curve in Fig. 2.13. Unfortunately, few studies have been performed to extensively understand the variation of n with relative depth for common pipe materials. However, in the absence of such data, the variable n curve of Fig. 2.13 provides a good estimation for design purposes for most common materials. For reader's interested in HDPE, the author is of opinion that the the work of Devkota et al. (2012) (mentioned above) provides the most comprehensive investigation of the variation of roughness with relative depth available at the data of publication.

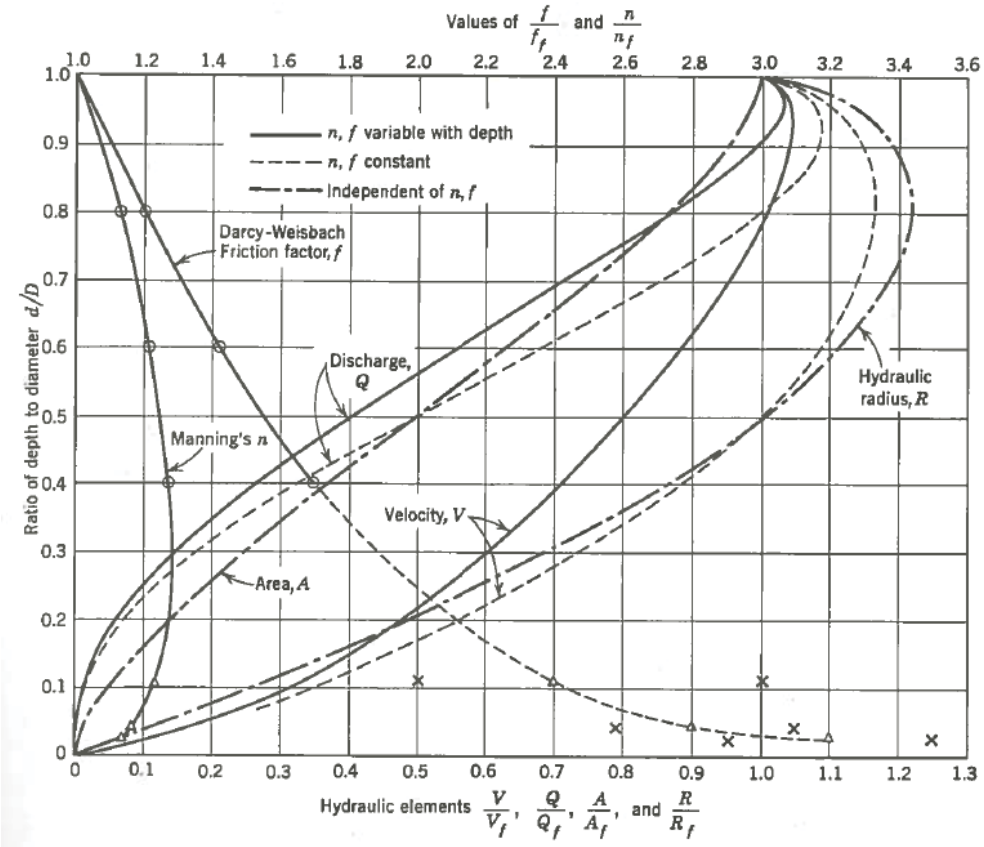

Figure 2.13: Hydraulic elements graph of circular sewers (Langworthy and Bargman, 1967).

2.4 Common Baffle Forms

Many baffle designs for use in corrugated steel pipe culverts have been proposed over the past half century. The hydraulics of the most popular baffle designs have been extensively studied by a group of Canadian scientists directed by Rajaratnam over the course of five consecutive studies performed at the University of Alberta in the late 1980's and early 1990's (Rajaratnam et al., 1988, 1989, Rajaratnam and Katopodis, 1990, 1991) and in a subsequent study a decade later by Ead et al. (2002). These six papers investigated the hydraulics of culverts retrofitted with offset baffles, spoiler baffles, slotted-weir baffles, weir baffles, Alberta fishweir and Alberta fishbaffle systems. The general form and characteristic dimensions of each of these baffles are presented in Fig. 2.14. Baffles are usually installed with equidistant spacing (L), usually a fixed ratio of the culvert's diameter, along the invert of the culvert. The baffle height (h) is also a fixed ratio of the diameter of the culvert. Since the publication of these studies, a few of these baffles have gained considerable popularity over others. Most notably the slotted weir

baffle (SWB) [Fig. 2.14(b)], the weir baffle (WB) [Fig. 2.14(c)] and the spoiler baffle (SPB) [Fig. 2.14(d)] which have seen widespread application in culverts due to their simplistic form and ease of installation.

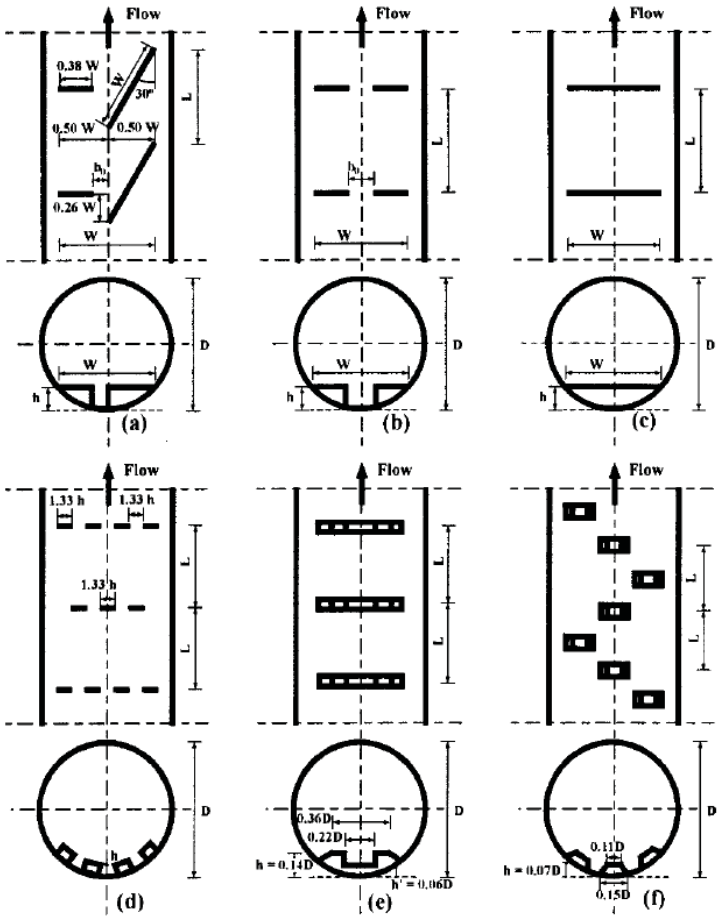

Figure 2.14: a) Offset baffle, (b) Slotted-weir baffle, (c) weir baffle, (d) spoiler baffle, (e) Alberta Fishweir (AFW), and (f) Alberta fishbaffle (Ead et al., 2002).

The following section presents the principal works which have investigated the hydraulics of the three most popular baffle configurations mentioned above. The contributions of other researchers into improving the understanding of the flow field of these configurations are highlighted. The general advantages and disadvantages of each baffle configuration in terms of its appropriateness for fish passage is also a central theme of the following subsections.

2.4.1 Weir and Slotted-Weir Baffles

The slotted-weir and weir baffle systems are in common use in the industry. They have been extensively studied under various scientific contexts over the last two decades since their

development and most notably by Rajaratnam et al. (1989) and Rajaratnam and Katopodis (1990), who proposed and studied both baffles configurations at the University of Alberta. The following section presents a brief overview of the objectives, experimental setups, methodologies used, results obtained and the conclusions that were drawn from these two experimental studies of the weir and slotted-weir baffle configurations.

These two studies (Rajaratnam et al., 1989 and Rajaratnam and Katopodis, 1990) both shared the same objectives; notably, the determination of equations to predict the flow depth for a given discharge, diameter and slope and also the development of an equation to predict velocity barriers at the baffle. The authors also wished to examine the effects of baffles on the discharge rate, visually assess the flow field, establish centerplane velocity profiles for important zones along the length of the model, and draw conclusions as to which baffle system would best allow for fish passage.

In an earlier study (Rajaratnam et al., 1988) it was found that the dimensionless discharge of a baffle retrofitted culvert is a function of the relative depth of the flow. This relation is expressed by the Eq. 2.7. Plotting Q_* against y_o/D for each baffle design provided design curves which can be approximated by Eq. 2.7. The coefficients (C) and (a) in the Eq. 2.8 are dependent on the physical configurations of the baffles (e.g., relative height and spacing). Equations 2.7 and 2.8 were both applied in Rajartnam et al. (1989, 1990) and can be used to provide an accurate means to determine the depth for various slopes and culvert diameters given a known discharge.

$$Q_* = \frac{Q}{\sqrt{g S_o D^5}} = f\left(\frac{y_o}{D}\right) \tag{2.7}$$

$$Q_* = C\left(\frac{y_o}{D}\right)^a \tag{2.8}$$

Where:

Q_* = dimensionless discharge
Q = discharge (m^3/s)
D = culvert diameter (m)
y_o = water depth (m)
S_o = bed slope
g = gravitational constant (m/s^2)

In the study of the slotted-weir baffle (Rajaratnam et al., 1989), baffle heights of 0.15D were configured with four baffle spacings ($\lambda = 0.3D$, $0.6D$, $1.2D$ and $2.4D$). A baffle height of $0.1D$ was also tested, however only with two baffle spacings ($0.6D$ and $1.2D$), for a total of six tested combinations. Each configuration was then installed and studied inside a smooth plastic pipe with diameter 0.305 m and length 6.3 m. Each of the six combinations were placed at three different slopes (1, 3 and 5%), under inlet control, in both supercritical and subcritical flows in order to study a variety of hydraulic conditions. Velocity profiles were obtained at the slot and half way upstream between the next baffle. The two combinations that were tested with a spacing of $0.6D$ were found to be the most effective at producing higher depths of flow and lower barrier velocities (where velocity barrier can be defined as the maximum exhibited velocity). In general, it was observed that during low flows the water moved as a jet between each cell separating any two baffles, however, as the flow increased, water height also increased and a lower recirculation zone appeared below the high velocity upper water layer. The dimensionless discharge (Q^*) was plotted against relative depth (y/D) (Fig. 2.15) and the coefficients for a regression equation relating Q^* as a function of (y/d see Eq. 2.8) were calculated. The fitted curves can be seen in Fig. 2.15. The dimensionless discharge curves can be used to predict the flow depth for any of the baffle configurations presented in Rajaratnam et al. (1989).

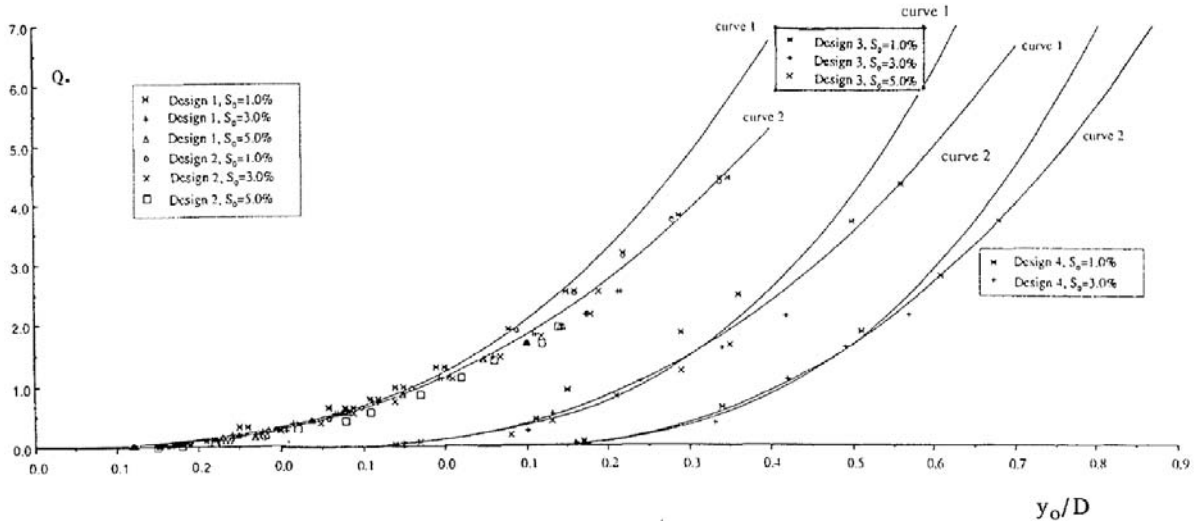

Figure 2.15: Dimensionless discharge curves for the slotted-weir baffle system for a variety of designs and slope combinations (Rajaratnam et al., 1989).

The weir baffle was investigated in the second study (Rajaratnam and Katopodis, 1990).

Rajaratnam proposed the design, stating that it would be cheaper to install (seeing how only one single piece of metal needs to be welded) and likely just as effective as the slotted-weir baffle system. For this study, two baffle heights (h) were studied (h=0.15D and 0.10D), with two baffle spacings (L=0.6D and L=1.2D) to make four tested configurations. The baffles were fixed into a smooth plastic pipe of 0.305 m diameter, having a length of 6.3 m. In the preliminary observations, it was said that the baffles had a significant effect on the relative flow depth during low flow rates and barely any effect once the depth of the water reached a certain level above the baffles. In the latter case, the baffles were said to merely act as bed roughness. Velocity profiles were determined for five vertical regions along the center line of the culvert. The velocity profiles were experimentally determined using a 3 mm Prandtl tube. The velocity barrier was determined to be located over top of the baffles and the maximum backward velocities were found to be less than one third the maximum forward velocity. Similar to the slotted-weir baffle study, the dimensionless discharge (Q^*) was plotted against relative depth (y/D) (similar to Fig. 2.15) and the coefficients for the dimensionless discharge regression Eq. 2.8, were also calculated for each of the weir baffle configurations.

Rajaratnam and Katopodis (1990) conclude that the weir baffle system appears to function just as effectively at reducing velocity and developing depth as the slotted-weir baffle, and therefore may be the preferred option of the two, because of the weir baffles simpler installation. The study also concludes that a baffle spacing of 0.6D should be preferred over larger spacings in an attempt to reduce velocity barriers to fish passage.

2.4.2 Spoiler baffles

Spoiler baffles [2.14(d)] are an attractive alternative to the WB and SPB baffle configurations for use in HDPE slipliner culverts for a number of reasons. To begin with, spoiler baffles can be flexibly arranged along the invert of the culvert. For example, laterally separating baffles from each other in function of a fish's body length allows the design to be adapted to the needs of individual fish species (i.e., body width, length). Similarly, baffle height (h) can be readily adjusted to aid in tailoring the inter-baffle flow depth to the fish's body height. Furthermore, spoiler baffles have been shown to improve fish passage success in smooth concrete culverts with similar roughness coefficients to that of HDPE culverts (Macdonald and Davies, 2007; Stevenson et al., 2008). Moreover, spoiler baffles have been demonstrated to reduce

the level of confusion which fish manifest when contemplating the direction to be taken to proceed upstream compared to Alberta fish-weirs (a baffle which closely resembles the weir baffle)(Feurich et al., 2012). Additionally, spoiler baffles produce a high density of low velocity resting zones, attributable to the close proximity of the baffles, then other forms of baffles (i.e., weir and slotted weir baffles). The higher density of resting zones is likely to improve ascent success rates over longer culverts by providing resting zones for smaller and or weaker fish species to recuperate. The presence of these low velocity resting zones was confirmed in a numerical simulation by Feurich et al. (2012).

Spoiler baffles are also attractive for a number of practical hydraulic engineering considerations. The open flow field they develop likely improves sediment transport through the culvert and streamlined spoiler baffle variations can be anticipated to reduce debris snags. However, these last two points have yet to be rigorously examined and further study in these areas is warranted.

Macdonald and Davies (2007) are likely the sole researchers who have thoroughly investigated the effectiveness of spoiler baffles on fish passage with live specimens. They quantified and compared fish passage success rates through a control (bare) concrete culvert (with diameter of 1.5 m) with those for an adjacent culvert of exactly the same dimensions fitted with three different spoiler baffle configurations. Two baffle heights were studied ($h = 0.019D$ and $0.037D$). The authors investigated in-line spoiler baffles (1-1-1) at two different longitudinal spacings (0.33 m and 0.66 m) and also a 2-1-2 configuration (where X-X-X refers to the number of baffles in the first, second and third row after which the pattern repeats). Figure 2.16b presents the passage success findings obtained by Macdonald and Davies (2007) for passage of common jollytails (*Galaxias maculatus*) through three spoiler baffle arrangements (Fig. 2.16a) for three test velocities (0.35, 0.70 and 1.00 m/s where only 0.35 and 0.70 m/s are shown in Fig. 2.16b). Macdonald and Davies (2007) found that the most complex arrangement (2-1-2) was the most effective at passing fish, with fish being 21 times more likely to traverse the baffled culvert compared to the bare control. The inline 1-1-1 spoiler baffle configuration at the smallest longitudinal spacing was also rather effective, but considerably less so than the 2-1-2 configuration. In contrast, the inline 1-1-1 at the 0.66 m longitudinal spacing only marginally improved passage success compared the control culvert. A principal finding from Macdonald and Davies (2007) is that passage success improves with increasing baffle complexity, as can

be seen from the Fig. 2.16b where the baffle arrangement (C) significantly outperformed the control culvert and the baffle arrangements (A) and (B). Finally, the most promising advantage spoiler baffles offer stems from the fact that they have been shown to significantly improve fish passage even at very low baffle heights ($h < 0.05D$). Macdonald and Davies (2007) concluded that both of these baffle heights - which are much smaller compared to those studied by Rajaratnam et al. (1991) - improved passage success rates considerably compared to a bare control culvert. Interestingly, Macdonald and Davies (2007) demonstrated that the larger h value baffle only marginally improved passage rates compared to the smaller h value baffle. These findings may have important implications for the design of baffles for use in HDPE slipliner culverts where the baffle height is thought to play a key role in the production of barrel friction losses.

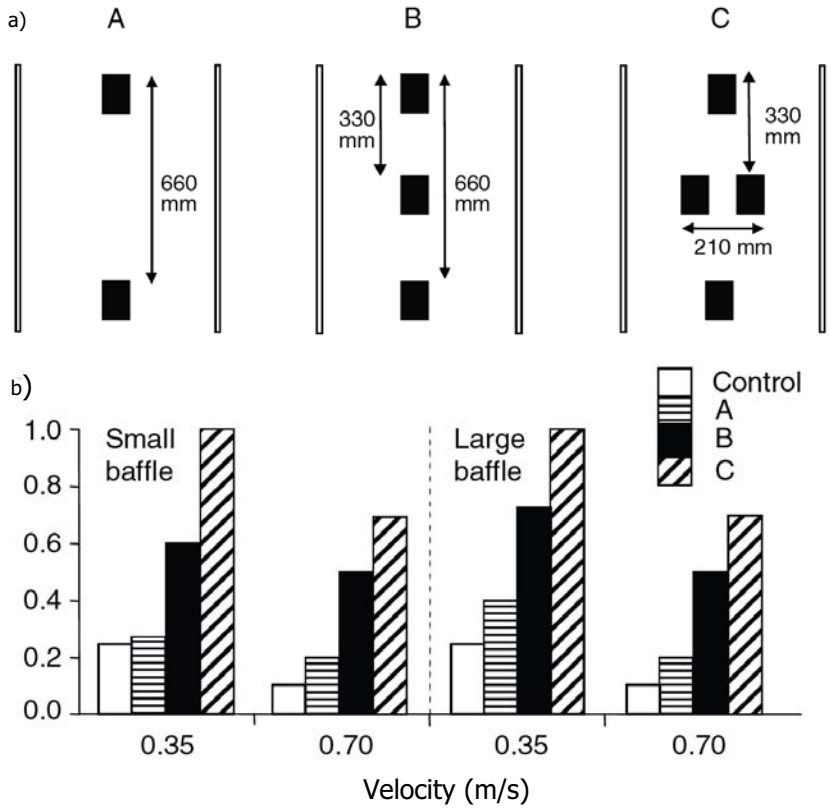

Figure 2.16: (a) the three spoiler baffle configurations studied by Macdonald and Davies (2007). (b) proportion of individuals successfully passing the test section for: Trial series 1 common jollytails. Control trials and trials with small (100 x 70 x 28 mm) and large (100 x 70 x 56 mm) baffles in three arrangements (A, B, C) at two test velocities (0.35, 0.70 m/s).(Caption partially reproduced from Macdonald and Davies (2007).

2.5 Hydraulic design of Culverts

The purpose of the following section is to briefly explain the important considerations in the design of culverts for hydraulic capacity. Many reference books and design manuals have been published which enter into much finer detail than presented here. A few recommended works include the HDS-5 by the Federal Highway Administration (Norman et al., 2001) of the United States as well as the *Manuel de conception des ponceaux* by the Transport Ministry of Québec and the reader is directed towards these sources for further information. The concept of the hydraulic control section of a culvert is explained and the effects of HDPE sliplining and sliplining with fish baffles on the hydraulic capacity are examined. Near the end of the section, the energy equation is developed as it applies to culverts. Furthermore, various scientific articles which have investigated entrance and exit conditions on hydraulic capacity are summarized.

2.5.1 The culvert design process

The first step performed in the culvert design process is to determine the peak design flow which must be conveyed through the culvert. This is done through statistical hydrological analysis of the upstream portion of the watershed in question. The concept of the return period is an important culvert design parameter. It gives the designer a sense of the probability that a flood event with a specific discharge will occur during the lifetime of the culvert. To illustrate, a flow rate with a return period of 20 years is expected to occur once every 20 years. However, it is not guaranteed to occur in this time period, it may occur every year for three years in a row and then not again for the following 50 years. Yet, over a sufficiently long period of time, it should occur on average once every 20 years. Regulatory bodies perform risk analysis to determine the appropriate return period discharge which will serve as the peak design flow rate for a given culvert. The chosen return period will depend on many factors including the culvert's level of risk to the public (e.g., proximity to urban centers, importance of the road or rail line under which it is installed), its construction costs and the potential costs for repairs due to flood damage. What is important to retain is that every culvert is designed to convey a peak design flow rate. Failure for the culvert to convey the specified discharge may result in damage to infrastructure, elevated repair costs, possible damage downstream and possible loss of life.

Once the peak design discharge has been established a maximum upstream head water

level is determined. The choice of head water level is usually, but not always, taken at a level near the elevation of the pavement or the low point of the shoulder of the highway embankment plus an appropriate safety margin. After the maximum head water level is established, the engineer will begin to iteratively analyze various culvert forms (concrete box culverts, corrugated steel pipe, multiple culverts, etc.) of various diameters and dimensions. During the design it will also be verified that the culvert respects the maximum head water level under both inlet and outlet control. The process continues until a culvert design is attained which conveys the required discharge without excessive headwater ponding, while also respecting budgetary and other practical constraints (e.g., construction feasibility). The following subsections present a brief explanation of the two control types.

Inlet control

The hydraulic capacity of an inlet controlled culvert is largely limited by the geometry of the entrance of the culvert. In other words, the barrel of the culvert is capable of passing a greater flow than the inlet is capable of letting enter the culvert. Flow contraction at the inlet of the culvert diminishes the effective flow area and consequently reduces the discharge capacity. Many inlet geometries have been developed with the intent of reducing flow contraction. The majority of short culverts are controlled at the inlet since the barrel length is not sufficient to produce an appreciable amount of friction losses to cause the culvert to be controlled at the outlet (explained in greater detail further on). Parameters affecting inlet control include: the head water level, inlet shape, inlet area and the inlet edge configuration (Norman et al., 2001). It is important to underline that the hydraulic capacity of an inlet controlled culvert is not affected by barrel roughness.

Outlet control

The hydraulic capacity of outlet controlled culverts is determined by the discharge capacity of the culvert's barrel. In other words, the inlet is able to let more flow into the culvert than the barrel is capable of evacuating. The same parameters that affect inlet control also affect outlet control. However, in addition, outlet controlled culverts are also affected by barrel roughness, barrel slope, barrel length and barrel area. A number of water surface profiles are possible

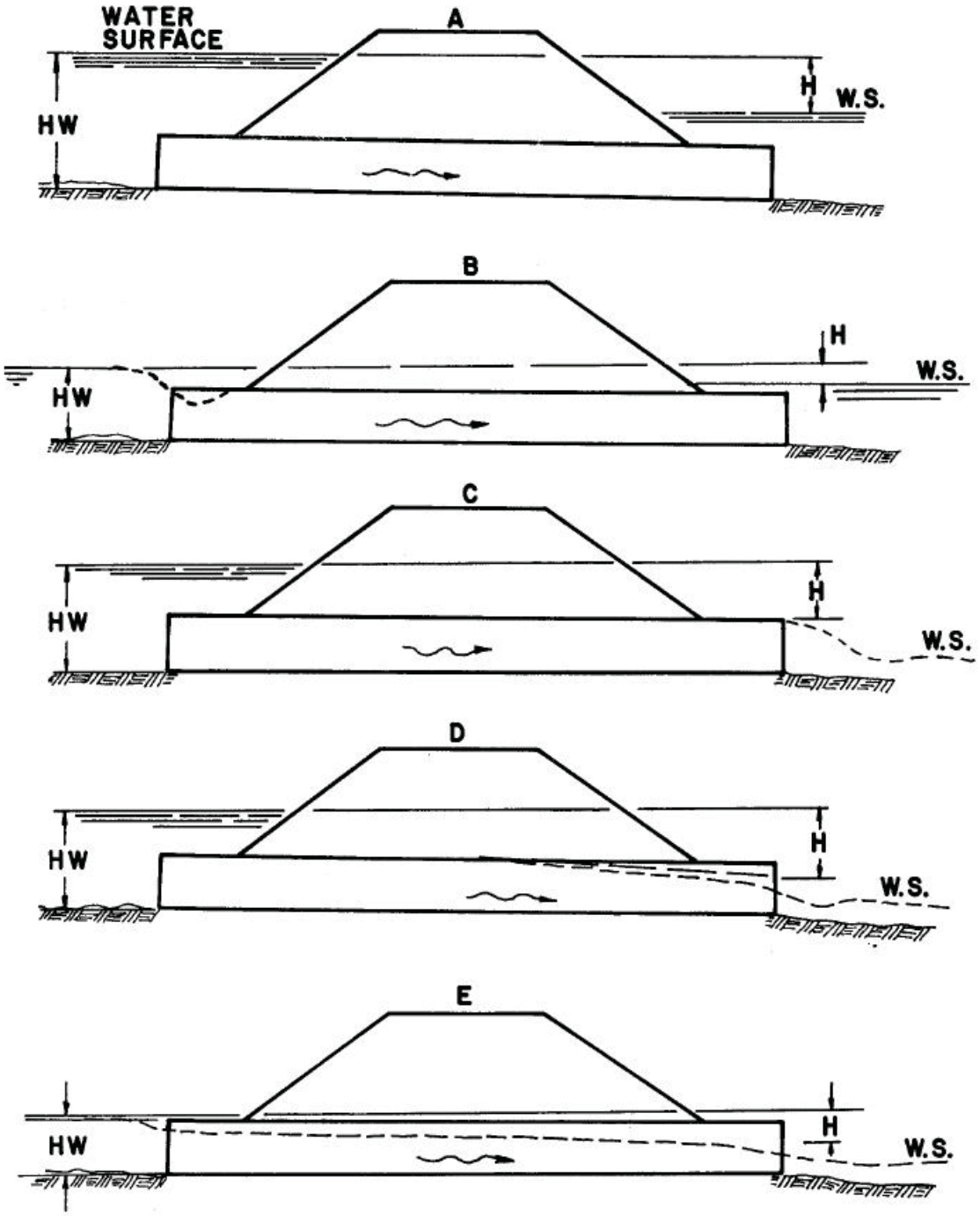

Figure 2.17: The five possible types of outlet control: (A) classic full flow condition, (B) outlet submerged inlet unsubmerged, (C) entrance submerged outlet unsubmerged, (D) entrance submerged and outlet flows freely, (E) both inlet and outlet unsubmerged yet the culvert flows partially full (Norman et al., 2001).

along the length of a culvert flowing under outlet control as shown in Fig. 2.17. In most cases the culvert runs full along the majority of its length. Exceptionally, however, the culvert may run less than full at the inlet due to flow contraction or less than full near the outlet as flow passes through critical depth and draws the water surface profile down before the exit. To simplify the definition for the purpose of this thesis, the term outlet control evokes that the culvert runs full along its entire length and the inlet and outlet are submerged as illustrated in Fig. (2.17A). In such an arrangement, the culvert essentially acts as a pipe connecting two reservoirs and is the control scenario most susceptible to barrel roughness.

2.5.2 The energy equation applied to culverts

The following section develops the energy equation used to determine the hydraulic capacity of an outlet controlled culvert. The energy equation 2.9 implies that the energy available upstream of the culvert is equal to the energy downstream of the culvert plus the friction losses occurring at the inlet, over the barrel and at the exit of the culvert.

$$LS_o + HW + \frac{V_1^2}{2g} = h_o + H + \frac{V_2^2}{2g} \tag{2.9}$$

Where:

$$\begin{aligned} L &= \text{culvert length (m)} \\ HW &= \text{headwater elevation (m)} \\ V_1 &= \text{upstream velocity (m/s)} \\ V_2 &= \text{downstream velocity (m/s)} \\ H &= \text{energy losses (m)} \\ h_o &= \text{outlet datum (m)} \\ S_o &= \text{bed slope} \\ g &= \text{gravitational constant (m/s}^2\text{)} \end{aligned}$$

The energy loss term (H) can be further decomposed into three terms: singular inlet losses (h_{in}), singular outlet losses (h_{out}), and friction losses along the barrel (h_f). The Eq. 2.10 gives an expression for this decomposition.

$$H = h_{in} + h_{out} + h_f \tag{2.10}$$

The velocity head $\frac{V^2}{2g}$ is a common factor for all three terms that compose the loss term

(H) V is the average velocity in the barrel. For the calculation of the inlet and outlet losses the average barrel velocity (V) is used. The singular losses at the inlet of a culvert under outlet control are given by Eq. 2.11 where k_e is the entrance loss coefficient.

$$h_{in} = k_e \frac{V^2}{2g} \tag{2.11}$$

Where:

V = average barrel velocity (m/s)

The losses at the outlet depend on the change in the water's velocity as it exits the barrel. Equation 2.12 presents this relationship. For the case where the flow suddenly expands at the culvert's outlet, k_o is usually taken to be equal to 1.

$$h_{out} = k_o(\frac{V^2}{2g} - \frac{V_2^2}{2g}) \tag{2.12}$$

The downstream velocity is usually neglected and Eq. 2.12 and when k_o is equal to one the exit losses equal the full flow barrel velocity head of the culvert (Eq. 2.13).

$$h_{out} = (\frac{V^2}{2g}) \tag{2.13}$$

Friction losses along the barrel of the culvert are calculated using the Eq. 2.14 or Eq. 2.15, depending on the preferance for Manning's n or Darcy's friction factor f.

$$h_f = (\frac{2gn^2L}{R^{1.33}})\frac{V^2}{2g} \tag{2.14}$$

$$h_f = f\frac{LV^2}{D2g} \tag{2.15}$$

Where:

n = Manning's friction factor
R = hydraulic radius
V = barrel velocity (m/s)
f = Darcy's friction factor
D = culvert diameter (m)
g = gravitational constant (m/s^2)

The three friction loss terms are expressed in Eq. 2.16 below.

$$H = \left\{ k_e + k_o + \frac{2gn^2L}{R^{1.33}} \right\} \frac{V^2}{2g} \tag{2.16}$$

The determination of the three coefficients k_e, k_o, and n, is necessary to design the culvert to properly accommodate the peak design discharge. It can be seen from Eq. 2.16 that reductions in k_e, k_o, and n will improve the discharge for a fixed head water level. Equation 2.16 is used as the theoretical basis of an analysis presented in the discussion of the article of chapter 4. The discussion examines how roughness reductions and radial reductions between the parent and slipliner culvert interact.

2.5.3 The effect of HDPE Sliplining on Hydraulic Capacity

The practice of rehabilitating failing culverts with HDPE slipliners poses a number of problems towards respecting the peak design discharge that the parent culvert was designed to convey. These risks were briefly explained in chapter 1. Here, they are further developed within the context of inlet and outlet control.

Sliplining inevitably decreases the available flow area at the entrance and along the barrel of the culvert. This has the direct consequence of reducing the discharge capacity of the culvert. For a fixed friction factor (f), energy losses through a pipe h_f, or in this case a culvert, are inversely proportional to culvert diameter as shown in the widely accepted Darcy-Weisbach headloss relation for turbulent flow (Eq. 2.15). Additionally, it can be seen that h_f increases exponentially with V. Furthermore, velocities must increase in the smaller diameter slipline culvert to respect the same discharge rate passing through the larger diameter parent culvert.

The singular losses at the inlet of the culvert are also inversely proportional to the inlet diameter as can be seen in Eq. 2.17. Consequently, reductions in diameter will have an important influence on the inlet energy losses for a given flow rate.

$$h_e = \frac{2k_eQ^2}{D^4g} \tag{2.17}$$

Where:

L = culvert length (m)
h_e = friction losses (m)
k_e = entrance loss coefficient

$$Q \quad = \quad \text{barrel velocity (m/s)}$$

The increased energy losses at the inlet and through the barrel of the culvert consequently require an increase in energy to drive the flow. For the case of a culvert, this energy is found in the form of hydraulic head available in the upstream approach. Unfortunately, as previously explained, the upstream head water level is normally a fixed value and provides little flexibility. Therefore, allowing increases in head water level is not an option for increasing the available energy in the system. HDPE slipliners attempt to compensate for the loss in diameter by providing a very low f value which helps reduce the required energy. In many cases this is feasible, especially for outlet controlled culverts heavily dominated by barrel losses. However, as will be detailed in chapter 4, the advantage of the reduced f value only compensates for a small range of reductions in diameter (0 to 20%). Short inlet controlled culverts witness zero improvement in hydraulic capacity after HDPE sliplining. In fact, one study found that in many cases the hydraulic capacity of inlet controlled culverts failed to respect the peak discharge capacity after sliplining (Luo and Peng 2010), attributable to increased inlet losses. To summarize, the practice of HDPE sliplining cannot guarantee that the original peak design discharge of the parent culvert will be respected. The actual discharge capacity of the slipliner will largely depend on the degree to which the diameter is restricted as well as the decrease in roughness between parent and slipline culvert.

2.5.4 The effect of baffles on hydraulic capacity

Although there are a large number of studies which have treated friction losses pertaining to culverts, very few have directly assessed the effect of baffles on the hydraulic capacity of slipline culverts. Within the context of a master's thesis performed at Utah State University (United States), Olsen (2011) evaluated the effects of a single design of baffle (slanted weir-baffle) on the hydraulic capacity, the velocity and turbulence profiles of a slip-lined culvert. Manning's n values were experimentally determined for various discharges up to the culvert's full capacity. Non-pressurized and pressurized tests were performed. For the non-pressurized tests, a Manning's roughness coefficient was determined for a number of measured flows (up to full capacity) and at a range of inclinations using the Manning equation for open channel flow. For the pressurized tests, the Manning's coefficient was determined by calculating the friction losses from the pressure differential on a horizontal 50.9 m (167 ft) section of baffled pipe.

Overall, the study concluded that the addition of baffles in a slip-lined culvert decreased the flow capacity by 74% compared to a regular smooth walled slipline culvert of the same length. Although, the publication has identified baffle presence as a potential risk to hydraulic capacity in slip-line culverts, the author examined the effects of only one baffle size and configuration and attempts at developing a new baffle configuration or identifying the best performing configuration in terms of hydraulic capacity were not performed. The results published by Olsen (2011) will be beneficial for comparison purposes with the results of the present study.

Investigations were performed on determining the effects of weir and slotted weir baffles on hydraulic capacity in two papers headed by Rajaratnam and his collegues (Rajaratnam et al., 1989, Rajaratnam and Katopodis, 1990). The researchers, implicitly examined how baffles affect discharge capacity by examining the variation in depth between the bare and baffled pipe for fixed discharges and slopes. The authors did not explicitly determine roughness coefficients by performing pressurized tests as Olsen did. Therefore the data is presented in a less explicit fashion than the work of Olsen (2011). The following paragraphs outline the methodology used by Rajaratnam et al. (1989) and Rajaratnam and Katopodis (1990), while also highlighting their findings and conclusions.

For a given dimensionless discharge Q_*, let η_o $(=y/D)$ be the dimensionless depth for a culvert without baffles and η be the corresponding value for the same pipe fitted with any of the slotted-weir or weir baffle configurations tested by Rajaratnam et al. (1989), Rajaratnam and Katopodis (1990). Then the dimensionless discharges for the plain or baffled culverts can be expressed using the Eqs. 2.18 and 2.19.

$$Q_* = C_o(\eta_o)^{\eta_o} \tag{2.18}$$

$$Q_* = C(\eta)^{\eta} \tag{2.19}$$

Where:

C = coefficient dependent on baffle configuration
C_o = coefficient dependent on baffle configuration

If $\Delta\eta$ is the increase in η, then $\Delta\eta$ is defined by;

$$\Delta\eta = \eta - \eta_o \tag{2.20}$$

From which it can be shown that;

$$\frac{\Delta\eta}{\eta_o} = \frac{\left(\frac{Q_*}{c}\right)^{\frac{1}{\alpha}} - \left(\frac{Q_*}{c_o}\right)^{\frac{1}{\alpha_o}}}{\left(\frac{Q_*}{c_o}\right)^{\frac{1}{\alpha_o}}} \tag{2.21}$$

Equation 2.21 was used to evaluate all the slotted weir and weir baffle designs by substituting the values of C and n for the respective baffle configurations. These coefficients can be found in the respective articles of the baffle in question. The data were plotted to obtain Fig. 2.18, which displays the influence of the various baffle configurations on flow depth. From Fig. 2.18 it can be seen that the tallest baffle configurations (SWB D1 and D1 WB) - which had the tallest baffle heights of 0.15D and the closest baffle spacings of 0.6D - developed the largest values of $\Delta\eta/\eta_o$. From these results one could predict that larger more closely spaced baffles will have the greatest influence on full flow hydraulic capacity.

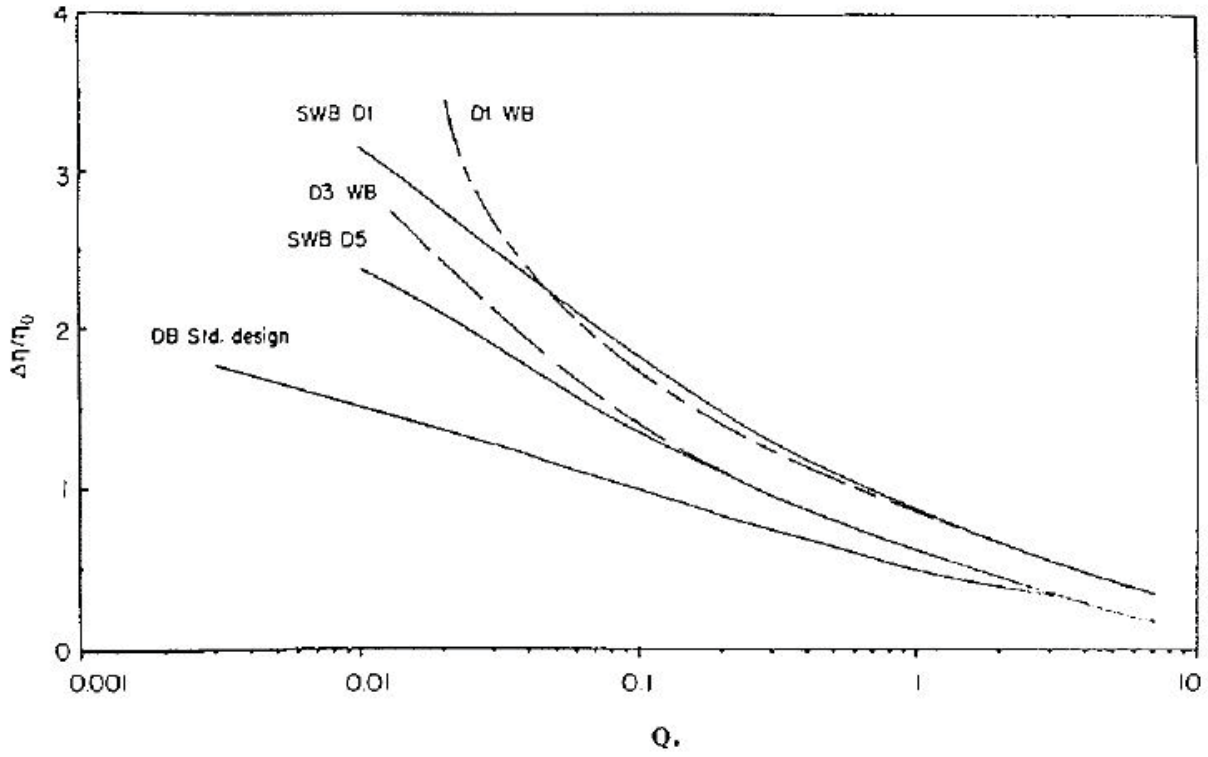

Figure 2.18: Variation in flow depth ($\frac{\Delta\eta}{\eta}$) versus dimensionless discharge (Q_*) (Rajaratnam and Katopodis, 1990).

It is worthy to note that the primary objectives of Rajaratnam et al. (1989) and Rajaratnam and Katopodis (1990) were focused on assessing the hydraulic characteristics of the baffle designs for fish passage and not necessarily for determining hydraulic capacity. Equation 2.21 was evaluated for values of Q_* producing relative depths (y_o/D) for the most part less than 0.6 and therefore greatly less than the culvert's full flow design capacity. Direct conclusions about the effects of baffles on the outlet control hydraulic capacity (e.g., Manning's n or Darcy friction factors) were not made and cannot be extracted from the data published by Rajaratnam et al. (1989) and Rajaratnam and Katopodis (1990), since this data was obtained for partially full flow. However, the findings of Rajaratnam et al. (1989, 1990), specifically their published discharge and depth data, can be used to back calculate the configurations open channel Manning's roughness coeffcients. Despite the fact that Rajaratnam et al. (1989) and Rajaratnam and Katopodis (1990) findings were from open channel flow experiments, calculated roughness findings may prove beneficial to compare with the present study's experimental roughness results. This subject is treated in further detail later in chapter 4.

2.5.5 Inlet and Outlet coefficients

A study performed by Tullis and Anderson (2010) investigated the effects of various inlet end treatments on the hydraulic capacity of slipline culverts. Specifically, the authors determined the effects of several inlet end treatments on the loss coefficient (k_e) and the inlet control head-discharge relationship. The experimental study consisted of a laboratory model of a 12" (0.604 m) slipline pipe constructed from a smooth walled PVC 12" (0.604 m) inside diameter pipe fitted inside a larger diameter PVC pipe. The annular space was grouted and four different inlet end treatments composed of two pipe projection/diameter ratios (P/D = 0.17 and 0.34) and two tapered pipe projection/diameter ratios (P/D = 0.17 and 0.34) were applied and tested separately. The authors published results of the obtained k_e values (Fig. 2.19) for the four inlet end treatments and also a head-discharge relation under inlet control. The results indicate that k_e increases up to $H_w/D = 1.3$; greater depths decrease k_e, until the values begin to plateau near H_w/D = 2.5, where H_w is the headwater level upstream of the test pipe. The results also indicate much lower k_e values for the tapered inlet treatments. These findings are of great importance to slipline culvert designers interested in reducing the overall losses incurred in their design. Installing an appropriate inlet treatment would have a positive effect

on the hydraulic capacity, and could prove especially useful for slipline culverts equipped with baffles. The inlet treatment may in some cases prove to sufficiently offset the additional losses introduced by the baffle roughness. This is an avenue of research explored further in detail in chapter 4.

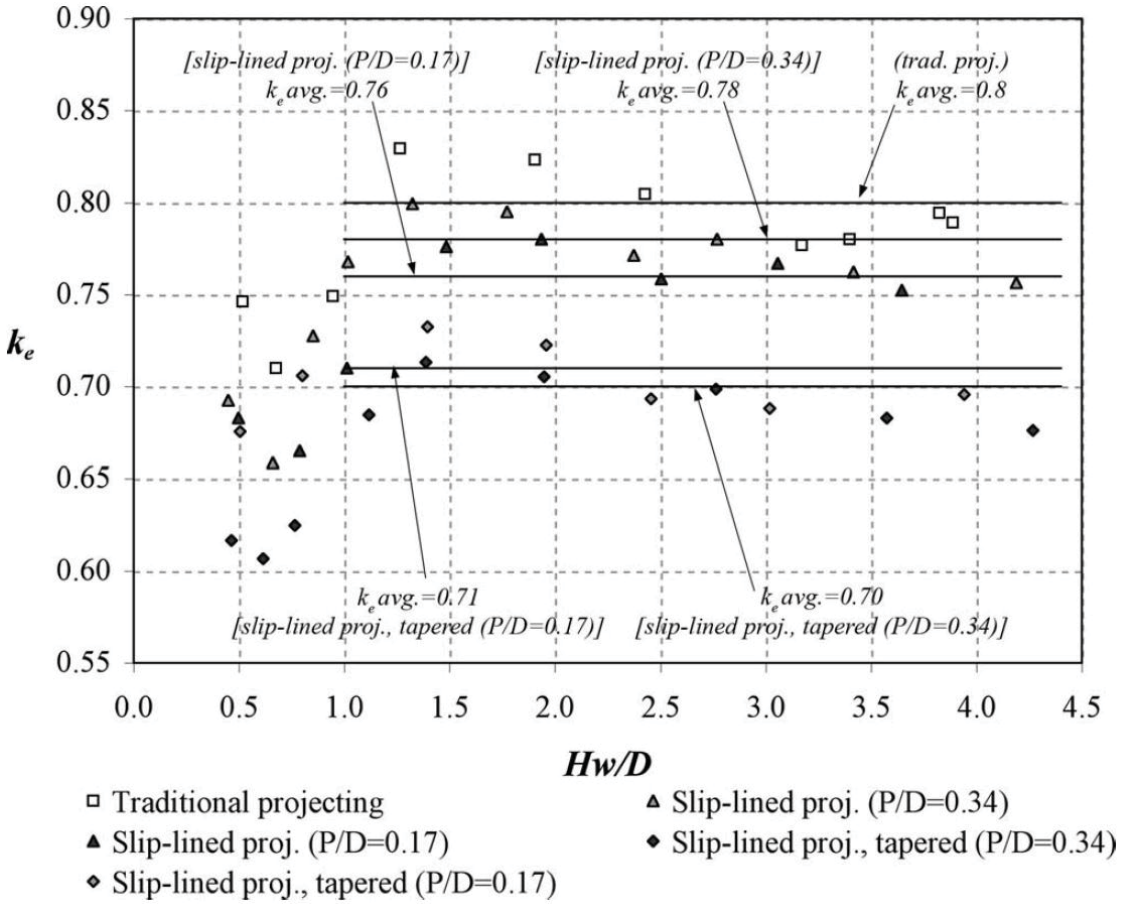

Figure 2.19: Entrance loss coefficients as a function of (H_w/D) under outlet control conditions (Tullis and Anderson, 2010).

Tullis et al. (2008), investigated the errors associated with using a k_o=1 in Eq. 2.12, a common practice recommended in HDS-5, and also with using the Borda-Carnot method (Eq. 2.22) for determining k_o for predicting experimental determined exit loss values. The experimental details of the five runs they performed are presented in Table 2.10 and the errors associated with the HDS-5 and Borda-Carnot method are presented in Table 2.11.

$$h_{out} = k_o \frac{V^2}{2g},\ k_o = \left(1 - \frac{A_p}{A_c}\right)^2 \tag{2.22}$$

Where:

A_p = Pipe area (m^2)
A_c = downstream channel area (m^2)

Tullis et al. (2008) determined that using the Borda-Carnot method (Eq. 2.22) for estimating the k_o significantly improved the prediction of energy losses incurred at the outlet of a culvert compared to assuming a k_o=1 (as recommended in the HDS-5) or using Eq. 2.12 with a known downstream velocity (V_2). The prediction of outlet barrel losses for an submerged outlet with the Borda-Carnot method was only 6.2% superior to the experimentally determined value. In contrast the assumption of k_o=1 overestimated exit losses by 187%. The findings of Tullis et al. (2008) may be of particular interest to culvert designers looking for methods to improve their predictions of discharge through baffled HDPE slipliners.

Table 2.10: Exit loss test conditions and data from Tullis et al. (2008).

Run No.	D (m)	Pipe exit condition	R pipe	F pipe	Δz (m)	Percent full pipe (%)	Tw/D	A_c/A_p	Experimental exit loss (m)
1	0.3	Submerged	722,450	—	0.77	100	1.99	45.9	0.360
2	0.61	Submerged	651,033	—	0.65	100	1.26	12.4	0.128
3	0.61	Unsubmerged	827,299	0.97	0.65	69	0.75	13.2	0.143
4	1.22	Unsubmerged	1,304,322	0.72	0.36	53	0.57	4.1	0.079
5	1.52	Unsubmerged	2,104,402	0.52	0.22	64	0.68	2.5	0.040

After having experimentally determined k_o, Tullis et al., 2008 concluded that the Borda-Carnot method for calculating the outlet loss coefficient k_o is a more accurate method than assuming $k_o = 1$. This can be observed by comparing the theoretically determined k_o values with the experimentally determined k_o values presented in Table 2.11.

Table 2.11: Experimental and theoretical exit loss coefficient comparison Tullis et al. (2008).

Run	K_0 exp.	K_0 theor.	Percent error (%)
Eq. (1)			
1	0.93	1.00	7.3
2	0.88	1.00	13.9
3	0.84	1.00	18.9
4	0.63	1.00	60.0
5	0.41	1.00	143.1
Eq. (2)			
1	0.93	1.00	7.3
2	0.87	1.00	14.6
3	0.84	1.00	19.6
4	0.60	1.00	69.9
5	0.35	1.00	187.3
Eq. (4)			
1	0.93	0.96	2.7
2	0.87	0.85	3.1
3	0.84	0.85	2.2
4	0.60	0.58	2.2
5	0.35	0.37	6.2

2.6 Flow regime

Flow over baffles will develop one of three possible flow regimes: isolated roughness flow, wake-interference flow or quasi-smooth flow (sometimes skimming flow) depending on the baffle spacing (λ) used. Isolated roughness flow occurs when the wake zone developed behind a baffle is fully dispersed before reaching the next downstream baffle. In this situation the baffles act as isolated roughness elements hence the term *isolated roughness flow*. Wake-interference flow occurs when the baffles are spaced sufficiently close so that the dispersion of the wake zones shedding from a baffle are interrupted by the next downstream baffle. The third and final flow type, quasi-smooth flow occurs when baffles are closely spaced enough so that the majority of the flow skims above the roughness crests leaving spinning vortices in the interbaffle region. Figure 2.20 demonstrates the three flow types.

Morris (1955) demonstrated that f is dependent on Reynold's number (**R**) and the predominant flow regime. Isolated roughness and quasi-smooth flow develop descending f-**R** curves

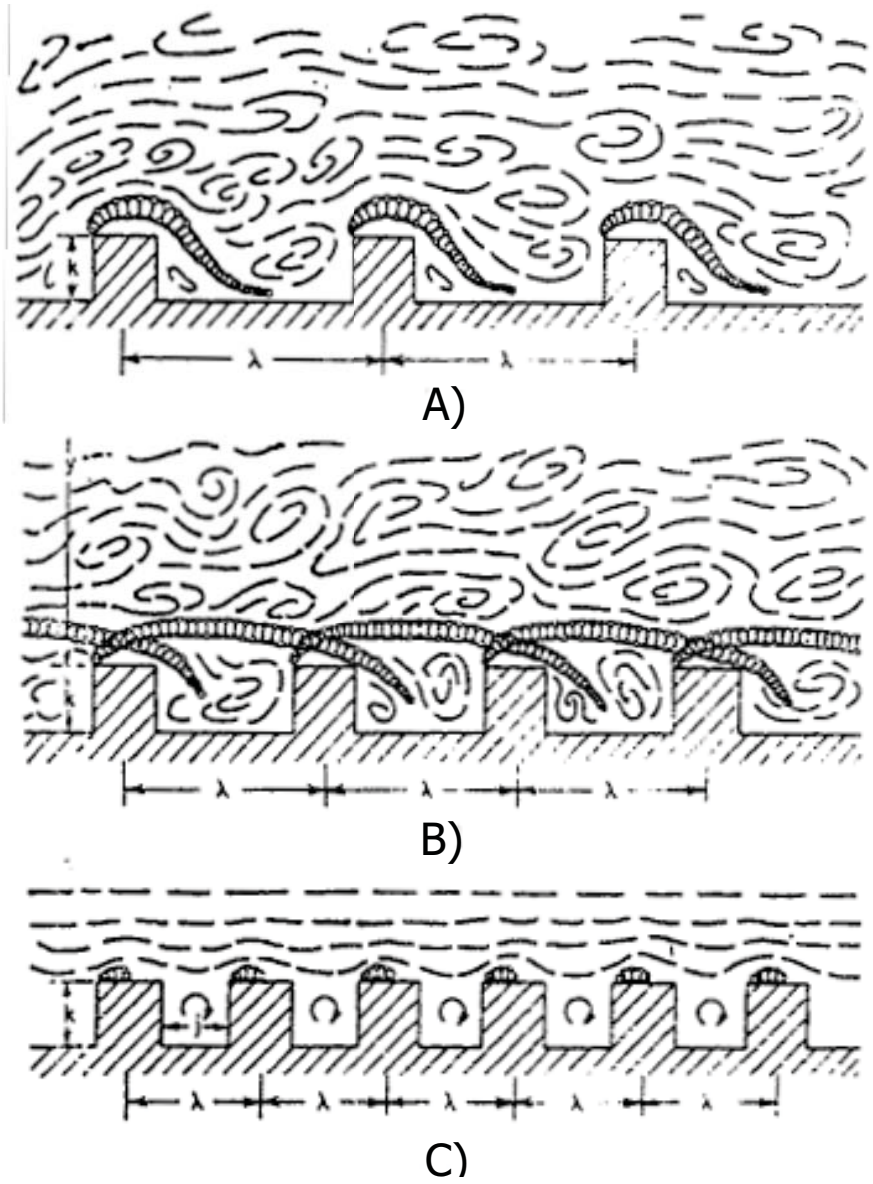

Figure 2.20: Sketch of the three principle flow types : (a) isolated roughness flow, (b) wake-interference flow, (c) quasi-smooth flow (unidentifiable source).

whereas wake-interference flow is characterized by a rising f-**R** curve. At a sufficiently high **R** number, f will attain a constant value for each of these three flow regimes. When this occurs it is said that f is demonstrating Reynold's independence. Early work by Straub and Morris (1951) on corrugated steel pipes produced increasing f-**R** curves. The corrugations on the pipe act as roughness elements which alter the near wall flow. Baffles, can be thought of as roughness elements, not unlike those used in works reviewed by Morris (1955) and consequently much of the theory he presented can be applied to understanding the relationship of f-**R** in baffled HDPE slipliners.

The importance of studying roughness **R** dependence over roughness elements lies in the fact that f-**R** curves rise for wake interference flow. Thus, baffle configurations studied at moderate Reynold's numbers (somewhat objective, yet for the purpose of this thesis **R** values < than 5E5 will be considered moderate) need to rule out wake interference flow as a possibility. Both isolated roughness and skimming flow f-**R** curves show descending trends, and therefore experimentally determined values from flows exhibiting these two flow regimes will be more conservative than those obtained from a wake interference flow regime. The interested reader is directed towards Morris (1955) for detailed derivations of equations for use in determining friction losses over roughness elements establishing either of the three flow regimes presented above. The Fig. 2.21 shows the roughness data obtained by Straub and Morris (1951) from their work on corrugated steel culverts. A clear ascending trend of f with **R** can be seen.

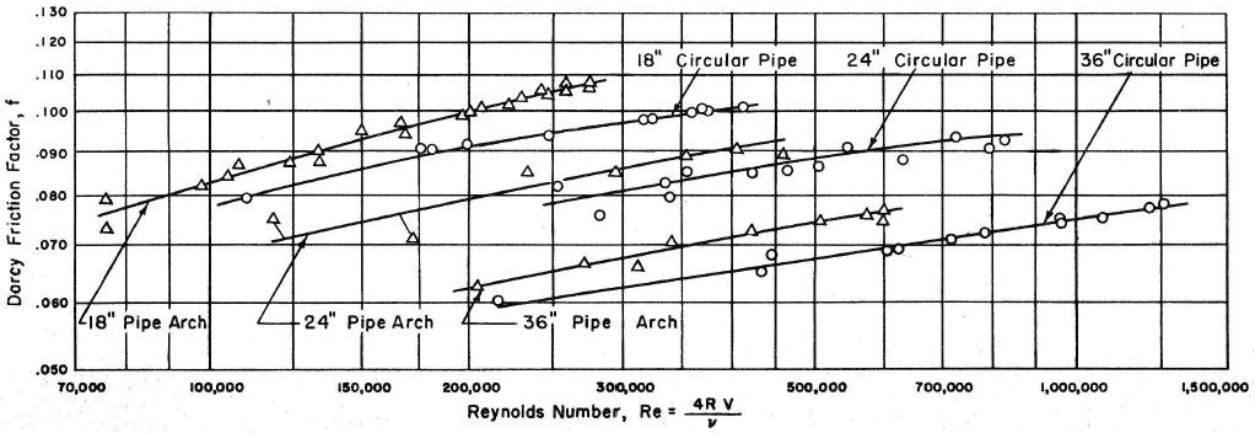

Figure 2.21: Variation of friction factor with Reynolds number for full flowing corrugated steel pipes (Straub and Morris, 1951).

Olsen and Tullis (2013) published f-**R** data for a single trial of their friction loss tests on a

baffled HDPE culvert. Figure 2.22 presents the clear descending trend of f versus **R** established by their experimental data. Olsen and Tullis (2013) tested a 0.6D spacing 0.15D high weir baffle. The descending character of their roughness curve suggests isolated roughness flow. It is doubtful that the baffles, with a 0.6D spacing, were close enough from one and other to establish a skimming flow regime. Olsen and Tullis (2013) findings will prove useful for comparative purposes during the discussion of the experimentally determined roughness findings from this study.

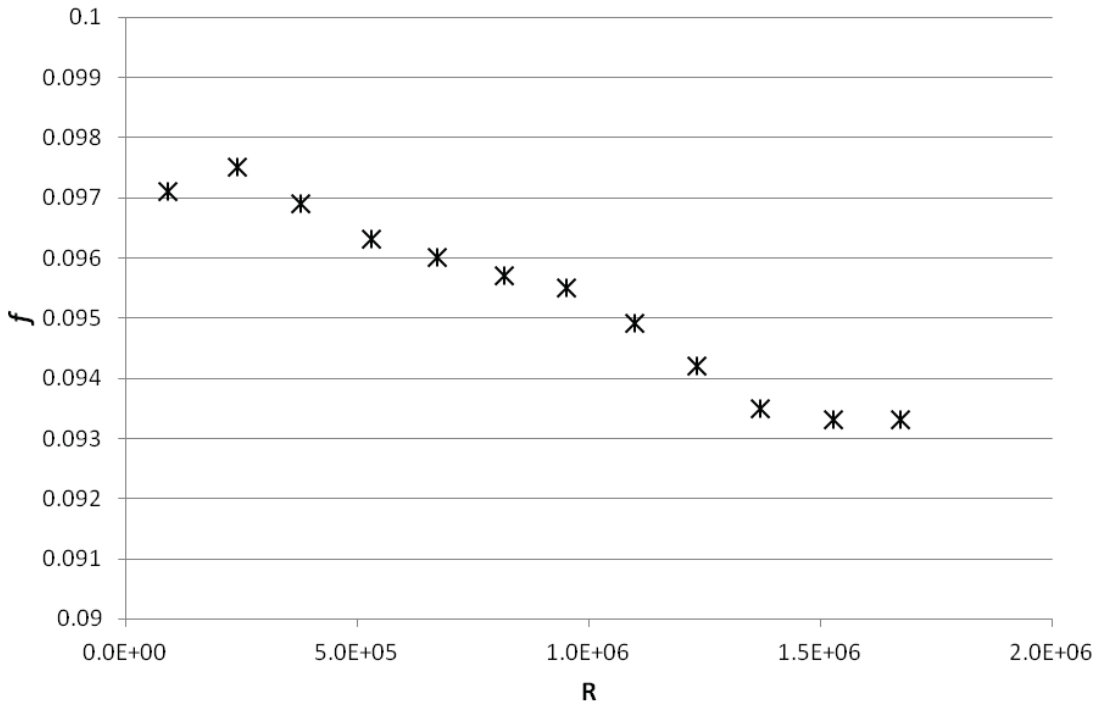

Figure 2.22: Variation of the friction factor with increasing Reynold's number for full flow over a weir baffle configuration (Olsen and Tullis, 2013).

Chapter 3

Effects of Sliplining on Depth and Velocity

3.1 Introduction

The passage from a larger diameter rough walled corrugated steel culvert to a smaller diameter smooth walled HDPE slipliner insert has consequences on the mean flow depth and velocities through which fish are required to navigate. The loss in flow depth and the increase in velocity can pose substantial barriers to fish movements. The extent to which these two flow parameters vary after HDPE sliplining has received little attention from the research community. Consequently, a simple analytical study employing Manning's open channel flow equation would be beneficial to estimate the extents to which HDPE slipliners influence depths and velocities. It is common to use Manning's uniform open channel flow equation to predict normal depth and velocities in culverts; however, the use of Manning's formula assumes a constant Manning's coefficient (n). Yet, a number of studies have shown that n varies with depth in corrugated steel and HDPE culverts as was shown in chapter 2 (e.g., 2.9 and 2.11). The variable nature of n with depth raises the question: Which values of n should be used for both the parent (usually corrugated steel) and HDPE slipliner culvert to accurately estimate the change in y and V? The variant nature of n introduces the possibility for substantial error in the estimation of depths and velocities in culverts for fish passage design purposes.

An answer to this last question would be to determine the minimum and maximum values of n for corrugated steel and HDPE and then use these values in an analytical study employing Manning's equation to estimate the possible range of variation of y and V. The literature review in chapter 2 synthesized roughness data from multiple sources which can be used to assess the extents of the roughness range for corrugated steel and HDPE culverts. However, obtaining an accurate range of roughness variation solves only half the puzzle. The choice of the appropriate combination of minimum and maximum values to be used in the analysis still needs consideration. Should the *minimum* roughness coefficient for the corrugated steel culvert be analyzed with the *minimum* roughness coefficient for the HDPE culvert? Or should *maximum* and *maximum* be analyzed together? One option is to use the *maximum* roughness value for corrugated steel to calculate depth in the parent culvert and then use the *minimum* roughness value for the HDPE culvert to calculate the depth in the slipline culvert. Comparing the depth change between the parent culvert and the HDPE culvert for this *maximum-minimum* pairing will result in the most conservative estimate, or in other words, the worst case scenario

which presents the largest decrease in depth and greatest increase in velocity. In contrast, a *minimum-minimum* or a *maximum-maximum* pairing will result in less drastic variations in depth and velocity, which may or may not be representative of reality. Yet another possibility is to analyze the *average-average* pairing and give the *average-minimum* pairing as the worse case scenario (for fish passage) and the *average-maximum* pairing as the best case scenario. This last option is retained for the purposes of this chapter. Comments on the *maximum-minimum* paring will also be discussed. It should be noted that no clear answer to the question of how much y and V are affected by HDPE sliplining is possible due to the variant nature of Manning's roughness with depth. Rather, the best approach is to propose an estimated range of variation and this is the motivation behind the work presented in the following pages.

3.2 Methodology

3.2.1 Theory

A typical cross section of a partially full pipe is presented by Fig. 3.1. The area (A) of flow in a partially filled culvert is a function of the radius (r) and the angle (θ in radians) between the centerline of the pipe and a line drawn from the center of the circle to the union of the free surface and the culvert wall. A θ of π indicates a culvert flowing half full whereas a θ of 2π would be a culvert flowing full.

Equation 3.1 is Manning relation used to determine the flow rate in open channel flow, where (R_h) is the hydraulic radius and (S_o) is the slope of the culvert. The area occupied by a given flow depth in a circular culvert is given by Eq. 3.2.

$$Q = \frac{1}{n} A R_h^{2/3} S_o^{1/2} \tag{3.1}$$

$$A = r^2 \left(\theta - \frac{sin(2\theta)}{2} \right) \tag{3.2}$$

The wetted perimeter (P) of a partially full pipe is given by Eq. 3.3 and the hydraulic radius (R_h) is then expressed by Eq. 3.4.

$$P = 2r\theta \tag{3.3}$$

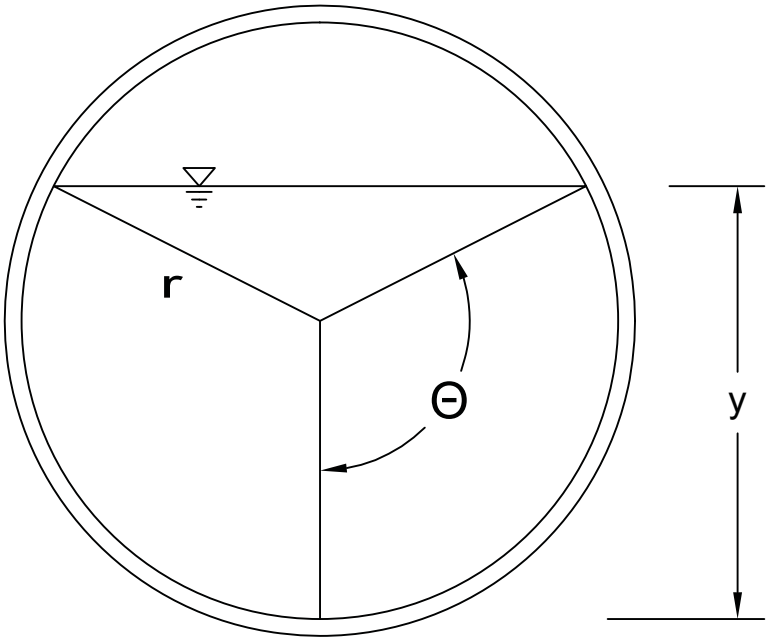

Figure 3.1: Schematic of y as a function of r and Θ.

$$R_h = \frac{r}{2}\left(1 - \frac{sin(2\theta)}{2\theta}\right) \tag{3.4}$$

The average velocity (V_o) over a cross section of the pipe can then be determined by applying Eq. 3.5. Once the average velocity is found, the flow rate (Q) can be resolved by multiplying V_o by the area as presented in Eq. 3.6.

$$V_o \cong \frac{\alpha}{n}\left[\frac{r}{2}\left(1 - \frac{sin(2\theta)}{2\theta}\right)\right]^{2/3} S_o^{1/2} \tag{3.5}$$

$$Q = V_o r^2 \left(\theta - \frac{sin(2\theta)}{2}\right) \tag{3.6}$$

The difficulty of using Eqs. 3.5 and 3.6 to determine V and y is that θ is unknown (and consequently neither is the normal flow depth, y). In order to use Manning's formula to evaluate the variation of velocity and flow depth when passing from a corrugated steel culvert to a smooth HPDE culvert, a value of y/D must be selected in the corrugated steel culvert (y/D is a function of θ which can be determined from trigonometry). Once θ is determined in can then be applied in Eqs. 3.5 and 3.6 to determine the corresponding Q. This flow rate is then applied

to the slipliner, however, Eq. 3.6 must be solved iteratively for θ to yield the resulting y_i/D_i and V_i for Q in the slipliner.

3.2.2 Testing

After examining the results of the literature review in chapter 2 it was decided that two roughness values for the CSP would be tested: an average value of $n = 0.024$ and a maximum value of $n = 0.028$. The average roughness value of 0.024 was used since the mean of all the values in Fig. 2.10 was very near 0.024 and also because most references suggests the use of 0.024 for use in the hydraulic calculations implicating corrugated steel culverts. The maximum value of 0.028 corresponds to the highest values in Fig. 2.10 were sufficient data is available. Higher roughness values are likely (i.e., 0.034) for very low relative depths, however it was judged that an accurate estimate of roughness at those depths was impossible due to insufficient roughness data at these low relative depths. An accurate minimum n value was also impossible to obtain since the literature review failed to demonstrate valid n values lower than 0.024 and therefore lower values of n in corrugated steel will not be considered.

The parent culvert was given a diameter of 0.671 m and only a single radial reduction of 10% was used when simulating the change in pipe radius due to the slipliner process. The radial reduction that occurs during the sliplining process will influence depths and velocities to a certain degree. However, after preliminary study, this effect was found to be minimal and are discussed in further detail in section 3.4.3 below. Therefore, for the purpose of this study only the single radial reduction was retained.

A total of six scenarios were tested and are summarized in Table 3.1. Scenarios 1, 2 and 3 correspond to y/D values of 0.1, 0.2 and 0.3 respectively in a CSP with the average n value of 0.024. Scenarios 4, 5 and 6, on the other hand, also correspond to y/D values of 0.1, 0.2 and 0.3 in a CSP, however with the maximum n value of 0.028. Each of the six scenarios were tested for three slopes (0.001, 0.005 and 0.02) and a mimimum ($n = 0.004$), average ($n = 0.009$) and maximum ($n = 0.012$) roughness estimate for the HDPE slipliner pipe. This range of roughness was taken from the work of the various authors presented previously in chapter 2. From the work of Devkota et al. (2012) the minimum n value was taken to be 0.004 ($n/n_f \cong 0.4$) and the maximum n value was determined to be 0.012. It is true that Devkota et al. (2012) did demonstrate roughness values somewhat lower than 0.004, however a large group

of data clusters near 0.004 (Fig. 2.11) and this is believed to provide a more reliable minimum value for n. Olsen's values suggest a higher maximum n being closer to 0.014, however, this point may be considered an outlier and a more realistic maximum would be 0.012 as shown in Devkota et al. (2012). A value of 0.009 was taken as the average roughness for the HDPE culvert since this is generally considered to be the design roughness for full flowing HDPE pipe (Devkota et al., 2012,Olsen and Tullis, 2013 and ISCO, 2013).

Table 3.1: Assumed Manning's roughnesses and y/D values in the CSP for the six tested scenarios.

Scenario #	*y/D in CSP*	*n value of CSP*
1	0.1	0.024
2	0.2	0.024
3	0.3	0.024
4	0.1	0.028
5	0.2	0.028
6	0.3	0.028

The analysis will be performed on the *average-average* pairing as well as the *average-minimum* and the *average-maximum* to gauge the effect of HDPE sliplining on y and V as was discussed in the introduction of this chapter. The possible influence of a higher maximum n value for the corrugated steel (e.g., $n = 0.034$) calculated from the raw depth and discharge data of Richmond et al. (2007) is briefly discussed in the conclusions below.

The theory detailed above (subsection 3.2.1) was used to solve for the flow rates corresponding to the six scenarios in a 0.671 m corrugated steel pipe culvert (CSP) for each of the three slopes. The resulting flow rates were then used to determine the flow depths and corresponding velocities that would theoretically be developed in a HDPE slipliner culvert at each of the three Manning's roughnesses (minimum = 0.004, average = 0.009 and maximum = 0.012).

3.3 Results

The flow rates required to develop the respective relative depths in the corrugated steel culverts are presented in Tables 3.3 (scenarios 1, 2 and 3) and 3.3 (scenarios 4, 5, and 6). The largest flow rate of 0.124 m^3/s was found for a y/D of 0.3 at a slope of 0.02. A very small flow rate of 0.0029 m^3/s was determined for the y/D condition of 0.1 at a slope of 0.001. The flow rates are higher for scenarios 1, 2 and 3 compared to those of scenarios 4, 5 and 6 because the

lower n value of the CSP for scenarios 1, 2 and 3 requires increased flow to develop the fixed values of y/D (0.1, 0.2 and 0.3).

Table 3.2: Velocities, depth, flow rate and Froude number developed for scenarios 1, 2 and 3 (n=0.024).

Scenario #	*S*	V (m/s)	y (m)	*Q (m^3/s)*	*Froude Number*
1	0.001	0.1608	0.067	0.003	0.198
	0.005	0.3595	0.067	0.007	0.443
	0.02	0.7191	0.067	0.013	0.887
2	0.001	0.246	0.134	0.012	0.215
	0.005	0.5512	0.134	0.028	0.481
	0.02	1.1024	0.134	0.056	0.962
3	0.001	0.311	0.201	0.028	0.221
	0.005	0.6956	0.201	0.062	0.495
	0.02	1.3912	0.201	0.124	0.991

Table 3.3: Velocities, depth, flow rate and Froude number developed for scenarios 4, 5 and 6 (textitn=0.028).

Scenario #	*S*	V (m/s)	y (m)	*Q (m^3/s)*	*Froude Number*
4	0.001	0.1378	0.067	0.003	0.170
	0.005	0.3082	0.067	0.006	0.380
	0.02	0.6163	0.067	0.011	0.760
5	0.001	0.211	0.134	0.011	0.184
	0.005	0.4724	0.134	0.024	0.412
	0.02	0.9449	0.134	0.048	0.824
6	0.001	0.266	0.201	0.024	0.189
	0.005	0.596	0.201	0.053	0.424
	0.02	1.192	0.201	0.106	0.849

The resulting depths and velocities after sliplining with an HDPE pipe (with a 10% reduction in diameter) are presented in Tables 3.4 and 3.5. Velocities are seen to vary between the range of 0.265 m/s to 5 m/s.

The velocity (C_v) and depth (C_y) change coefficients presented in Tables 3.6 and 3.7 were obtained by dividing the velocity v (or depth y) in the HDPE culvert by the velocity V_o (or depth y_o) in the corrugated steel culvert corresponding to the same slope and y/D value. The coefficients represent the factor by which velocity and depth have changed and provide a convenient fashion to compare the results of the scenarios.

Table 3.4: Velocities (V) and depths (y) produced in the HDPE slipliner culvert for scenarios 1, 2 and 3 at the three Manning's roughness values studied (low = 0.004, average = 0.009 and high = 0.012) with a radial reduction of $\beta = 10\%$.

Scenario #	*S*	V (m/s)			y (m)			Froude Number		
		n=0.004	n = 0.009	n = 0.012	n=0.004	n = 0.009	n = 0.012	n=0.004	n = 0.009	n = 0.012
1	0.001	0.569	0.324	0.265	0.030	0.043	0.050	1.048	0.498	0.378
	0.005	1.272	0.724	0.592	0.030	0.043	0.050	2.344	1.114	0.845
	0.020	2.543	1.447	1.184	0.030	0.043	0.050	4.688	2.227	1.690
2	0.001	0.878	0.498	0.407	0.058	0.086	0.099	1.165	0.542	0.413
	0.005	1.965	1.114	0.910	0.058	0.086	0.099	2.605	1.213	0.923
	0.020	3.929	2.228	1.820	0.058	0.086	0.099	5.209	2.425	1.847
3	0.001	1.119	0.632	0.515	0.086	0.127	0.147	1.218	0.566	0.429
	0.005	2.501	1.413	1.152	0.086	0.127	0.147	2.723	1.266	0.959
	0.020	5.003	2.826	2.305	0.086	0.127	0.147	5.447	2.532	1.919

Table 3.5: Velocities (V) and depths (y) produced in the HDPE slipliner culvert for scenarios 4, 5 and 6 at the three Manning's roughness values studied (low = 0.004, average = 0.009 and high = 0.012) with a radial reduction of $\beta = 10\%$.

Scenario #	*S*	V (m/s)			y (m)			Froude Number		
		n=0.004	n = 0.009	n = 0.012	n=0.004	n = 0.009	n = 0.012	n=0.004	n = 0.009	n = 0.012
4	0.001	0.543	0.309	0.252	0.028	0.040	0.046	1.044	0.491	0.375
	0.005	1.213	0.690	0.565	0.028	0.040	0.046	2.333	1.102	0.840
	0.020	2.427	1.380	1.130	0.028	0.040	0.046	4.667	2.195	1.680
5	0.001	0.839	0.476	0.389	0.054	0.080	0.092	1.151	0.538	0.410
	0.005	1.875	1.064	0.869	0.054	0.080	0.092	2.574	1.201	0.917
	0.020	3.751	2.127	1.738	0.054	0.080	0.092	5.148	2.406	1.834
6	0.001	1.068	0.604	0.493	0.079	0.118	0.136	1.210	0.562	0.427
	0.005	2.389	1.351	1.102	0.079	0.118	0.136	2.707	1.256	0.954
	0.020	4.778	2.701	2.203	0.079	0.118	0.136	5.413	2.512	1.908

$$V = C_v V_o \tag{3.7}$$

$$y = C_y y_o \tag{3.8}$$

Table 3.6: Velocity (C_v) and depth (C_y) change coefficients determined for the passage from a CSP to an HDPE slipliner pipe for scenarios 1, 2 and 3.

Scenario #	*S*	C_v			C_y		
		n=0.004	n = 0.009	n = 0.012	n=0.004	n = 0.009	n = 0.012
	0.001	3.54	2.01	1.65	0.448	0.642	0.746
1	0.005	3.54	2.01	1.65	0.448	0.642	0.746
	0.02	3.54	2.01	1.65	0.448	0.642	0.746
	0.001	3.57	2.02	1.65	0.433	0.642	0.739
2	0.005	3.56	2.02	1.65	0.433	0.642	0.739
	0.02	3.56	2.02	1.65	0.433	0.642	0.739
	0.001	3.60	2.03	1.66	0.428	0.632	0.731
3	0.005	3.60	2.03	1.66	0.428	0.632	0.731
	0.02	3.60	2.03	1.66	0.428	0.632	0.731

Table 3.7: Velocity (C_v) and depth (C_y) change coefficients determined for the passage from a CSP to an HDPE slipliner pipe for scenarios 4, 5 and 6.

Scenario #	*S*	C_v			C_y		
		n=0.004	n = 0.009	n = 0.012	n=0.004	n = 0.009	n = 0.012
	0.001	3.94	2.24	1.83	0.411	0.602	0.688
4	0.005	3.94	2.24	1.83	0.411	0.597	0.688
	0.02	3.94	2.24	1.83	0.411	0.602	0.688
	0.001	3.97	2.25	1.84	0.404	0.595	0.683
5	0.005	3.97	2.25	1.84	0.404	0.597	0.683
	0.02	3.97	2.25	1.84	0.404	0.595	0.683
	0.001	4.02	2.27	1.85	0.395	0.587	0.676
6	0.005	4.01	2.27	1.85	0.395	0.587	0.676
	0.02	4.01	2.27	1.85	0.395	0.587	0.676

3.4 Analysis and discussion

3.4.1 Effect on velocity and depth

From Tables 3.6 and 3.7 it can be observed that the average cross-sectional velocities vary drastically between the three Manning's roughness coefficients used for the HDPE culvert. When an n value of 0.004 is assumed for the HDPE culvert and a n of 0.024 for the CSP, velocity increases by a factor (C_v) of between 3.54 and 3.60 (scenarios 1, 2 and 3) compared to the original depth in the CSP. The C_v values increase slightly when the n of the CSP is assumed to be 0.028 (scenarios 4, 5 and 6), varying between 3.94 and 4.01. These values indicate that the velocity is a factor of C_v higher than the velocity in the CSP. A C_v of 1 indicates no variation from the velocity in the CSP.

When the average value of $n = 0.009$ is assumed for the HDPE pipe, velocity increases by

a factor of approximately 2 for scenarios 1, 2 and 3 and by approximately 2.25 for scenarios 4, 5 ad 6. A HDPE n value of (0.012) causes velocities to increase by a factor of approximately 1.65 for the first three scenarios and by approximately 1.84 for the last three scenarios. The high variation in velocity with the chosen Manning's roughness coefficient for the HDPE culvert demonstrates that large errors in predicted velocities are possible if n values are not appropriately chosen. Also the significant increase in C_v factors between the first three (CSP $n = 0.024$) and last three scenarios (CSP $n = 0.028$) suggests that a prudent choice for the n value of the parent CSP culvert is required.

The variability of the CSP and HDPE roughnesses can introduce unexpected errors while identifying whether or not fish passage barriers may develop for a given sliplining project. To illustrate, from the results for scenarios 1, 2 and 3 it can be concluded that the use of $n = 0.009$ overestimates the velocity by a factor of approximately 0.37 (or 37%) if in fact the HDPE slipliner has a true n value of 0.012. For scenarios 4, 5 and 6 this error increases to 51%. Similarly, from the results for scenarios 1, 2 and 3, assuming $n = 0.009$ underestimates the velocity by a factor of 1.65 (or 165%) if in fact the true n value of the HDPE slipliner was 0.004, or by approximately 174% for scenarios 4, 5 and 6. These values were obtained by averaging the difference between the C_v coefficients for n in Tables 3.6 and 3.7.

The effect of sliplining on flow depth presents the opposite pattern to the one presented above for velocity. When an n value of 0.004 is assumed for the HDPE culvert in the first three scenarios, the (C_y) is approximately 0.448 (or a 55.2% decrease), for $n = 0.009$ depths reduce by a factor of 0.642 (or a 35.8% decrease) and for $n = 0.012$ depth reduces by a factor of 0.746 (or a 25.4% decrease). For the scenarios 4, 5 and 6 the respective decreases in depth are 59%, 41% and 32%.

If an n value of 0.009 is assumed for the HDPE culvert for the first three scenarios, but in fact the true value is 0.012, depth will be underestimated by approximately 10%, or approximately 8% for the last three scenarios. If an n value of 0.009 is assumed for the HDPE culvert, but in fact the true value is 0.004, depth will be overestimated by approximately 20% for all six scenarios. These error estimates demonstrate that an incorrect choice of n value for the HDPE culvert can introduce significant error in the estimation of the depth in the HDPE culvert.

Slight increases in C_v and slight decreases in C_y are observed with increasing values of y/D imposed on the CSP (see Tables 3.6 and 3.7). These slight variations stem from the fact that

depths vary more rapidly at low relative depths (e.g., $y/D = 0.1$) than at higher relative depths (e.g., $y/D = 0.3$). This is purely due to the circular geometry of the culvert since available flow area is not a linear function of flow depth. Therefore, flow rates developing a low relative depth in the corrugated steel culvert (e.g., $y/D = 0.1$) will demonstrate a slightly greater variation in depth after sliplining than for flows developing a higher relative depth in the corrugated steel culvert (e.g., $y/D = 0.3$). In a similar fashion, the average cross sectional velocities also vary more rapidly at lower relative depths. However, the effect of the geometry of the culvert on velocity and depth are very small and can likely be neglected.

3.4.2 Effect on the Froude number

The Froude number (Fr) can be used to determine whether a free surface flow is a shallow, fast supercritical flow (Fr > 1) or a relatively deeper and slower subcritical flow (Fr < 1). Since minimum velocities and maximum depths are preferred for fish passage, subcritical flows are desirable in culverts where fish passage is of concern. Sliplining increases the Froude number significantly, as can be seen by comparing the Froude numbers in the host CSP culvert 3.2 and 3.3 respectively with the Froude numbers in the HDPE slipline culvert 3.4 and 3.5. Increases in slope and decreases in the assumed roughness of the HDPE slipiner have a profound effect on Fr, which often times attains a value > 4.0. For the slope of 0.05% virtually all of the scenarios are supercritical after sliplining. Also, the assumption of an $n$value of 0.004 for the HDPE surface guarantees a supercritical flow at each of the three values of slope studied. The addition of baffles increases surface roughness, developing flow depths and decreasing average cross-sectional velocities which in turn help to promote the development of the subcritical normal depth along the culvert.

3.4.3 A word on radial reductions

There is a slight dependence of depth and velocity with increases in the radial reduction of the slipliner, however, the change is not very significant when the radial reduction is within reasonable limits (i.e., $\beta < 20\%$). To illustrate, for the mildest slope studied ($S = 0.001$) and the lowest relative depth imposed in the corrugated steel culvert ($y/D = 0.1$ similar to scenario 1) a radial reduction of 20% increases the flow depth in the slipliner culvert by 2% compared to the 10% condition, whereas velocity increases by only 3%. Similar variations are seen for the other slopes and y/D values studied. These very small increases in depth and velocity

demonstrate that radial reductions can be considered negligible.

3.5 Conclusion

The results of this brief analytical study demonstrate that velocities are expected to increase and depths are expected to decrease drastically before and after the sliplining procedure. Velocities are estimated to increase anywhere from 65% to 300% depending on the actual Manning's roughness of the HDPE slipliner and parent culvert. Depths are estimated to decrease anywhere from 25% to 60%, also depending on the actual roughness of the HDPE slipline and parent culvert. These are significant variations which have important negative effects on fish passage through the slipliner culvert.

Given the fact that there is a larger range of n values below 0.009 compared to the range of values above 0.009 as seen in Fig. 2.11, there is a greater probability that velocity will be underestimated and flow depth overestimated if the average n value of 0.009 is assumed. It is therefore suggested that a lower n value of 0.004 for the HDPE culvert and a value of 0.028 for the CSP be used to obtain the most conservative estimates of velocity and depth. For very low relative depths even higher values of n in the CSP may possibly occur (i.e., $n = 0.034$) as was seen in the data of Richmond et al. (2007). Such values would introduce even greater errors in the estimation of depth and velocity if the average n value of 0.024 was assumed for the parent CSP culvert. However, the lack of experimental roughness data at low relative depths in corrugated steel culverts makes it difficult to asses this error with certitude.

The findings of this study demonstrate the need for the installation of baffles (or suitable alternative) in HDPE culverts to decrease velocities and increase depths. In many cases failure to install baffles will result in excessive velocities posing barriers to fish movements. To illustrate with the scenarios studied here, CSP culverts rehabilitated with HDPE slipliners on slopes greater than 0.02 will likely produce average cross-sectional velocities with magnitudes larger than 4 m/s (see Tables. 3.4 and 3.5). Such elevated velocities would meet or surpass the burst-speed of a number of the fish species presented in Fig. 2.1, such as brown trout, cutthroat trout, whitefish and suckers. Consequently, rehabilitated culverts of excessive length would require fish to maintain burst-speeds for an extended period of time, therefore hindering their chances of ascending the entire culvert length. The installation of baffles is therefore a recommended practice for use in HDPE culverts. Further investigations into this field of study are warranted

in order to improve baffle designs for both the needs of fish passage and hydraulic capacity.

3.5.1 Future work

This study has raised a few research questions that merit further investigation. As previously mentioned in chapter 2, the focus by the industry on the full flow roughness of corrugated steel pipes has drawn considerable attention away from the partially full roughness of corrugated steel pipes. Therefore, a comprehensive study with the objective to fully understand the evolution of n/n_f at low relative depths is warranted. Furthermore, an experimental study carried out under controlled laboratory conditions to determine depths and velocities before and after sliplining a corrugated steel culvert with an HDPE culvert would be beneficial to validate the results of this analytical study. Finally, a formula that is independent of Manning's n, yet dependent on an easily measured geometrical parameter such as roughness height or corrugation height should be developed and tested in order to eliminate the error associated with the variant Manning's n. There is some work which has proceeded in this direction (Mangin, 2010); the interested reader is directed to this work for details), however, still much more refinement is necessary and different approaches to determining depth could be applied.

Chapter 4

The Effects of Fish Baffles on the Hydraulic Capacity of Slipline Rehabilitated Culverts

Avant-propos

Authors and affiliations:

Jason Duguay

Department of Civil Engineering, University of Sherbrooke, Quebec, Canada

Jay Lacey

Department of Civil Engineering, University of Sherbrooke, Quebec, Canada

Submission date: September 28, 2013

Journal: Journal of Hydraulic Engineering

Title: The Effect of Fish Baffles on the Hydraulic Capacity of Slipline Rehabilitated Culverts

Contribution to the thesis:

The following article resumes the experimental work that was performed to obtain roughness coefficients of various fish baffle configurations. A complete description of the experimental setup is included along with a presentation of the results and a subsequent analysis and discussion of the implications of the findings for culvert design.

Proof of Submission:

Proof of submission is given in Appendix B in the form of letter presenting the Journal of Hydraulic Engineering associate editor's comments.

Note:

Following the corrections recommended by the reviewers of the Journal of Hydraulic Engineering the article pending acceptation differs in some aspects to the article presented here.

Abstract:

The use of fish baffles in HDPE slipliners is growing in popularity to improve hydraulic conditions for fish passage, yet little is known on how baffles affect the outlet controlled discharge capacity of these types of culverts. To fill this gap in knowledge, roughness coefficients (Manning's h and friction factor f values) were experimentally determined for weir baffle, slotted weir baffle and spoiler baffle configurations at four baffle spacings ($\lambda = 0.6$D, 1.2D, 1.8D, 2.4D) and three baffle heights ($h = 0.15$D, 0.10D, 0.05D), where D is the nominal diameter of the culvert. Roughness height was found to be the determinant geometric parameter affecting hydraulic roughness. Roughness spacing is found to play a important secondary role. An analytical model was developed and analyzed to determine the effects of roughness reduction (α), radial reduction (β), barrel length (L) and inlet treatments (k_e) on the hydraulic capacity of corrugated steel culverts after being sliplined with baffled HDPE culverts. Results demonstrate that many HDPE slipliner culverts can house baffles with α values in the range of 0.5 to 0.9. Design recommendations for the use of baffles in short and long slipline culverts are discussed.

CE database subject headings: Culverts; Design; Fish Management; Hydraulic Roughness

Author Keywords: Culvert roughness, Baffled culverts, Culvert Rehabilitation, Fish Passage, Manning's roughness , Slip-lined HDPE culverts

4.1 Introduction

Culverts are often used to provide road crossings over ditches, streams and small rivers. Corrugated steel culverts installed under roadways during the past half a century are reaching the end of their lifespan and in many cases require immediate replacement or rehabilitative work. There exist many trenchless culvert rehabilitation technologies which may be applied to extend the life of failing culverts besides the conventional open cut/dig and replace method. A survey of twenty state transport departments in the United States concluded that sliplining is the most popular trenchless culvert rehabilitation technique followed secondly by cured in place linings and thirdly by invert repair techniques (Syachrani et al., 2010). In brief, the sliplining process requires light machinery and a small maintenance crew to insert an HDPE culvert inside a failing culvert. The insert culvert is held securely in place by filling the annular space created between the two culverts with sealing grout. HDPE slipliner installation is considerably less costly, quicker to perform, and poses much less inconvenience to the public compared to many other culvert rehabilitation and replacement methods (Thomas, 1990; Hollingshead and Tullis, 2009). With sliplining, the original design flow capacity for an outlet controlled parent culvert is thought to be generally respected since the slipliner's smooth interior surface (i.e., lower surface roughness) increases velocities, thus compensating for the loss in flow area caused by the reduction in interior diameter (Webb and Hotchkiss, 2009; Hollingshead and Tullis, 2009; Tullis et al., 2008).

Although sliplining presents numerous advantages over the traditional cut/dig and replace technique, it regrettably poses major disadvantages with regards to aquatic organism passage. Foremost, the smooth interior surface of the HDPE pipe is known to produce elevated barrel and outlet velocities (Olsen and Tullis, 2013; Devkota et al., 2012). Extensive reaches of increased velocity may present passage barriers for one or more fish species who must pass the culvert to continue their migration (Rayamajhi et al., 2012; Haro et al., 2004; Katopodis and Gervais, 2012). Moreover, supercritical flows are often developed over the smooth surface and flow depths fall lower than those required for fish to maintain an adequate level of respiratory and swimming capacity (Clay, 1995; Makrakis et al., 2012). High exit velocities may also increase scour hole depth downstream, possibly leading to an impassable perched culvert (Makrakis et al., 2012).

The installation of baffles is a promising solution to the aforementioned problems. Various configurations of baffles (explained in greater detail below) have long been used to: reduce average cross-sectional velocities, increase flow depths and develop a heterogeneous flow field favorable for fish passage in traditional culverts. Only fairly recently have they begun to be installed in slipline culverts. Despite their benefits for fish passage, the installation of baffles in outlet controlled slipline culverts

negates the advantage of the low hydraulic roughness of the HDPE walls.

If an HDPE slipline insert fitted with standard baffles is found not to respect the parent culvert's design discharge, one of the following three solutions will likely ensue: (I) the baffles will not be installed, (II) the baffles will be installed regardless of the increased risk to roadway overtopping or, (III) a new culvert designed with fish passage in mind will be constructed to replace the failing culvert. The first solution is the most economical and will likely respect the parent culvert's outlet control design discharge, however does little to promote fish passage. The second solution will provide for fish passage, yet at an increased risk to roadway overtopping and damage to infrastructure. The third solution, though ideal for fish passage and hydraulic conveyance, places substantial demands on what are likely already overextended road maintenance budgets. Society can benefit from the low costs associated with the use of HDPE culverts to rehabilitate failing culverts. However, currently little knowledge is available on how to best optimize baffle design for the case specific needs of both fish passage and adequate hydraulic conveyance for slipline rehabilitated culverts.

4.1.1 Baffles

Three main baffle types are commonly used by practitioners: a) slotted weir baffles (SWB), b) weir baffles (WB), and c) spoiler baffles (SPB) [Figs. 4.1(a), (b), (c)]. The SWB was first proposed by Rajaratnam et al. (1989) as a simpler alternative to more complex baffle designs. Two wedges of fixed roughness height, h (relative to culvert diameter, D) made of metal or other suitable material are installed laterally across the center line of the pipe separated by a gap of fixed width b [Fig. 4.1(a)]. Weir baffles resemble their SWB counterpart with the exception that they are made of one solid piece of material. The WB [Fig. 4.1(b)] was proposed by Rajaratnam and Katopodis (1990) as a less costly to install alternative to the SWB. In practice, both the SWB and WB are fitted along the invert of a culvert at fixed roughness spacing (λ) (relative to culvert D).

In their most simplistic form, spoiler baffles (SPB) consist of rows of cubes placed equidistantly along the invert of the culvert. Spoiler baffles provide great flexibility in their number of possible configurations as they can be grouped in alternating rows of two and three or any other similar combination as site specific constraints impose. Streamlined alternatives to the block form have also been proposed by Rajaratnam et al. (1991). A study performed by Macdonald and Davies (2007) showed that spoiler baffles improve fish passage (by nearly 10 fold) compared to a bare smooth surfaced concrete culvert. The authors also demonstrated that fish passage success rates improve with increased spoiler baffle arrangement complexity (i.e., number of baffles per row and by fashions of staggering the baffles). Furthermore, Macdonald and Davies (2007) suggested that scaling baffle height to fish size, rather than

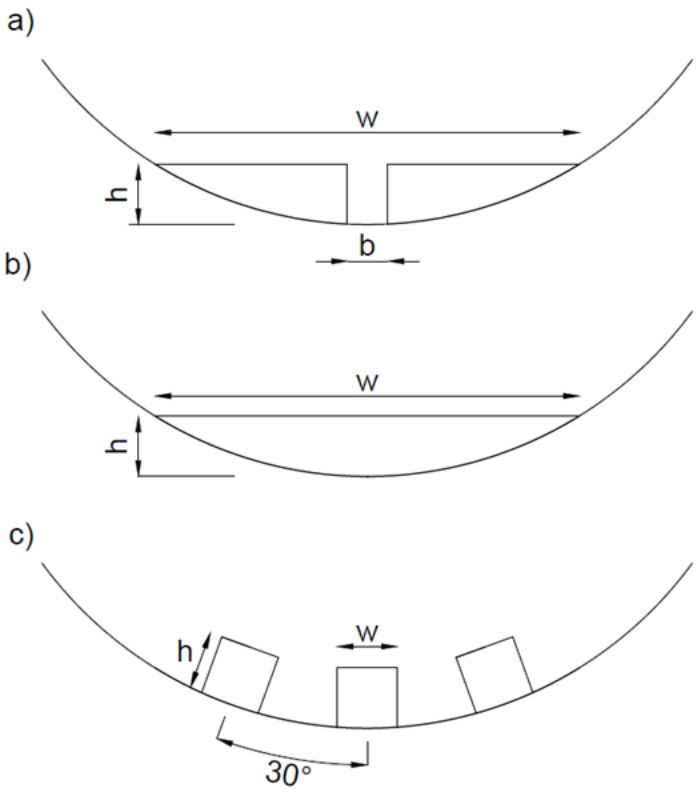

Figure 4.1: Baffle forms: a) slotted-weir baffle (WB), b) weir baffle (SWB), (c) spoiler baffle (SPB)

culvert diameter is an appropriate method for choosing baffle heights. A similar study by Feurich et al. (2012) support this conclusion after identifying that fish passage success rates through a culvert fitted with spoiler baffles did not noticeably improve with further increases in baffle height beyond a certain height. Moreover, Feurich et al. (2012) observed that fish demonstrated decreased confusion as to which direction to swim when navigating spoiler baffle arrangements compared to weir and slotted-weir baffles. This suggests that spoiler baffles may allow fish to swim more efficiently through the culvert, thus decreasing energy expenditures necessary to successfully continue migration.

Various authors have suggested optimal baffle heights and spacings to improve the flow field (depths and velocities) for fish passage in culverts. For example, in a comprehensive study of WB, SWB and SPB designs, Ead et al. (2002) suggested practical baffle heights fall within the range of 0.1D and 0.15D and should be placed no further than 1D apart in order to maximize depths and reduce barrier velocities. Love and Bates (2009) recommend a minimum spacing of 1.52 m between baffles. They further suggested that weir and corner baffle (which is a weir baffle inclined at an angle of 10 to 30 degrees from the horizontal) heights be chosen to be almost completely submerged at the highest fish passage design discharge.

4.1.2 Hydraulic Capacity

Partially Full Flow

Partially full roughness in bare (non-baffled) HDPE pipes was shown by Devkota et al. (2012) to vary considerably for y/D <20% with Manning's values ranging from 0.004 to 0.011. The findings of Devkota et al. (2012) suggest that the velocities calculated for fish passage purposes using full flow roughness values ($n = 0.009$) may greatly underestimate actual velocity magnitudes observed in HDPE pipes at low relative depths. Velocities therefore may exceed recommended limits for target species and develop barriers to fish passage. These findings stress the need for further investigations into promoting fish passage in HDPE pipes.

The effect of baffles on hydraulic capacity in culverts under free surface flow conditions has been the subject of a number of studies. Rajaratnam et al. (1989; 1990; 1991) studied the effects of SWB, WB and SPB on the flow depth of a 0.3 m diameter PVC pipe over a variety of slopes and discharges. Although the effect on depth was studied, full flow roughness coefficients were not determined. Feurich et al. (2012) determined the effects that various arrangements of spoiler baffles have on free surface depths in inlet controlled culverts. Their findings showed that flow was reduced by approximately 8% compared to an equivalent depth in bare pipes.

Full Flow

A study by Luo and Peng (2010) employing an analytical model determined that 4 of the 15 culverts examined along an existing stretch of highway would fail to respect the 100 year discharge, Q_{100}, after slipline rehabilitation. The cause was attributed to increased inlet losses due to reduction in pipe diameter. The authors concluded that the smooth interior surface of a slipline pipe ($n = 0.009$) does not guarantee adequate discharge capacity after rehabilitation since the majority of the investigated culverts were controlled at the inlet, where barrel roughness has no effect on discharge capacity. A study was undertaken by Tullis et al. (2008) to determine the effectiveness of various inlet end treatments (projecting and tapered projecting treatments) on improving the hydraulic capacity of inlet and outlet controlled sliplined culverts. They concluded that inlet treatments can improve the hydraulic capacity of short to medium length inlet and outlet controlled culverts, yet minimal effects on longer outlet controlled culverts.

An adequate understanding of barrel roughness is essential for the proper hydraulic design of outlet controlled culverts. Improper evaluation of barrel roughness can lead to incorrect culvert sizing and

possible roadway overtopping. The full flow roughness values of standard materials for bare culverts have been extensively studied and can be used with confidence for new culvert designs (e.g., corrugated steel, steel plate, HDPE, concrete). The Manning's roughness of bare HDPE pipe at full flow has been determined experimentally to be approximately 0.009 to 0.0095 (Olsen and Tullis, 2013, ISCO, 2013). This is significantly lower than the commonly used $h = 0.024$ for corrugated steel pipe.

Roughness values of culverts retrofitted with baffles have not yet received the same level of attention and presently there exists little information available on this subject. To the authors' knowledge, only one study performed by Olsen and Tullis (2013) has investigated the effect of baffles on the full flow hydraulic capacity of an HDPE culvert. In their study, a single weir baffle configuration with $h = 0.15$D and $\lambda = 0.9$D was tested for hydraulic roughness in an 18 m long, 0.61 m diameter HDPE culvert under non-pressurized and pressurized conditions. An average fully pressurized Manning's coefficient of 0.0254 ± 2.8E-4 was determined as well as roughness coefficients for non-pressurized full flow over a variety of bed slopes. Olsen and Tullis (2013) determined that baffles in HDPE pipe reduced hydraulic capacity by 50 to 70% compared to a bare HDPE culvert. This finding demonstrates that baffles have an appreciable effect on hydraulic capacity. It is worthy to note that this finding compares culverts of equal diameter made of the same material. These conditions do not necessarily reflect capacity losses that may be observed when refitting a larger corrugated steel culvert with a smaller diameter HDPE baffle fitted culvert typical to normal field applications. Furthermore, there exist many other possible baffle configurations than the one studied by Olsen and Tullis (2013) which may better respond to the site specific needs of both fish passage and hydraulic discharge for which their contribution to hydraulic roughness is little understood.

4.1.3 Objectives

The objectives of our study were to: (1) determine Manning's roughness coefficients of common slotted-weir (SWB), weir (WB) and spoiler baffle (SPB) configurations for fully pressurized flow, (2) gain insights into how roughness spacing (λ) and roughness height (h) affect hydraulic roughness, (3) develop an analytical model to examine the associated risks of installing baffles on the hydraulic capacity of slipline culverts, (4) present design suggestions to facilitate the determination of an optimal baffle configuration tailored to the site specific needs for both hydraulic capacity and fish passage. Physical experiments were performed at the hydraulic laboratory at the Université de Sherbrooke in the goal of obtaining these objectives. The results of this study are novel and provide urgently needed knowledge to aid hydraulic engineers in assessing the risks associated with baffle installation for slipline rehabilitation projects.

4.2 Experimental setup

A physical model of a slipline culvert was constructed using a 0.254 m nominal diameter PVC pipe of 7.35 m in length at the Hydraulics Laboratory at the Université de Sherbrooke. The test pipe was placed in an 8 m long, 0.5 m wide and 0.55 m deep hydraulic flume. A PVC coupler was fitted into the head which separated the flume from a 1.43 m^3 stilling tank upstream [Fig. 4.2]. A 6 m section of 0.254 m inside diameter PVC pipe was attached to the coupler. The pipe length was extended with a 1.35 m long piece of pipe placed (with the aid of a another coupler) at the downstream end of the 6 m long section (i.e., total length of the model was 7.35 m). A 0.152 m diameter circular orifice was fitted over the downstream end of the extension pipe. The orifice was installed to fulfill three functions: ensure fully pressurized flow over the entire test section of the pipe; stabilize fluctuations in the piezometer levels; and elevate the hydraulic grade line so that it could easily be read in the piezometers (above the glass sides of the flume in Fig. 4.2). Thin transverse slits (25 in total) approximately 1.5 mm wide and 20.5 cm long were cut at regular 0.6D m intervals along a 4.11 m section of the pipe. The furthest upstream slit was cut 1.5 m from the head tank in order to allow sufficient distance for the vena-contracta at the entrance to expand to the full diameter of the pipe before entering the test section. The reservoir was fed from a constant head (approx. 11 m) roof reservoir supplied by a 30 HP pump. Flow rates were measured using an HTTF Transit Time Ultrasonic flow meter with a manufacturer stated accuracy of 1%. The flow meter was installed according to manufacturer specifications on the main line supplying the flume.

Three sets of paired (top and side) piezeometers were installed upstream of the first baffle [Fig. 4.3]. The piezometers were spaced at intervals of 0.6D m starting at 0.6D upstream of the first baffle and continuing further upstream. In a similar fashion, another group of 4 paired piezometers was installed 0.6D downstream of the last baffle (with 0.6D spacing between each). Preliminary tests concluded that the first downstream piezometer levels were significantly lower compared to the downstream group average. This decrease was likely caused by flow expansion after the last baffle. Therefore readings from this piezometer were not taken into consideration. Using a laser level, the test pipe and flume were set to a zero slope for all trails. In the absence of slope only the headwater height provides the necessary energy to induce flow. A laser level was also used to level the piezometers. Figs. (4.2 and 4.3) illustrate the laboratory setup.

Laboratory experiments were conducted on three common baffle types [Fig. 4.1]; the slotted weir baffle (SWB), weir baffle (WB) and spoiler baffle (SPB) of roughness height (h) of 0.15D, 0.1D, 0.05D and roughness spacing (λ) of 0.6D, 1.2D, 1.8D and 2.4D as shown in Table 4.1. The respective areas

Figure 4.2: Laboratory flume with reservoir, headwall, test culvert and piezometers (flow is from left to right)

of each baffle type normal to the flow are also presented in Table 4.1. The SPB were placed in rows of three (laterally spaced) with one at the centerline of the pipe and the other two spaced at 30° from the centerline as indicated in Fig. 4.1(c). All of the baffles were precision cut by laser from 18 gauge galvanised steel. The notation used for reference to a particular baffle configuration is as follows: baffle type-h-λ. For example a weir baffle with $h = 0.15$D and $\lambda = 0.6$D has the notation WB-0.15D-0.6D.

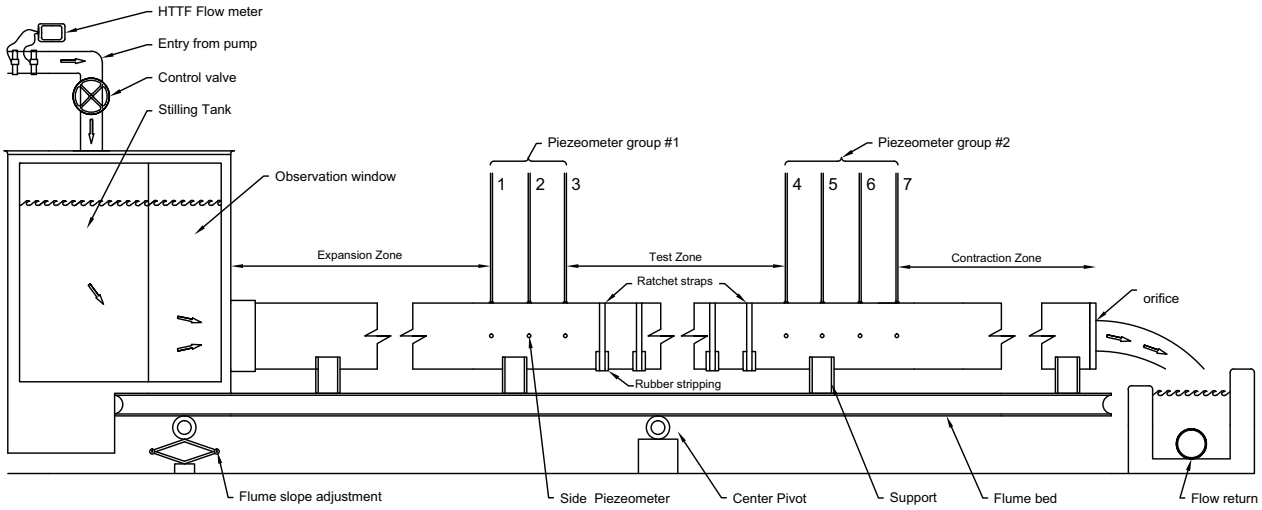

Figure 4.3: Schematic of laboratory test pipe (scale not respected). The flow is measured by the HTTF flow meter (1), and is controlled by a locking valve (2), it then passes through a diffuser (3) before arriving in the settling tank (4). Flow then proceeds through the test pipe past the expansion zone (5), past piezeometer group #1 (6), over the baffle test section (7), past piezeometer group #2 (8), over the contraction zone (9) before exiting out the orifice (10) into the flow return tank (11). The test pipe is encapsulated in a hydraulic flume not shown for purposes of clarity.

Baffles were inserted by hand into the slits at the specified λ value for each test. With the baffles in place, the slits were sealed with 4 mm thick, 0.3 m long rubber stripping held in place with ratchet straps to ensure the test pipe did not leak. The baffles were orientated along the bottom of the culvert during the tests to avoid possible air bubble entrapment. When it was necessary to change baffle configurations the entire conduit was floated, pulled out of the headwall and rotated to provide easy access to manipulate the baffles.

Table 4.1: Dimensions and areas of tested baffle configurations

Baffle type	*h*	*h (m)*	*w (m)*	*b (m)*	*A (mm^2)*
WB	0.15D	38.0	208.0	-	4833
	0.10D	25.5	183.2	-	2699
	0.05D	12.5	150.6	-	999
SWB	0.15D	38.0	208.0	25.5	3865
	0.10D	25.5	183.2	25.5	2052
	0.05D	12.5	150.6	25.5	667
*SPB**	0.15D	38.0	38.0	-	4332
	0.10D	25.5	25.5	-	1951
	0.05D	12.5	12.5	-	469

* areas are for all three spoiler baffles

4.3 Methodology

Each baffle configuration was tested at 9 flow rates. The flows ranged from 0.025 to 0.045 m^3/s in equal increments of 0.0025 m^3/s. Any small deviations from the intended intervals of 0.0025 m^3/s were due to the difficulty in precisely controlling the flow rate with the head tank valve. The headwater level was measured by means of a meterstick fixed on the outside of the glass observation window upstream of the headwall. The headwater levels as well as the flow rates were noted at the beginning and at the end of each flow rate trail. This was done in order to verify that the flow as well as the headwater level remained constant over the duration of the trial. The hydraulic grade line was calculated using the difference of the average height of the 6 upstream piezeometers compared to the average height of the six downstream piezeometers. The difference in head was attributed solely to friction losses along the baffle test length.

Prior to baffle insertion, the Manning's roughness coefficient for the smooth pipe was determined to be $h = 0.0104$. This value is in good agreement with h values determined by Olsen and Tullis (2013) for a bare HDPE pipe $h = 0.009$ and a stated HDPE pipe manufacturer values of $h = 0.0091$ (ISCO, 2013). The close proximity between our value for PVC pipe and previously stated values for HDPE pipe serves to validate the experimental setup and demonstrates that PVC pipe can be used to conservatively simulate HDPE pipe in roughness trials.

4.4 Theory

The bulk Reynolds number for the conduit (**R**) is expressed as a function of mean longitudinal velocity (V), the density of water (ρ), the interior diameter of the pipe (D) as well as the viscosity of water (μ).

$$\mathbf{R} = \frac{\rho V D}{\mu} \tag{4.1}$$

Turbulent friction losses (h_f) over a given length (L) of pipe is a function of the Darcy friction factor (f), D, V as well as the gravitational constant (g) as expressed by the Darcy-Weisbach relation Eq. 4.2.

$$h_f = f \frac{LV^2}{D2g} \tag{4.2}$$

The Chézy-Manning relation Eq. 4.3 expresses the Manning's roughness coefficient (n) as a function of f and the hydraulic radius ($\mathbf{R}$).

$$n = R^{\frac{1}{6}} \sqrt{\frac{f}{8g}} \tag{4.3}$$

For each baffle configuration tested, roughness coefficients (n and f) were calculated with Eqs. (4.1-4.3) using the difference in elevation between the mean of the upstream and downstream piezometer water levels. From Eq. 4.2 it is seen that h_f does not depend on slope. It is for this reason that the tests were performed at the horizontal (i.e., for full pipe flow, the roughness developed is not dependent on the pipe's slope).

4.5 Results and Analysis

4.5.1 Baffle roughness

Figure 4.4 presents the Manning's roughness coefficients h along with the corresponding $\sqrt{f}$ values obtained for each of the nine baffle configurations tested over the entire flow range and the four λ values. Since f is proportional to the square of h in the Chézy-Manning relation (Eq. 4.3), the square root of f is shown so that the left and right ordinate axis of the Fig. 4.4 can share the same data series. This facilitates the presentation of flow rates and their corresponding $\mathbf{R}$ values on the lower and upper abscissa, respectively. Figure 4.5 presents the mean roughness coefficients of each of the baffle configuration series presented in Fig. 4.4. Roughness spacing (λ) is presented on the abscissa and both h and $\sqrt{f}$ on the left and right ordinate axis. Table 4.2 presents the mean roughness values plotted in Fig. 4.5 with standard deviations in brackets.

As can be seen in Fig. 4.4, roughness values for each of the nine tested flow rates are randomly scattered about the mean of the series of the respective configurations. It is not possible to establish clear trends between $\mathbf{R}$ and $\sqrt{f}$ over the range of $\mathbf{R}$ for any of the baffle configurations tested suggesting $\mathbf{R}$ and $\sqrt{f}$ independence. Roughness coefficients are the highest for the SPB-0.15D baffle configuration for

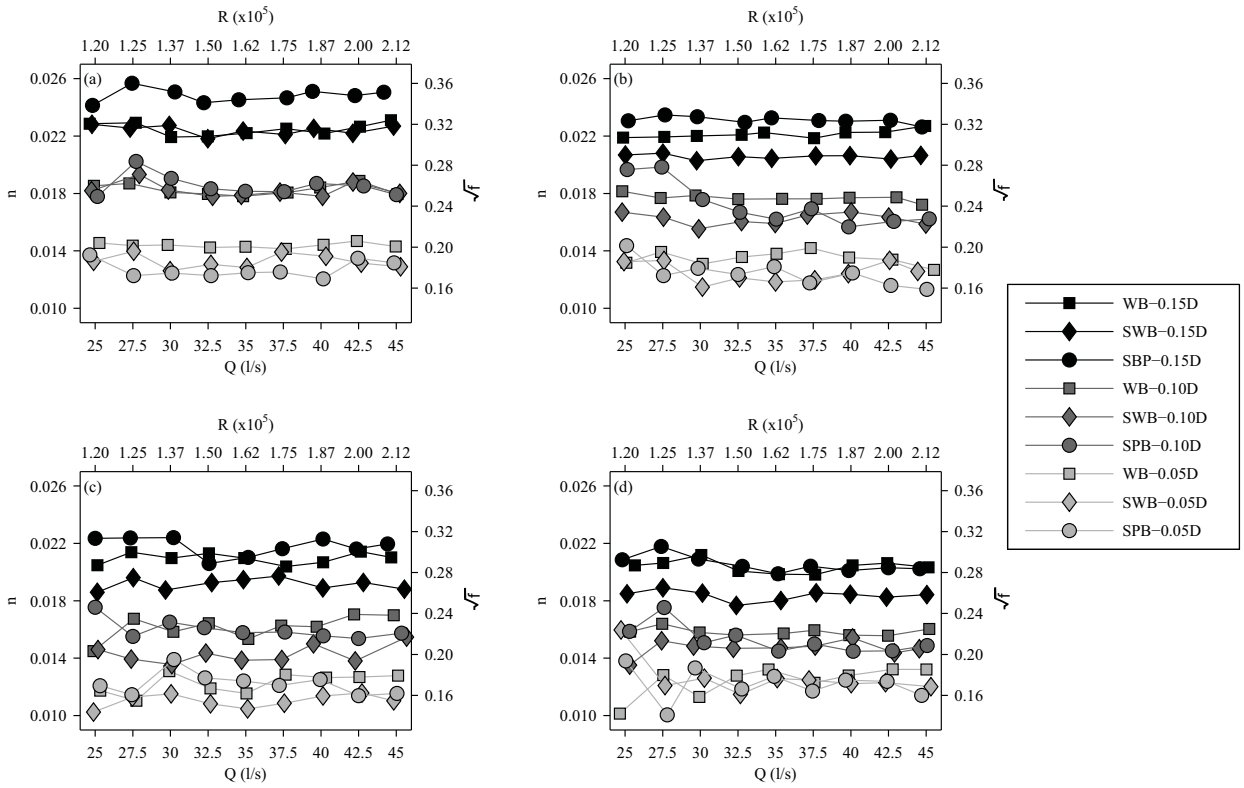

Figure 4.4: Individual Manning roughness n and $\sqrt{f}$ trail data versus flow rate and corresponding **R** for each of the baffle configurations tested at λ of a) 0.6D, b) 1.2D, c) 1.8D, d) 2.4D.

the four values of λ tested with the exception of SPB-0.15D-2.4D which is approximately equal to WB-0.15D-2.4D. The SWB configurations demonstrate consistently lower roughness coefficients than the WB configurations. This difference is likely explained by the reduction in area for the flow to impinge upon and develop form drag on the SWB configurations.

As expected the largest baffles (WB, SWB and SPB at heights of 0.15D) produce higher roughness values across all four tested λ values than the two smaller (0.10D and 0.05D) values of h tested as seen in Fig. 4.5. A consistent descending trend in roughness is visible with increasing λ values. The SWB configurations develop lower roughness coefficients than both the WB and SPB configurations for $h =$ 0.15D and 0.1D. Roughness values for the $h = 0.05D$ trails are higher for the WB configurations for $\lambda =$ 0.6D and $\lambda = 1.2$D. For $\lambda = 1.8$D and $\lambda = 2.4$D, h coefficients stabilize at approximately 0.012 with the exception of the SWB-0.05D at $\lambda = 1.8$D trial which produced an$h$ value of 0.0108. It is also interesting to note that the SPB-0.15D-0.6D ($A_{surf} = 4833$ mm^2) configuration produced a higher roughness value than the WB-0.15D-0.6D ($A_{surf} = 4332$ mm^2) configuration despite having a lower surface area normal to the flow. The SPB protrudes higher into the flow field than the WB and this could partially account

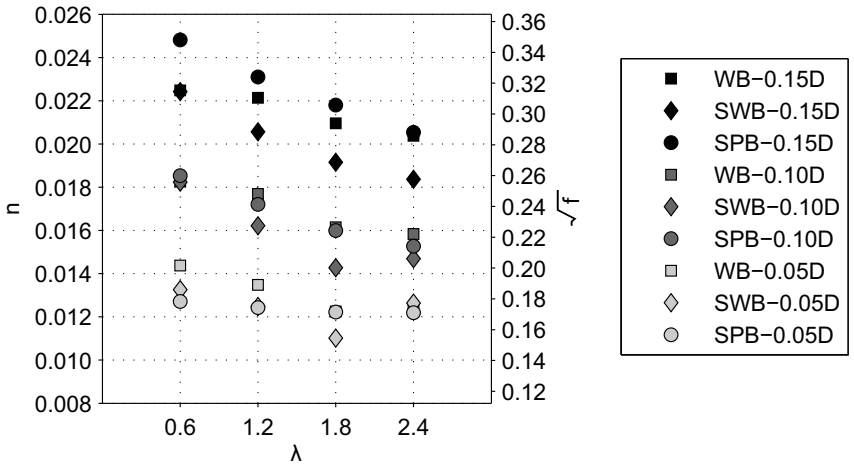

Figure 4.5: Mean Manning's and Darcy-Weisbach roughness coefficients versus baffle spacing (λ).

for the higher roughness value. Furthermore, the SPB configuration is geometrically more complicated than the WB, increasing the length of edges available for flow to contour and generate energy losses due to vortex dissipation.

Figure 4.5 demonstrates that h is indeed much more influential on roughness than is λ when only a single baffle type and height is analyzed at a time. To illustrate, h values can be seen to decrease by an average of 0.073% (WB), 0.108% (SWB) and 0.090% (SPB) as spacing is increased by a factor of 0.05D, while roughness values decrease by 20.3% (WB), 20.3% (SWB) and 24.1% (SPB) as h is decreased by increments of 0.05D.

$$n = \beta_1 + \beta_o \lambda \tag{4.4}$$

Trends relating Manning's n, h and λ are clearly identifiable in Fig. 4.5. Assuming a linear relationship exist between h and λ, an ordinary least square (OLS) regression model was performed for each baffle configuration (type and height) using Excel's data analysis package. The obtained regression coefficients β_1, β_o for use with Eq. 5.1 as well as the coefficients of determination ($\mathbf{R}^2$) were determined and are presented in Table 4.3. The $\mathbf{R}^2$ demonstrate that the majority OLS model fits the observed data for the majority of the baffle configurations. Only the SWB-0.05D demonstrated a low $\mathbf{R}^2$ value. Therefore the linear regression model (Eq. 5.1) in conjunction with the coefficients presented in Table 4.3 can be used as valuable tool to predict roughness values for baffle spacings between 0.6D and 2.4D which were not presented herein.

Table 4.2: Friction factors (n and f) for tested baffle configurations with standard deviations presented in parenthesis.

		0.6D Spacing				1.2D Spacing			
Baffle Type	***h***	***n***		***f***		***n***		***f***	
WB-	0.15D	0.0222	(0.0004)	0.0971	(0.0035)	0.0219	(0.0002)	0.0940	(0.0021)
	0.1D	0.0180	(0.0003)	0.0641	(0.0025)	0.0169	(0.0015)	0.0566	(0.0089)
	0.05D	0.0142	(0.0002)	0.0397	(0.0009)	0.0139	(0.0008)	0.0379	(0.0043)
SWB-	0.15D	0.0220	(0.0004)	0.0956	(0.0037)	0.0196	(0.0019)	0.0766	(0.0127)
	0.1D	0.0180	(0.0005)	0.0639	(0.0034)	0.0153	(0.0015)	0.0464	(0.0083)
	0.05D	0.0131	(0.0004)	0.0337	(0.0022)	0.0121	(0.0007)	0.0289	(0.0033)
SPB-	0.15D	0.0242	(0.0011)	0.1156	(0.01)	0.0229	(0.0002)	0.1028	(0.0016)
	0.1D	0.0183	(0.0007)	0.0660	(0.0052)	0.0170	(0.0014)	0.0569	(0.0095)
	0.05D	0.0126	(0.0006)	0.0311	(0.0028)	0.0122	(0.0009)	0.0296	(0.0044)

		1.8D Spacing				2.4D Spacing			
Baffle Type	***h***	***n***		***f***		***n***		***f***	
WB-	0.15D	0.0207	(0.0003)	0.0846	(0.0027)	0.0199	(0.0008)	0.0783	(0.0058)
	0.1D	0.0159	(0.0009)	0.0498	(0.0052)	0.0157	(0.0022)	0.0493	(0.0141)
	0.05D	0.0121	(0.0007)	0.0289	(0.0032)	0.0124	(0.001)	0.0304	(0.0046)
SWB-	0.15D	0.0195	(0.0016)	0.0754	(0.013)	0.0184	(0.0009)	0.0665	(0.0068)
	0.1D	0.0141	(0.0006)	0.0392	(0.0033)	0.0140	(0.0013)	0.0387	(0.0068)
	0.05D	0.0106	(0.0012)	0.0222	(0.0045)	0.0118	(0.0006)	0.0275	(0.0026)
SPB-	0.15D	0.0215	(0.0006)	0.0912	(0.0054)	0.0204	(0.0006)	0.0816	(0.0047)
	0.1D	0.0158	(0.0006)	0.0492	(0.004)	0.0151	(0.0009)	0.0448	(0.0053)
	0.05D	0.0121	(0.0007)	0.0288	(0.0036)	0.0120	(0.001)	0.0288	(0.0048)

Table 4.3: Linear regression coefficients and $\mathbf{R}^2$ values.

Baffle Type	***h***	β_1	β_o	R^2
WB-	0.15D	0.023	-0.0012	0.96
	0.1D	0.019	-0.0014	0.94
	0.05D	0.015	-0.0012	0.85
SWB-	0.15D	0.023	-0.0022	0.97
	0.1D	0.019	-0.0021	0.82
	0.05D	0.013	-0.0005	0.20
SPB-	0.15D	0.026	-0.0023	0.99
	0.1D	0.019	-0.0018	0.98
	0.05D	0.013	-0.0003	0.90

4.6 Discussion

4.6.1 Flow regime and Reynold's independence

Flow over baffles will develop one of three possible flow regimes: isolated roughness flow, wake-interference flow or quasi-smooth flow (*skimming flow*) depending on the baffle spacing (λ) used. Morris

(1955) demonstrated that f is dependent on **R** and the predominant flow regime. Isolated roughness and quasi-smooth flow develop descending f-**R** curves whereas wake-interference flow is characterized by rising f-**R** curve. At a sufficiently high **R** number f will attain a constant value for each of these three flow regimes. When this occurs it is said that f is now Reynold's independent. The establishment of Reynold's independence is important if the experimentally determined roughness coefficients presented in Table 4.2 are to be confidently used in baffled culvert design. From Fig. 4.4 it can be seen that trends of f with **R** are not apparent. Thus, Reynold's independence is plausible. However, because of the limited range of **R** values tested in this study (1.1e5 to 2.3e5), absolute certainty of Reynold's independence is difficult to establish. The following arguments, however, give reason to believe that the roughness values in Table 4.2 for the λ = 1.2D, 1.8D and 2.4D are conservative estimates. The question of λ = 0.6D is treated further on.

Isolated roughness flow over baffles is characterized by decreasing f values with increasing values of λ. This inverse relationship arises because spacing baffles further apart reduces the number of vortex shedding structures (and related drag) which is largely responsible for the induced pressure losses over a given length of pipe. This relationship is evident in Fig. 4.5 and is indicative of isolated roughness flow.

As stated above, Morris (1955) demonstrated that f-**R** curves for the isolated roughness regime characteristically descend with increasing **R** values. Olsen and Tullis (2013), show a descending trend in their study of full flow roughness of a WB-0.15D-0.9D baffle configuration over a wide range of **R** values (9.2e4 to 1.67e6), where f fell marginally (yet consistently) from 0.0971 to 0.0933. This implies that if our assumption of **R** independence is incorrect than the experimentally determined roughness coefficients for the λ = 1.2D, 1.8D and 2.4D configurations presented in Table 4.2 are conservative for culverts running full at **R** values greater than 2.3e5.

Exceptionally, it is possible that our baffles spaced at λ = 0.6D may be in the wake interference flow regime. The worry with wake interference flow is that it is known to be characterized by increasing f-**R** curves for reasons describe by Morris (1955). Such ascending f-**R** curves were found by Straub and Morris (1951) in corrugated steel pipes. Friction factors varied from approximately 0.08 to 0.10 (or n, 0.022 to 0.025) over a range of **R** from 1e5 to 3e5 in a full flowing 18" (0.457 m) diameter culvert. Corrugations were 0.5" (12.7 mm) high (or h = 0.05D) and 2'(2/3)" (68 mm) crest to crest (or λ = 0.15D). Roughness of closely spaced baffles may behave in a similar manner to roughness in corrugated steel pipes. Thus, the experimentally determined roughness values in Table 4.2 for λ values of 0.6D may underestimate the maximum f value at high **R**. Regretfully, the range of **R** in Fig. 4.4(a) is not

wide enough to reveal any such trends. However, it is doubtful that f will increase with **R** larger than a factor of 1.25 as witnessed in the trials on corrugated steel pipe by Straub and Morris (1951). In light of the possibility of wake-interference flow, designers may wish to increase the values in Table 4.2 for the $\lambda = 0.6$D baffle configurations by a factor of 1.25 to obtain a more conservative design. Further investigations of the $\lambda = 0.6$D baffle configurations at higher values of **R** is warranted in order to verify the presence of wake interference flow (through analysis of the flow structure in the proximity of the baffle) and also to better understand the variation of f with increasing values of **R**.

4.6.2 Comparison with previous work

Mean velocity depth profiles for the SWB-0.15D-0.6D and WB-0.15D-0.6D presented by Rajaratnam et al. (1989) and Rajaratnam et al. (1990) were used to obtain Manning's roughness coefficients using for the largest relative depths studied (y/D of 0.79 and 0.81) at the lowest slopes tested (1%), in order to best compare their values with the current studies' values. The h values obtained with Rajaratnam's data were 0.022 for both the SWB and WB configurations. These values, though derived from partially full flow data, are very near to the values obtained in the current study for the same heights and spacings (both WB and SWB of 0.022). The values obtained from Rajaratnam's work were derived from high relative depths nearing full flow and thus can likely be considered to be near the full flow roughness value. The roughness coefficient of $h = 0.0251$ determined by Olsen and Tullis (2013) for a WB-0.15D-0.9D configuration under fully pressurized flow is slightly higher than the value obtained in the present study ($n = 0.0221$) for the WB-0.15D-0.6D. However, the difference is minor and shows a significant amount of agreement with the present studies' values and those determined from Rajaratnam et al. (1989) and Rajaratnam and Katopodis (1990).

4.6.3 Retrofit effect on discharge

Slipliner culverts must respect the parent culvert's design discharge capacity if they are to be an acceptable alternative. An equation relating the hydraulic capacity of the slipline culvert (Q) as a ratio of the known parent culvert's hydraulic capacity (Q_o) was developed and analyzed in a number of slipline rehabilitation scenarios with various diameter and roughness reductions for outlet control conditions. This was done in order to asses, with culvert theory, to what extent the increased roughness caused by baffles as well as radial reductions and culvert length have on the discharge capacity of the culvert after rehabilitation.

The energy equation applied to an outlet controlled culvert running under fully pressurized flow is presented in Eq. 4.5 where L is the culvert length, S_1 is the bed slope of the culvert, Y_1 is the headwater level (m), V_1 and V_2 are respectively the upstream and downstream velocities (m/s), Y_2 is the water

level (m) and H (m) is the total headlosses occurring over the length of the culvert. The sum of the left hand terms gives the total available head upstream of the culvert entrance which must be accounted for downstream of the culvert in the sum of the right hand terms. Eq. 4.5 can be applied to both the parent and the slipliner culverts. The upstream water surface level is considered to coincide with the energy grade line and therefore the term containing V_1 in Eq. 4.5 is ignored. The term V_2 is generally represented as a loss coefficient (k_{out} equal to 1) and is included in the energy loss term H.

Before and after slipline rehabilitation (L), (S_o), (Y_1) and (Y_2) are assumed to be unchanged. The total head loss (H) therefore remains as the sole variable and consequently the only parameter determining if the slipline culvert design will respect the parent culvert's original design discharge.

$$LS_o + Y_1 + \frac{V_1^2}{2g} = Y_2 + H + \frac{V_2^2}{2g} \tag{4.5}$$

The total head loss (H) is composed of entrance, barrel and exit losses. The barrel velocity head $\frac{V^2}{2g}$ is common to all three loss terms as is shown in terms of discharge (Q) in Eq. 4.6.

$$H = \left[k_{in} + k_{out} + \frac{19.63n^2L}{R^{1.33}}\right]\frac{Q^2}{2gA^2} \tag{4.6}$$

Where k_{in} is the inlet loss coefficient, k_{out} is the outlet loss coefficient, **R** is the hydraulic radius and the exit loss coefficient is taken to be equal to 1. Equating H (slipline culvert) to H_o (the subscript refers to the parent culvert) permits a direct assessment of the discharge ratio, $\frac{Q}{Q_o}$, as shown in Eq. 4.7, where $C_1 = 49.35$ in SI units, r is the nominal radius of the culvert. Hence, the parent culvert discharge capacity can only be respected after rehabilitation if $H \leq H_o$ or in other words if $\frac{Q}{Q_o}$ is equal than or greater than unity.

$$\frac{Q}{Q_o} = \frac{\left[k_{in}^o + k_{out}^o + \frac{C_1Ln_o^2}{r_o^{1.33}}\right]}{\left[k_{in} + k_{out} + \frac{C_1Ln^2}{r^{1.33}}\right]}\frac{r}{r_o}^2 \tag{4.7}$$

Letting roughness reduction $\alpha = \frac{n}{n_o}$ and radial reduction $\beta = \frac{r}{r_o}$ and substituting in Eq. 4.7, a more intuitive expression for $\frac{Q}{Q_o}$ results [Eq. 4.8].

$$\frac{Q}{Q_o} = \frac{\left[k_{in}^o + k_{out}^o + \frac{C_1Ln_o^2}{r_o^{1.33}}\right]}{\left[k_{in} + k_{out} + \frac{C_1Ln_o^2\alpha^2}{r_o^{1.33}\beta^{1.33}}\right]}\beta^2 \tag{4.8}$$

Holding all other variables constant, the effects of α and β on discharge can be assessed. It is reasonable to assume that the entrance and exit loss coefficients will remain unchanged in both conditions,

unless entrance improvements such as a beveled inlet or hydraulic bell are installed on the refit culvert. If such is the case, the appropriate entrance loss coefficient should be used.

An analysis of Eq. 4.8 was performed to better understand the effects of L, α and β on $\frac{Q}{Q_o}$. Two culvert lengths, short (10 m) and long (80 m) were studied for two values of radial reduction ($\beta = 0.90$ and $\beta = 0.85$), seven values of roughness reduction ($\alpha = 1.0, 0.9, 0.8, 0.7, 0.6, 0.5, 0.4$) and with and without an inlet treatment. The two inlet conditions imposed were (*i*) $k_{in} = 0.9$ and (*ii*) $k_{in} = 0.2$. Condition (*i*) reflects the value suggested for a corrugated steel culvert projecting from the fill with no headwall by the Federal Highway Administration (Norman et al., 2001). Whereas condition (*ii*) is a reasonable value for an energy efficient inlet (e.g., beveled inlet, side or slope tapered inlet or other commercially available product) that is installed or constructed at the inlet of the slipline culvert in order to reduce contraction losses. The parent culvert was assumed to have $k_{in} = 0.9$. Figure 4.6 (a and b) presents the solutions to Eq. 4.8 for the 10 m culvert at $\beta = 0.90$ and $\beta = 0.85$, respectively. Figure 4.6 (c and d) presents the solutions to Eq. 4.8 for the 80 m culvert at $\beta = 0.90$ and $\beta = 0.85$, respectively. It should be noted that the y-axis was converted from $\frac{Q}{Q_o}$ to percent change in discharge capacity in order to clarify the presentation. The various α values corresponding to the baffle configurations of the present study are presented in Table 4.4, and are discussed further on.

Several general observations related to the effect of radial and roughness reductions are apparent in Fig. 4.6. First, discharge always improves with decreasing values of α (barrel roughness). This is an obvious result and can be deduced from Eq. 4.8 as α is in the denominator. Secondly, discharge always decreases with increasing radial reductions and for values of β inferior to 0.85 [Figs. 4.6(c and d)] it becomes difficult to respect the required discharge without resorting to the installation of an inlet treatment (e.g., hydraulic bell) and a sever reduction in barrel roughness. In fact, on graphs of Eq. 4.8 with 20% reduction in radius (not shown) it is nearly impossible to attain $\frac{Q}{Q_o} > 1.0$ in practical applications. Compared to the 10 m culvert, the 80 m culvert shows much more improvement with reductions in α.

A part from these general observations, more specific trends are revealed from analyzing each culvert length individually. The 10 m culvert demonstrates a significant improvement in hydraulic capacity when a hydraulic bell is applied to the slipliner entrance [Fig. 4.6(a and b)]. This can be explained from the fact that total energy losses in shorter culverts are heavily dominated by entrance losses. It is interesting to note that the discharge capacity of the 10 m culvert improves only moderately with decreasing roughness. Reductions in roughness have less impact on hydraulic capacity in shorter culverts since the barrel is not of sufficient length to develop considerable friction losses. In contrast to the 10 m length,

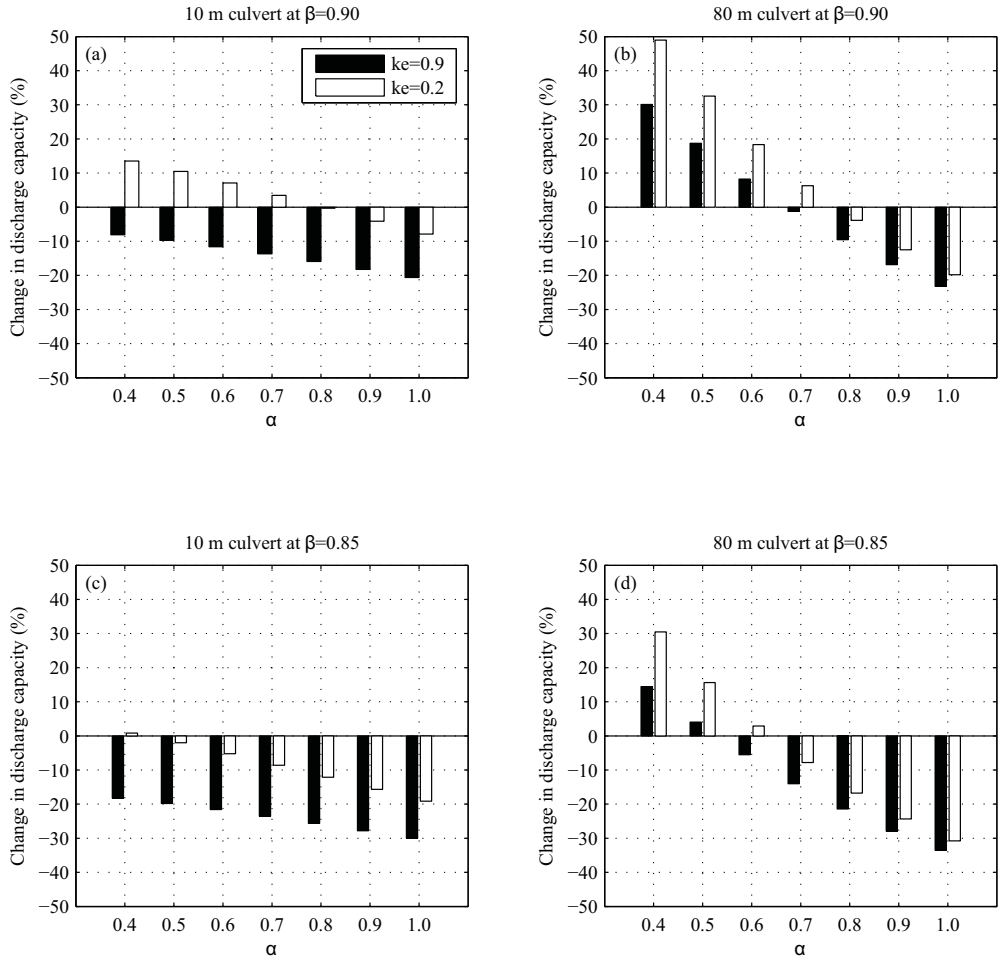

Figure 4.6: Percent change in discharge capacity for slipline rehabilitations of a; (a) 10 m culvert with $\beta = 0.90$, (b) 80 m culvert with $\beta = 0.85$, (c) 10 m culvert with $\beta = 0.85$, (d) 80 m culvert with $\beta = 0.85$.

the 80 m culvert shows considerable improvement in discharge as roughness is decreased. This reflects the fact that friction losses dominate the total energy loss term in the energy equation (Eq. 4.5).

From Figs. 4.6(a and b) it can be seen that it is not necessarily true that the smooth slipliner surface (approximately $h = 0.009$ or $\alpha = 0.4$) can sufficiently compensate for the discharge reduction caused by the loss in radius in a short outlet controlled culvert. However, for the longer 80 m culvert [Figs. 4.6(b and d)] the same alpha value ($\alpha = 0.4$) would enhance hydraulic capacity.

4.6.4 Baffle choice for outlet controlled culverts

Recommendations for baffle use in short and long culverts

Table 4.4 presents the relative reduction in roughness (α values) for the various baffle configurations tested in our experiments. A Manning's h value of 0.024 was used in the calculation of the α values since

Table 4.4: α values for the tested baffle configurations.

		α			
Baffle Type	***h***	**ʎ=0.6**	**ʎ=1.2**	**ʎ=1.8**	**ʎ=2.4**
WB-	0.15D	0.95	0.89	0.84	0.00
	0.1D	0.75	0.73	0.66	0.65
	0.05D	0.59	0.55	0.50	0.51
SWB-	0.15D	0.92	0.84	0.79	0.75
	0.1D	0.75	0.67	0.59	0.60
	0.05D	0.54	0.51	0.45	0.52
SPB-	0.15D	1.02	0.95	0.89	0.84
	0.1D	0.76	0.71	0.66	0.63
	0.05D	0.52	0.51	0.50	0.50

this is commonly accepted for use in corrugated steel culverts. From Table 4.4 it can be noted that the larger ($h = 0.15$D) baffle configurations produce α values in the range of 0.85 to 1.0, the intermediate ($h = 0.1$D) baffles are in the range of 0.60 to 0.76 and the smaller ($h = 0.05$D) are mostly in the range of 0.5 to 0.6. The obtained experimental α values can be used in combination with Eq. 4.8 to gain insights on how to best optimize the hydraulic capacity of short and long culverts outlet controlled culverts.

Short culverts outlet control

With reference to Fig. 4.6(a), the $k_e = 0.2$ condition is shown to attain a 0% change in discharge at an α value of approximately 0.8. The $k_e = 0.9$ condition never attains the 0% change in discharge within the practical range of α values of 1 to 0.4. This supports the findings of Luo and Peng (2010). Consequently, efforts to significantly increase or maintain the discharge capacity of a short outlet controlled slipline culvert by installing a baffle configuration with a low α value is not a recommended design practice. Instead, energy losses at the inlet of the slipline culvert should be addressed with the application of a beveled inlet or similar low energy loss inlet treatment. For the conditions used to produce Fig. 4.6(a), the use of such an inlet treatment would permit the installation of baffle configurations with α values in the range of 0.7 to 0.85. As shown in Table 4.4, this range includes the baffles of medium height at a spacing of 0.6D (e.g., WB-0.10D, SWB-0.10D). Fortunately, These baffles have been shown by Ead et al. (2002) to produce adequate hydraulic conditions (ex. depths and velocities) for fish passage. It should be noted however, that shorter culverts are rarely controlled by barrel losses and are instead usually controlled at the inlet, therefore the added roughness of baffles on very short culverts can likely be neglected. For this reason, very short culverts (controlled at the inlet) are likely to be able to house any of the baffle configurations investigated in the current study without posing significant risk to hydraulic

capacity.

Long culverts outlet control

In contrast to short culverts, it can be seen from the $k_e = 0.9$ conditions in Figs. 4.6(b and d) that the hydraulic capacity of long culverts improves immensely with reductions in barrel roughness with 0% change in discharge being attained at approximately $\alpha = 0.65$. Further decreases in α (≤ 0.65) demonstrate a drastic improvement in hydraulic capacity. The $k_e = 0.2$ in Figs. 4.6(b and d) improves hydraulic capacity over the $k_e = 0.9$ condition, yet to a lesser extent than is developed for the short culvert. The hydraulic capacity of longer slipline culverts which are heavily controlled by barrel losses should benefit significantly from the installation of baffles with low α values. For the conditions studied to produce Figs. 4.6(b and d), α values less than 0.65 would suffice. The application of a low energy loss inlet treatment would increase the upper limit of α values to 0.75. As can be seen in Table 4.4, this upper limit of allowable α value would still permit the installation of most of the baffle configurations with $h = 0.10D$ (e.g., WB-0.10D, SWB-0.10D).

Comments on Spoiler baffle height and spacing

Pertaining to spoiler baffle arrangements, Feurich et al. (2012) found that a spoiler baffle height scaled to the body size of the target species successfully passed the target fish over a wide range of culvert diameters. This manner of determining baffle height is an alternative approach to the more common practice in which baffle height is scaled to barrel diameter. Feurich et al. (2012) findings may have profound implications for the use of baffles in slipline culverts. To illustrate, a standardized spoiler baffle height for trout (say $h = 10$ cm) would have an $h = 0.1$D in a 1 m diameter culvert and an $h = 0.05$D in a 2 m culvert. Consequently, the hydraulic capacity of larger slipliner culvert diameters would benefit from the lower α values that are characteristic of baffle configurations with low roughness heights (e.g., $h = 0.05$D). Furthermore, this approach would allow the installation of baffles in a larger number of slipliner culverts where larger baffles ($h = 0.10$D and $h = 0.15$D) would be impossible to install and still respect hydraulic conveyance requirements.

Can baffles be excluded?

The exclusion of baffles in an HDPE slipline retrofit may be appropriate if the following 2 criteria are respected: 1) the average barrel velocities are low enough to allow the target fish species to navigate a culvert over its entire length, and 2) adequate flow depths are present during the migratory periods of

the year as to not inhibit fish passage. If one of these criteria is not met the culvert will likely impede fish passage. Findings from Olsen and Tullis (2013) suggest that HDPE culverts at very mild slopes develop low average cross sectional velocities conducive to fish passage. Olsen and Tullis (2013) showed that sexually mature wild brown trout (*salmo trutta*) (body length $\geq$ 203 mm) demonstrated high passage rates ($>$ 65%) through a non-baffled 18 m long HDPE horizontal culvert with velocities in the range of 0.65 to 0.90 m/s. Passage success rates decreased to roughly 40% at the slightly steeper slope of 0.5% and velocities in the range of 1.0 to 1.45 m/s. Passage rates were very low (roughly 10%) at 1% slopes with velocities in the 1.45 to 1.55 m/s range. These findings demonstrate that velocities in smooth HDPE culverts may act as a significant barrier to fish passage even at relatively mild slopes.

Elevated flow velocities in culverts of excessive length inhibit passage by fatiguing fish before the end of the culvert is attained. The Washington Department of Fish and Wildlife have produced a list of recommended average flow velocities as a function of culvert length for trout and a cohort of salmon species (Bates et al. 2003). A maximum velocity of 1.22 m/s is recommended for adult trout (ex. salvelinus fontinalis, salmo trutta) navigating culverts of lengths between 3 and 30 m. With reference to the findings of Olsen and Tullis (2013) this recommended velocity would produce a roughly 35% passage rate in a HDPE culvert of 18 m length. This low passage success rate suggests that a more conservative velocity threshold (0.9 m/s) may be appropriate when deciding on whether or not to install baffles to promote the passage of trout.

A secondary effect of baffles is that they increase flow depths and thus may be necessary in HDPE culverts where low barrel roughness often produce shallow and rapid supercritical flow conditions (Froude number $>$ 1). Water depths should be adequate to completely submerge the largest fish which the culvert intends to pass. Gregory and McEnroe (2004) found that baffles improved passage success and attributed this success largely to increased depths compared to bare control culverts. Free surface depth calculations should be performed to check that adequate water levels are developed in HDPE culverts for passage of the largest individuals of the target species with appropriate design discharges. Ultimately the choice of excluding baffles from the design should be based on sound fish passage theory backed by experienced judgment. However, it is reasonable that non-baffled HDPE culverts on very mild slopes (S_o $<$ 0.25%) with low average velocities (V $<$ 1 m/s) and adequate depths during migratory periods of the year are likely not to pose a barrier to mature salmonid individuals.

4.7 Conclusions and Recommendations

The full flow baffle roughness coefficients determined herein represent unique and beneficial data which should be of value to practitioners involved in the design of HDPE retrofit culverts. Full flow

roughness coefficients (Manning's h and Darcy-Weisbach's friction factor f) were determined for a wide array of baffle types (weir, slotted weir and spoiler baffles), roughness heights (h = 0.15D, 0.10D and 0.05D) and roughness spacings (λ = 0.6D, 1.2D, 1.8D, 2.4D). An analytical model was derived from the energy equation to determine the effects of roughness reduction (α), radial reduction (β), inlet loss coefficient (k_e) and culvert length (L) on two practical slipline rehabilitation scenarios. Results from the analytical model suggest that baffling slipline culverts is a feasible practice in many situations to improve hydraulic conditions for fish passage and still respect the parent culvert's original design discharge. The increased discharge capacity caused by the hydraulically smooth surface of HDPE slipliner culverts was shown to not necessarily be sufficient to compensate for radial reductions in shorter culverts. Furthermore, the wide variation in the experimentally determined roughness coefficients (n varied between 0.012 and 0.024) demonstrates that culvert designers have considerable flexibility in their choice of baffle when attempting to optimize fish passage conditions and the needs of hydraulic capacity. Also the following conclusions were made:

Baffles are likely not a feasible option when radial reductions are inferior to $\beta < 0.80$. This general limit can be increased under certain circumstances where the culvert is very long and fitted with an inlet treatment and a low α value baffle configuration is installed.

- Baffle roughness height (h) was determined to be the primary geometric parameter affecting roughness.
- Roughness spacing (α) plays a secondary, yet important role in determining hydraulic roughness.
- The hydraulic capacity of shorter outlet controlled culverts is most improved by the installation of an inlet treatment followed secondly by choosing a low α value baffle configuration.
- In combination with an appropriate inlet treatment, baffle configurations with larger α values (i.e., 0.8) can likely be used in shorter outlet controlled culverts as well as short inlet controlled culverts (with or without inlet treatment) with little risk of significantly decreasing hydraulic capacity.
- Improving hydraulic capacity by choosing a low α value baffle configuration is a recommended practice for longer culverts that are heavily controlled by barrel friction losses.

Performing a thorough investigation of the effectiveness of low λ and α value spoiler baffles in HDPE culverts with live specimens of various fish species would be an insightful endeavor. Such a study would draw conclusions on whether low roughness baffle configurations can effectively develop proper hydraulic conditions necessary for successful fish passage over a range of slopes, discharges and lengths.

4.8 Acknowledgements

The authors would like to thank the NSERC, the groupe de recherche interuniversitaire en limnologie et en environnement aquatique (GRIL) as well as Hydro-Québec for providing the funding necessary to perform this project. We would also like to give our immense appreciation to Normand Bergeron (INRS) for his priceless advice on how best to install the baffles and Nicolas Simard for his invaluable technical assistance during the laboratory phase of this project.

4.9 Notation

The following symbols are used in this paper:

b = slot width (SWB) [L];
C_1 = 49.32 [L/T^2];
D = interior diameter [L] ;
f = Darcy-Weisbach friction factor [-];
g = gravitational constant [L/T^2] ;
h = baffle height [L];
h_f = friction losses [L];
k_{in} = entrance loss coefficient [-];
k_{out} = exit loss coefficient [-];
k_b = constant 49.35 (S.I.);
L = length [L];
n = Manning's roughness coefficient [-];
Q_o = discharge of parent culvert [L^3/T];
Q = discharge of slipliner [L^3/T];
Q_{100} = 100 year design discharge [L^3/T];
r = inside radius of slipliner culvert [L];
r_o = inside radius of parent culvert [L];
$\mathbf{R}$ = bulk Reynold's number [-];
R = hydraulic radius [L];
R^2 = coefficient of determination [-];
S = culvert slope [-];
V = velocity [L/T];
w = baffle width [L];
y = depth [L];

Y_1 = upstream water level [L];

Y_2 = downstream water level [L];

α = roughness reduction ratio [-];

β = radius reduction ratio [-];

β_o = slope of the linear regression Eq.(refregression) [-];

β_1 = y-intercept of the linear regression Eq.(refregression) [-];

λ = baffle spacing [-];

ρ = density [M/L^3];

μ = viscosity [M/(LT)]; d

Chapter 5

Additional Spoiler Baffle Testing

5.1 Introduction

The literature review presented in chapter 2, section 2.4 lists a number of advantages inherent to the spoiler baffle (SPB) configuration. Work by Macdonald and Davies (2007) demonstrated that passage success rates markedly improved with increasing spatial complexity. In-line rows of single spoiler baffles significantly underperformed more spatially complex SPB arrangements (i.e. rows of two SPB followed by rows of three SPB). The baffles studied were of very low height ($h = 0.018$D and $h = 0.037$D), and regardless of their small size, greatly outperformed bare control culverts in fish passage success tests. A principal finding of the work in chapter 4 of the present thesis was that baffle height is the dominant parameter affecting energy losses for fully pressurized flow. Thus baffle height is directly related to hydraulic capacity and therefore decreases in baffle height will result in improved conveyance. Furthermore, the findings of Macdonald and Davies (2007) suggests that low height, spatial complex spoiler baffle configurations may potentially be used to improve fish passage through HDPE slipliner culverts, while simultaneously reducing the baffles' effect on hydraulic capacity. Consequently, well designed SPB arrangements may be able to address a larger number of failing culverts through the use of the economically advantageous HDPE slipliner culvert, yet still adhere to environmental regulations requiring measures to ensure fish passage (i.e., the installation of baffles).

The work presented in the following chapter has the objective of determining fully pressurized roughness coefficients for a number of spoiler baffle configurations of varying spatial complexity and baffle height. It is intended as a compliment to the work of chapter 4. The experimental setup used to investigate the spoiler baffle configurations was identical to that described in chapter 4 section 4.2. The following sections describe the geometry of the spoiler baffle configurations studied, the obtained roughness results, analysis and subsequent discussion.

5.1.1 Tested Spoiler Baffle Configurations

A total of four SPB configurations were tested for fully pressurized roughness coefficients. The first configuration [Fig. 5.1(a)] consisted of alternating rows of two and three spoiler baffles. A 30° angle of separation was used between the vertical and the center line of the exterior baffles for the rows of three baffles (see Fig. 4.1). A 15° angle of separation from the vertical was used for the rows composed of two baffles. The second configuration [Fig. 5.1(b)] was composed of rows of two spoiler baffles, again with a 15° angle of separation from the vertical. The third configuration [Fig. 5.1(c)] consisted of alternating rows of one and two spoiler baffles with an angle of separation from the vertical of 15°. Finally, the fourth configuration [Fig. 5.1(d)] was simply composed of rows of a single spoiler baffle. Each of the four spoiler baffle configurations were tested at the following four spacings ($\lambda = 0.6$D, 1.2D,

1.8D and 2.4D). Furthermore, each configuration was tested at three baffle heights (h=0.15D, h=0.10D and h=0.05D). Figure 4.1 in chapter 4 presents the geometric parameters defining the dimensions of the tested spoiler baffles. The reader is directed towards chapter 4 section 4.2 for a thorough explanation of the experimental design as well as the theory that was applied to determine the roughness coefficients.

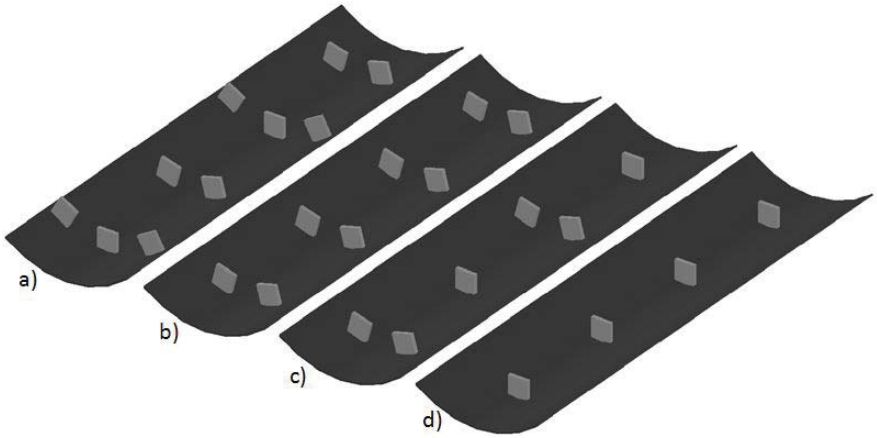

Figure 5.1: The four supplementary spoiler baffles configurations; (a) the 3-2-3 configuration, (b) 2-2-2, (c) 2-1-2 and (d) 1-1-1.

5.2 Results and Analysis

Figure 5.2 presents the individual trial results for each of the spoiler baffle configurations tested. The left y-axis of Fig. 5.2(a-d) displays the scaling for the roughness value n. In contrast, the right y-axis displays the scaling for $\sqrt{f}$. The square root of f was used in order to present n and f values on the same series. This is unavoidable since n and f are not linearly related to each other in the Chezy-Manning relation (Eq. 4.3). The nine tested flow rates appear on the bottom x-axis and their corresponding **R** values appear on the upper x-axis. Complete tables of the raw experimental data are available for viewing in the appendix A for each of the four supplementary baffle configurations tested.

Figure 5.3 presents the average roughness values for each of the flow rate series presented in Fig. 5.2. Standard error bars were omitted from Fig. 5.3 for reasons of clarity. Table 5.1 presents the same data as Fig. 5.3 along with an error estimation expressed as the standard deviation of each respective roughness trial data series.

Roughness values for each of the nine tested flow rates are randomly scattered about the mean of the series of each of the respective configurations presented in Figs. 5.2(a - d). It is not possible to establish clear trends between **R** and $\sqrt{f}$ over the range of **R** for any of the baffle configurations tested; suggesting **R** and $\sqrt{f}$ independence. Roughness coefficients are the highest for the SPB-3-2-3-0.15D baffle configuration for the four values of λ tested.

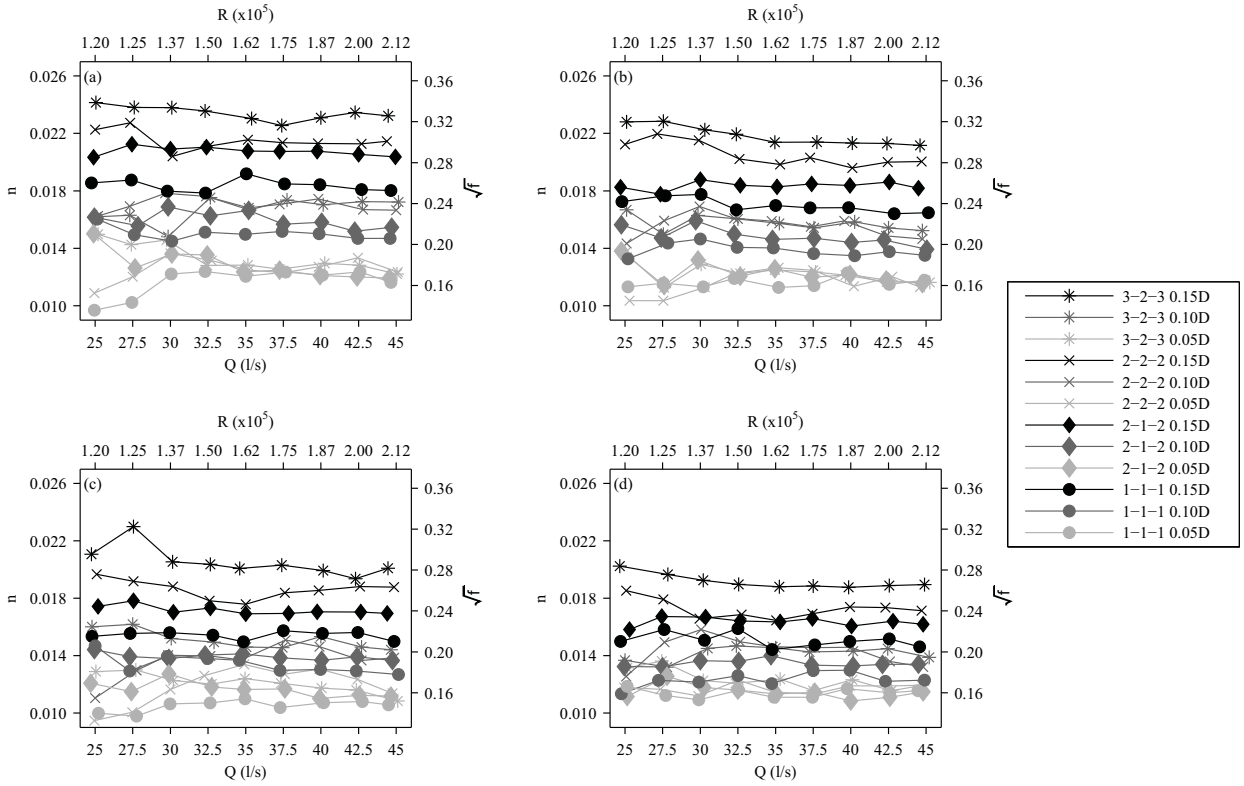

Figure 5.2: Individual Manning roughness n and $\sqrt{f}$ trial data versus flow rate and corresponding **R** for each of the four spoiler baffle configurations tested at λ of a) 0.6D, b) 1.2D, c) 1.8D, d) 2.4D

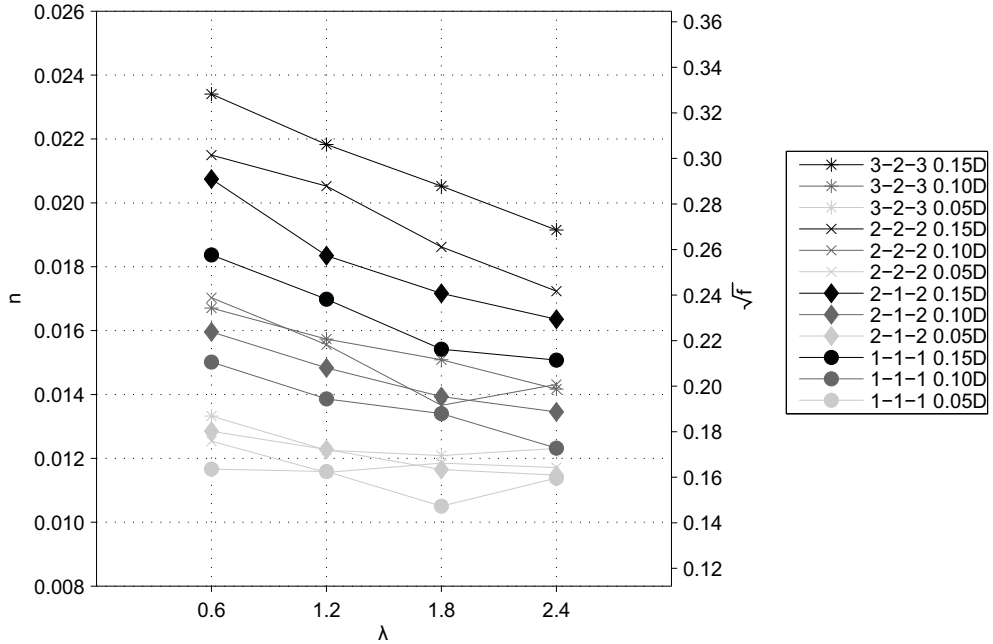

Figure 5.3: Series averaged roughness values for each of the spoiler baffle configurations tested

Table 5.1: Series averaged roughness coefficients for each of the spoiler baffle configurations tests. Error is expressed as standard deviation in parenthesis

Baffle Type	h	λ=0.6D				λ=1.2D Spacing				λ=1.8D Spacing				λ=2.4D Spacing			
		n		f		n		f		n		f		n		f	
3-2-3	0.15D	0.0234	(0.0005)	0.1078	(0.0042)	0.0218	(0.0006)	0.0938	(0.0054)	0.0205	(0.001)	0.0830	(0.0082)	0.0191	(0.0005)	0.0722	(0.0036)
	0.1D	0.0167	(0.0008)	0.0550	(0.0051)	0.0157	(0.0005)	0.0487	(0.0032)	0.0151	(0.0006)	0.0448	(0.0037)	0.0142	(0.0005)	0.0395	(0.0025)
	0.05D	0.0133	(0.0009)	0.0351	(0.005)	0.0123	(0.0007)	0.0296	(0.0034)	0.0121	(0.0006)	0.0288	(0.0029)	0.0123	(0.0006)	0.0299	(0.0032)
2-2-2	0.15D	0.0215	(0.0006)	0.0910	(0.0054)	0.0205	(0.0008)	0.0830	(0.0064)	0.0186	(0.0006)	0.0683	(0.0044)	0.0172	(0.0006)	0.0585	(0.0043)
	0.1D	0.0170	(0.0005)	0.0571	(0.0032)	0.0156	(0.0008)	0.0477	(0.0047)	0.0137	(0.0011)	0.0369	(0.0055)	0.0143	(0.001)	0.0405	(0.0053)
	0.05D	0.0125	(0.0008)	0.0310	(0.0037)	0.0116	(0.0008)	0.0264	(0.0036)	0.0118	(0.0013)	0.0279	(0.0057)	0.0117	(0.0003)	0.0270	(0.0015)
2-1-2	0.15D	0.0207	(0.0003)	0.0847	(0.0023)	0.0183	(0.0003)	0.0662	(0.0019)	0.0172	(0.0003)	0.0580	(0.002)	0.0164	(0.0003)	0.0526	(0.0018)
	0.1D	0.0160	(0.0005)	0.0502	(0.0034)	0.0148	(0.0006)	0.0433	(0.0034)	0.0139	(0.0002)	0.0382	(0.0012)	0.0135	(0.0002)	0.0356	(0.0013)
	0.05D	0.0128	(0.001)	0.0326	(0.0051)	0.0123	(0.0007)	0.0298	(0.0037)	0.0116	(0.0005)	0.0267	(0.0023)	0.0115	(0.0005)	0.0259	(0.0022)
1-1-1	0.15D	0.0184	(0.0004)	0.0664	(0.003)	0.0170	(0.0005)	0.0568	(0.003)	0.0154	(0.0003)	0.0468	(0.0016)	0.0151	(0.0005)	0.0448	(0.0028)
	0.1D	0.0150	(0.0004)	0.0444	(0.0025)	0.0139	(0.0004)	0.0378	(0.0023)	0.0134	(0.0006)	0.0354	(0.0033)	0.0123	(0.0005)	0.0299	(0.0023)
	0.05D	0.0117	(0.0009)	0.0269	(0.0041)	0.0116	(0.0003)	0.0264	(0.0015)	0.0105	(0.0004)	0.0217	(0.0015)	0.0114	(0.0003)	0.0255	(0.0013)

Clear descending trends in roughness with increasing values of λ are observed in Fig. 5.3. This is especially true for the spoiler baffle configurations with larger roughness heights of $h = 0.15$D and $h = 0.10$D. The descending trend for the smaller $h = 0.05$D configurations, however, are more subtle. Clear variations in roughness for the larger $h = 0.15$D and $h = 0.10$D spoiler baffle height are apparent. Furthermore, roughness varies markedly between baffle configuration spatial complexities for $h = 0.15$D than it does for $h = 0.10$D and $h = 0.05$D. To illustrate, the difference in Manning's roughness between SPB 3-2-3-0.15D-0.6D and SPB 1-1-1-0.15D-0.6D is a reduction of approximately 21%. However, only 10% reduction is exhibited between SPB 3-2-3-0.10D-0.6D and SPB 1-1-1-0.10D-0.6D.

In order to confirm that negative correlations do indeed exist between roughness and λ, an ordinary least squares regression analysis was performed. The linear regression model takes the form of Eq. 5.1, where β_1 and β_o are the regression coefficients and respectively represent the y-intercept and the slope of the regression line. The regression coefficients β_1 and β_o along with the R^2 were determined and are presented in 5.2. P-values for each of the equations were also obtained and are useful for determining if the calculated regression coefficients β_1 and β_o are derived by chance or are indeed due to a statistically significant correlation. Regression coefficients having P-values less than 0.05 are generally considered to provide accurate estimations of the variables in question.

$$n = \beta_1 + \beta_o \lambda \tag{5.1}$$

As can be seen in Table 5.2, the P-values for β_1 are all < 0.05 demonstrating that the y-intercept of

the regression equation is statistically relevant. The *P*-values for β_o, on the other hand show much more variability. Of the 12 configurations tested, four configurations (SPB 3-2-3-0.05D, SPB 2-2-2-0.05D, SPB 2-2-2-0.10D and SPB 1-1-1-0.05D) surpass the *P*-value threshold of 0.05. Interestingly, three of these four configurations are for $h = 0.05$D baffle heights. Furthermore, the β_o values for these same four configurations are nearly horizontal, thus any descending trends with λ for $h = 0.05$D spoiler baffles are likely due to chance. For the larger baffle heights ($h = 0.15$D and $h = 0.10$D) the *P*-values for the β_o all respect the 0.05 threshold with the exception of the SPB 2-2-2-0.10D, with a *P*-value of 0.12. In spite of this elevated *P*-value, a clear descending trend for this configuration is visible in Fig. 3. The elevated *P*-value is likely due to a rather low roughness value at $\lambda = 1.8$D, a small sample size (i.e., n=4) and possible experimental errors. The OLS regression model is therefore a useful tool for estimating the roughness coefficients of spoiler baffles with λ values intermediate to those tested here with heights of $h = 0.15$D and $h = 0.10$D.

Table 5.2: Results from the ordinary least squares analysis performed on the series averaged roughness data versus λ

Baffle Type	***h***	β_1	β_o	R^2	β_1			
					P-value	Low 95%	High 95%	P-value
3-2-3	0.15D	0.025	-0.0023	0.998	0.000	0.024	0.025	0.001
	0.1D	0.017	-0.0014	0.995	0.000	0.017	0.018	0.003
	0.05D	0.013	-0.0005	0.543	0.002	0.011	0.016	0.263
2-2-2	0.15D	0.0231	-0.0024	0.987	0.0002	0.0217	0.0246	0.0068
	0.1D	0.0177	-0.0017	0.762	0.0038	0.0130	0.0223	0.1272
	0.05D	0.0125	-0.0004	0.427	0.0016	0.0103	0.0146	0.3468
2-1-2	0.15D	0.022	-0.0024	0.939	0.001	0.019	0.025	0.031
	0.1D	0.017	-0.0014	0.970	0.000	0.015	0.018	0.015
	0.05D	0.013	-0.0008	0.956	0.000	0.012	0.014	0.022
1-1-1	0.15D	0.019	-0.0019	0.946	0.001	0.017	0.022	0.027
	0.1D	0.016	-0.0014	0.976	0.000	0.015	0.017	0.012
	0.05D	0.012	-0.0003	0.219	0.004	0.009	0.015	0.532

5.3 Analysis and discussion

The roughness results presented in Fig. 5.3 display a wide range of variation in roughness between the SPB configurations. Culvert designers can use this variability to their advantage when choosing a configuration to best meet the hydraulic conveyance requirements of the culvert as well as those for fish passage. To address the concern of hydraulic capacity, the roughness coefficients presented in Table 5.1 can be applied to determine the configuration's influence on hydraulic capacity with Eq. 4.8. Baffles

can be selected based on their ability to respect discharge requirements. However, the choice of an appropriate baffle for fish passage is a more delicate matter. Revisiting the findings of Macdonald and Davies (2007) and coupling them with a discussion of the present studies findings provides insights on this matter.

Before proceeding, it is useful to underline some important differences between the present study and that of Macdonald and Davies (2007). The smallest baffle height configurations tested here was $h =$ 0.05D. This is slightly higher than the baffles used by Macdonald and Davies (2007). Their baffles were also wider (70 mm) than the baffles used in the present study, especially for the $h = 0.05$D configurations which had a width of 12.7 mm. Unfortunately, the effect of spoiler baffle width was not examined herein and it is therefore not certain how spoiler baffle width affects hydraulic roughness. It should be kept in mind that the work of Macdonald and Davies (2007) involved smaller fish species indigenous to Australia (*Galaxias maculatus*) which may not necessarily reflect the swimming capacities and passage needs of native North American fish species. However, this opens the door for a study orientated towards the passage of North American species through spoiler baffled HDPE culverts.

To begin with, the findings of Macdonald and Davies (2007) demonstrated that spoiler baffles with $h <$ 0.05D are still very effective at improving fish passage. Table 5.3 presents the alpha values of the various spoiler baffles to be used in conjunction with Eq. 4.8 in chapter 4 to determine discharge variation. As a reminder to the reader, the α value is calculated by dividing the experimentally determined roughness Manning's roughness coefficient by the commonly accepted h value for corrugated steel (n = 0.024). From Table 5.3 it can be seen that the $h = 0.05$D spoiler baffles produce alpha values in the range of α=0.56 and 0.50 - only slightly higher than the alpha value of a bare HDPE culvert (0.38). Low alpha values for a particular configuration indicates that it will have a limited impact on the discharge. Therefore, small h spoiler baffles, such as the 0.05D configurations studied herein can be used to provide for fish passage with limited risk to hydraulic capacity.

Macdonald and Davies (2007) demonstrated that fish passage success is positively correlated to spoiler baffle spatial complexity. The authors attributed this correlating to the greater number of available low velocity resting zones formed behind individual baffles as well as the shorter lateral and longitudinal navigable distances separating them. From Table 5.3 it can be seen that even the most spatially complex baffle configuration (3-2-3) at $h = 0.05$D and $\lambda = 0.6$D has a very low alpha value ($\alpha = 0.56$). Furthermore, in Fig. 5.3, it is observed that roughness shows very little variation with increased baffle complexity at baffle heights of 0.05D (the values vary sporadically about a mean of approximately $n =$ 0.012). Therefore, spatially complex 3-2-3 baffle configurations at $h = 0.05$D and $\lambda = 0.6$D can be used

		α			
Baffle Type	***h***	**λ=0.6**	**λ=1.2**	**λ=1.8**	**λ=2.4**
3-2-3	0.15D	0.98	0.91	0.86	0.80
	0.1D	0.70	0.66	0.63	0.59
	0.05D	0.56	0.51	0.50	0.51
2-2-2	0.15D	0.90	0.86	0.78	0.72
	0.1D	0.71	0.65	0.57	0.60
	0.05D	0.52	0.48	0.49	0.49
2-1-2	0.15D	0.86	0.76	0.72	0.68
	0.1D	0.66	0.62	0.58	0.56
	0.05D	0.54	0.51	0.49	0.48
1-1-1	0.15D	0.77	0.71	0.64	0.63
	0.1D	0.63	0.58	0.56	0.51
	0.05D	0.49	0.48	0.44	0.47

Table 5.3: Alpha values of the tested spoiler baffle configurations (a bare HDPE slipliner has an α value of 0.038)

instead of baffle configurations with less spatial complexity (i.e., 2-2-2, 2-1-2, 1-1-1) to improve fish passage without substantially compromising hydraulic capacity. It can be speculated that even further increases in spatial complexity (e.g., alternating rows of three and four or even four and five) would cause only slight increases in roughness.

Even though inline 1-1-1 baffles were shown by Macdonald and Davies (2007) to be ineffective for passing fish compared to the more spatially complex configurations, the roughness coefficients of 1-1-1 baffles are still of interest. In very long culverts a series of large resting zones would likely improve fish passage. The use of larger spoiler baffles interspersed among smaller more spatially complex baffle configurations would produce such resting habitats. Fish may use the lower velocity wake zones developed downstream of the larger baffles to rest before attempting subsequent ascents. The hydraulic roughness of a heterogeneous baffle height configuration would likely be dominated by the roughness developed by the higher baffles and be only marginally influenced by the shorter baffles. Consequently, the roughness of the combined baffle configuration would likely equal that developed by a 1-1-1 spoiler baffle configuration for an appropriately chosen value of h and λ. Further investigations are needed to determine the effectiveness of such a combined design at passing fish and also to ascertain if indeed the corresponding roughness coefficients could be approximated by the roughness values of the 1-1-1 configurations.

5.3.1 Reynolds independence

Similar to the discussion presented on Reynold's independence for WB, SWB and the 3-3-3 spoiler baffle arrangements in chapter 4, section 4.5, the lack of any linear (or other) correlation between n and **R** in Fig. 5.2 suggests Reynolds independence over the range of Reynolds numbers studied. From Fig. 5.3 it can be seen that roughness values for the various configurations have not yet attained a plateau with decreasing λ. This is indicative of isolated roughness flow which has been shown by Morris (1955) to develop curves of descending f values for increasing **R** values. In theory, for an isolated roughness regime, roughness values will drop with increasing **R**, and therefore the values presented in Table 5.1 should be conservative estimates of the full flow barrel roughness for culvert designs at higher **R** values.

5.3.2 Discussion on the experimental design

Concern may be given as to whether testing the roughness of 2D steel plates can accurately represent the roughness induced by plastic streamlined 3D spoiler baffles commonly used (though blocks are used often as well) in slipline culverts. The majority of 3D baffle forms can be decomposed into constituent ellipsoidal, conic or cubic 3D bodies. Even though the respective drag coefficients of these streamlined forms are highly dependent on a number of geometric parameters, the most conservative estimates are nearly half that of a two dimensional flat plate White (2009). Therefore it goes to reason that the use of 2D plates is a conservative approach for estimating the friction coefficients of more streamlined 3D baffles. Furthermore, Christodoulou (2013) found that arrays of rounded edge objects immersed in steep open channel flows produced significantly smaller n values than similar sized objects with sharp edges. It is also likely that inserting and sealing plate spoiler baffles into a full diameter HDPE slipline culvert from the exterior may prove to be a more practical and less costly installation technique compared to traditional plastic welding methods necessary for 3D forms. This installation method would also facilitate the use of baffles inside HDPE culverts of small diameter which inhibit workers from entering. Care should be taken to ensure that the edges of the chosen baffle are smooth as to not injure fish.

5.4 Conclusions and Further Research

The roughness coefficients obtained in this study demonstrate that spoiler baffle configurations do exist to meet the hydraulic capacity of HDPE slipliners. Spoiler baffle configurations with low relative roughness heights ($h = 0.05$D), similar to those demonstrated by Macdonald and Davies (2007) which were shown to significantly improve fish passage, were found to produce roughness coefficients slightly higher than bare (HDPE) pipe. Furthermore, the lowest baffle height configurations studied demonstrated very little variance in roughness among themselves with increasing spatial complexity. For these

reasons the installation of 3-2-3 (and possible even more spatially complex designs) spoiler baffles with low relative roughness heights is likely the most appropriate action to address the problem of fish passage in HDPE culverts without causing substantial detriment to the hydraulic capacity.

The analysis of these supplementary spoiler baffle configurations brings to the surface a few research questions that warrant further investigation. First of all, would the use of larger baffles interspersed among a standard configuration of spoiler baffles improve fish passage by providing relatively large resting zones in their wake? Also, how would such an arrangement affect hydraulic roughness? Passage success was shown by Macdonald and Davies (2007) to improve with increasing spatial complexity, however, what are the appropriate limits for the lateral and longitudinal spacing between spoiler baffles? Should these limits be tailored to the characteristic swimming abilities of individual species? How should baffle height be adjusted for individual fish species? Surely larger fish require deeper inter-baffle water depths to properly swim. Very little has been done to improve the understanding on the effectiveness of various spoiler baffle forms at reducing debris blockage and improving sediment transport in slipliner culverts. These questions should all be thoroughly investigated if spoiler baffles are to be widely accepted as an appropriate candidate as a standard baffle configuration for use in slipliner culverts.

Chapter 6

Conclusion

6.1 Introduction

From a practical perspective, high density polyethylene sliplining is an ideal method to address the problems associated with failing culverts. Sliplining reduces costs, construction delays and consequently the impact on the smooth operation of highways and rail lines. However, recent research has shown that HDPE sliplining leaves much to be desired from the perspective of fish passage. The smooth surface of the HDPE culvert drastically increase velocities and reduces depths - both of which pose potential passage barriers. In an ideal world, every culvert would be replaced by a wide span bridge replete with natural substrate. Unfortunately, such a world is unlikely due to cost contraints. Consequently society is confided with the responsibility of identifying a compromise between the practical constraints that transport agencies are required to operate under (mainly funding and project deadlines) and the often far too lofty ideals of sustainable development. This thesis endeavored to do just that. Four research questions were posed in the introductory pages of this text with the intent of structuring a research approach with the objective of improving fish passage and hydraulic capacity of HDPE slipliner culverts. The principal contributions stemming from this research are summarized in the following sections.

6.1.1 How does HDPE sliplining affect depth and velocities?

The study presented in chapter 3 revealed the consequences of replacing a corrugated steel pipe with an HDPE slipliner on depth and velocity. The use of the Manning's open channel equation along with minimum and maximum roughness coefficients provided an estimation of the maximum possible variation of velocity and depth. Velocity was found to increase anywhere from 65 to 300% percent depending on the values of n used for the corrugated steel culvert and the HDPE slipliner. Depth was found to vary between -25% and -60%, also depending on the roughness of the two culverts. The use of the average n value of 0.024 for corrugated steel and an n value 0.009 for HDPE produced an estimated percent change in depth of -36% and velocity of 102%. If the actual n value of the corrugated steel was higher (e.g., $n = 0.034$), as it often is for flow at low relative depths, then the variation in depth and velocity would be increased by an even larger factor. The lowest values of n for HDPE was taken to be 0.004 from findings of Devkota et al. (2012). When this value was applied for the HDPE slipliner, velocities increased even further to 260% and depths decreased by -58%. In light of these findings, a conservative approach to estimating the variation in depth and velocity would be to use $n = 0.004$ instead of using the full flow value of 0.009 for HDPE slipliner culverts. Given the substantial depth and velocity variations estimated from this analytical study, it is strongly suggested that attempts at improving the flow field be undertaken to alleviate fish passage difficulty in HDPE culverts. This findings fully justified the research efforts of Chapters 4 and 5. A study aimed at experimentally verifying these analytical

findings would be beneficial.

6.1.2 How does a baffle configuration's geometric parameters affect energy losses?

The work performed in Chapters 4 and 5 provided insights pertaining to the effects of baffle geometries on energy losses. First, it was determined that the baffle height (h) was the predominant parameter affecting energy losses. To illustrate, the $h = 0.15D$ baffle configurations (WB, SWB and SPB) all produced much higher n values than the $h = 0.10$D and 0.05D configurations. Manning's n values decreased only marginally with increased spacing for all of the configurations tested. Regarding spoiler baffles, it was found that increasing spatial complexity does increase energy losses however to a lesser degree than baffle height (see Fig. 5.3). Therefore, energy losses are best reduced by decreasing the height of the baffles rather than increasing the spacing between baffles or decreasing the spatial complexity of spoiler baffle arrangements.

On another note, the results of chapter 4 demonstrated Reynold's independence for fully pressurized flow over the tested baffle configurations. It is likely that baffles with scaled geometries to fit larger real life culvert diameters will also demonstrate Reynold's independence, or if not complete Reynold's independence, a descending f-R curve representative of isolated roughness flows. Reynold's dependence is correlated to baffle spacing and if baffles are too closely spaced, a rising f-R curve indicative of wake interference flow may prevail. As a word of caution, testing closely spaced baffles at low Reynold's numbers may have the consequence of underestimating the roughness coefficients.

6.1.3 Can baffles be used in HDPE slipliner rehabilitaitons?

Unfortunately, there is not a black or white answer to this third question given its highly dependent nature on a wide range of parameters. If it can be shown that the slipliner culvert will run under inlet control, then baffle installation is a promising option. This is because inlet controlled culverts are not affected by barrel roughness and consequently baffles will have no affect on the hydraulic capacity of the culvert. There is one exception to this last statement, there is the possibility that roughness can be increased so much by the presence of baffles that the culvert will switch from an inlet control regime to an outlet control regime - the designer should be wary of this. However, if the parent culvert was designed to run under outlet control, or it can be shown that the slipliner culvert will run under outlet control, then determining if installing baffles is appropriate will require further analysis. From results obtained from an analytical model (Eq. 4.8) derived from the energy equation in Chapter 4 it was determined that HDPE slipliners with radial reductions greater than 15% will not be able to house baffles. Fortunately,

the majority of culverts are designed to run under inlet control and therefore the use of baffles is likely an acceptable practice for a large number of culverts (though the possibility of a control regime shift should be analyzed). However, in the case of outlet controlled culverts, it was shown in chapters 4 and 5 that many low roughness baffle configuration options are possible. Further increases in hydraulic capacity can be gained from the installation of end treatments such as a hydraulic bell at the inlet. The combination of an inlet treatment and a low roughness baffle configuration is likely to respect the hydraulic conveyance requirements in HDPE slipliner culverts.

6.1.4 How can practitioners optimize hydraulic capacity and fish passage in HDPE slipliners?

This last question is by large the most important for practitioners involved in the design of HDPE culverts. Certainly the findings of the present thesis can be used to provide recommendations for improving both fish passage and hydraulic capacity in HDPE culverts; however, more research with live fish species representative of wild fish populations is required. We now know that energy losses are most highly influenced by baffle height, therefore smaller baffles heights should be preferred. However, how small is too small? The work of MacDonald and Davies (2007) found that small spoiler baffles significantly improved fish passage through a smooth concrete culvert. However, they studied a very small fish species and therefore it is not known whether small baffles would also be effective for larger fish such as the trout and salmon species native to North America.

Nevertheless, if hydraulic discharge is of great concern then reducing baffle height will significantly improve capacity. The author is of opinion that spoiler baffles (or possibly stream lined spoiler baffles) are the superior choice over WB and SWB and other larger baffle designs for use in HDPE slipline culverts. Spoiler baffles have been shown to considerably reduce fish passage times through test culverts compared to other baffle forms (Feurich et al. 2012) and they are known to improve passage success rates at very low baffle heights (MacDonald and Davies 2012). Further research into the development and testing of a streamlined spoiler baffle with live adult and juvenile fish native to North America will likely culminate in a baffle design that most closely approaches the ideal for HDPE slipline culverts. However, until such research is performed, the author suggests the installation of (at minimum) a 2-1-2 spoiler baffle configuration with baffle heights of $h < 0.10D$. Arguably, spoiler baffle configurations of increased spatial complexity are likely to improve fish passage with only marginal costs to hydraulic capacity. Regardless of the chosen spatial complexity, the suggestion by Feurich et al. (2012) to scale baffle height to fish size should be followed. Therefore, for large diameter culverts (> 1 m) it is likely unnecessary to continue scaling the baffle height with culvert diameter. Instead baffle height could be limited, for example, to 0.1

m. Further research is needed in this area to determine appropriate minimal baffle heights for species of fish of high socioeconomic importance to North America.

6.1.5 Concluding Remarks

This project proved to be an enriching introduction to the growing field of ecohydraulic engineering. Countless hours of sifting through the works of those that have come before me has opened my eyes to the importance of ensuring the perennial connectivity of our streams and rivers if we wish to continue benefiting from the joy they offer. It will take a concerted effort from all levels of government and industry to successfully address this problem in its entirety. The work of this thesis is but a small contribution to this task. Nevertheless, the author is hopeful that the insights gained by this project will be of benefit to engineers, biologists, slipline manufactures, industry and government representatives alike.

6.2 Conclusion version française

6.2.1 Introduction

D'un point de vue pratique, la réhabilitation des ponceaux en tôle ondulée par l'insertion d'un ponceau en polyéthylène haute densité (PEHD) est une méthode idéale pour résoudre les problèmes liés à des ponceaux défaillants. Cette pratique réduit les coûts, les délais de construction et l'impact sur le bon fonctionnement des routes et des voies ferroviaires. Cependant, des recherches récentes ont montré que cette pratique laisse quelque peu à désirer en ce qui concerne le passage des poissons. Cela est entre autre dû à la surface lisse du ponceau en PEHD qui augmente considérablement les vitesses et réduit les profondeurs. Optimalement, un ponceau défaillant serait remplacé par un pont à travée large rempli de substrat naturel. Malheureusement, en raison de contraintes budgétaires, il est souvent nécessaire de faire un compromis entre les contraintes subites par les organismes de transport et les principes du développement durable. Quatre questions de recherche ont été posées dans les premières pages de ce mémoire afin de structurer une démarche de recherche ayant pour objectif d'améliorer le passage des poissons et la capacité hydraulique de ponceaux réfectionnés par des ponceaux en PEHD. Les principales contributions découlant de ces recherches sont résumées dans les sections suivantes.

6.2.2 Qu'arrive- t-il aux vitesses et profondeurs après qu'un ponceau en tôle ondulée soit réfectionné par un ponceau en PEHD?

L'étude présentée dans le chapitre 3 a révélé les conséquences que le remplacement d'un tuyau en acier ondulé par un ponceau en PEHD peut avoir sur la profondeur et la vitesse de l'écoulement.

L'utilisation de l'équation de l' Manning pour les écoulements à surface libre avec des coefficients de rugosité minimal et maximal fournit une estimation de la variation maximale possible de la vitesse et de la profondeur. La vitesse s'est avérée augmenter entre 65 à 300 % en fonction des valeurs de n utilisés pour décrire la rugosité du ponceau en tôle ondulée et le ponceau en PEHD. La profondeur variait également entre -25 % et -60 %, en fonction de la rugosité des deux ponceaux. L'utilisation de la valeur moyenne de n de 0,024 pour l'acier ondulé et un n valeur de 0,009 pour le ponceau en PEHD produit une variation approximative de profondeur de -36 % et une variation de la vitesse de 102 %. Si la valeur réel de n de la tôle ondulée était plus élevée (par exemple, $n = 0{,}034$), comme c'est souvent le cas pour les écoulements à des profondeurs relativement faibles, alors la variation de la profondeur et de la vitesse serait augmentée d'un facteur encore plus élève. La valeur le plus faible probable de $n = 0.004$ pour PEHD a été prise à partir des résultats de Devkota et al. (2012). Lorsque cette valeur a été appliquée pour le ponceau en PEHD, les vitesses augmentaient davantage pour atteindre 260 % et les profondeurs ont diminué de -58 %. À la lumière de ces résultats, une approche prudente à l'estimation de la variation de la profondeur et de la vitesse serait d'utiliser $n = 0{,}004$ au lieu d'utiliser la valeur pour un écoulement plein de 0,009 pour les ponceaux en PEHD. Compte tenu des variations importantes de la profondeur et de la vitesse estimées à partir de cette étude analytique, il est fortement recommandé que les tentatives soient prises afin d'atténuer les problématiques nuisant au passage des poissons dans des ponceaux en PEHD. Ces conclusions justifient pleinement les efforts de recherche des chapitres 4 et 5. Une étude visant à vérifier expérimentalement ces résultats d'analyse serait bénéfique.

6.2.3 Qu'est-ce que la relation entre les paramètres géométriques des chicanes à poisson et les pertes d'énergie engendrées dans le système?

Les travaux effectués dans les chapitres 4 et 5 fournissent des connaissances relatives aux effets qui peut avoir les géométries de chicanes sur les pertes d'énergie. Tout d'abord, il a été déterminé que la hauteur de la chicane (h) est le paramètre prépondérant affectant les pertes d'énergie. Pour illustrer, les configurations de chicanes ayant $h = 0{,}15D$ ont toutes les valeurs de n plus élevées que les configurations ayant $h = 0.10$D ou 0.05D. Par ailleurs, les valeurs de Manning ne diminuent que légèrement lorsque l'espacement augment pour toutes les configurations testées. En ce qui concerne les chicanes de type spoiler, il a été constaté que l'augmentation de la complexité spatiale fait accroître les pertes d'énergie, mais à un degré moindre qu'observé par une augmentation de la hauteur de la chicane (voir Fig. **??**) . Par conséquent, il est plus facile de réduire les pertes d'énergie en diminuant la hauteur des déflecteurs plutôt qu'en augmentant l'espacement entre les déflecteurs ou en diminuant la complexité

spatiale (dans le cas des chicanes de type spoiler). Sur une autre note, les résultats du chapitre 4 ont suggéré l'indépendance de Reynold pour l'écoulement sous pression pour les configurations de chicanes testées. Il est fort probable que des chicanes ayant des géométries mises à l'échelle réelle démontreraient également l'indépendance de Reynold, ou au moins une courbe de f-R descendante représentative des écoulements au travers des éléments de rugosité isolés. La dépendance de Reynold est corrélée à l'espacement de chicanes et si celles-ci sont trop rapprochées, une courbe f - R ascendant indicative d'un écoulement de type wake-interference peut prévaloir. Par contre, tester des chicanes rapprochées à des numéros de Reynold faibles peut avoir comme conséquence de sous-estimer les coefficients de rugosité. C'est pour cette raison que de futurs travaux devraient être réalisée afin d'en tenir compte.

6.2.4 L'utilisation des déversoirs dans les ponceaux en PEHD

Malheureusement, il n'existe pas de réponse claire et précise à cette troisième question compte tenu de sa nature fortement dépendante d'un large éventail de paramètres. Si l'on pourrait démontrer avec certitude que le ponceau réfectionné en PEHD serait contrôlé à l'entrée, alors on pourrait dire que l'installation serait une option prometteuse. Ceci découle du fait que les ponceaux contrôlés à l'entrée ne sont pas affectés par la rugosité du baril et par conséquent la présence des chicanes n'aurait aucune incidence sur la capacité hydraulique du ponceau. Il existe néanmoins une exception à cette dernière affirmation. Il est possible que la rugosité puisse être quelque peu augmentée par la présence de chicanes et qu'ainsi, le ponceau passe d'un régime de contrôle à l'entrée à un régime de contrôle à la sortie - le concepteur doit se méfier de cette possibilité. Toutefois, si le ponceau défaillant a été conçu pour être contrôlé à la sortie, ou il peut être démontré que le ponceau réfectionné serait contrôlé à la sortie avec certitude. Il est à important de mentionner qu'une analyse plus approfondie est requise afin de valider si l'installation des chicanes est appropriée. À partir des résultats obtenus par l'étude du modèle analytique (équation 4.8) dérivé de l'équation de l'énergie dans le chapitre 4, il a été déterminé que les ponceaux réfectionnés par des ponceaux en PEHD ayant des réductions radiales supérieures à 15 % ne seront pas en mesure d'héberger des chicanes à poissons. Heureusement, la majorité des ponceaux sont conçus pour fonctionner sous contrôle à l'entrée et donc l'utilisation de chicanes est probablement une pratique acceptable pour un grand nombre de ponceaux (bien que la possibilité d'un changement de régime de contrôle doive être analysée). Toutefois, dans le cas d'un ponceau contrôlé à la sortie, il a été montré dans les chapitres 4 et 5 que de nombreuses options de configuration chicanes à poissons ayant de faibles coefficients de rugosité sont disponibles. D'autres augmentations de capacité hydraulique peuvent être tirées de la mise en place de traitements à l'entrée du ponceau tel qu'une cloche hydraulique ou un autre traitement similaire. La combinaison d'un traitement à l'entrée et l'utilisation d'une configuration

de chicane à poisson de faible rugosité demeure indéniablement une méthode efficace qui permet de respecter la capacité hydraulique du design et de promouvoir le passage des poissons dans les ponceaux contrôlés à la sortie.

6.2.5 Comment optimiser la capacité hydraulique et le passage des poissons dans les ponceaux en PHED utilisé pour réfectionner les ponceaux défaillants?

Cette dernière question est de la plus grande importance pour les praticiens impliqués dans la conception des ponceaux en PEHD. Les conclusions de la présente thèse peuvent être utilisées pour fournir des recommandations ayant pour but d'améliorer à la fois le passage du poisson et de la capacité hydraulique des ponceaux en PEHD. Néanmoins, des recherches plus approfondies sur différentes espèces de poissons et cela dans un environnement de laboratoire contrôlé ou en milieu naturel seraient nécessaire. Sachant maintenant que les pertes d'énergie sont plus fortement influencées par la hauteur de la chicane, les chicanes de faible hauteur devraient être préférées dans les cas ou la capacité hydraulique et le facteur limitant. Cependant, jusqu'à quel point peut-on réduire la hauteur des chicanes sans compromettre leur efficacité pour améliorer le champ d'écoulement pour le passage des poissons? Lors de sa recherche, MacDonald et Davies (2007) ont constaté que des chicanes à faible hauteur ont sensiblement amélioré le passage des poissons dans un ponceau en béton lisse. Cependant, ils ont étudié une espèce de poisson de petite taille et donc, on ne peut pas dire avec certitude que les chicanes de faible hauteur seraient également efficaces pour les espèces de poisson plus large tel que les truites et de saumons indigènes de l'Amérique du Nord. L'auteur est d'avis que l'utilisation des chicanes de type spoiler représente le meilleur choix pour les ponceaux en PEHD utilisé pour réfectionner les ponceaux défaillants en tôle ondulée. Par exemple, les chicanes de type spoiler réduisent considérablement les temps de passage des poissons dans les ponceaux par rapport à d'autres formes de chicane (Feurich et al. 2012) et des observations ont démontrée l'amélioration du taux de réussite de passage de poisson même à des hauteurs de chicanes très faible (MacDonald et Davies 2012). Des recherches plus poussées ciblant le développement d'une chicane de spoiler aérodynamique ciblant les stades adultes et juvéniles des espèces de poissons d'importance socioéconomique en Amérique du Nord aboutiraient probablement à une conception de chicane se rapprochant la forme de chicane idéale. Toutefois, jusqu'à ce que cette recherche soit effectuée, l'auteur suggère l'installation d'une configuration de chicane de type spoiler ayant une complexité spatiale d'au moins 2-1-2 à une hauteur $h < 0{,}10D$. Indubitablement, les configurations chicanes de type spoiler d'une complexité spatiale plus importante (e.g., 3-2-3 et 4-3-4) sont susceptibles d'améliorer le passage des poissons sans avoir des effets néfastes sur la capacité hy-

draulique. Quelle que soit la complexité spatiale choisie, la suggestion par Feurich et al. (2012) d'opter pour la hauteur des chicanes en fonction de la taille des poissons devrait être prise en compte au lieu de choisir la hauteur des chicanes en fonction du diamètre du ponceau. Des recherches supplémentaires sont nécessaires dans ce domaine afin de déterminer la hauteur des chicanes appropriées pour les différentes espèces de poissons d'importance socio-économique en Amérique du Nord.

6.2.6 Mot final

Ce projet s'est avéré être une introduction enrichissante dans le domaine d'écohydraulique. D'innombrables heures de tamisage à travers les œuvres de mes prédécesseurs m'ont ouvert mes yeux sur l'importance d'assurer la connectivité entre les habitats aquatiques Il faudra un effort mutuel du gouvernement et de l'industrie pour lutter efficacement contre ce problème dans son intégralité. Le travail de cette thèse n'est qu'une petite contribution à cette tâche. Néanmoins, l'auteur espère que les connaissances acquises par ce projet seront bénéfiques pour les ingénieurs, les biologistes, l'industrie ainsi que des représentants gouvernementaux.

Appendices

Appendix A

Experimental Data

Baffle type:	Slotted-weir (SWB)
Baffle height (h):	0.15D

Experimental data | **Calculated Roughness coefficients**

Λ	Q_1 (l/s)	Q_2 (l/s)	Q_a (l/s)	H_{res1} (mm)	H_{res2} (mm)	Piezometer # 1	2	3	4	5	6	7	8	9	10	11	12	H_{upavg} (mm)	$H_{downavg}$ (mm)	ΔH (m)	n	n_{avg}	σ	f	f_{avg}	σ	$\sqrt{f}$	$\sqrt{f_{avg}}$	σ
						H_{up} (mm)								H_{down} (mm)																	
	44.74	44.91	44.83	1040	1040	973	973	972	973	969	970	904	904	906	906	906	906	971.7	905.3	0.066	0.0224			0.0989			0.315		
	42.04	42.19	42.12	941	940	880	881	880	880	876	879	824	824	824	822	823	824	879.3	823.5	0.056	0.0219			0.0943			0.307		
	39.64	39.40	39.52	845	843	790	790	790	790	789	790	739	739	739	739	739	739	789.8	739.0	0.051	0.0223			0.0976			0.312		
	37.42	37.83	37.63	773	773	724	724	724	724	722	722	679	679	679	679	679	679	723.3	679.0	0.044	0.0218			0.0939			0.306		
0.6D	34.73	34.64	34.69	691	692	646	647	646	646	646	646	611	611	609	610	611	611	646.2	610.5	0.036	0.0213	0.0220	0.0004	0.0889	0.0956	0.0037	0.298	0.30901	0.00060
	32.56	32.41	32.49	619	620	581	581	581	581	580	580	548	548	549	549	549	549	580.7	548.7	0.032	0.0215			0.0909			0.301		
	30.12	29.72	29.92	568	568	535	535	535	535	534	534	505	505	505	505	505	505	534.7	505.0	0.030	0.0225			0.0993			0.315		
	27.32	27.32	27.32	505	506	479	479	479	479	476	476	454	454	454	454	454	454	478.0	454.0	0.024	0.0221			0.0964			0.310		
	24.86	24.72	24.79	441	441	420	420	420	420	419	419	399	398	400	399	399	400	419.7	399.2	0.021	0.0225			0.1000			0.316		
	44.72	44.57	44.65	1024	1024	955	955	955	955	954	954	900	900	901	901	901	901	954.7	900.7	0.054	0.0203			0.0812			0.285		
	42.55	42.75	42.65	951	951	886	886	887	887	884	885	836	836	838	838	838	838	885.8	837.3	0.049	0.0202			0.0799			0.283		
	39.96	39.92	39.94	860	861	806	806	806	806	804	803	761	761	762	762	762	762	805.2	761.7	0.044	0.0204			0.0817			0.286		
	37.67	37.65	37.66	781	781	751	751	751	751	751	751	681	681	681	681	681	681	716.0	681.0	0.035	0.0194			0.0740			0.272		
1.2D	34.82	34.66	34.74	680	680	638	638	638	638	636	636	605	605	605	605	605	605	637.3	605.0	0.032	0.0202	0.0202	0.0003	0.0803	0.0803	0.0025	0.283	0.2833	0.00045
	32.42	32.64	32.53	628	630	590	590	590	590	589	589	561	561	561	561	561	561	589.7	561.0	0.029	0.0203			0.0812			0.285		
	29.88	29.63	29.76	560	560	527	527	527	527	525	525	503	503	503	503	503	503	526.3	503.0	0.023	0.0200			0.0790			0.281		
	27.42	27.6	27.51	511	511	483	483	483	483	480	480	461	461	461	461	461	461	482.0	461.0	0.021	0.0206			0.0832			0.288		
	24.92	25.12	25.02	450	450	427	427	427	427	427	427	409	409	410	411	410	410	427.0	409.8	0.017	0.0204			0.0822			0.287		
	45.38	45.70	45.54	1040	1030	976	976	975	975	975	974	928	929	928	928	928	928	975.2	928.2	0.047	0.0186			0.0679			0.261		
	42.72	42.86	42.79	955	953	890	890	890	890	887	888	844	845	846	846	846	846	889.2	845.5	0.044	0.0191			0.0715			0.267		
	40.10	40.15	40.13	844	844	789	789	786	786	785	785	749	750	750	750	750	750	786.7	749.8	0.037	0.0187			0.0686			0.262		
	37.27	37.12	37.20	755	753	705	705	704	704	701	702	668	668	668	670	670	670	703.5	669.0	0.035	0.0195			0.0747			0.273		
1.8D	34.92	34.78	34.85	678	676	634	634	633	634	630	632	602	602	604	604	604	604	632.8	603.3	0.030	0.0192	0.0189	0.0004	0.0728	0.071	0.0028	0.270	0.2666	0.00053
	32.60	32.88	32.74	628	627	587	587	587	587	585	586	561	561	561	561	561	561	586.5	561.0	0.026	0.0190			0.0713			0.267		
	29.48	29.86	29.67	559	559	525	525	525	525	523	524	504	504	505	505	505	505	524.5	504.7	0.020	0.0185			0.0675			0.260		
	27.59	27.47	27.53	503	503	474	474	474	474	473	473	455	455	455	455	455	455	473.7	455.0	0.019	0.0194			0.0738			0.272		
	25.02	25.17	25.10	448	448	423	423	424	424	422	422	409	409	409	409	409	409	423.0	409.0	0.014	0.0184			0.0666			0.258		
	44.95	45.14	45.05	1030	1030	941	941	941	941	940	939	895	895	897	897	897	897	940.5	896.3	0.044	0.0182			0.0652			0.255		
	42.37	42.37	42.37	918	918	855	855	855	855	853	853	818	818	815	815	815	815	854.3	816.0	0.038	0.0180			0.0640			0.253		
	40.16	39.75	39.96	834	833	779	779	779	779	775	776	743	743	743	743	743	743	777.8	743.0	0.035	0.0182			0.0654			0.256		
	37.61	37.78	37.70	755	753	705	705	705	705	702	703	670	671	674	674	674	674	704.2	672.8	0.031	0.0183			0.0661			0.257		
2.4D	35.14	35.55	35.35	677	680	635	635	635	635	634	633	605	606	610	610	610	610	634.5	608.5	0.026	0.0178	0.0182	0.0003	0.0624	0.065	0.0023	0.250	0.2555	0.00046
	32.3	32.47	32.39	604	605	565	565	565	565	565	565	542	542	545	545	545	545	565.0	544.0	0.021	0.0175			0.0600			0.245		
	30.28	30	30.14	555	555	521	521	521	521	521	521	499	499	502	502	502	502	521.0	501.0	0.020	0.0183			0.0660			0.257		
	27.51	27.51	27.51	492	492	464	464	464	464	464	464	450	446	446	446	446	446	464.0	446.7	0.017	0.0187			0.0686			0.262		
	25.13	25.1	25.12	450.00	450.00	426	426	425	426	425	425	411	411	412	412	412	412	425.5	411.7	0.014	0.0183			0.0657			0.256		

Baffle type:	Slotted-weir (SWB)
Baffle height (h):	0.10D

Experimental data | **Calculated Roughness coefficients**

Λ	Q_1 (l/s)	Q_2 (l/s)	Q_a (l/s)	H_{res1} (mm)	H_{res2} (mm)	Piezometer # 1	2	3	4	5	6	7	8	9	10	11	12	H_{upavg} (mm)	$H_{downavg}$ (mm)	ΔH (m)	n	n_{avg}	σ	f	f_{avg}	σ	$\sqrt{f}$	$\sqrt{f_{avg}}$	σ
						H_{up} (mm)								H_{down} (mm)																
	45.22	45.25	45.24	1044	1045	974	974	974	974	974	974	933	933	930	932	932	929	974.0	931.5	0.043	0.0178			0.0623			0.250		
	42.25	42.00	42.13	929	927	868	868	868	868	867	868	827	827	828	829	827	828	867.8	827.7	0.040	0.0186			0.0678			0.260		
	40.04	40.16	40.10	860	860	804	804	804	804	803	803	771	771	771	771	771	771	803.7	771.0	0.033	0.0176			0.0609			0.247		
	37.25	37.31	37.28	752	751	705	705	704	705	704	703	674	675	674	676	676	676	704.3	675.2	0.029	0.0179			0.0629			0.251		
0.6D	34.80	34.62	34.71	676	676	635	635	635	635	634	634	609	609	610	611	610	611	634.7	610.0	0.025	0.0177	0.0180	0.0005	0.0614	0.0639	0.0034	0.248	0.2527	0.0067
	32.78	32.81	32.80	627	627	589	589	589	589	588	588	566	566	567	567	568	567	588.7	566.8	0.022	0.0176			0.0608			0.247		
	29.71	30.00	29.86	556	556	525	525	525	525	525	525	505	505	506	507	506	507	525.0	506.0	0.019	0.0180			0.0639			0.253		
	27.96	27.90	27.93	511	511	485	485	485	485	483	483	465	465	466	466	466	466	484.3	465.7	0.019	0.0191			0.0717			0.268		
	24.78	24.73	24.76	438	438	419	419	419	419	418	418	405	405	406	406	406	406	418.7	405.7	0.013	0.0180			0.0636			0.252		
	44.85	45.11	44.98	1000	1001	927	927	927	927	927	927	895	895	894	894	894	894	927.0	894.3	0.033	0.0157			0.0484			0.220		
	42.35	42.68	42.52	906	906	845	845	845	845	845	845	814	814	814	814	814	814	845.0	814.0	0.031	0.0162			0.0514			0.227		
	40.21	39.83	40.02	810	809	755	755	755	755	755	755	725	725	727	727	727	727	755.0	726.3	0.029	0.0165			0.0536			0.232		
	37.18	37.03	37.11	730	730	681	651	681	681	681	681	657	657	657	657	657	657	676.0	657.0	0.019	0.0145			0.0414			0.203		
1.2D	35	34.95	34.98	658	658	614	614	614	614	614	614	595	595	593	594	594	594	614.0	594.2	0.020	0.0157	0.0157	0.0006	0.0486	0.0487		0.220	0.2220	0.0086
	32.85	32.61	32.73	600	600	562	562	562	562	562	562	545	545	544	544	544	544	562.0	544.3	0.018	0.0159			0.0494			0.222		
	29.82	29.79	29.81	539	540	506	506	506	506	506	506	493	493	492	492	492	492	506.0	492.3	0.014	0.0153			0.0461			0.215		
	27.55	27.56	27.56	484	484	466	466	466	466	466	466	443	443	443	443	443	443	454.5	443.0	0.012	0.0152			0.0454			0.213		
	24.71	24.9	24.81	423	424	401	401	401	401	401	401	390	390	390	390	390	390	401.0	390.0	0.011	0.0165			0.0536			0.231		
	45.62	45.76	45.69	1030	1030	960	961	961	961	960	960	927	928	929	928	930	929	960.5	928.5	0.032	0.0153			0.0459			0.214		
	42.34	42.20	42.27	950	950	845	845	845	845	844	844	821	821	824	823	824	824	844.7	822.8	0.022	0.0136			0.0366			0.191		
	39.81	39.18	39.50	802	801	749	749	748	748	746	747	726	726	725	725	725	725	747.8	725.3	0.023	0.0148			0.0432			0.208		
	37.50	37.29	37.40	748	748	697	697	697	697	696	696	680	680	679	679	679	679	696.7	679.3	0.017	0.0137			0.0372			0.193		
1.8D	34.70	34.75	34.73	660	661	617	617	617	617	615	615	601	602	601	601	602	602	616.3	601.5	0.015	0.0137	0.0141	0.0006	0.0369	0.0393	0.0033	0.192	0.1988	0.0083
	32.22	32.49	32.36	604	604	565	565	565	565	565	565	552	551	551	551	551	551	565.0	551.2	0.014	0.0142			0.0396			0.199		
	30.06	30.12	30.09	550	550	516	516	516	516	515	515	505	505	505	505	505	505	515.7	505.0	0.011	0.0134			0.0353			0.188		
	27.47	27.31	27.39	499	499	468	468	470	470	470	470	460	460	460	460	460	460	469.3	460.0	0.009	0.0138			0.0373			0.193		
	25.06	25.21	25.14	444	444	420	420	421	421	420	420	413	413	411	411	411	411	420.3	411.7	0.009	0.0145			0.0411			0.203		
	44.95	45.1	45.03	1030	1030	920	920	921	921	921	921	890	890	891	891	891	891	920.7	890.7	0.030	0.0150			0.0444			0.211		
	42.64	42.71	42.68	906	907	846	846	846	846	846	846	820	820	820	820	820	820	846.0	820.0	0.026	0.0147			0.0428			0.207		
	40.06	40	40.03	815	814	761	761	761	761	761	761	736	736	736	736	736	736	761.0	736.0	0.025	0.0154			0.0468			0.216		
	37.54	37.54	37.54	731	732	683	683	683	683	683	683	662	662	663	663	663	663	683.0	662.7	0.020	0.0148			0.0432			0.208		
2.4D	35.13	35.24	35.19	677	675	629	629	629	629	629	629	611	611	611	611	611	611	629.0	611.0	0.018	0.0149	0.0149	0.0002	0.0436	0.0444	0.0014	0.209	0.2092	0.0034
	32.6	32.69	32.65	600	600	563	563	563	563	563	563	548	548	548	548	548	548	563.0	548.0	0.015	0.0146			0.0422			0.205		
	30.26	30.26	30.26	548	543	515	515	515	515	515	506	500	500	500	500	500	500	513.5	500.0	0.014	0.0150			0.0442			0.210		
	27.38	27.73	27.56	492	492	463	463	463	463	463	463	452	452	452	452	452	452	463.0	452.0	0.011	0.0149			0.0434			0.208		
	25.16	24.88	25.02	435	433	410	410	410	410	410	410	400	400	402	402	402	402	410.0	401.3	0.009	0.0145			0.0415			0.204		

Baffle type:	Slotted-weir (SWB)
Baffle height (h):	0.05D

	Experimental data					Piezometer #															Calculated Roughness coefficients											
								H_{up} (mm)					H_{down} (mm)																			
Λ	Q_1 (l/s)	Q_2 (l/s)	Q_a (l/s)	H_{res1} (mm)	H_{res2} (mm)	1	2	3	4	5	6	7	8	9	10	11	12	H_{upavg} (mm)	$H_{downavg}$ (mm)	ΔH (m)	n	n_{avg}	σ	f	f_{avg}	σ	$\sqrt{f}$	$\sqrt{f_{avg}}$	σ
	45.14	45.44	45.29	1016	1016	946	946	946	946	946	946	925	926	923	924	923	924	946.0	924.2	0.022	0.0127			0.0319			0.179		
	42.54	42.81	42.68	919	919	856	856	855	855	856	855	835	836	835	835	836	835	855.5	835.3	0.020	0.0130			0.0332			0.182		
	40.51	40.14	40.33	830	830	775	775	775	775	775	775	756	755	756	756	755	756	775.0	755.7	0.019	0.0135			0.0356			0.189		
	37.49	37.26	37.38	738	736	689	689	689	689	689	689	672	672	671	672	672	671	689.0	671.7	0.017	0.0138	0.0131	0.0004	0.0372	0.0337	0.0022	0.193	0.1834	0.00061
0.6D	35.29	34.92	35.11	664	665	623	623	623	623	623	623	610	610	610	610	610	610	623.0	610.0	0.013	0.0127			0.0316			0.178		
	32.74	32.63	32.69	610	610	572	572	572	571	571	571	560	560	560	560	560	560	571.5	560.0	0.012	0.0128			0.0323			0.180		
	29.89	30.07	29.98	549	549	517	517	517	517	517	517	508	508	508	507	508	508	517.0	507.8	0.009	0.0125			0.0306			0.175		
	27.38	27.73	27.56	496	496	470	470	470	469	469	469	461	460	460	460	460	460	469.5	460.2	0.009	0.0137			0.0368			0.192		
	24.87	24.92	24.90	433	433	414	414	413	413	413	413	406	406	407	406	407	406	413.3	406.3	0.007	0.0131			0.0339			0.184		
	44.54	44.34	44.44	957	955	890	890	890	890	890	890	870	870	870	870	870	870	890.0	870.0	0.020	0.0124			0.0304			0.174		
	42.59	42.56	42.58	884	882	823	823	823	823	823	823	803	803	802	802	802	802	823.0	802.3	0.021	0.0132			0.0342			0.185		
	39.91	39.75	39.83	782	780	727	727	727	727	727	727	712	712	712	712	712	712	727.0	712.0	0.015	0.0120			0.0283			0.168		
	37.8	37.4	37.60	707	706	658	658	658	658	658	658	645	645	645	645	645	645	658.0	645.0	0.013	0.0118			0.0276			0.166		
1.2D	34.76	35.23	35.00	640	639	596	596	596	596	596	596	585	585	585	585	585	585	596.0	585.0	0.011	0.0117	0.0121	0.0007	0.0269	0.0289	0.0033	0.164	0.170	0.00096
	32.23	32.98	32.61	579	577	540	540	540	540	540	540	530	530	530	530	530	530	540.0	530.0	0.010	0.0120			0.0282			0.168		
	30.25	30.02	30.14	529	530	496	496	496	496	496	496	489	489	489	489	489	489	496.0	489.0	0.007	0.0108			0.0231			0.152		
	27.44	27.73	27.59	478	479	450	450	450	450	450	450	443	443	443	443	443	443	450.0	443.0	0.007	0.0118			0.0276			0.166		
	24.78	25.08	24.93	425	426	404	404	404	404	404	404	397	397	397	397	397	397	404.0	397.0	0.007	0.0131			0.0338			0.184		
	44.5	45.16	44.83	980	984	906	906	906	906	906	906	891	891	890	890	890	890	906.0	890.3	0.016	0.0109			0.0234			0.153		
	42.63	42.8	42.72	911	912	849	849	850	850	849	850	835	834	833	834	833	834	849.5	833.8	0.016	0.0114			0.0257			0.160		
	40.1	40.17	40.14	817	818	762	762	762	762	761	761	749	749	748	748	748	748	761.7	748.3	0.013	0.0112			0.0248			0.158		
	37.69	37.43	37.56	736	736	686	686	685	685	685	685	675	675	674	675	674	675	685.3	674.7	0.011	0.0107	0.0109	0.0004	0.0227	0.0223	0.0018	0.151	0.153	0.00060
1.8D	34.81	35.44	35.13	662	664	618	618	618	618	618	618	610	610	609	609	609	609	618.0	609.3	0.009	0.0103			0.0211			0.145		
	32.71	32.61	32.66	602	602	563	563	563	563	563	563	555	555	555	555	555	555	563.0	555.0	0.008	0.0107			0.0225			0.150		
	30.14	29.95	30.05	547	547	514	514	513	513	512	512	506	506	505	505	505	505	513.0	505.3	0.008	0.0114			0.0255			0.160		
	27.54	27.42	27.48	489	488	460	461	460	460	460	460	454	454	454	454	454	454	460.2	454.0	0.006	0.0112			0.0245			0.156		
	24.89	24.8	24.85	435	435	411	411	411	411	411	411	406	407	407	407	407	407	411.0	406.8	0.004	0.0101			0.0202			0.142		
	44.81	44.75	44.78	955	955	888	888	888	888	885	885	869	869	867	867	867	867	887.0	867.7	0.019	0.0121			0.0289			0.170		
	42.57	42.42	42.50	864	867	805	805	805	805	802	803	788	788	788	788	788	788	804.2	788.0	0.016	0.0117			0.0268			0.164		
	39.98	39.88	39.93	778	777	724	724	723	723	721	721	707	707	707	707	707	707	722.7	707.0	0.016	0.0122			0.0295			0.172		
	37.63	37.51	37.57	700	701	653	653	653	653	650	650	640	640	639	639	639	639	652.0	639.3	0.013	0.0117			0.0269			0.164		
2.4D	34.88	34.63	34.76	630	631	590	590	590	590	588	588	577	577	577	577	577	577	589.3	577.0	0.012	0.0125	0.0121	0.0003	0.0306	0.029	0.0015	0.175	0.170	0.00045
	32.88	32.72	32.80	580	580	542	542	542	542	540	540	533	533	531	531	531	531	541.3	531.7	0.010	0.0117			0.0269			0.164		
	29.85	30.22	30.04	523	522	491	491	491	491	489	489	481	481	481	481	481	481	490.3	481.0	0.009	0.0126			0.0310			0.176		
	27.81	27.58	27.70	479	479	451	451	451	451	449	449	444	444	442	442	442	442	450.3	442.7	0.008	0.0123			0.0300			0.173		
	25.16	25.2	25.18	418	418	397	397	396	396	395	395	390	390	390	390	390	390	396.0	390.0	0.006	0.0120			0.0284			0.168		

Baffle type:	Weir Baffle (WB)
Baffle height (h):	0.15D

	Experimental data																				Calculated Roughness coefficients								
						Piezeometer #																								
Λ	Q_1 (l/s)	Q_2 (l/s)	Q_a (l/s)	H_{res1} (mm)	H_{res2} (mm)	1	2	3	4	5	6	7	8	9	10	11	12	H_{upavg} (mm)	$H_{downavg}$ (mm)	ΔH (m)	n	n_{avg}	σ	f	f_{avg}	σ	$\sqrt{f}$	$\sqrt{f_{avg}}$	σ
						H_{up} (mm)						H_{down} (mm)																		
	44.86	44.44	44.65	1045	1045	974	974	975	976	968	968	903	903	905	906	905	904	972.5	904.3	0.068	0.0228			0.1025			0.320		
	42.59	42.59	42.59	963	963	905	905	905	905	904	902	842	842	846	846	846	846	904.3	844.7	0.060	0.0224			0.0986			0.314		
	40.21	40.24	40.23	879	879	823	823	822	822	819	820	770	770	771	771	770	771	821.5	770.5	0.051	0.0219			0.0945			0.307		
	37.76	37.63	37.70	780	778	730	730	728	729	725	727	682	682	682	682	682	682	728.2	682.0	0.046	0.0222			0.0974			0.312		
0.6D	34.94	35.19	35.07	701	701	657	657	657	657	654	656	617	617	618	617	618	618	656.3	617.5	0.039	0.0219	0.0222	0.0004	0.0947	0.0971	0.0035	0.308	0.3116	0.0056
	32.32	32.65	32.49	631	631	593	593	594	594	592	590	560	560	560	560	560	560	592.7	560.0	0.033	0.0217			0.0928			0.305		
	30.11	29.98	30.05	576	577	542	542	542	542	541	540	513	513	514	514	514	514	541.5	513.7	0.028	0.0217			0.0924			0.304		
	27.76	27.63	27.70	519	519	490	490	490	490	489	490	464	464	464	464	464	464	489.8	464.0	0.026	0.0227			0.1009			0.318		
	24.73	24.56	24.65	441	441	420	420	420	420	420	420	399	399	400	400	400	400	420.0	399.7	0.020	0.0226			0.1003			0.317		
	44.9	44.96	44.93	1040	1040	973	973	973	973	969	969	906	905	905	905	905	905	971.7	905.2	0.067	0.0224			0.0987			0.314		
	42.45	42.12	42.29	956	956	895	895	895	894	893	892	835	836	838	837	838	839	894.0	837.2	0.057	0.0220			0.0953			0.309		
	39.53	39.74	39.64	857	853	799	799	799	799	795	796	746	746	746	749	749	749	797.8	747.5	0.050	0.0221			0.0960			0.310		
	37.65	37.45	37.55	775	775	726	726	725	725	724	723	680	680	682	682	683	683	724.8	681.7	0.043	0.0216			0.0918			0.303		
1.2D	34.72	34.34	34.53	687	688	645	645	645	645	642	643	607	607	607	607	607	607	644.2	607.0	0.037	0.0218	0.0219	0.0002	0.0934	0.0940	0.0021	0.306	0.307	0.0034
	32.83	32.65	32.74	634	634	596	596	596	596	594	595	562	562	562	562	562	562	595.5	562.0	0.034	0.0218			0.0937			0.306		
	29.73	29.8	29.77	566	566	534	534	532	533	531	531	505	505	505	505	505	505	532.5	505.0	0.028	0.0217			0.0930			0.305		
	27.43	27.78	27.61	517	518	490	490	489	489	486	487	465	465	465	465	465	465	488.5	465.0	0.024	0.0217			0.0924			0.304		
	24.88	24.86	24.87	447	449	425	425	426	425	424	425	406	406	406	406	406	406	425.0	406.0	0.019	0.0216			0.0921			0.303		
	44.69	44.64	44.67	1025	1025	956	956	956	956	954	953	897	895	900	900	900	900	955.2	898.7	0.057	0.0208			0.0849			0.291		
	42.74	42.55	42.65	960	960	896	896	896	896	892	895	841	841	842	842	842	842	895.2	841.7	0.054	0.0212			0.0882			0.297		
	40.14	40.15	40.15	861	861	805	805	805	805	804	803	759	759	761	761	761	761	804.5	760.3	0.044	0.0204			0.0821			0.287		
	37.73	37.64	37.69	771	771	721	721	720	720	717	718	679	679	682	682	682	682	719.5	681.0	0.039	0.0203			0.0813			0.285		
1.8D	35.04	34.77	34.91	687	687	645	645	644	644	642	640	607	607	610	610	610	610	643.3	609.0	0.034	0.0207	0.0207	0.0003	0.0845	0.0850	0.0027	0.291	0.2911	0.0046
	32.77	32.34	32.56	638	639	597	597	597	597	595	594	565	565	565	565	566	566	596.2	565.3	0.031	0.0211			0.0872			0.295		
	30.15	29.99	30.07	564	563	530	530	529	529	529	528	503	503	504	504	504	504	529.2	503.7	0.025	0.0207			0.0845			0.291		
	27.48	27.32	27.40	502	502	475	475	474	474	473	473	452	452	452	452	452	452	474.0	452.0	0.022	0.0211			0.0878			0.296		
	25.13	25.17	25.15	446	446	422	422	422	422	421	422	405	404	405	405	405	405	421.8	404.8	0.017	0.0202			0.0806			0.284		
	44.96	45.19	45.08	1030	1030	960	960	960	960	960	960	900	904	908	908	908	908	960.0	906.0	0.054	0.0201			0.0797			0.282		
	42.53	42.41	42.47	946	947	884	884	884	884	880	880	831	831	835	835	835	835	882.7	833.7	0.049	0.0203			0.0814			0.285		
	40.24	40.11	40.18	849	850	793	793	793	793	791	789	743	746	751	751	751	751	792.0	748.8	0.043	0.0202			0.0802			0.283		
	37.62	37.62	37.62	764	764	715	715	715	715	711	713	677	677	679	679	679	679	714.0	678.3	0.036	0.0196			0.0755			0.275		
2.4D	35.23	35.23	35.23	687	688	645	645	645	645	643	643	611	611	614	614	614	614	644.3	613.0	0.031	0.0196	0.0201	0.0004	0.0757	0.0800	0.0034	0.275	0.283	0.0060
	32.55	32.55	32.55	625	625	586	586	586	586	585	585	557	557	559	559	559	559	585.7	558.3	0.027	0.0198			0.0773			0.278		
	29.86	29.86	29.86	566	566	534	534	534	534	533	533	505	505	509	509	509	509	533.7	507.7	0.026	0.0211			0.0874			0.296		
	27.53	27.53	27.53	502	502	475	475	475	475	473	473	451	451	455	455	455	455	474.3	453.7	0.021	0.0204			0.0817			0.286		
	25.65	25.65	25.65	459	459	435	435		435	434	434	415	415	418	418	418	418	434.6	417.0	0.018	0.0202			0.0802			0.283		

Baffle type:	Weir Baffle (WB)
Baffle height (h):	0.10D

	Experimental data																					Calculated Roughness coefficients								
						Piezometer #																								
								H_{up} (mm)				H_{down} (mm)																		
Λ	Q_1 (l/s)	Q_2 (l/s)	Q_a (l/s)	H_{res1} (mm)	H_{res2} (mm)	1	2	3	4	5	6	7	8	9	10	11	12	H_{upavg} (mm)	$H_{downavg}$ (mm)	ΔH (m)	n	n_{avg}	σ	f	f_{avg}	σ	$\sqrt{f}$	$\sqrt{f_{avg}}$	σ
	45.21	44.95	45.08	1025	1025	956	956	956	956	955	954	913	914	913	912	914	915	955.5	913.5	0.042	0.0177			0.0619			0.249		
	42.42	42.69	42.56	939	939	878	878	878	878	876	877	836	835	836	837	836	837	877.5	836.2	0.041	0.0186			0.0684			0.262		
	39.74	40.15	39.95	844	844	790	790	790	790	787	789	753	753	755	756	755	756	789.3	754.7	0.035	0.0182			0.0651			0.255		
	37.68	37.87	37.78	771	771	721	721	721	721	720	720	689	690	691	692	691	692	720.7	690.8	0.030	0.0178			0.0627			0.250		
0.6D	34.80	34.86	34.83	678	678	636	636	635	635	635	635	610	610	611	611	611	611	635.3	610.7	0.025	0.0176	0.0180	0.0003	0.0609	0.0641	0.0025	0.247	0.2531	0.0049
	32.68	32.30	32.49	618	618	581	581	581	581	580	581	558	558	559	560	559	560	580.8	559.0	0.022	0.0178			0.0620			0.249		
	29.98	30.01	30.00	558	559	526	526	526	526	525	525	506	506	507	507	507	508	525.7	506.8	0.019	0.0179			0.0627			0.250		
	27.23	27.31	27.27	497	497	471	471	471	471	470	470	454	454	454	454	454	454	470.7	454.0	0.017	0.0185			0.0672			0.259		
	24.89	24.95	24.92	440	440	420	420	418	418	418	418	405	405	405	405	405	405	418.7	405.0	0.014	0.0183			0.0660			0.257		
	44.7	44.76	44.73	1020	1020	950	950	950	950	950	950	912	912	912	912	912	912	950.0	912.0	0.038	0.0170			0.0569			0.239		
	42.85	43.21	43.03	962	962	905	905	905	905	905	905	867	867	868	868	868	868	905.0	867.7	0.037	0.0175			0.0604			0.246		
	40.07	39.74	39.91	852	852	797	797	797	797	797	797	765	765	765	765	765	765	797.0	765.0	0.032	0.0175			0.0602			0.245		
	37.69	37.75	37.72	771	771	723	723	723	723	723	723	694	694	695	695	695	695	723.0	694.7	0.028	0.0174			0.0597			0.244		
1.2D	35.42	35.44	35.43	698	699	655	655	655	655	655	655	630	630	630	630	630	630	655.0	630.0	0.025	0.0174	0.0174	0.0002	0.0597	0.0594	0.0014	0.244	0.2444	0.0030
	32.64	32.4	32.52	631	630	592	592	592	592	592	592	571	571	571	571	571	571	592.0	571.0	0.021	0.0174			0.0595			0.244		
	29.58	29.78	29.68	563	561	530	530	530	530	530	530	512	512	512	512	512	512	530.0	512.0	0.018	0.0176			0.0612			0.247		
	27.36	27.36	27.36	514	514	485	485	485	485	485	485	470	470	470	470	470	470	485.0	470.0	0.015	0.0175			0.0601			0.245		
	24.81		24.81	447	448	436	436	436	436	436	436	412	412	413	413	413	413	424.3	412.7	0.012	0.0170			0.0568			0.238		
	44.82	44.84	44.83	1010	1005	938	938	939	940	933	934	899	900	901	902	901	902	937.0	900.8	0.036	0.0166			0.0539			0.232		
	42.20	42.19	42.20	913	913	852	852	852	852	850	851	820	820	817	818	817	818	851.5	818.3	0.033	0.0168			0.0558			0.236		
	39.73	39.70	39.72	826	825	770	770	770	770	769	769	741	742	744	744	744	744	769.7	743.2	0.027	0.0160			0.0504			0.224		
	37.43	37.28	37.36	740	739	691	691	690	690	688	688	665	665	666	666	667	667	689.7	666.0	0.024	0.0161			0.0508			0.225		
1.8D	35.08	35.27	35.18	678	679	634	634	634	634	632	632	614	614	615	615	615	615	633.3	614.7	0.019	0.0152	0.0159	0.0008	0.0452	0.0500	0.0046	0.213	0.224	0.0105
	32.66	32.44	32.55	608	607	570	570	570	569	569	569	551	551	551	551	551	551	569.5	551.0	0.019	0.0163			0.0523			0.229		
	30.47	29.92	30.20	550	550	516	516	516	516	516	516	501	501	501	502	501	502	516.0	501.3	0.015	0.0157			0.0482			0.220		
	27.56	27.58	27.57	499	499	470	470	470	470	469	469	456	456	456	456	456	456	469.7	456.0	0.014	0.0166			0.0539			0.232		
	24.93	24.85	24.89	435	435	411	411	411	411	410	410	401	401	403	403	403	403	410.7	402.3	0.008	0.0143			0.0403			0.201		
	45.3	45.1	45.20	1030	1030	947	947	947	947	946	946	913	913	913	913	913	913	929.8	913.0	0.017	0.0112			0.0247			0.157		
	42.25	42.69	42.47	910	909	847	847	847	847	847	847	819	819	819	819	819	819	847.0	819.0	0.028	0.0154			0.0465			0.216		
	39.94	39.84	39.89	819	818	764	764	764	764	763	762	738	738	739	739	739	739	763.5	738.7	0.025	0.0154			0.0468			0.216		
	37.53	37.61	37.57	741	741	693	693	693	693	693	693	670	670	670	670	670	670	693.0	670.0	0.023	0.0158			0.0488			0.221		
2.4D	35.32	35.75	35.54	677	677	635	635	635	635	635	635	615	615	615	615	615	615	635.0	615.0	0.020	0.0155	0.0151	0.0014	0.0475	0.0455	0.0075	0.218	0.212	0.0198
	32.44	32.22	32.33	600	600	563	563	563	563	563	563	547	547	547	547	547	547	563.0	547.0	0.016	0.0153			0.0459			0.214		
	30.17	29.73	29.95	547	547	514	514	514	514	514	514	499	499	500	500	500	500	514.0	499.7	0.014	0.0156			0.0479			0.219		
	27.6	27.31	27.46	492	492	464	464	464	464	464	464	451	451	451	451	451	451	464.0	451.0	0.013	0.0162			0.0517			0.227		
	25.13	25.37	25.25	444	445	421	421	421	421	421	421	410	410	411	411	411	411	421.0	410.7	0.010	0.0157			0.0486			0.220		

Baffle type:	Weir Baffle (WB)
Baffle height (h):	0.05D

	Experimental data																				Calculated Roughness coefficients								
						Piezometer #																								
Λ	Q_1 (l/s)	Q_2 (l/s)	Q_a (l/s)	H_{res1} (mm)	H_{res2} (mm)	1	2	3	4	5	6	7	8	9	10	11	12	H_{upavg} (mm)	$H_{downavg}$ (mm)	ΔH (m)	n	n_{avg}	σ	f	f_{avg}	σ	$\sqrt{f}$	$\sqrt{f_{avg}}$	σ
						H_{up} (mm)						H_{down} (mm)																		
	44.99	44.93	44.96	1000	1002	932	932	932	932	932	932	906	907	905	904	906	905	932.0	905.5	0.027	0.0141			0.0393			0.198		
	42.41	42.38	42.40	917	916	857	857	856	856	856	855	831	831	831	832	832	831	856.2	831.3	0.025	0.0145			0.0414			0.203		
	40.05	40.28	40.17	832	831	777	777	776	776	776	775	754	754	755	755	755	755	776.2	754.7	0.022	0.0142			0.0399			0.200		
	37.49	37.84	37.67	754	754	705	705	705	705	705	705	687	687	687	686	687	687	705.0	686.8	0.018	0.0140	0.0142	0.0002	0.0384	0.0397	0.0009	0.196	0.1993	0.00022
0.6D	35.10	34.87	34.99	670	671	629	629	628	628	628	628	613	613	612	612	612	612	628.3	612.3	0.016	0.0141			0.0392			0.198		
	32.56	32.70	32.63	606	606	570	570	569	568	569	569	556	556	555	555	555	555	569.2	555.3	0.014	0.0141			0.0389			0.197		
	29.88	29.76	29.82	543	541	511	511	511	511	511	511	499	498	499	500	499	500	511.0	499.2	0.012	0.0142			0.0399			0.200		
	27.48	27.50	27.49	497	497	470	470	470	470	470	470	460	460	460	460	460	460	470.0	460.0	0.010	0.0142			0.0397			0.199		
	25.04	25.51	25.28	445	445	424	424	424	423	424	423	415	415	415	415	415	415	423.7	415.0	0.009	0.0144			0.0407			0.202		
	45.5	45.54	45.52	995	995	923	923	923	923	923	923	901	901	902	902	902	902	923.0	901.7	0.021	0.0125			0.0309			0.176		
	42.82	42.7	42.76	898	898	836	836	836	836	836	836	815	815	815	815	815	815	836.0	815.0	0.021	0.0132			0.0344			0.186		
	39.82	39.94	39.88	806	806	751	751	751	751	751	751	733	733	732	732	732	732	751.0	732.3	0.019	0.0134			0.0352			0.188		
	37.39	37.27	37.33	719	717	670	670	670	670	670	670	652	652	652	652	652	652	670.0	652.0	0.018	0.0140	0.0139	0.0008	0.0387	0.0379	0.0043	0.197	0.194	0.00112
1.2D	35.12	35.01	32.76	656	656	612	612	612	612	612	612	597	597	597	597	597	597	612.0	597.0	0.015	0.0146			0.0419			0.205		
	32.58	32.94	30.16	593	593	555	555	555	555	556	556	542	542	543	543	543	543	555.3	542.7	0.013	0.0146			0.0417			0.204		
	30.11	30.21	27.40	543	543	510	510	510	510	510	510	500	500	500	500	500	500	510.0	500.0	0.010	0.0142			0.0399			0.200		
	27.56	27.24	25.03	483	483	456	456	455	455	455	455	446	446	446	446	446	446	455.3	446.0	0.009	0.0151			0.0447			0.211		
	25.03	25.03	25.03	430	430	407	407	407	407	407	407	400	400	400	400	400	400	407.0	400.0	0.007	0.0130			0.0335			0.183		
	42.25	45.00	43.63	1000	1000	931	931	931	931	931	931	910	910	909	909	910	910	931.0	909.7	0.021	0.0131			0.0336			0.183		
	42.65	42.45	42.55	903	902	841	841	840	840	839	839	821	821	821	822	821	822	840.0	821.3	0.019	0.0125			0.0309			0.176		
	40.35	40.32	40.34	830	830	773	773	773	773	772	772	756	756	756	756	756	756	772.7	756.0	0.017	0.0125			0.0307			0.175		
	37.59	37.70	37.65	735	735	685	685	685	685	685	685	670	670	670	670	670	676	685.0	671.0	0.014	0.0123			0.0296			0.172		
1.8D	35.07	35.03	35.05	663	664	620	620	619	620	618	618	609	609	608	609	609	609	619.2	608.8	0.010	0.0113	0.0121	0.0007	0.0252	0.0229	0.0032	0.159	0.170	0.00095
	32.61	32.70	32.66	606	606	566	566	566	566	565	565	556	556	556	556	556	556	565.7	556.0	0.010	0.0118			0.0272			0.165		
	29.80	30.04	29.92	542	542	510	510	510	510	510	510	500	501	500	500	500	500	510.0	500.2	0.010	0.0129			0.0329			0.181		
	27.03	27.84	27.44	491	491	461	461	461	461	461	461	455	455	455	455	455	455	461.0	455.0	0.006	0.0110			0.0239			0.155		
	25.33	25.35	25.34	438	437	415	415	414	414	414	414	408	408	409	409	409	409	414.3	408.7	0.006	0.0116			0.0265			0.163		
	45.02	45.1	45.06	990	990	915	915	915	915	915	915	893	893	892	892	892	892	915.0	892.3	0.023	0.0130			0.0335			0.183		
	42.81	42.74	42.78	889	885	827	827	827	827	827	827	805	805	805	805	805	805	827.0	805.0	0.022	0.0135			0.0360			0.190		
	37.6	37.57	37.59	717	717	669	669	668	668	668	668	655	655	654	654	654	654	668.3	654.3	0.014	0.0123			0.0297			0.172		
	39.85	39.84	39.85	786	786	734	734	732	732	731	731	716	716	715	715	715	715	732.3	715.3	0.017	0.0128			0.0321			0.179		
2.4D	34.77	34.29	34.53	635	635	595	595	595	595	593	593	581	581	581	581	581	581	594.3	581.0	0.013	0.0131	0.0124	0.0010	0.0335	0.0300	0.0046	0.183	0.174	0.00141
	32.3	32.53	32.42	581	582	545	545	545	545	545	545	534	534	534	534	534	534	545.0	534.0	0.011	0.0126			0.0314			0.177		
	29.93	29.95	29.94	535	534	502	502	502	502	502	502	495	495	494	494	494	494	502.0	494.3	0.008	0.0114			0.0256			0.160		
	27.65	27.44	27.55	485	485	456	456	456	456	456	456	448	448	448	448	448	448	456.0	448.0	0.008	0.0127			0.0316			0.178		
	24.51	24.8	24.66	422	424	400	400	400	400	400	400	396	396	396	396	396	396	400.0	396.0	0.004	0.0100			0.0197			0.140		

Baffle type:	**Spoiler Baffle (SPB) 3-3-3**
Baffle height (h):	**0.15D**

Experimental data | **Calculated Roughness coefficients**

Λ	Q_1 (l/s)	Q_2 (l/s)	Q_a (l/s)	H_{res1} (mm)	H_{res2} (mm)	Piezeometer # 1	2	3	4	5	6	7	8	9	10	11	12	H_{upavg} (mm)	$H_{downavg}$ (mm)	ΔH (m)	n	n_{avg}	σ	f	f_{avg}	σ	$\sqrt{f}$	$\sqrt{f_{avg}}$	σ
								H_{up} (mm)						H_{down} (mm)																	
	44.17	44.18	44.18	1040	1040	964	964	964	964	961	963	883	885	885	885	886	887	963.3	885.2	0.078	0.0247			0.1201			0.346		
	42.25	42.25	42.25	972	972	908	908	907	907	905	904	834	834	838	840	835	835	906.5	836.0	0.071	0.0245			0.1184			0.344		
	39.37	39.50	39.44	863	860	805	805	805	805	804	802	741	741	745	742	740	740	804.3	741.5	0.063	0.0248			0.1211			0.348		
	37.72	37.75	37.74	790	790	740	740	740	740	736	738	683	683	682	685	684	684	739.0	683.5	0.056	0.0244			0.1168			0.342		
0.6D	34.60	34.47	34.54	690	690	647	647	647	647	644	643	597	597	601	603	600	601	645.8	599.8	0.046	0.0242	0.0246	0.0004	0.1156	0.1189	0.0039	0.340	0.3447	0.0056
	32.30	32.13	32.22	634	632	594	594	594	594	594	594	550	550	555	555	554	554	594.0	553.0	0.041	0.0245			0.1184			0.344		
	30.30	30.30	30.30	585	585	550	550	550	550	550	550	511	511	515	515	513	513	550.0	513.0	0.037	0.0248			0.1208			0.348		
	27.30	27.60	27.45	520	520	490	491	495	495	495	495	460	460	462	463	465	460	493.5	461.7	0.032	0.0254			0.1266			0.356		
	24.80	24.84	24.82	450	450	426	426	426	426	430	430	402	402	405	405	406	406	427.3	404.3	0.023	0.0239			0.1119			0.335		
	44.81	44.63	44.72	1045	1044	970	970	970	970	976	967	900	900	903	904	905	908	970.5	903.3	0.067	0.0226			0.1007			0.317		
	42.68	42.58	42.63	971	971	902	902	902	902	900	901	840	840	840	840	838	838	901.5	839.3	0.062	0.0228			0.1025			0.320		
	39.74	39.58	39.66	852	850	795	795	794	795	790	790	737	737	742	742	740	740	793.2	739.7	0.054	0.0228			0.1019			0.319		
	37.8	37.95	37.88	792	793	742	742	742	742	740	740	691	691	693	693	693	693	741.3	692.3	0.049	0.0228			0.1024			0.320		
1.2D	34.63	34.83	34.73	688	688	645	645	645	645	641	642	602	602	602	602	602	602	643.8	602.0	0.042	0.0230	0.0229	0.0002	0.1040	0.1028	0.0016	0.322	0.3221	0.0025
	32.71	33.2	32.96	640	641	602	602	601	601	599	599	562	562	565	565	565	565	600.7	564.0	0.037	0.0227			0.1012			0.318		
	29.89	29.7	29.80	565	565	532	532	533	533	530	530	500	501	500	500	502	501	531.7	500.7	0.031	0.0231			0.1047			0.324		
	27.84	27.47	27.66	516	516	488	488	488	488	485	485	460	460	460	460	460	460	487.0	460.0	0.027	0.0232			0.1058			0.325		
	25.33	25.1	25.22	454	455	431	431	431	431	430	430	408	408	409	409	410	410	430.7	409.0	0.022	0.0228			0.1021			0.320		
	44.50	44.34	44.42	1020	1020	953	953	954	954	950	950	893	893	895	895	886	888	952.3	891.7	0.061	0.0216			0.0922			0.304		
	42.30	42.39	42.35	944	944	881	881	881	881	877	877	826	826	826	826	826	826	879.7	826.0	0.054	0.0214			0.0897			0.300		
	40.14	40.12	40.13	856	857	800	800	800	800	796	796	747	747	747	747	748	748	798.7	747.3	0.051	0.0220			0.0955			0.309		
	37.59	37.30	37.45	758	758	710	710	710	710	706	706	665	665	665	665	670	670	708.7	666.7	0.042	0.0214			0.0898			0.300		
1.8D	35.23	35.09	35.16	683	683	640	640	640	640	638	638	605	605	605	605	605	605	639.3	605.0	0.034	0.0206	0.0215	0.0006	0.0832	0.0911	0.0054	0.289	0.3022	0.0090
	32.56	32.57	32.57	620	622	583	583	583	583	580	581	554	554	552	552	554	554	582.2	553.3	0.029	0.0204			0.0815			0.285		
	30.25	30.16	30.21	567	568	535	535	535	535	533	533	505	505	505	505	505	505	534.3	505.0	0.029	0.0221			0.0964			0.310		
	27.40	27.20	27.30	501	501	475	475	475	475	472	472	450	450	450	450	450	450	474.0	450.0	0.024	0.0222			0.0965			0.311		
	25.00	25.00	25.00	441	441	420	420	420	420	420	420	400	400	400	400	400	400	420.0	400.0	0.020	0.0221			0.0959			0.310		
	44.67	44.5	44.59	1030	1030	959	959	958	959	952	952	902	902	905	905	906	906	956.5	904.3	0.052	0.0200			0.0787			0.280		
	42.5	42.47	42.49	940	940	881	881	880	880	876	876	830	830	831	831	833	833	879.0	831.3	0.048	0.0201			0.0792			0.281		
	40	39.72	39.86	842	842	786	786	786	786	784	784	744	743	744	744	745	745	785.3	744.2	0.041	0.0199			0.0777			0.279		
	37.36	37.28	37.32	765	765	714	714	714	714	712	713	675	675	676	676	678	678	713.5	676.3	0.037	0.0202			0.0800			0.283		
2.4D	35.21	35.12	35.17	687	687	642	642	642	642	640	640	610	610	610	610	610	610	641.3	610.0	0.031	0.0196	0.0204	0.0006	0.0759	0.0882	0.0047	0.276	0.2855	0.0082
	32.74	32.84	32.79	629	630	590	590	590	590	587	587	560	560	560	560	561	561	589.0	560.3	0.029	0.0202			0.0799			0.283		
	30	29.75	29.88	560	560	525	525	525	525	525	525	500	500	500	500	500	500	525.0	500.0	0.025	0.0207			0.0840			0.290		
	27.34	27.46	27.40	505	505	478	478	478	478	478	478	455	455	455	455	456	455	478.0	455.2	0.023	0.0215			0.0912			0.302		
	24.81	24.81	24.81	445	445	423	423	423	423	423	423	404	404	408	404	405	405	423.0	405.0	0.018	0.0211			0.0876			0.296		

Baffle type:	Spoiler Baffle (SPB) 3-3-3
Baffle height (h):	0.10D

	Experimental data																				Calculated Roughness coefficients								
						Piezometer #																								
Λ	Q_1 (l/s)	Q_2 (l/s)	Q_a (l/s)	H_{res1} (mm)	H_{res2} (mm)	1	2	3	4	5	6	7	8	9	10	11	12	H_{upavg} (mm)	$H_{downavg}$ (mm)	ΔH (m)	n	n_{avg}	σ	f	f_{avg}	σ	$\sqrt{f}$	$\sqrt{f_{avg}}$	σ
								H_{up} (mm)						H_{down} (mm)																
	45.02	45.00	45.01	103	103	950	950	950	950	949	948	910	909	908	907	906	908	949.5	908.0	0.042	0.0177			0.0614			0.248		
	42.80	42.86	42.83	941	945	878	878	878	878	877	878	837	836	838	838	838	838	877.8	837.5	0.040	0.0183			0.0659			0.257		
	39.90	39.50	39.70	827	825	772	773	772	772	770	769	736	737	735	735	736	739	771.3	736.3	0.035	0.0184			0.0666			0.258		
	37.40	37.70	37.55	757	757	708	710	707	707	705	706	677	678	677	677	678	678	707.2	677.5	0.030	0.0179	0.0183	0.0007	0.0631	0.0660	0.0052	0.251	0.25667	0.00988
0.6D	35.03	34.92	34.98	675	675	634	632	632	632	631	631	606	606	606	605	607	607	632.0	606.2	0.026	0.0179			0.0633			0.252		
	32.68	32.58	32.63	620	621	583	586	582	582	581	582	558	559	560	560	560	561	582.7	559.7	0.023	0.0181			0.0647			0.254		
	30.01	30.10	30.06	559	557	525	527	524	524	523	523	503	502	503	503	505	504	524.3	503.3	0.021	0.0188			0.0697			0.264		
	27.54	27.90	27.72	503	504	477	480	477	480	480	477	460	457	457	460	456	460	478.5	458.3	0.020	0.0200			0.0787			0.280		
	25.05	25.25	25.15	469	439	415	415	415	415	416	416	400	402	402	402	406	403	415.3	402.5	0.013	0.0176			0.0608			0.247		
	45.2	45.2	45.20	1030	1030	958	957	957	957	956	956	921	921	921	921	925	925	956.8	922.3	0.035	0.0160			0.0506			0.225		
	42.85	42.85	42.85	950	954	885	885	886	886	885	885	855	855	855	855	855	855	885.3	855.0	0.030	0.0159			0.0495			0.223		
	39.94	39.76	39.85	830	835	775	775	775	775	775	775	750	750	750	750	750	750	775.0	750.0	0.025	0.0155			0.0472			0.217		
	37.61	37.14	37.38	741	741	692	692	692	692	691	691	666	666	666	666	666	666	691.7	666.0	0.026	0.0167	0.0170	0.0014	0.0551	0.0570	0.0096	0.235	0.2382	0.0193
1.2D	35.04	34.98	35.01	664	664	621	621	621	621	620	620	600	600	600	600	600	600	620.7	600.0	0.021	0.0160			0.0505			0.225		
	32.53	32.73	32.63	615	614	576	576	575	575	575	575	556	556	557	557	556	556	575.3	556.3	0.019	0.0165			0.0535			0.231		
	30	30.3	30.15	558	559	525	525	525	525	525	525	507	507	507	507	507	507	525.0	507.0	0.018	0.0174			0.0593			0.244		
	27.44	27.3	27.37	495	464	470	470	470	470	470	470	451	451	451	451	451	451	470.0	451.0	0.019	0.0197			0.0760			0.276		
	25.14	25.1	25.12	438	437	419	419	419	419	415	415	403	403	402	402	403	403	417.7	402.7	0.015	0.0190			0.0712			0.267		
	45.30	45.40	45.35	1020	1020	943	943	943	943	940	940	910	910	908	908	910	910	942.0	909.3	0.033	0.0156			0.0476			0.218		
	42.40	42.60	42.50	929	929	863	863	863	863	861	861	835	835	835	835	835	835	862.3	835.0	0.027	0.0152			0.0454			0.213		
	40.15	40.15	40.15	836	836	778	778	778	778	778	778	754	754	753	753	752	752	778.0	753.0	0.025	0.0154			0.0465			0.216		
	37.70	37.50	37.60	743	739	691	691	691	691	691	691	668	668	668	668	669	669	691.0	668.3	0.023	0.0156			0.0481			0.219		
1.8D	34.70	34.90	34.80	662	661	620	620	620	620	618	618	600	600	600	600	600	600	619.3	600.0	0.019	0.0156	0.0158	0.0006	0.0478	0.0490	0.0040	0.219	0.2222	0.0088
	32.50	32.00	32.25	601	601	564	564	564	564	562	562	546	546	546	546	546	546	563.3	546.0	0.017	0.0159			0.0500			0.223		
	29.80	30.10	29.95	551	551	519	519	519	519	519	519	504	504	503	503	503	503	519.0	503.3	0.016	0.0163			0.0523			0.229		
	27.50	27.50	27.50	493	493	465	465	465	465	465	465	453	453	454	454	453	453	465.0	453.3	0.012	0.0153			0.0462			0.215		
	25.00	25.00	25.00	434	435	415	415	414	414	411	411	401	401	401	401	401	401	413.3	401.0	0.012	0.0173			0.0591			0.243		
	45.03	45.1	45.07	1010	1010	935	935	935	935	932	931	905	905	905	905	905	905	933.8	905.0	0.029	0.0147			0.0426			0.206		
	42.72	42.8	42.76	927	928	865	865	865	865	864	864	840	840	840	840	840	840	864.7	840.0	0.025	0.0143			0.0404			0.201		
	40	40.3	40.15	835	836	779	779	779	779	777	777	756	756	757	757	757	757	778.3	756.7	0.022	0.0143			0.0403			0.201		
	37.66	37.5	37.58	748	746	696	696	696	696	695	695	675	675	675	675	676	676	695.7	675.3	0.020	0.0148			0.0432			0.208		
2.4D	35.4	35	35.20	676	675	632	632	632	632	631	631	615	615	615	615	615	615	631.7	615.0	0.017	0.0143	0.0151	0.0009	0.0403	0.0450	0.0053	0.201	0.2111	0.0120
	32.5	32.2	32.35	596	593	559	559	559	559	557	557	542	542	542	542	542	542	558.3	542.0	0.016	0.0154			0.0468			0.216		
	30.1	30.4	30.25	551	551	519	519	519	519	517	517	505	505	505	505	505	505	518.3	505.0	0.013	0.0149			0.0437			0.209		
	27.6	27.6	27.60	495	495	470	470	470	470	470	470	455	455	455	455	456	456	470.0	455.3	0.015	0.0171			0.0577			0.240		
	25.4	25.2	25.30	443	444	420	420	421	421	420	420	410	410	410	410	410	410	420.3	410.0	0.010	0.0157			0.0484			0.220		

Baffle type:	**Spoiler Baffle (SPB) 3-3-3**
Baffle height (h):	**0.05D**

Experimental data | **Calculated Roughness coefficients**

Λ	Q_1 (l/s)	Q_2 (l/s)	Q_a (l/s)	H_{res1} (mm)	H_{res2} (mm)	Piezometer # 1	2	3	4	5	6	7	8	9	10	11	12	H_{upavg} (mm)	$H_{downavg}$ (mm)	ΔH (m)	n	n_{avg}	σ	f	f_{avg}	σ	$\sqrt{f}$	$\sqrt{f_{avg}}$	σ
						H_{up} (mm)						H_{down} (mm)																			
	44.90	44.80	44.85	998	998	908	908	907	907	907	907	885	885	885	885	885	885	907.3	885.0	0.022	0.0130			0.0333			0.182		
	42.60	42.30	42.45	896	893	834	834	834	834	834	834	814	814	813	813	812	812	834.0	813.0	0.021	0.0133			0.0349			0.187		
	40.10	40.20	40.15	815	819	760	760	760	760	760	760	745	745	745	745	745	745	760.0	745.0	0.015	0.0119			0.0279			0.167		
	37.34	37.25	37.30	726	727	676	676	676	676	676	676	662	662	662	662	662	662	676.0	662.0	0.014	0.0124			0.0302			0.174		
0.6D	35.00	35.30	35.15	656	659	614	614	614	614	614	614	603	603	602	602	600	600	614.0	601.7	0.012	0.0123	0.0126	0.0006	0.0299	0.0311	0.0028	0.173	0.1762	0.0077
	32.60	32.80	32.70	597	600	561	561	560	560	560	560	550	550	550	550	550	550	560.3	550.0	0.010	0.0121			0.0290			0.170		
	30.10	30.10	30.10	547	548	512	512	515	515	515	515	505	505	505	505	505	505	514.0	505.0	0.009	0.0123			0.0298			0.173		
	27.70	27.40	27.55	485	485	456	456	456	456	456	456	450	450	448	448	448	448	456.0	448.7	0.007	0.0121			0.0290			0.170		
	24.70	24.60	24.65	420	420	402	402	400	400	400	400	393	393	393	393	394	394	400.7	393.3	0.007	0.0136			0.0362			0.190		
	45.2	44.9	45.05	990	990	918	918	918	918	917	917	900	900	903	903	900	906	917.7	902.0	0.016	0.0108			0.0231			0.152		
	42.5	42.8	42.65	910	910	844	844	844	844	843	843	828	828	828	828	828	828	843.7	828.0	0.016	0.0115			0.0258			0.161		
	40.3	39.9	40.10	805	805	750	750	750	750	750	750	735	735	733	733	734	734	750.0	734.0	0.016	0.0123			0.0298			0.173		
	37.4	37.14	37.27	723	725	675	675	675	675	674	674	663	663	661	661	663	663	674.7	662.3	0.012	0.0116			0.0266			0.163		
1.2D	34.9	34.9	34.90	646	646	605	605	605	605	605	605	592	592	592	592	592	592	605.0	592.0	0.013	0.0128	0.0122	0.0009	0.0320	0.0296	0.0044	0.179	0.172	0.0125
	32.5	32.5	32.50	595	595	555	555	556	556	555	555	545	545	545	545	545	545	555.3	545.0	0.010	0.0122			0.0293			0.171		
	30	29.7	29.85	534	535	500	500	505	505	502	502	492	492	492	492	495	495	502.3	493.0	0.009	0.0126			0.0314			0.177		
	27.6	27.5	27.55	485	486	460	460	457	457	458	458	451	451	451	451	451	451	458.3	451.0	0.007	0.0121			0.0290			0.170		
	25.1	25.1	25.10	430	430	411	411	411	411	410	410	402	402	403	403	402	402	410.7	402.3	0.008	0.0142			0.0396			0.199		
	44.96	45.15	45.06	1015	1015	938	938	937	937	937	937	920	920	920	920	920	920	937.3	920.0	0.017	0.0114			0.0256			0.160		
	42.40	42.60	42.50	912	912	847	847	847	847	847	847	831	831	831	831	834	834	847.0	832.0	0.015	0.0112			0.0249			0.158		
	40.10	39.80	39.95	808	805	754	754	750	750	749	749	735	735	735	735	735	735	751.0	735.0	0.016	0.0124			0.0300			0.173		
	37.24	37.21	37.23	721	721	674	674	673	673	672	672	660	660	660	660	660	660	673.0	660.0	0.013	0.0120			0.0281			0.168		
1.8D	34.90	34.82	34.86	657	656	615	615	615	615	612	612	602	602	602	602	602	602	614.0	602.0	0.012	0.0123	0.0121	0.0007	0.0296	0.029	0.0036	0.172	0.169	0.0102
	32.30	32.30	32.30	526	526	562	562	560	560	560	560	550	550	550	550	550	550	560.7	550.0	0.011	0.0125			0.0306			0.175		
	30.16	30.30	30.23	544	542	514	514	510	510	510	510	500	500	500	500	500	500	511.3	500.0	0.011	0.0137			0.0372			0.193		
	27.33	27.54	27.44	484	485	456	456	456	456	456	456	449	449	450	450	450	450	456.0	449.7	0.006	0.0113			0.0252			0.159		
	25.33	25.34	25.34	435	435	411	411	411	411	411	411	405	405	405	405	405	405	411.0	405.0	0.006	0.0119			0.0280			0.167		
	44.7	44.7	44.70	990	990	915	915	915	915	915	915	900	900	895	895	900	900	915.0	898.3	0.017	0.0113			0.0250			0.158		
	42.5	42.4	42.45	906	906	844	844	845	845	845	845	827	827	827	827	827	827	844.7	827.0	0.018	0.0122			0.0294			0.171		
	39.5	39.8	39.65	805	804	750	750	750	750	749	749	734	734	734	734	734	734	749.7	734.0	0.016	0.0123			0.0299			0.173		
	37.5	37.4	37.45	730	731	680	680	681	681	681	681	668	668	668	668	669	669	680.7	668.3	0.012	0.0116			0.0264			0.162		
2.4D	35	34.8	34.90	657	655	614	614	615	615	614	614	602	602	601	601	602	602	614.3	601.7	0.013	0.0126	0.0120	0.0010	0.0312	0.029	0.0048	0.177	0.169	0.0145
	32.7	32.8	32.75	601	600	563	563	563	563	562	562	553	553	553	553	553	553	562.7	553.0	0.010	0.0117			0.0270			0.164		
	29.8	29.5	29.65	537	535	505	505	505	505	504	504	495	495	494	494	495	495	504.7	494.7	0.010	0.0132			0.0341			0.185		
	27.6	28	27.80	493	495	465	465	465	465	465	465	460	460	460	460	460	460	465.0	460.0	0.005	0.0099			0.0194			0.139		
	25	25.1	25.05	435	436	414	414	414	414	414	414	407	407	406	406	406	406	414.0	406.3	0.008	0.0136			0.0366			0.191		

Baffle type:	**Spoiler Baffle (SPB) 3-2-3**
Baffle height (h):	**0.15D**

	Experimental data																				Calculated Roughness coefficients											
						Piezometer #																											
Λ	Q_1 (l/s)	Q_2 (l/s)	Q_a (l/s)	H_{res1} (mm)	H_{res2} (mm)	1	2	3	4	5	6	7	8	9	10	11	12	H_{upavg} (mm)	$H_{downavg}$ (mm)	ΔH (m)	n	n_{avg}	σ	f	f_{avg}	σ	$\sqrt{f}$	$\sqrt{f_{avg}}$	σ		
								H_{up} (mm)						H_{down} (mm)																			
	25.00	25.10	25.05	454	455	430	432	434	430	430	431	408	409	407	405	407	407	431.2	407.2	0.024	0.0241			0.1146			0.339				
	27.60	27.60	27.60	516	516	489	484	490	489	482	482	458	459	456	455	459	459	486.0	457.7	0.028	0.0238			0.1115			0.334				
	29.90	30.30	30.10	573	573	539	541	540	538	536	536	505	504	505	504	505	505	538.3	504.7	0.034	0.0238			0.1114			0.334				
	32.40	32.20	32.30	628	627	589	590	589	590	587	586	550	550	551	552	550	550	588.5	550.5	0.038	0.0236			0.1092			0.330				
0.6D	35.20	35.60	35.40	705	705	660	662	660	660	657	656	614	615	615	616	616	617	659.2	615.5	0.044	0.0230	0.0234	0.0005	0.1044	0.1078	0.00442	0.323	0.32833	0.00064		
	37.50	37.30	37.40	764	764	713	714	712	713	712	710	666	665	665	665	667	666	712.3	665.7	0.047	0.0225			0.1000			0.316				
	40.20	39.80	40.00	863	863	805	805	805	806	803	801	748	747	747	748	750	749	804.2	748.2	0.056	0.0231			0.1049			0.324				
	42.40	42.15	42.28	955	955	889	889	889	890	887	885	824	824	823	824	824	823	888.2	823.7	0.065	0.0234			0.1082			0.329				
	44.53	44.40	44.47	1041	1041	968	967	966	967	965	964	895	894	895	896	898	899	966.2	896.2	0.070	0.0232			0.1061			0.326				
	25.1	25.1	25.10	454	453	431	433	435	433	430	431	410	410	412	410	411	411	432.2	410.7	0.022	0.0228			0.1023			0.320				
	27.4	27.7	27.55	515	514	487	489	490	488	488	486	461	462	463	462	462	462	488.0	462.0	0.026	0.0228			0.1027			0.320				
	30.2	30.4	30.30	574	573	540	541	542	540	538	539	510	510	511	510	510	510	540.0	510.2	0.030	0.0223			0.0974			0.312				
	32.4	32.4	32.40	620	619	584	585	585	583	580	580	549	550	550	549	551	549	582.8	549.7	0.033	0.0219			0.0947			0.308				
1.2D	35	34.9	34.95	695	694	650	652	652	651	650	648	614	613	613	614	615	614	650.5	613.8	0.037	0.0214	0.0218	0.0006	0.0900	0.0938	0.00548	0.300	0.3006	0.00888		
	37.6	37.9	37.75	785	786	734	734	735	735	733	731	691	690	690	691	692	691	733.7	690.8	0.043	0.0214			0.0901			0.300				
	40	40.2	40.10	869	870	812	812	811	812	810	808	761	760	762	763	766	765	810.8	762.8	0.048	0.0213			0.0895			0.299				
	42.4	42.4	42.40	950	952	886	886	886	887	888	887	831	831	833	833	835	836	886.7	833.2	0.054	0.0213			0.0892			0.299				
	44.5	44.7	44.60	1032	1032	958	957	958	959	955	953	897	896	897	898	900	901	956.7	898.2	0.059	0.0212			0.0881			0.297				
	24.70	24.80	24.75	440	440	420	420	421	420	421	420	401	403	403	402	403	403	420.3	402.5	0.018	0.0211			0.0873			0.295				
	27.60	27.50	27.55	510	510	484	480	489	490	489	487	461	460	460	460	460	460	486.5	460.2	0.026	0.0230			0.1040			0.322				
	30.20	30.10	30.15	573	573	539	540	540	541	540	539	514	515	515	514	515	515	539.8	514.7	0.025	0.0205			0.0830			0.288				
	32.70	32.60	32.65	628	629	590	591	591	590	589	588	560	559	561	560	562	563	589.8	560.8	0.029	0.0204			0.0815			0.286				
1.8D	34.60	34.60	34.60	685	685	640	641	643	641	639	638	609	608	608	608	610	609	640.3	608.7	0.032	0.0201	0.0205	0.0010	0.0793	0.0833	0.00822	0.282	0.2882	0.01377		
	37.40	37.40	37.40	768	767	719	718	720	719	717	715	679	678	680	680	680	684	718.0	680.2	0.038	0.0203			0.0811			0.285				
	40.10	40.20	40.15	866	865	809	808	808	809	805	803	764	763	763	763	768	769	807.0	765.0	0.042	0.0199			0.0781			0.279				
	42.50	42.10	42.30	933	934	870	870	869	870	867	864	822	823	824	824	826	827	868.3	824.3	0.044	0.0194			0.0737			0.271				
	44.60	44.30	44.45	1032	1031	957	957	957	956	958	956	903	902	904	903	907	908	956.8	904.5	0.052	0.0201			0.0794			0.282				
	24.7	24.6	24.65	439	439	419	418	421	419	420	420	402	403	402	405	402	405	419.5	403.2	0.016	0.0202			0.0806			0.284				
	27.8	27.9	27.85	511	512	485	483	484	483	485	485	464	465	466	464	465	463	484.2	464.5	0.020	0.0197			0.0760			0.276				
	30.2	30.2	30.20	563	563	532	530	532	530	530	531	508	509	510	507	510	508	530.8	508.7	0.022	0.0192			0.0728			0.270				
	32.6	32.5	32.55	622	621	585	584	585	584	584	585	559	560	558	560	559	561	584.5	559.5	0.025	0.0190			0.0707			0.266				
2.4D	35.4	35.1	35.25	682	682	640	639	640	639	640	638	609	608	612	610	613	611	639.3	610.5	0.029	0.0188	0.0191	0.0005	0.0696	0.072	0.0036	0.264	0.269	0.0065		
	37.5	37.5	37.50	764	763	715	713	713	714	714	713	680	680	682	680	683	680	713.7	680.8	0.033	0.0189			0.0700			0.265				
	39.8	39.9	39.85	844	843	787	786	788	787	786	785	749	749	751	749	751	750	786.5	749.8	0.037	0.0188			0.0692			0.263				
	42.6	42.5	42.55	955	955	888	888	887	888	885	886	844	843	845	845	845	846	887.0	844.7	0.042	0.0189			0.0701			0.265				
	45.1	44.7	44.90	102.9	102.8	953	953	953	953	950	948	902	902	905	904	906	906	951.7	904.2	0.048	0.0189			0.0706			0.266				

Baffle type:	**Spoiler Baffle (SPB) 3-2-3**
Baffle height (h):	**0.10D**

	Experimental data																				Calculated Roughness coefficients								
						Piezometer #																								
Λ	Q_1 (l/s)	Q_2 (l/s)	Q_a (l/s)	H_{res1} (mm)	H_{res2} (mm)	1	2	3	4	5	6	7	8	9	10	11	12	H_{upavg} (mm)	$H_{downavg}$ (mm)	ΔH (m)	n	n_{avg}	σ	f	f_{avg}	σ	$\sqrt{f}$	$\sqrt{f_{avg}}$	σ
						H_{up} (mm)						H_{down} (mm)																		
	25.00	25.20	25.10	443	443	422	420	423	421	421	420	410	411	410	409	412	410	421.2	410.3	0.011	0.0162			0.0515			0.227		
	27.30	27.30	27.30	496	496	470	468	469	465	468	466	455	456	453	452	459	453	467.7	454.7	0.013	0.0163			0.0523			0.229		
	29.80	29.90	29.85	557	558	523	520	522	520	522	519	508	509	509	506	509	508	521.0	508.2	0.013	0.0148			0.0432			0.208		
	32.40	32.90	32.65	622	623	586	584	587	585	585	584	563	564	565	563	564	563	585.2	563.7	0.022	0.0175	0.0167	0.0008	0.0604	0.0550	0.0051	0.246	0.2343	0.0112
0.6D	35.10	35.40	35.25	688	688	644	643	646	643	643	643	620	623	621	619	623	620	643.7	621.0	0.023	0.0167			0.0547			0.234		
	37.80	37.70	37.75	768	768	720	718	718	718	717	717	690	690	690	689	691	689	718.0	689.8	0.028	0.0174			0.0592			0.243		
	40.20	40.10	40.15	850	850	792	792	793	792	791	791	760	760	763	760	763	761	791.8	761.2	0.031	0.0170			0.0570			0.239		
	42.90	42.60	42.75	946	946	880	880	880	880	879	880	844	843	845	844	845	844	879.8	844.2	0.036	0.0172			0.0585			0.242		
	45.20	45.10	45.15	1040	1041	963	962	964	963	962	963	923	923	922	922	925	924	962.8	923.2	0.040	0.0172			0.0583			0.241		
	44.7	44.8	44.75	1018	1017	939	938	939	940	937	938	907	907	907	908	910	909	938.5	908.0	0.031	0.0152			0.0456			0.214		
	42.5	42.5	42.50	922	922	857	858	857	857	855	856	830	829	827	828	829	828	856.7	828.5	0.028	0.0154			0.0467			0.216		
	40.2	40.3	40.25	841	840	785	784	785	784	781	782	757	756	756	757	757	758	783.5	756.8	0.027	0.0158			0.0493			0.222		
	37.6	37.5	37.55	754	754	703	703	703	703	700	702	681	680	680	680	680	681	702.3	680.3	0.022	0.0154	0.0157	0.0005	0.0468	0.0487	0.0032	0.216	0.2221	0.0071
1.2D	35.3	35.2	35.25	674	674	633	631	632	631	629	630	611	611	611	610	611	611	631.0	610.8	0.020	0.0157			0.0486			0.221		
	32.5	32.5	32.50	608	609	572	570	573	570	570	570	553	553	554	552	553	553	570.8	553.0	0.018	0.0160			0.0506			0.225		
	30	29.7	29.85	546	546	517	515	516	512	511	511	499	498	499	497	498	498	513.7	498.2	0.015	0.0163			0.0521			0.228		
	27.5	27.6	27.55	495	496	470	467	466	467	466	466	455	453	458	456	456	457	467.0	455.8	0.011	0.0150			0.0441			0.210		
	25.2	25	25.10	439	440	420	418	421	418	418	418	407	406	409	406	408	408	418.8	407.3	0.012	0.0167			0.0547			0.234		
	44.60	44.70	44.65	1000	1000	926	926	925	926	923	924	899	898	897	896	900	897	925.0	897.8	0.027	0.0144			0.0408			0.202		
	42.70	42.70	42.70	929	928	862	861	862	863	860	861	835	836	836	835	837	837	861.5	836.0	0.026	0.0146			0.0419			0.205		
	40.00	40.00	40.00	833	831	775	775	775	775	773	774	750	749	750	749	750	751	774.5	749.8	0.025	0.0153			0.0462			0.215		
	37.30	37.60	37.45	745	745	695	694	695	695	693	694	674	674	675	674	676	676	694.3	674.8	0.020	0.0146			0.0417			0.204		
1.8D	35.00	35.10	35.05	662	663	621	619	621	619	618	619	602	602	602	602	603	603	619.5	602.3	0.017	0.0146	0.0151	0.0006	0.0419	0.0445	0.0037	0.205	0.2122	0.0086
	32.80	33.00	32.90	615	615	578	576	578	576	575	575	560	559	561	560	562	561	576.3	560.5	0.016	0.0149			0.0438			0.209		
	30.10	30.00	30.05	546	546	516	514	516	514	513	514	501	500	501	500	502	501	514.5	500.8	0.014	0.0152			0.0454			0.213		
	27.40	27.60	27.50	492	493	467	466	466	464	465	464	452	453	451	452	453	453	465.3	452.3	0.013	0.0162			0.0515			0.227		
	25.00	24.60	24.80	431	431	412	411	412	410	412	410	400	400	401	400	404	400	411.2	400.8	0.010	0.0160			0.0504			0.224		
	45.1	45.3	45.20	1022	1025	948	947	948	948	946	947	921	922	922	922	921	921	947.3	921.5	0.026	0.0139			0.0379			0.195		
	42.6	42.3	42.45	907	905	843	843	843	844	841	842	819	818	818	817	817	818	842.7	817.8	0.025	0.0145			0.0413			0.203		
	40.2	40.1	40.15	838	837	779	778	779	779	778	779	757	757	757	756	758	757	778.7	757.0	0.022	0.0143			0.0403			0.201		
	37.3	37.2	37.25	743	742	693	693	694	693	691	693	675	674	675	674	674	674	692.8	674.3	0.019	0.0143			0.0400			0.200		
2.4D	34.9	35.1	35.00	661	661	620	618	621	619	619	618	602	601	602	602	603	603	619.2	602.2	0.017	0.0145	0.0142	0.0005	0.0416	0.0400	0.0025	0.204	0.199	0.0065
	32.5	32.3	32.40	607	607	570	568	571	569	570	567	554	554	554	554	555	555	569.2	554.3	0.015	0.0147			0.0424			0.206		
	30.3	30.7	30.50	559	661	528	526	530	528	529	526	515	514	516	514	516	515	527.8	515.0	0.013	0.0145			0.0413			0.203		
	27.8	27.8	27.80	498	497	471	469	467	466	467	467	459	458	460	457	461	459	467.8	459.0	0.009	0.0132			0.0343			0.185		
	25	25	25.00	432	432	413	411	410	410	411	410	401	402	405	402	406	403	410.8	403.2	0.008	0.0137			0.0368			0.192		

Baffle type:	**Spoiler Baffle (SPB) 3-2-3**
Baffle height (h):	**0.05D**

Experimental data | **Calculated Roughness coefficients**

Δ	Q_1 (l/s)	Q_2 (l/s)	Q_a (l/s)	H_{res1} (mm)	H_{res2} (mm)	Piezometer # 1	2	3	4	5	6	7	8	9	10	11	12	H_{upavg} (mm)	$H_{downavg}$ (mm)	ΔH (m)	n	n_{avg}	σ	f	f_{avg}	σ	$\sqrt{f}$	$\sqrt{f_{avg}}$	σ
						H_{up} (mm)						H_{down} (mm)																			
	44.90	45.20	45.05	1008	1007	931	931	932	932	930	931	912	912	910	911	913	910	931.2	911.3	0.020	0.0122			0.0293			0.171		
	42.50	42.60	42.55	907	907	842	841	840	840	840	841	821	821	821	822	821	821	840.7	821.2	0.020	0.0128			0.0323			0.180		
	40.20	40.30	40.25	823	822	767	765	765	766	764	765	748	747	748	747	747	748	765.3	747.5	0.018	0.0130			0.0330			0.182		
	37.30	37.20	37.25	729	729	680	679	678	678	678	679	665	664	665	664	664	664	678.7	664.3	0.014	0.0125	0.0133	0.0009	0.0310	0.03551	0.00550	0.176	0.18669	0.00131
0.6D	35.20	35.10	35.15	671	671	628	626	627	626	626	626	614	613	613	613	613	613	626.5	613.2	0.013	0.0128			0.0323			0.180		
	32.50	32.40	32.45	600	600	564	563	561	561	560	560	550	550	550	549	551	551	561.5	550.2	0.011	0.0128			0.0323			0.180		
	29.90	29.60	29.75	537	537	509	508	508	507	507	506	495	495	496	495	495	495	507.5	495.2	0.012	0.0146			0.0418			0.204		
	27.40	27.40	27.40	487	488	464	461	462	461	461	460	451	452	451	450	453	452	461.5	451.5	0.010	0.0142			0.0399			0.200		
	25.30	25.10	25.20	434	434	416	415	416	414	417	414	406	405	406	406	407	406	415.3	406.0	0.009	0.0150			0.0441			0.210		
	45.3	45.2	45.25	1014	1014	937	937	937	938	936	937	920	919	918	918	920	918	937.0	918.8	0.018	0.0116			0.0266			0.163		
	42.5	42.3	42.40	914	914	848	848	847	848	847	848	830	831	831	832	834	832	847.7	831.7	0.016	0.0116			0.0267			0.163		
	39.8	39.5	39.65	811	811	755	754	754	755	753	754	740	739	739	738	739	739	754.2	739.0	0.015	0.0121			0.0289			0.170		
	37.7	37.6	37.65	742	742	692	691	692	692	692	691	677	678	678	677	678	677	691.7	677.5	0.014	0.0123	0.0123	0.0007	0.0300	0.02966	0.00034	0.173	0.1722	0.00096
1.2D	35	34.9	34.95	661	661	618	617	618	617	617	617	605	605	605	604	605	605	617.3	604.8	0.013	0.0125			0.0307			0.175		
	32.6	32.7	32.65	602	602	566	565	566	564	564	563	555	554	554	553	555	554	564.7	554.2	0.011	0.0123			0.0295			0.172		
	30	30.1	30.05	545	546	515	514	517	515	515	513	505	504	506	505	505	505	514.8	505.0	0.010	0.0129			0.0326			0.181		
	27.7	27.5	27.60	489	490	461	460	463	463	463	460	455	455	457	455	455	455	461.7	455.3	0.006	0.0113			0.0249			0.158		
	25	25	25.00	431	430	412	411	411	410	412	410	403	402	405	403	404	403	411.0	403.3	0.008	0.0137			0.0368			0.192		
	45.20	45.00	45.10	1006	1005	928	928	928	929	928	929	912	912	912	913	915	912	928.3	912.7	0.016	0.0108			0.0231			0.152		
	42.30	42.40	42.35	900	899	836	836	836	837	835	836	819	819	820	820	823	820	836.0	820.2	0.016	0.0116			0.0265			0.163		
	40.20	39.90	40.05	818	817	762	761	761	761	760	761	747	747	745	746	748	746	761.0	746.5	0.015	0.0117			0.0271			0.165		
	37.40	37.30	37.35	727	728	680	679	679	678	677	678	666	665	665	665	665	665	678.5	665.2	0.013	0.0121	0.0121	0.0006	0.0286	0.02929	0.00029	0.169	0.1700	0.00088
1.8D	35.00	34.90	34.95	658	657	617	617	614	614	613	614	603	603	602	602	602	603	614.8	602.5	0.012	0.0124			0.0303			0.174		
	32.70	32.80	32.75	603	602	566	565	564	564	563	563	555	554	554	553	554	554	564.2	554.0	0.010	0.0120			0.0284			0.169		
	30.30	30.10	30.20	549	549	519	518	517	516	515	516	508	508	508	508	508	507	516.8	507.8	0.009	0.0123			0.0296			0.172		
	27.70	27.70	27.70	491	491	465	464	463	463	463	463	455	455	455	454	456	455	463.5	455.0	0.009	0.0130			0.0332			0.182		
	25.00	25.10	25.05	432	4432	412	410	412	410	410	410	404	404	404	403	404	404	410.7	403.8	0.007	0.0129			0.0326			0.181		
	44.8	44.7	44.75	996	997	924	923	923	924	923	924	905	905	905	905	904	905	923.5	904.8	0.019	0.0119			0.0279			0.167		
	42.6	42.8	42.70	919	919	854	854	853	854	852	852	837	837	837	837	837	838	853.2	837.2	0.016	0.0116			0.0263			0.162		
	40	40.2	40.10	829	828	771	771	771	772	770	771	755	755	755	755	755	755	771.0	755.0	0.016	0.0123			0.0298			0.173		
	37.6	37.4	37.50	736	737	687	686	687	687	687	686	674	674	674	674	675	675	686.7	674.3	0.012	0.0116			0.0263			0.162		
2.4D	35.2	35.4	35.30	666	666	624	622	625	623	625	623	612	612	611	610	611	611	623.7	611.2	0.013	0.0124	0.0123	0.0006	0.0301	0.0300	0.0032	0.173	0.1730	0.0090
	32.5	32.2	32.35	595	595	559	557	560	557	560	557	549	548	548	548	548	549	558.3	548.3	0.010	0.0121			0.0286			0.169		
	30.2	30.2	30.20	548	548	517	515	517	515	517	515	507	506	507	507	508	507	516.0	507.0	0.009	0.0123			0.0296			0.172		
	27.5	27.4	27.45	485	485	461	459	460	458	460	458	450	451	450	450	450	450	459.3	450.2	0.009	0.0136			0.0365			0.191		
	25.2	25.1	25.15	433	433	414	412	414	413	415	413	406	406	406	406	407	407	413.5	406.3	0.007	0.0131			0.0340			0.184		

Baffle type:	**Spoiler Baffle (SPB) 2-2-2**
Baffle height (h):	**0.15D**

	Experimental data																				Calculated Roughness coefficients								
						Piezometer #																								
Λ	Q_1 (l/s)	Q_2 (l/s)	Q_a (l/s)	H_{res1} (mm)	H_{res2} (mm)	1	2	3	4	5	6	7	8	9	10	11	12	H_{upavg} (mm)	$H_{downavg}$ (mm)	ΔH (m)	n	n_{avg}	σ	f	f_{avg}	σ	$\sqrt{f}$	$\sqrt{f_{avg}}$	σ
						H_{up} (mm)						H_{down} (mm)																		
	44.20	44.56	44.38	1050	1050	975	975	975	975	974	973	913	913	915	916	916	917	974.5	915.0	0.060	0.0215			0.0905			0.301		
	42.80	42.60	42.70	980	980	910	910	910	910	906	907	853	853	854	856	856	856	908.8	854.7	0.054	0.0213			0.0890			0.298		
	40.00	39.60	39.80	867	865	811	811	811	811	809	809	760	760	764	767	763	765	810.3	763.2	0.047	0.0213			0.0892			0.299		
	37.40	37.50	37.45	782	782	732	732	732	732	730	730	687	687	687	693	690	692	731.3	689.3	0.042	0.0214			0.0898			0.300		
0.6D	35.10	35.20	35.15	701	701	658	660	660	660	656	660	620	623	620	622	620	623	659.0	621.3	0.038	0.0216	0.0215	0.0006	0.0914	0.0910	0.0054	0.302	0.30115	0.00088
	32.50	32.60	32.55	623	623	585	590	590	590	585	587	557	557	557	557	556	557	587.8	556.8	0.031	0.0211			0.0877			0.296		
	30.00	30.30	30.15	577	580	544	547	548	548	545	548	521	521	522	522	522	523	546.7	521.8	0.025	0.0204			0.0819			0.286		
	27.35	27.30	27.33	507	506	483	483	483	483	483	483	457	457	456	456	460	460	483.0	457.7	0.025	0.0227			0.1017			0.319		
	25.00	25.00	25.00	450	450	432	431	432	432	430	430	410	411	411	411	411	411	431.2	410.8	0.020	0.0223			0.0975			0.312		
	44.6	44.8	44.70	1045	1050	974	974	973	973	972	972	920	920	921	921	920	920	973.0	920.3	0.053	0.0200			0.0790			0.281		
	42.4	42.5	42.45	956	957	894	894	895	895	895	895	846	846	847	848	847	850	894.7	847.3	0.047	0.0200			0.0787			0.281		
	40	40.2	40.10	863	866	807	807	809	809	807	810	765	765	769	770	768	769	808.2	767.7	0.041	0.0196			0.0755			0.275		
	37.4	37.2	37.30	772	771	724	725	723	726	723	725	685	685	687	689	686	688	724.3	686.7	0.038	0.0203			0.0811			0.285		
1.2D	35.3	35.3	35.30	702	702	661	661	660	660	660	660	626	626	630	630	628	629	660.3	628.2	0.032	0.0198	0.0205	0.0008	0.0774	0.0830	0.0064	0.278	0.2888	0.00110
	32.4	32.8	32.60	633	634	600	600	597	600	595	598	567	569	571	571	571	570	598.3	569.8	0.029	0.0202			0.0804			0.284		
	30	29.8	29.90	570	567	540	540	540	540	538	539	510	514	513	513	510	514	539.5	512.3	0.027	0.0215			0.0911			0.302		
	27.2	27.1	27.15	501	501	480	480	480	480	480	480	456	456	456	456	458	458	480.0	456.7	0.023	0.0220			0.0949			0.308		
	25	25	25.00	449	449	431	430	430	432	428	430	411	410	413	412	411	413	430.2	411.7	0.019	0.0212			0.0887			0.298		
	44.70	45.00	44.85	1040	1040	965	965	965	965	964	965	920	920	919	919	915	917	964.8	918.3	0.047	0.0188			0.0693			0.263		
	42.80	42.40	42.60	951	948	886	886	885	885	881	884	842	842	842	842	843	843	884.5	842.3	0.042	0.0188			0.0696			0.264		
	40.00	39.70	39.85	852	851	795	796	795	795	793	794	757	758	759	759	760	760	794.7	758.8	0.036	0.0185			0.0676			0.260		
	37.80	37.40	37.60	770	770	720	720	721	721	719	719	687	687	689	691	687	691	720.0	688.7	0.031	0.0184			0.0664			0.258		
1.8D	34.80	35.20	35.00	689	690	644	647	645	645	645	645	619	619	620	622	620	622	645.2	620.3	0.025	0.0176	0.0186	0.0006	0.0608	0.0688	0.0044	0.246	0.2261	0.00085
	32.60	32.60	32.60	630	630	590	595	591	595	590	591	568	568	569	571	571	572	592.0	569.8	0.022	0.0178			0.0625			0.250		
	30.25	30.10	30.18	570	570	540	537	540	539	537	537	517	517	518	518	515	518	538.3	517.2	0.021	0.0188			0.0697			0.264		
	27.50	27.60	27.55	509	510	485	485	486	484	485	485	466	467	465	465	469	468	485.0	466.7	0.018	0.0192			0.0724			0.269		
	25.10	25.10	25.10	450	450	430	430	430	430	430	430	412	412	415	415	415	415	430.0	414.0	0.016	0.0197			0.0761			0.276		
	44.8	44.6	44.70	1040	1040	960	960	961	960	960	960	920	920	923	922	922	923	960.2	921.7	0.039	0.0171			0.0578			0.240		
	42.3	42.3	42.30	941	940	876	876	877	877	876	878	839	839	842	843	842	843	876.7	841.3	0.035	0.0173			0.0592			0.243		
	40	39.9	39.95	845	845	788	788	790	790	790	790	756	756	757	758	759	760	789.3	757.7	0.032	0.0174			0.0595			0.244		
	37.6	37.3	37.45	760	760	710	710	713	715	713	715	685	685	687	687	687	687	712.7	686.3	0.026	0.0169			0.0563			0.237		
2.4D	35	35.1	35.05	687	685	641	645	646	644	643	643	621	621	623	623	620	623	643.7	621.8	0.022	0.0165	0.0172	0.0006	0.0533	0.0559	0.0043	0.231	0.2422	0.00087
	32.7	32.8	32.75	633	634	594	596	594	598	594	596	575	575	576	576	574	576	595.3	575.3	0.020	0.0169			0.0559			0.236		
	30	29.9	29.95	567	567	537	535	537	537	535	534	519	519	520	520	520	520	535.8	519.7	0.016	0.0166			0.0540			0.232		
	27.5	27.6	27.55	507	507	482	482	482	482	482	482	466	466	466	465	467	466	482.0	466.0	0.016	0.0179			0.0632			0.251		
	24.9	25.25	25.08	447	448	430	430	430	430	430	430	415	416	416	416	416	416	430.0	415.8	0.014	0.0185			0.0675			0.260		

Baffle type:	**Spoiler Baffle (SPB) 2-2-2**
Baffle height (h):	**0.10D**

	Experimental data																				Calculated Roughness coefficients								
						Piezometer #																								
Λ	Q_1 (l/s)	Q_2 (l/s)	Q_a (l/s)	H_{res1} (mm)	H_{res2} (mm)	1	2	3	4	5	6	7	8	9	10	11	12	H_{upavg} (mm)	$H_{downavg}$ (mm)	ΔH (m)	n	n_{avg}	σ	f	f_{avg}	σ	$\sqrt{f}$	$\sqrt{f_{avg}}$	σ
								H_{up} (mm)						H_{down} (mm)																
	45.00	45.00	45.00	1030	1030	953	953	953	953	954	954	915	915	916	917	918	918	953.3	916.5	0.037	0.0166			0.0545			0.233		
	42.80	42.80	42.80	947	947	883	883	884	884	884	884	849	849	850	851	851	851	883.7	850.2	0.034	0.0167			0.0548			0.234		
	39.75	39.90	39.83	839	836	781	781	783	784	780	783	750	750	751	751	750	750	782.0	750.3	0.032	0.0174			0.0598			0.245		
	37.30	37.20	37.25	757	757	708	710	709	710	707	709	681	680	682	682	682	687	708.8	682.3	0.027	0.0171			0.0572			0.239		
0.6D	35.10	35.30	35.20	683	685	640	642	643	643	640	642	620	620	617	617	619	619	641.7	618.7	0.023	0.0168	0.0170	0.0005	0.0556	0.0571	0.0032	0.236	0.2388	0.00067
	32.34	32.40	32.37	614	616	580	580	581	581	580	580	560	560	557	557	560	560	580.3	559.0	0.021	0.0176			0.0610			0.247		
	29.70	29.60	29.65	554	551	524	524	523	523	523	523	505	505	505	506	503	506	523.3	505.0	0.018	0.0178			0.0625			0.250		
	27.50	27.10	27.30	490	490	465	465	465	465	465	465	451	451	451	451	451	451	465.0	451.0	0.014	0.0169			0.0563			0.237		
	25.10	25.30	25.20	450	450	430	430	431	431	431	432	420	419	420	420	420	420	430.8	419.8	0.011	0.0162			0.0519			0.228		
	44.7	44.8	44.75	1005	1007	933	933	934	934	933	933	905	905	905	905	905	906	933.3	905.2	0.028	0.0146			0.0422			0.205		
	42.4	42.3	42.35	931	930	867	867	867	867	865	865	840	840	840	840	840	842	866.3	840.3	0.026	0.0149			0.0434			0.208		
	39.75	39.4	39.58	822	820	765	765	770	770	765	765	741	741	740	740	741	741	766.7	740.7	0.026	0.0159			0.0498			0.223		
	37.4	37.3	37.35	745	741	695	695	697	697	694	694	673	673	673	673	673	675	695.3	673.3	0.022	0.0155			0.0473			0.217		
1.2D	34.7	34.8	34.75	671	670	630	630	631	631	629	629	609	610	610	610	610	611	630.0	610.0	0.020	0.0159	0.0156	0.0008	0.0496	0.0477	0.0047	0.223	0.218	0.00107
	32.4	32.1	32.25	600	600	565	565	565	565	563	564	546	546	546	546	548	549	564.5	546.8	0.018	0.0161			0.0509			0.226		
	30	29.9	29.95	554	554	524	524	524	524	520	524	506	506	505	505	508	509	523.3	506.5	0.017	0.0169			0.0562			0.237		
	27.7	27.5	27.60	501	500	475	475	475	475	471	474	460	460	462	461	462	464	474.2	461.5	0.013	0.0159			0.0498			0.223		
	25	25.2	25.10	440	440	420	421	420	420	419	419	410	411	412	411	413	411	419.8	411.3	0.009	0.0143			0.0404			0.201		
	44.90	44.80	44.85	1015	1015	940	940	940	940	940	940	915	915	914	914	915	915	940.0	914.7	0.025	0.0139			0.0377			0.194		
	42.60	42.80	42.70	931	931	867	867	867	867	867	867	845	845	845	845	844	844	867.0	844.7	0.022	0.0137			0.0367			0.192		
	40.00	39.80	39.90	842	842	785	785	785	785	785	785	762	764	762	762	762	764	785.0	762.7	0.022	0.0146			0.0420			0.205		
	37.60	37.70	37.65	760	761	710	713	711	713	711	711	690	690	690	690	690	692	711.5	690.3	0.021	0.0151			0.0448			0.212		
1.8D	34.80	34.60	34.70	669	669	625	627	625	627	626	627	612	613	610	611	610	612	626.2	611.3	0.015	0.0137	0.0137	0.0011	0.0369	0.037	0.0055	0.192	0.192	0.0152
	32.60	32.70	32.65	622	622	583	585	582	585	582	585	570	571	570	570	569	570	583.7	570.0	0.014	0.0140			0.0384			0.196		
	29.90	29.80	29.85	556	556	522	522	522	522	521	521	510	510	511	511	509	510	521.7	510.2	0.011	0.0140			0.0387			0.197		
	27.70	27.80	27.75	509	510	482	482	482	482	483	483	474	474	474	474	473	474	482.3	473.8	0.009	0.0130			0.0331			0.182		
	24.90	25.10	25.00	440	441	420	420	420	420	421	421	415	415	416	416	415	415	420.3	415.3	0.005	0.0110			0.0240			0.155		
	44.9	44.7	44.80	1010	1010	933	933	933	933	933	933	909	909	910	910	911	911	933.0	910.0	0.023	0.0132			0.0343			0.185		
	42.7	42.5	42.60	932	930	867	867	867	867	867	867	845	845	846	846	844	844	867.0	845.0	0.022	0.0136			0.0363			0.191		
	39.9	40.1	40.00	840	839	784	784	784	784	785	785	762	762	762	762	762	762	784.3	762.0	0.022	0.0146			0.0418			0.205		
	37.6	37.6	37.60	755	755	705	706	706	705	705	707	686	686	686	686	686	686	705.7	686.0	0.020	0.0146			0.0417			0.204		
2.4D	34.7	34.9	34.80	673	674	630	634	630	634	632	633	615	615	615	615	615	616	632.2	615.2	0.017	0.0146	0.0143	0.0010	0.0421	0.040	0.0053	0.205	0.201	0.0133
	32.7	32.6	32.65	614	614	576	576	579	579	579	579	562	562	562	562	562	564	578.0	562.3	0.016	0.0150			0.0440			0.210		
	30.1	30	30.05	560	560	530	530	531	531	530	530	515	515	515	517	515	516	530.3	515.5	0.015	0.0158			0.0492			0.222		
	27.65	27.6	27.63	502	502	476	476	477	477	477	477	465	466	465	467	463	467	476.7	465.5	0.011	0.0149			0.0439			0.209		
	24.9	25.25	25.08	443	443	421	421	422	422	422	422	415	415	415	415	416	415	421.7	415.2	0.007	0.0126			0.0310			0.176		

Baffle type:	Spoiler Baffle (SPB) 2-2-2
Baffle height (h):	0.05D

	Experimental data																				Calculated Roughness coefficients									
						Piezometer #																									
Λ	Q_1 (l/s)	Q_2 (l/s)	Q_a (l/s)	H_{res1} (mm)	H_{res2} (mm)	1	2	3	4	5	6	7	8	9	10	11	12	H_{upavg} (mm)	$H_{downavg}$ (mm)	ΔH (m)	n	n_{avg}	σ	f	f_{avg}	σ	$\sqrt{f}$	$\sqrt{f_{avg}}$	σ
						H_{up} (mm)						H_{down} (mm)																			
	45.00	45.20	45.10	1002	1002	933	933	933	933	933	933	912	912	913	913	913	913	933.0	912.7	0.020	0.0123			0.0300			0.173		
	42.60	42.30	42.45	922	920	859	859	859	859	860	860	839	839	839	839	837	837	859.3	838.3	0.021	0.0133			0.0349			0.187		
	40.00	39.70	39.85	835	832	778	778	778	778	779	779	760	762	760	763	760	764	778.3	761.5	0.017	0.0127			0.0318			0.178		
	37.60	37.50	37.55	748	748	700	700	698	699	697	698	685	685	683	684	685	686	698.7	684.7	0.014	0.0123			0.0298			0.173		
0.6D	35.20	35.20	35.20	676	676	635	635	635	635	635	636	623	624	620	624	620	624	635.2	622.5	0.013	0.0125	0.0125	0.0008	0.0306	0.0310	0.0037	0.175	0.1759	0.0108
	32.60	32.90	32.75	619	619	584	584	580	583	584	584	572	572	569	572	570	571	583.2	571.0	0.012	0.0131			0.0340			0.184		
	30.00	30.00	30.00	552	552	524	524	522	523	522	523	513	512	510	513	512	512	523.0	512.0	0.011	0.0136			0.0366			0.191		
	27.60	27.40	27.50	500	500	475	475	475	475	475	475	466	466	469	469	468	469	475.0	467.8	0.007	0.0120			0.0284			0.169		
	25.00	24.90	24.95	435	434	416	416	415	415	415	415	410	410	411	411	410	411	415.3	410.5	0.005	0.0109			0.0233			0.153		
	44.8	44.4	44.60	990	990	916	916	917	917	916	917	899	899	900	903	899	899	916.5	899.8	0.017	0.0113			0.0251			0.158		
	42.8	42.7	42.75	925	925	861	861	861	861	862	862	844	844	845	846	842	843	861.3	844.0	0.017	0.0120			0.0284			0.169		
	40.2	40.2	40.20	841	842	784	784	785	785	784	784	770	770	770	772	770	772	784.3	770.7	0.014	0.0114			0.0253			0.159		
	37.5	37.5	37.50	749	749	700	702	699	702	699	700	685	685	687	687	686	686	700.3	686.0	0.014	0.0125			0.0305			0.175		
1.2D	35.2	35.2	35.20	675	675	635	635	634	634	630	634	619	619	620	623	620	623	633.7	620.7	0.013	0.0126	0.0116	0.0008	0.0314	0.0264	0.0036	0.177	0.162	0.0113
	32.4	32.3	32.35	609	608	574	574	570	572	570	572	560	562	563	563	560	562	572.0	561.7	0.010	0.0123			0.0296			0.172		
	30.3	30.3	30.30	556	556	525	525	525	525	525	523	517	517	517	517	517	517	524.7	517.0	0.008	0.0113			0.0250			0.158		
	27.7	27.4	27.55	499	499	471	471	471	471	471	468	465	465	465	465	465	466	470.5	465.2	0.005	0.0103			0.0211			0.145		
	25.3	25.3	25.30	446	448	428	428	426	426	426	426	422	422	422	422	422	423	426.7	422.2	0.005	0.0103			0.0211			0.145		
	44.75	44.75	44.75	1005	1007	932	932	932	932	932	932	915	915	915	915	915	915	932.0	915.0	0.017	0.0114			0.0254			0.160		
	42.55	42.30	42.43	919	917	854	854	854	854	854	854	836	836	836	836	836	836	854.0	836.0	0.018	0.0123			0.0300			0.173		
	39.90	39.90	39.90	828	827	775	775	773	773	771	774	756	756	755	756	755	756	773.5	755.7	0.018	0.0131			0.0336			0.183		
	37.50	37.70	37.60	745	743	697	697	694	696	695	697	681	681	680	682	680	682	696.0	681.0	0.015	0.0127			0.0318			0.178		
1.8D	34.90	34.90	34.90	673	673	632	632	633	633	631	631	617	617	618	619	616	619	632.0	617.7	0.014	0.0134	0.0118	0.0013	0.0353	0.0288	0.0057	0.188	0.166	0.0178
	32.30	32.20	32.25	610	610	575	575	575	575	575	575	565	565	563	565	562	565	575.0	564.2	0.011	0.0126			0.0312			0.177		
	30.00	30.00	30.00	556	558	526	526	527	527	528	528	520	520	519	520	517	518	527.0	519.0	0.008	0.0116			0.0266			0.163		
	27.55	27.40	27.48	496	496	470	470	470	470	470	470	465	465	466	465	464	465	470.0	465.0	0.005	0.0100			0.0199			0.141		
	24.70	25.20	24.95	437	438	418	418	418	418	419	419	415	416	415	416	413	413	418.3	414.7	0.004	0.0095			0.0177			0.133		
	44.8	44.6	44.70	1000	1000	925	925	925	925	926	926	906	906	907	908	906	907	925.3	906.7	0.019	0.0119			0.0280			0.167		
	42.4	42.4	42.40	920	920	856	856	856	856	857	857	839	839	840	840	839	841	856.3	839.7	0.017	0.0119			0.0278			0.167		
	40	39.9	39.95	830	827	773	773	773	773	773	773	758	759	757	760	756	759	773.0	758.2	0.015	0.0119			0.0279			0.167		
	37.55	37.5	37.53	749	748	701	701	701	701	701	701	690	690	690	690	686	689	701.0	689.2	0.012	0.0113			0.0252			0.159		
2.4D	35	34.8	34.90	675	678	636	636	635	635	636	636	626	626	626	626	623	624	635.7	625.2	0.011	0.0115	0.0117	0.0003	0.0258	0.0207	0.0015	0.161	0.164	0.0045
	32.5	32.6	32.55	615	615	580	580	580	580	580	580	570	570	570	570	567	570	580.0	569.5	0.011	0.0123			0.0297			0.172		
	29.75	30	29.88	552	553	523	523	522	522	522	522	515	515	515	515	515	515	522.3	515.0	0.007	0.0112			0.0246			0.157		
	27.3	27.4	27.35	494	493	467	467	466	466	467	467	460	460	460	460	460	460	466.7	460.0	0.007	0.0117			0.0267			0.163		
	25	24.9	24.95	439	437	419	420	418	418	418	418	413	413	413	413	413	412	418.5	412.8	0.006	0.0118			0.0273			0.165		

Baffle type:	**Spoiler Baffle (SPB) 2-1-2**
Baffle height (h):	**0.15D**

Experimental data | **Calculated Roughness coefficients**

Λ	Q_1 (l/s)	Q_2 (l/s)	Q_a (l/s)	H_{res1} (mm)	H_{res2} (mm)	Piezometer # 1	2	3	4	5	6	7	8	9	10	11	12	H_{upavg} (mm)	$H_{downavg}$ (mm)	ΔH (m)	n	n_{avg}	σ	f	f_{avg}	σ	$\sqrt{f}$	$\sqrt{f_{avg}}$	σ
						H_{up} (mm)								H_{down} (mm)																	
	45.10	44.80	44.95	1040	1040	967	966	967	968	965	966	911	910	911	911	914	912	966.5	911.5	0.055	0.0204			0.0816			0.286		
	42.50	42.50	42.50	947	948	883	883	883	884	881	882	832	831	832	833	835	833	882.7	832.7	0.050	0.0205			0.0830			0.288		
	39.80	39.70	39.75	857	857	801	801	799	800	797	798	755	754	754	754	755	756	799.3	754.7	0.045	0.0208			0.0847			0.291		
	37.30	37.20	37.25	761	761	714	713	712	713	710	711	675	673	672	673	672	673	712.2	673.0	0.039	0.0207	0.0207	0.0003	0.0846	0.0847	0.0023	0.291	0.2910	0.0040
0.6D	35.00	35.30	35.15	703	702	660	659	657	658	655	656	624	623	622	623	621	622	657.5	622.5	0.035	0.0208			0.0849			0.291		
	32.30	32.50	32.40	634	634	597	598	595	595	593	594	564	566	565	565	565	564	595.3	564.8	0.031	0.0210			0.0871			0.295		
	30.10	29.90	30.00	570	569	538	539	535	536	534	535	511	512	510	510	510	509	536.2	510.3	0.026	0.0209			0.0860			0.293		
	27.40	27.50	27.45	507	508	478	479	480	480	479	480	457	460	456	456	456	457	479.3	457.0	0.022	0.0213			0.0888			0.298		
	24.90	24.90	24.90	445	445	423	423	424	424	423	423	406	407	406	407	407	406	423.3	406.5	0.017	0.0203			0.0814			0.285		
	44.6	44.4	44.50	1023	1023	947	948	947	948	944	945	903	903	904	904	903	904	946.5	903.5	0.043	0.0182			0.0651			0.255		
	42.7	42.4	42.55	947	948	882	882	881	882	880	878	840	840	839	840	839	840	880.8	839.7	0.041	0.0186			0.0682			0.261		
	40	39.9	39.95	854	853	796	796	795	796	794	795	760	760	759	760	760	761	795.3	760.0	0.035	0.0184			0.0664			0.258		
	37.5	37.3	37.40	766	766	718	717	716	717	714	715	685	684	685	685	685	685	716.2	684.8	0.031	0.0185	0.0183	0.0003	0.0671	0.0662	0.0019	0.259	0.257	0.0038
1.2D	35	35.2	35.10	686	685	641	641	641	642	639	640	614	613	613	614	614	614	640.7	613.7	0.027	0.0183			0.0657			0.256		
	32.6	32.7	32.65	617	617	580	580	579	580	577	578	555	555	555	556	555	556	579.0	555.3	0.024	0.0184			0.0665			0.258		
	30	30	30.00	566	566	532	532	530	531	530	531	510	510	510	510	510	511	531.0	510.2	0.021	0.0188			0.0694			0.263		
	27.2	27.5	27.35	499	499	471	472	471	471	468	468	454	454	455	456	454	455	470.2	454.7	0.016	0.0178			0.0621			0.249		
	24.8	24.6	24.70	440	440	419	418	418	418	418	420	405	406	404	405	405	406	418.5	405.2	0.013	0.0182			0.0655			0.256		
	44.50	44.30	44.40	994	995	922	922	923	923	922	920	884	883	887	885	885	885	922.0	884.8	0.037	0.0169			0.0565			0.238		
	42.60	42.70	42.65	948	946	878	878	878	879	878	877	842	842	845	843	845	843	878.0	843.3	0.035	0.0170			0.0571			0.239		
	39.70	39.80	39.75	834	834	778	778	777	778	778	777	747	746	749	747	749	747	777.7	747.5	0.030	0.0171			0.0572			0.239		
	37.80	37.90	37.85	764	764	715	713	714	713	714	712	687	687	687	685	688	685	713.5	686.5	0.027	0.0169	0.0172	0.0003	0.0565	0.0581	0.0020	0.238	0.241	0.0040
1.8D	35.00	35.00	35.00	676	676	635	634	635	633	634	633	610	611	613	610	612	610	634.0	611.0	0.023	0.0169			0.0563			0.237		
	32.40	32.90	32.65	620	621	584	584	585	582	584	582	561	563	563	562	564	562	583.5	562.5	0.021	0.0173			0.0590			0.243		
	30.00	30.40	30.20	557	559	529	526	529	526	528	525	509	510	509	510	510	511	527.2	509.8	0.017	0.0170			0.0570			0.239		
	27.40	27.70	27.55	503	503	479	478	476	477	475	477	460	462	460	462	460	463	477.0	461.2	0.016	0.0178			0.0625			0.250		
	25.30	25.10	25.20	446	446	426	424	427	424	427	424	411	413	411	413	413	415	425.3	412.7	0.013	0.0174			0.0598			0.245		
	44.6	45	44.80	1023	1024	949	949	948	949	945	946	912	913	915	912	914	913	947.7	913.2	0.035	0.0162			0.0515			0.227		
	42.7	42.9	42.80	955	955	889	888	887	888	885	887	854	854	856	855	856	855	887.3	855.0	0.032	0.0164			0.0529			0.230		
	40	40.1	40.05	846	846	789	788	788	789	787	788	760	760	763	760	763	760	788.2	761.0	0.027	0.0161			0.0508			0.225		
	37.5	37.4	37.45	762	761	711	711	713	711	712	710	685	685	687	685	688	686	711.3	686.0	0.025	0.0166			0.0541			0.233		
2.4D	35.4	35.2	35.30	688	688	647	644	644	645	644	643	621	623	624	622	624	622	644.5	622.7	0.022	0.0163	0.0164	0.0003	0.0525	0.0533	0.0018	0.229	0.229	0.0040
	32.7	32.6	32.65	622	622	585	585	584	585	585	582	565	566	566	564	567	565	584.3	565.5	0.019	0.0164			0.0530			0.230		
	30.3	30.4	30.35	570	570	538	538	538	535	536	535	518	520	521	518	523	519	536.7	519.8	0.017	0.0167			0.0548			0.234		
	27.4	27.5	27.45	503	503	476	474	474	477	473	476	460	462	459	462	461	463	475.0	461.2	0.014	0.0167			0.0550			0.235		
	25.3	25.3	25.30	446	447	424	424	427	424	428	425	415	416	412	416	414	416	425.3	414.8	0.011	0.0158			0.0492			0.222		

Baffle type:	Spoiler Baffle (SPB) 2-1-2
Baffle height (h):	0.10D

	Experimental data																				Calculated Roughness coefficients								
						Piezometer #																								
Λ	Q_1 (l/s)	Q_2 (l/s)	Q_a (l/s)	H_{res1} (mm)	H_{res2} (mm)	1	2	3	4	5	6	7	8	9	10	11	12	H_{upavg} (mm)	$H_{downavg}$ (mm)	ΔH (m)	n	n_{avg}	σ	f	f_{avg}	σ	$\sqrt{f}$	$\sqrt{f_{avg}}$	σ
						H_{up} (mm)						H_{down} (mm)																		
	44.60	44.80	44.70	1023	1024	948	948	947	948	946	947	915	916	917	915	917	916	947.3	916.0	0.031	0.0155			0.0470			0.217		
	42.20	42.30	42.25	923	924	858	858	858	859	856	857	830	831	830	830	833	830	857.7	830.7	0.027	0.0152			0.0453			0.213		
	40.20	39.90	40.05	842	841	784	784	784	784	785	782	758	757	758	758	757	757	783.8	757.5	0.026	0.0158			0.0492			0.222		
	37.30	37.70	37.50	757	758	708	706	708	706	708	705	685	684	683	683	685	685	706.8	684.2	0.023	0.0157			0.0483			0.220		
0.6D	35.00	35.40	35.20	691	689	649	648	649	647	648	646	626	625	625	626	625	625	647.8	625.3	0.023	0.0166	0.0160	0.0005	0.0544	0.0502	0.0034	0.233	0.2238	0.0075
	32.70	32.60	32.65	617	617	581	580	580	578	580	577	561	562	560	561	561	560	579.3	560.8	0.019	0.0163			0.0520			0.228		
	29.70	30.00	29.85	554	554	525	524	525	523	524	522	508	509	506	507	507	506	523.8	507.2	0.017	0.0169			0.0561			0.237		
	27.90	27.80	27.85	511	511	484	482	484	482	484	481	470	471	470	470	470	472	482.8	470.5	0.012	0.0156			0.0477			0.218		
	24.90	25.00	24.95	439	439	420	418	421	419	419	422	409	410	408	409	408	411	419.8	409.2	0.011	0.0162			0.0514			0.227		
	44.9	45.2	45.05	1019	1018	943	943	943	944	944	942	918	917	917	916	919	917	943.2	917.3	0.026	0.0139			0.0382			0.195		
	42.4	42	42.20	914	913	849	849	849	850	851	849	825	824	825	825	824	825	849.5	824.7	0.025	0.0146			0.0418			0.204		
	39.9	40.2	40.05	843	844	785	785	786	785	786	784	763	763	764	763	764	763	785.2	763.3	0.022	0.0144			0.0408			0.202		
	37.4	37.7	37.55	753	754	705	702	705	703	705	702	684	683	684	683	684	684	703.7	683.7	0.020	0.0147			0.0425			0.206		
1.2D	34.9	34.7	34.80	663	664	623	620	623	620	623	620	604	604	605	604	605	605	621.5	604.5	0.017	0.0146	0.0148	0.0006	0.0421	0.0433	0.0034	0.205	0.2208	0.0081
	32.3	32.2	32.25	605	605	570	569	570	568	570	567	553	553	554	553	555	554	569.0	553.7	0.015	0.0150			0.0442			0.210		
	29.8	29.6	29.70	546	546	517	516	517	515	515	514	501	501	501	500	502	501	515.7	501.0	0.015	0.0159			0.0498			0.223		
	27.4	27.4	27.40	492	492	467	465	465	463	465	462	454	454	454	453	454	454	464.5	453.8	0.011	0.0147			0.0426			0.206		
	24.8	24.7	24.75	434	434	416	412	416	412	416	413	404	404	404	403	407	404	414.2	404.3	0.010	0.0156			0.0481			0.219		
	44.70	44.80	44.75	1007	1007	936	936	935	936	935	934	912	911	911	911	909	911	935.3	910.8	0.025	0.0137			0.0367			0.191		
	42.40	42.40	42.40	923	922	858	858	857	858	859	857	836	835	835	835	834	835	857.8	835.0	0.023	0.0139			0.0381			0.195		
	39.90	40.20	40.05	838	839	780	780	782	781	783	780	762	762	762	761	760	761	781.0	761.3	0.020	0.0137			0.0367			0.192		
	37.40	37.20	37.30	746	746	697	697	698	696	698	695	680	680	679	679	679	679	696.8	679.3	0.018	0.0138			0.0377			0.194		
1.8D	34.80	34.80	34.80	664	664	624	624	624	622	624	621	607	607	608	607	609	606	623.2	607.3	0.016	0.0141	0.0139	0.0002	0.0392	0.0378	0.0012	0.198	0.1955	0.0032
	32.40	32.20	32.30	603	603	567	568	567	566	567	565	553	554	553	552	555	552	566.7	553.2	0.014	0.0140			0.0388			0.197		
	29.80	30.00	29.90	554	554	525	524	524	523	523	522	510	512	513	512	514	513	523.5	512.3	0.011	0.0138			0.0374			0.193		
	27.30	27.30	27.30	489	489	464	464	465	463	464	463	454	455	453	455	456	453	463.8	454.3	0.010	0.0139			0.0382			0.195		
	25.00	24.90	24.95	438	438	418	420	420	417	420	418	409	410	411	410	412	410	418.8	410.3	0.009	0.0144			0.0409			0.202		
	44.6	44.4	44.50	1004	1005	933	932	933	932	932	931	909	909	908	908	909	910	932.2	908.8	0.023	0.0134			0.0353			0.188		
	42.2	42	42.10	912	911	847	847	848	847	847	849	828	827	826	827	825	827	847.5	826.7	0.021	0.0134			0.0352			0.188		
	40.1	40.2	40.15	839	839	780	781	781	781	781	783	762	762	762	762	765	762	781.2	762.5	0.019	0.0133			0.0347			0.186		
	37.5	37.3	37.40	743	743	693	694	695	696	692	695	677	677	677	678	678	680	694.2	677.8	0.016	0.0133			0.0350			0.187		
2.4D	34.7	34.7	34.70	665	664	622	624	625	625	622	624	608	607	607	609	608	610	623.7	608.2	0.016	0.0140	0.0135	0.0002	0.0386	0.0363	0.0013	0.196	0.1889	0.0033
	32.4	32.7	32.55	615	615	578	578	579	580	576	579	564	565	564	566	567	567	578.3	565.5	0.013	0.0136			0.0363			0.191		
	30	30	30.00	553	553	521	523	520	520	520	522	510	510	508	510	510	512	521.0	510.0	0.011	0.0136			0.0366			0.191		
	27.5	27.5	27.50	493	493	465	466	464	465	464	466	455	455	456	458	456	458	465.0	456.3	0.009	0.0132			0.0343			0.185		
	25.1	24.8	24.95	433	433	414	414	415	415	414	412	405	406	407	407	408	408	414.0	406.8	0.007	0.0132			0.0345			0.186		

Baffle type:	Spoiler Baffle (SPB) 2-1-2
Baffle height (h):	0.05D

	Experimental data																				Calculated Roughness coefficients									
						Piezometer #																									
Λ	Q_1 (l/s)	Q_2 (l/s)	Q_a (l/s)	H_{res1} (mm)	H_{res2} (mm)	1	2	3	4	5	6	7	8	9	10	11	12	H_{upavg} (mm)	$H_{downavg}$ (mm)	ΔH (m)	n	n_{avg}	σ	f	f_{avg}	σ	$\sqrt{f}$	$\sqrt{f_{avg}}$	σ
								H_{up} (mm)						H_{down} (mm)																
	44.60	44.50	44.55	987	988	913	913	915	914	914	913	895	895	894	897	894	896	913.7	895.2	0.019	0.0119			0.0279			0.167		
	42.20	42.60	42.40	925	926	859	859	860	859	859	860	842	841	842	844	842	843	859.3	842.3	0.017	0.0120			0.0283			0.168		
	40.00	39.90	39.95	835	834	775	775	777	778	776	778	761	761	760	763	760	762	776.5	761.2	0.015	0.0121			0.0288			0.170		
	37.20	37.30	37.25	742	742	692	694	693	695	692	694	680	678	679	680	678	680	693.3	679.2	0.014	0.0125	0.0128	0.0010	0.0306	0.0326	0.0051	0.175	0.18002	0.0135
0.6D	34.90	34.80	34.85	663	663	621	622	623	622	619	622	609	610	609	610	608	610	621.5	609.3	0.012	0.0124			0.0300			0.173		
	32.30	32.60	32.45	609	608	571	572	573	573	571	573	560	559	559	560	559	560	572.2	559.5	0.013	0.0135			0.0361			0.190		
	30.00	30.20	30.10	555	555	525	524	525	525	525	523	512	512	514	515	513	515	524.5	513.5	0.011	0.0136			0.0364			0.191		
	27.60	27.70	27.65	497	498	469	471	470	471	469	471	462	463	462	463	460	463	470.2	462.2	0.008	0.0126			0.0314			0.177		
	24.90	24.90	24.90	437	437	417	418	419	419	418	419	409	409	409	410	408	410	418.3	409.2	0.009	0.0150			0.0443			0.211		
	44.7	44.8	44.75	1008	1008	932	932	933	932	932	931	914	915	914	915	915	914	932.0	914.5	0.018	0.0115			0.0262			0.162		
	42.3	42.4	42.35	902	901	838	838	839	838	839	841	822	822	822	824	821	824	838.8	822.5	0.016	0.0118			0.0273			0.165		
	40.1	39.8	39.95	823	821	765	765	766	768	766	769	751	750	750	753	750	752	766.5	751.0	0.016	0.0122			0.0291			0.171		
	37.3	37.5	37.40	740	740	690	693	692	693	691	693	678	679	678	680	678	680	692.0	678.8	0.013	0.0120	0.0123	0.0007	0.0282	0.0298	0.0037	0.168	0.1722	0.0104
1.2D	35	34.9	34.95	668	669	624	626	627	626	625	627	613	612	612	615	614	613	625.8	613.2	0.013	0.0126			0.0311			0.176		
	32.7	32.6	32.65	607	606	568	570	571	570	568	570	559	558	559	561	558	561	569.5	559.3	0.010	0.0121			0.0286			0.169		
	30	29.7	29.85	543	543	510	513	514	513	510	514	501	502	502	504	503	501	512.3	502.2	0.010	0.0132			0.0342			0.185		
	27.5	27.7	27.60	493	493	464	466	464	466	463	465	458	458	458	459	458	458	464.7	458.2	0.007	0.0114			0.0256			0.160		
	24.8	24.7	24.75	428	428	406	409	411	410	407	410	404	404	400	404	401	394	408.8	401.2	0.008	0.0138			0.0375			0.194		
	44.70	44.60	44.65	991	993	920	920	921	920	920	923	904	903	904	905	903	907	920.7	904.3	0.016	0.0112			0.0246			0.157		
	42.50	42.60	42.55	914	915	850	850	852	851	851	853	836	835	835	837	835	839	851.2	836.2	0.015	0.0112			0.0248			0.158		
	40.00	39.80	39.90	828	828	768	767	769	768	769	768	755	755	755	757	755	756	768.2	755.5	0.013	0.0110			0.0238			0.154		
	37.60	37.60	37.60	742	742	691	695	695	695	692	694	683	680	679	683	679	682	693.7	681.0	0.013	0.0117	0.0116	0.0005	0.0269	0.0227	0.0023	0.164	0.1633	0.0069
1.8D	35.00	34.80	34.90	661	661	618	620	622	622	619	621	611	610	608	610	608	610	620.3	609.5	0.011	0.0116			0.0267			0.163		
	32.70	32.80	32.75	608	608	570	572	573	573	572	573	563	562	562	564	560	563	572.2	562.3	0.010	0.0118			0.0275			0.166		
	29.80	30.00	29.90	547	547	515	518	518	517	515	517	508	506	506	508	506	509	516.7	507.2	0.009	0.0127			0.0318			0.178		
	27.50	27.30	27.40	488	488	460	462	462	461	462	463	455	454	455	456	454	457	461.7	455.2	0.007	0.0115			0.0259			0.161		
	24.70	24.70	24.70	428	428	410	409	411	410	409	410	405	402	404	404	403	406	409.8	404.0	0.006	0.0121			0.0287			0.169		
	44.8	44.8	44.80	1004	1007	933	933	932	933	931	933	915	915	915	919	915	912	932.5	915.2	0.017	0.0115			0.0259			0.161		
	42.6	42.6	42.60	924	925	858	858	860	859	859	862	844	843	844	846	844	847	859.3	844.7	0.015	0.0111			0.0242			0.156		
	40.1	39.9	40.00	822	823	764	764	765	766	765	768	752	752	752	755	752	755	765.3	753.0	0.012	0.0108			0.0231			0.152		
	37.5	37.7	37.60	738	738	688	691	692	692	691	689	679	677	679	679	677	679	690.5	678.3	0.012	0.0115			0.0258			0.161		
2.4D	34.8	35.3	35.05	662	663	619	622	623	622	619	622	612	610	609	612	610	612	621.2	610.8	0.010	0.0113	0.0115	0.0005	0.0252	0.0226	0.0022	0.159	0.1611	0.0065
	32.5	32.5	32.50	600	600	563	565	566	565	563	565	556	555	554	556	554	556	564.5	555.2	0.009	0.0116			0.0265			0.163		
	30	30.5	30.25	558	558	525	524	525	525	524	527	517	516	516	518	515	518	525.0	516.7	0.008	0.0118			0.0273			0.165		
	27.7	27.9	27.80	499	499	470	473	473	473	469	474	465	464	463	465	462	465	472.0	464.0	0.008	0.0126			0.0310			0.176		
	25.1	25.2	25.15	439	441	417	420	422	422	420	422	415	415	414	416	415	417	420.5	415.3	0.005	0.0112			0.0245			0.156		

Baffle type:	**Spoiler Baffle (SPB) 1-1-1**
Baffle height (h):	**0.15D**

Experimental data | **Calculated Roughness coefficients**

Λ	Q_1 (l/s)	Q_2 (l/s)	Q_a (l/s)	H_{res1} (mm)	H_{res2} (mm)	Piezometer # 1	2	3	4	5	6	7	8	9	10	11	12	H_{upavg} (mm)	$H_{downavg}$ (mm)	ΔH (m)	n	n_{avg}	σ	f	f_{avg}	σ	$\sqrt{f}$	$\sqrt{f_{avg}}$	σ
						H_{up} (mm)						H_{down} (mm)																			
	44.70	44.60	44.65	1040	1040	965	965	965	965	964	964	922	923	922	922	922	922	964.7	922.2	0.043	0.0180			0.0639			0.253		
	42.80	42.60	42.70	970	968	902	901	902	901	900	899	861	860	863	865	861	860	900.8	861.7	0.039	0.0181			0.0644			0.254		
	40.05	39.80	39.93	865	862	808	808	809	808	806	806	772	771	771	775	772	771	807.5	772.0	0.036	0.0184			0.0668			0.258		
	37.55	37.60	37.58	787	787	739	736	737	738	737	735	705	704	705	708	705	705	737.0	705.3	0.032	0.0185	0.0184	0.0004	0.0672	0.0664	0.0030	0.259	0.2576	0.0057
0.6D	35.25	34.85	35.05	699	695	657	657	655	656	654	656	626	627	626	627	625	626	655.8	626.2	0.030	0.0192			0.0724			0.269		
	32.55	32.10	32.33	627	626	591	591	591	591	590	591	570	570	570	570	566	568	590.8	569.0	0.022	0.0178			0.0626			0.250		
	29.75	29.85	29.80	569	569	540	540	540	540	536	538	521	521	521	521	518	519	539.0	520.2	0.019	0.0180			0.0636			0.252		
	27.30	27.50	27.40	511	513	489	489	488	488	487	487	471	471	471	471	469	471	488.0	470.7	0.017	0.0188			0.0692			0.263		
	24.70	24.80	24.75	448	447	428	429	429	429	428	428	416	415	415	415	413	414	428.5	414.7	0.014	0.0185			0.0677			0.260		
	45.1	45.2	45.15	1050	1050	975	975	974	974	974	974	937	937	939	940	938	937	974.3	938.0	0.036	0.0165			0.0534			0.231		
	42.7	43.05	42.88	975	975	907	907	907	908	908	908	875	875	875	876	874	875	907.5	875.0	0.033	0.0164			0.0530			0.230		
	40	39.7	39.85	860	857	803	802	801	802	802	800	772	771	770	774	771	775	801.7	772.2	0.030	0.0168			0.0557			0.236		
	37.4	37.2	37.30	762	762	715	715	714	715	714	714	688	688	688	691	687	690	714.5	688.7	0.026	0.0168	0.0170	0.0005	0.0557	0.0568	0.0030	0.236	0.2382	0.0063
1.2D	34.8	35.2	35.00	694	695	655	655	653	654	653	653	632	630	630	632	629	631	653.8	630.7	0.023	0.0170			0.0567			0.238		
	32.3	32.5	32.40	627	626	591	591	588	590	590	590	571	570	572	572	571	569	590.0	570.8	0.019	0.0167			0.0547			0.234		
	29.95	30.15	30.05	569	570	541	540	540	539	539	540	521	520	520	523	520	523	539.8	521.2	0.019	0.0177			0.0620			0.249		
	27.55	27.8	27.68	511	511	487	486	487	486	487	487	472	470	472	472	471	469	486.7	471.0	0.016	0.0177			0.0613			0.248		
	24.9	24.7	24.80	444	445	425	425	423	425	425	424	412	410	412	414	413	414	424.5	412.5	0.012	0.0172			0.0585			0.242		
	44.80	44.90	44.85	1035	1040	962	962	964	963	961	962	932	932	931	933	933	935	962.3	932.7	0.030	0.0150			0.0442			0.210		
	42.50	42.40	42.45	949	948	884	884	884	884	885	883	855	854	854	856	855	857	884.0	855.2	0.029	0.0156			0.0480			0.219		
	40.10	40.10	40.10	854	855	800	797	798	799	799	797	773	772	772	774	772	774	798.3	772.8	0.026	0.0155			0.0475			0.218		
	37.50	37.50	37.50	771	771	723	723	720	722	723	723	700	699	698	701	699	700	722.3	699.5	0.023	0.0157			0.0487			0.221		
1.8D	34.80	34.90	34.85	686	686	645	645	645	645	645	645	628	627	626	627	627	628	645.0	627.2	0.018	0.0150	0.0154	0.0003	0.0440	0.0474	0.0016	0.210	0.2160	0.0036
	32.75	32.90	32.83	628	631	595	595	595	595	595	595	578	577	578	579	578	579	595.0	578.2	0.017	0.0154			0.0468			0.216		
	30.10	29.80	29.95	572	572	542	541	542	542	540	540	527	526	528	527	526	527	541.2	526.8	0.014	0.0156			0.0479			0.219		
	27.25	27.40	27.33	507	507	481	481	482	481	480	480	467	469	468	470	470	470	480.8	469.0	0.012	0.0155			0.0475			0.218		
	24.90	24.70	24.80	443	443	424	423	424	423	424	424	415	414	413	415	414	414	423.7	414.2	0.010	0.0153			0.0463			0.215		
	44.7	44.45	44.58	1013	1010	937	937	938	938	938	936	909	909	909	911	909	910	937.3	909.5	0.028	0.0146			0.0420			0.205		
	42.6	42.5	42.55	936	935	871	870	870	871	873	871	843	843	844	845	842	845	871.0	843.7	0.027	0.0152			0.0452			0.213		
	39.9	39.95	39.93	838	837	784	782	783	784	781	778	758	757	758	761	757	760	782.0	758.5	0.024	0.0150			0.0442			0.210		
	37.6	37.6	37.60	769	769	721	720	718	720	720	718	700	700	698	700	698	700	719.5	699.3	0.020	0.0147			0.0428			0.207		
2.4D	34.75	34.8	34.78	676	676	636	636	635	635	634	634	619	619	619	620	616	618	635.0	618.5	0.017	0.0144	0.0151	0.0005	0.0409	0.0455	0.0028	0.202	0.2111	0.0066
	32.6	32.4	32.50	620	620	584	585	582	583	584	582	565	565	565	567	565	568	583.3	565.8	0.018	0.0159			0.0497			0.223		
	30.15	30.4	30.28	568	568	539	538	538	538	537	534	524	523	522	524	524	525	537.3	523.7	0.014	0.0151			0.0447			0.211		
	27.7	27.5	27.60	505	505	480	480	480	479	479	478	468	467	465	467	466	468	479.3	466.8	0.013	0.0158			0.0492			0.222		
	24.7	24.7	24.70	438	437	419	420	419	419	418	417	411	410	408	410	410	409	418.7	409.7	0.009	0.0150			0.0442			0.210		

Baffle type:	**Spoiler Baffle (SPB) 1-1-1**
Baffle height (h):	**0.10D**

Experimental data | **Calculated Roughness coefficients**

Λ	Q_1 (l/s)	Q_2 (l/s)	Q_a (l/s)	H_{res1} (mm)	H_{res2} (mm)	Piezometer # 1	2	3	4	5	6	7	8	9	10	11	12	H_{upavg} (mm)	$H_{downavg}$ (mm)	ΔH (m)	n	n_{avg}	σ	f	f_{avg}	σ	$\sqrt{f}$	$\sqrt{f_{avg}}$	σ
						H_{up} (mm)								H_{down} (mm)																	
	44.50	44.70	44.60	1028	1024	950	950	950	950	949	948	920	920	921	924	920	923	949.5	921.3	0.028	0.0147			0.0424			0.206		
	42.40	42.50	42.45	941	941	877	877	876	877	878	876	851	850	852	854	849	852	876.8	851.3	0.026	0.0147			0.0424			0.206		
	39.75	40.00	39.88	845	845	791	789	789	790	791	789	766	765	766	768	765	768	789.8	766.3	0.024	0.0150			0.0443			0.210		
	37.35	37.50	37.43	763	763	716	716	713	715	715	713	692	695	693	695	692	694	714.7	693.5	0.021	0.0152			0.0453			0.213		
0.6D	34.95	35.00	34.98	683	682	639	642	643	643	639	641	621	623	625	624	622	624	641.2	623.2	0.018	0.0150	0.0150	0.0004	0.0441	0.0444	0.0025	0.210	0.2106	0.0058
	32.30	32.30	32.30	616	618	583	582	580	582	582	580	565	566	567	567	564	566	581.5	565.8	0.016	0.0151			0.0450			0.212		
	30.10	30.10	30.10	560	559	532	531	530	529	531	529	519	519	518	519	515	517	530.3	517.8	0.013	0.0145			0.0414			0.203		
	27.70	27.50	27.60	503	503	477	480	479	478	477	474	464	467	468	468	464	467	477.5	466.3	0.011	0.0149			0.0439			0.210		
	25.35	24.95	25.15	450	450	428	430	430	430	427	429	416	418	419	420	417	420	429.0	418.3	0.011	0.0160			0.0505			0.225		
	44.85	45	44.93	1025	1023	948	948	947	948	948	949	922	923	924	926	923	925	948.0	923.8	0.024	0.0135			0.0359			0.189		
	42.4	42.7	42.55	933	935	868	868	869	868	868	871	847	847	844	846	845	848	868.7	846.2	0.023	0.0138			0.0372			0.193		
	40.3	40.2	40.25	862	863	804	804	803	805	804	806	784	784	785	787	784	786	804.3	785.0	0.019	0.0135			0.0358			0.189		
	37.3	37.75	37.53	757	757	708	710	708	710	708	709	690	692	693	693	690	692	708.8	691.7	0.017	0.0136			0.0365			0.191		
1.2D	34.75	34.95	34.85	680	680	637	640	640	640	639	640	621	624	624	624	624	625	639.3	623.7	0.016	0.0140	0.0139	0.0004	0.0387	0.0378	0.0023	0.197	0.1944	0.0059
	32.5	32.4	32.45	622	622	585	587	587	587	587	586	570	572	574	574	573	574	586.5	572.8	0.014	0.0141			0.0389			0.197		
	30	30	30.00	559	559	531	530	530	530	530	530	515	517	518	518	519	518	530.2	517.5	0.013	0.0146			0.0422			0.205		
	27.8	27.9	27.85	514	514	485	487	488	488	486	486	474	475	476	477	477	478	486.7	476.2	0.011	0.0144			0.0406			0.201		
	25.2	25.2	25.20	447	445	423	425	425	426	425	426	416	416	417	418	419	420	425.0	417.7	0.007	0.0133			0.0346			0.186		
	45.30	45.00	45.15	1026	1025	950	950	950	950	950	952	928	930	928	932	927	928	950.3	928.8	0.022	0.0127			0.0316			0.178		
	42.50	42.20	42.35	931	929	865	865	865	865	865	868	845	845	846	848	843	848	865.5	845.8	0.020	0.0129			0.0329			0.181		
	40.10	39.85	39.98	837	837	780	781	780	780	780	782	762	762	764	765	761	762	780.5	762.7	0.018	0.0130			0.0334			0.183		
	37.35	37.20	37.28	749	749	699	702	700	701	699	701	683	685	687	687	683	685	700.3	685.0	0.015	0.0130			0.0331			0.182		
1.8D	34.80	34.35	34.58	663	662	621	623	623	623	621	622	607	607	609	609	605	608	622.2	607.5	0.015	0.0137	0.0134	0.0006	0.0368	0.0335	0.0033	0.192	0.1888	0.0087
	32.40	32.55	32.48	615	615	580	580	581	580	580	580	565	567	568	569	565	568	580.2	567.0	0.013	0.0138			0.0374			0.193		
	30.00	29.60	29.80	549	548	516	518	519	518	518	519	506	508	505	505	508	508	518.0	506.7	0.011	0.0139			0.0383			0.196		
	27.30	27.30	27.30	494	494	466	468	469	469	468	469	458	460	461	461	460	460	468.2	460.0	0.008	0.0129			0.0328			0.181		
	25.00	25.00	25.00	442	442	423	423	423	424	423	423	413	415	415	415	413	415	423.2	414.3	0.009	0.0147			0.0424			0.206		
	44.7	45.1	44.90	1020	1023	945	945	947	946	945	946	925	926	925	927	925	926	945.7	925.7	0.020	0.0123			0.0297			0.172		
	42.4	42.2	42.30	922	921	857	857	858	858	856	858	839	839	839	842	839	841	857.3	839.8	0.018	0.0122			0.0293			0.171		
	39.8	40.1	39.95	844	845	786	787	789	789	785	789	770	768	770	772	769	770	787.5	769.8	0.018	0.0130			0.0332			0.182		
	37.4	37.6	37.50	753	750	702	704	705	704	701	703	686	688	689	689	686	688	703.2	687.7	0.016	0.0130			0.0330			0.182		
2.4D	34.7	34.8	34.75	671	672	628	630	631	631	628	630	617	619	618	618	618	619	629.7	618.2	0.012	0.0120	0.0123	0.0005	0.0285	0.0300	0.0023	0.169	0.173	0.0066
	32.5	32.5	32.50	614	616	580	580	581	581	580	580	567	570	570	570	569	570	580.3	569.3	0.011	0.0126			0.0312			0.177		
	29.8	30	29.90	553	554	520	523	524	523	522	523	511	514	515	514	514	515	522.5	513.8	0.009	0.0122			0.0291			0.170		
	27.4	27.05	27.23	500	500	472	474	474	474	472	474	465	466	467	466	465	467	473.3	466.0	0.007	0.0123			0.0297			0.172		
	24.8	24.7	24.75	439	439	419	420	420	419	418	420	412	414	414	414	415	416	419.3	414.2	0.005	0.0113			0.0253			0.159		

Baffle type:	**Spoiler Baffle (SPB) 1-1-1**
Baffle height (h):	**0.05D**

Experimental data | **Calculated Roughness coefficients**

Λ	Q_1 (l/s)	Q_2 (l/s)	Q_a (l/s)	H_{res1} (mm)	H_{res2} (mm)	Piezometer # 1	2	3	4	5	6	7	8	9	10	11	12	H_{upavg} (mm)	$H_{downavg}$ (mm)	ΔH (m)	n	n_{avg}	σ	f	f_{avg}	σ	$\sqrt{f}$	$\sqrt{f_{avg}}$	σ
						H_{up} (mm)						H_{down} (mm)																			
	44.60	44.70	44.65	1004	1004	930	930	930	930	930	931	912	912	912	914	911	914	930.2	912.5	0.018	0.0116			0.0266			0.163		
	42.70	42.50	42.60	929	930	863	863	863	864	863	866	845	845	845	847	844	847	863.7	845.5	0.018	0.0124			0.0300			0.173		
	40.20	40.00	40.10	840	839	780	781	781	784	782	785	766	767	767	769	764	767	782.2	766.7	0.016	0.0121			0.0289			0.170		
	37.60	37.70	37.65	755	753	705	708	703	705	704	706	690	692	693	692	689	690	705.2	691.0	0.014	0.0123	0.0117	0.0009	0.0300	0.02699	0.00411	0.173	0.16336	0.00133
0.6D	35.10	34.90	35.00	678	675	634	636	634	636	632	635	624	624	624	623	620	622	634.5	622.8	0.012	0.0120			0.0285			0.169		
	32.30	32.30	32.30	607	606	573	573	570	572	570	572	562	561	562	562	560	560	571.7	561.2	0.011	0.0124			0.0302			0.174		
	29.90	30.20	30.05	558	558	525	527	525	527	525	528	516	518	519	518	516	517	526.2	517.3	0.009	0.0122			0.0293			0.171		
	27.40	27.50	27.45	497	497	468	470	469	470	470	469	464	465	464	465	463	464	469.3	464.2	0.005	0.0102			0.0206			0.143		
	25.00	24.90	24.95	438	438	416	418	416	419	415	418	415	414	414	414	411	411	417.0	413.2	0.004	0.0097			0.0185			0.136		
	44.9	44.9	44.90	1007	1007	933	933	934	933	933	938	915	915	914	917	914	919	934.0	915.7	0.018	0.0118			0.0273			0.165		
	42.4	42.7	42.55	928	929	863	863	863	863	862	865	846	846	847	850	846	850	863.2	847.5	0.016	0.0115			0.0259			0.161		
	39.8	39.75	39.78	834	833	777	778	776	778	777	779	762	761	764	764	759	761	777.5	761.8	0.016	0.0123			0.0297			0.172		
	37.35	37.75	37.55	757	756	707	709	707	709	706	709	697	695	697	697	694	695	707.8	695.8	0.012	0.0114	0.0116	0.0003	0.0255	0.02644	0.00115	0.160	0.163	0.00045
1.2D	35	35.4	35.20	678	677	633	636	633	636	633	635	623	623	625	625	624	624	634.3	624.0	0.010	0.0113			0.0250			0.158		
	32.4	32.1	32.25	599	597	562	563	561	562	561	563	551	551	554	554	552	552	562.0	552.3	0.010	0.0119			0.0279			0.167		
	30.2	30.2	30.20	559	559	525	527	525	527	527	527	518	517	520	520	518	519	526.3	518.7	0.008	0.0113			0.0252			0.159		
	27.6	27.5	27.55	495	495	468	470	470	470	468	470	461	461	464	464	463	463	469.3	462.7	0.007	0.0116			0.0263			0.162		
	25.2	25.2	25.20	445	445	425	425	425	425	423	425	420	420	420	420	418	418	424.7	419.3	0.005	0.0113			0.0252			0.159		
	44.40	44.60	44.50	965	966	894	893	894	895	893	895	880	880	879	883	877	878	894.0	879.5	0.015	0.0106			0.0219			0.148		
	42.70	42.80	42.75	905	905	839	839	840	841	839	841	825	825	825	828	825	827	839.8	825.8	0.014	0.0108			0.0230			0.152		
	40.15	40.20	40.18	823	824	765	767	765	767	765	768	755	754	755	755	752	753	766.2	754.0	0.012	0.0107			0.0226			0.150		
	37.30	37.30	37.30	721	721	674	675	673	674	672	674	665	664	665	665	661	663	673.7	663.8	0.010	0.0104	0.0105	0.0004	0.0212	0.0222	0.0015	0.146	0.147	0.0052
1.8D	35.00	34.90	34.95	667	665	615	615	615	614	614	615	606	605	606	605	604	604	614.7	605.0	0.010	0.0110			0.0237			0.154		
	32.67	32.60	32.64	603	603	565	568	565	566	565	567	559	559	559	559	555	557	566.0	558.0	0.008	0.0107			0.0225			0.150		
	30.00	29.95	29.98	544	544	510	513	513	513	510	513	507	506	505	505	504	505	512.0	505.3	0.007	0.0106			0.0222			0.149		
	27.80	27.70	27.75	494	494	467	467	466	467	465	466	463	462	462	461	461	460	466.3	461.5	0.005	0.0098			0.0188			0.137		
	25.25	25.20	25.23	439	439	418	418	419	419	418	419	415	414	414	414	414	415	418.5	414.3	0.004	0.0100			0.0196			0.140		
	44.4	44.5	44.45	996	996	923	923	922	923	922	924	905	905	905	907	905	906	922.8	905.5	0.017	0.0116			0.0263			0.162		
	42.4	42.75	42.58	932	932	865	865	866	866	866	869	850	850	850	853	849	852	866.2	850.7	0.016	0.0114			0.0256			0.160		
	39.8	39.7	39.75	830	830	773	774	773	775	774	776	760	759	762	762	757	760	774.2	760.0	0.014	0.0117			0.0269			0.164		
	37.4	37.5	37.45	745	746	695	698	695	697	695	697	686	685	686	686	682	684	696.2	684.8	0.011	0.0111			0.0242			0.156		
2.4D	35	34.8	34.90	674	673	632	633	630	632	630	631	623	622	622	622	620	620	631.3	621.5	0.010	0.0111	0.0114	0.0003	0.0242	0.0255	0.00113	0.156	0.160	0.00042
	32.4	32.7	32.55	605	605	567	567	567	569	569	570	558	558	560	560	558	559	568.2	558.8	0.009	0.0116			0.0264			0.162		
	29.7	30.1	29.90	504	503	525	527	526	528	525	528	520	518	520	520	520	519	526.5	519.5	0.007	0.0109			0.0235			0.153		
	27.8	27.6	27.70	504	503	475	477	477	478	475	476	470	470	470	470	470	470	476.3	470.0	0.006	0.0112			0.0247			0.157		
	25.1	25.2	25.15	444	444	425	425	425	425	424	425	420	419	420	420	418	417	424.8	419.0	0.006	0.0119			0.0276			0.166		

Appendix B

Letter from the Journal of Hydraulic Engineering

Ref.: Ms. No. HYENG-8713
The Effect of Fish Baffles on the Hydraulic Capacity of Slipline Rehabilitated Culverts
Jason Matthew Duguay, B. Eng.; R.W. Jay Lacey, Ph.D.

Dear Mr. Duguay,

Your Technical Paper, listed above, has completed a review for publication in ASCE's Journal of Hydraulic Engineering. The editor has requested that a revised manuscript be prepared based on the reviewers' evaluations (shown at the end of this email) and submitted for re-review by 02-16-2014.

You can view any reviewers' attachments by opening the attachments on this email OR by clicking on this link to see them in the system: ********. Please note, this link will only work one time.

When preparing the revised manuscript in accordance with the reviewers' concerns and suggestions, be sure to address the following additional requirements, if not already completed:

1. Please print out, sign, scan and upload a copy of our Copyright Transfer Agreement which can be found at:
http://www.asce.org/uploadedFiles/Publications/Permissions_Requirements/journalscta.pdf

2. Remove the figures from your manuscript text and upload them separately (one figure per file) in TIFF, EPS or PDF format. If uploading PDF figure files, please check to make sure the fonts are embedded (see http://www.asce.org/journals/pdf-figures/ for instructions for PDF figures). Also, please make sure to reference the figure number in each file name.

3. Please remove tables from within the text of your paper and place at the end of your paper after the references and figure captions list. If you upload them separately, please make sure they are uploaded in Microsoft Word/LaTex format.

Please submit the revised manuscript and a detailed response to the reviewers' criticisms by logging onto the editorial management system at http://jrnhyeng.edmgr.com/ and clicking on the "Submissions Needing Revision" link.

For your convenience, there is a calendar entry item attached that works with electronic calendars in the iCalendar format (e.g. Outlook, iCal, Google). To use, click to open the attachment, and then save it to your calendar.

Be advised that the editor may request further revision or decline your revised version if all of the reviewers' comments have not been adequately addressed.

Comments from the Editor and Reviewers can be found below.

We look forward to receiving your revised manuscript.

Sincerely,

Michelle English
Editorial Coordinator

Reviewers' comments:

Editor
In agreement with the reviewers and the AE, the authors are requested to submit a revised, shortened paper with a point by point response to each reviewer and AE comment along with an indication of the corresponding changes made in the paper (please refer to line numbers). Please include an ASCE sizing worksheet. Re-review is required.

Associate Editor
The paper has been reviewed by two experienced researchers on the subject of culvert fish baffles. Both reviewers find positive aspects of the paper, but have several objections to the presentation. Both reviewers point out several weaknesses of the paper that must be addressed before we can proceed any further. These include but are not limited to variables going undefined, a lack of understanding of limitations of the data, mistakes in some tables, and a paper that is simply too long and speculative. The applications at the end of the paper exceed the range of applicability of the results and in some cases the conclusions are trivial.

I have some critical comments of my own:
(1) The authors should be more careful with dimensionless values of the variables. Relative roughness (h/D) and relative spacing (lambda/D) should be used throughout the paper. The horizontal axis of Fig. 5, for example, should be labeled as lambda/D, not lambda. In addition, Eq. 4 should be based on lambda/D, not just lambda. Culvert length as L/D should also be given.
(2) In line 421, r is defined but not r_o. In addition, culverts are not specified by their radii; the authors should use "diameter" and "diameter reduction" instead.
(3) In line 430, the diameter of the hypothetical example is not given, and thus L/D cannot be determined. The authors should read Reviewer 1 comments on applicability of the results and relative inlet lengths very carefully. The authors are trying to stretch their results too far.
(4) Improve the technical language, e.g. "radial reductions are inferior? to <0.80"; Reynold's effects (should be Reynolds number effects); "parent culvert"?, etc.
(5) Reduce speculation on fish effects since the paper does not include fish experiments
(6) Shorten the article to accepted limits

My recommendation is to request a revision of the paper with responses to all reviewer and AE comments. The paper should be re-reviewed by both reviewers.

Reviewer #1: see attachment

Reviewer #2: The authors do a very good job describing what they did in their experimental setup. I appreciate the good drawing of the flume. The figures are also very useful.

It took me some time to realize that the authors were not really interested in fish passage but in checking the impact of baffles on capacity for a design-like discharge.

I have the following recommendations:

1.Define the term alpha in the abstract. Lamda and h are defined, but alpha is not. Alpha is defined in the paper, but some will only read the abstract. So put in a simple definition of alpha.

2. State the range of calculated full-flow velocities when the discharge range is mentioned. The values are from 0.49 to 0.89 m/s. I find this to be the most limiting part of the analysis. If the authors are really checking capactities as discharges high enough to fill the culvert to pressurized flow, I would expect velocities of greater than 2 m/s. I suppose the limitation on velocities is due to the pump capacity.

3. The authors discuss at length the plausibility of independence of roughness with Reynolds number. This is discussion is very important in light of my suggestion in item 2. I suggest the authors read Chapter 7 of the FHWA publication Hydraulic Design of Energy Dissipators for Culverts and Channels. There may be some comments there about this topic. If not, it's a standard reference that should have been cited in the paper.

4. The right hand side ordinate label in Figure 4 is illegible.

5. In the section headed, "Retrofit effect on discharge," it appears for a couple paragraphs to be almost a separate paper. I suggest the authors add a sentence in the opening paragraph that connects this section to the previous sections better.

6. I believe the references to Eq. 4 on lines 407 and 409 should be Eq. 5.

Bibliography

Bates, K. et al. (2003). *Design of Road Culverts for fish Passage*. Tech. rep. Washington Department of Fish and Wildlife (cit. on p. 20).

Castro-Santos, T. (2005). "Optimal swim speeds for traversing velocity barriers: An analysis of volitional high-speed swimming behavior of migratory fishes". In: *Journal of Experimental Biology* 208.3, pp. 421–432 (cit. on p. 16).

— (2006). "Modeling the effect of varying swim speeds on fish passage through velocity barriers". In: *Transactions of the American Fisheries Society* 135.5, pp. 1230–1237 (cit. on p. 16).

Chanson, H. (2004). *Environmental Hydraulics of Open Channel Flows*. Burlington, MA: Butterworth (cit. on p. 6).

Christodoulou, G. C. (2013). "Equivalent roughness of submerged obstacles in open channel flows". In: *Journal of Hydraulic Engineering* (cit. on p. 104).

Clark, S.P. and N. Kehler (2011). "Turbulent flow characteristics in circular corrugated culverts at mild slopes". In: *Journal of Hydraulic Research* 49.5, pp. 676–684 (cit. on pp. 17, 22).

Clay, Charles H. (1995). *Design of Fishways and Other Fish Facilities*. 2nd. London, England: Lewis (cit. on pp. 12, 71).

Davis, J.C. and G.A. Davis (2011). "The influence of stream-crossing structures on the distribution of rearing juvenile Pacific salmon". In: *Journal of the North American Benthological Society* 30.4, pp. 1117–1128 (cit. on p. 11).

Devkota, J.P. et al. (2012). "Variation in Manning's Roughness coefficient with diameter, discharge and slope in partially filled HDPE culverts". In: pp. 1716–1726 (cit. on pp. 21, 24, 25, 27, 56, 57, 71, 74).

Ead, S.A. et al. (2000). "Turbulent open-channel flow in circular corrugated culverts". In: *Journal of Hydraulic Engineering* 126.10, pp. 750–757 (cit. on p. 22).

Ead, S.A. et al. (2002). "Generalized study of hydraulics of culvert fishways". In: *Journal of Hydraulic Engineering* 128.11, pp. 1018–1022 (cit. on pp. 17, 28, 29, 73).

Enders, E.C. et al. (2003). "The effect of turbulence on the cost of swimming for juvenile Atlantic salmon (Salmo salar)". In: *Canadian Journal of Fisheries and Aquatic Sciences* 60.9, pp. 1149–1160 (cit. on p. 11).

Feurich, R. et al. (2012). "Improvement of fish passage in culverts using CFD". In: *Ecological Engineering* 47, pp. 1–8 (cit. on pp. 33, 73, 74).

Gregory, S. and J. McEnroe (2004). *Fish Passage through Retrofitted Culverts*. Tech. rep. FHWAORRD0505. Oregon Department of Transportation, pp. 37, 39, 42 (cit. on p. 91).

Haro, A. et al. (2004). "Swimming performance of upstream migrant fishes in open-channel flow: A new approach to predicting passage through velocity barriers". In: *Canadian Journal of Fisheries and Aquatic Sciences* 61.9, pp. 1590–1601 (cit. on p. 71).

Hollingshead, T. and B. Tullis (2009). *In-situ culvert rehabilitation: synthesis study and field evaluation*. Tech. rep. UT-09.16. Utah Department of Transportation Research Division (cit. on p. 71).

ISCO (2013). *Flow characteristics*. Tech. rep. http://www.culvertrehab.com/pdfs/2009$_m$*anual.pdf* : ISCO Industries (cit. on pp. 57, 75, 79).

Katopodis, C. and R. Gervais (2012). "Ecohydraulic analysis of fish fatigue data". In: *River Research and Applications* 28.4, pp. 444–456 (cit. on pp. 11, 13, 15, 16, 71).

Kemp, P.S. and J.G. Williams (2008). "Response of migrating Chinook salmon (Oncorhynchus Tshawytscha) smolts to in-stream structure associated with culverts". In: *River Research and Applications* 24.5, pp. 571–579 (cit. on p. 11).

Lacey, R.W.J. et al. (2012). "The ipos framework: Linking fish swimming performance in altered flows from laboratory experiments to rivers". In: *River Research and Applications* 28.4, pp. 429–443 (cit. on pp. 16–18).

Langworthy, V. W. and R.D. Bargman (1967). *Design and Construction of Sanitary and Storm Sewers*. Washington, D.C.: Water Pollution Controll Federation (cit. on pp. 26–28).

Liao, J.C. (2007). "A review of fish swimming mechanics and behaviour in altered flows". In: *Philosophical Transactions of the Royal Society B: Biological Sciences* 362.1487, pp. 1973–1993 (cit. on p. 16).

Love, M. and K. Bates (2009). *California Salmonid Stream Habitat Restoration Manual*. Tech. rep. State of California Department of fish, Game Wildlife, and Fisheries Division, p. XII 100 (cit. on p. 73).

Luo, Z. and M. Peng (2010). "Hydrology and hydraulic analysis for a drainage rehabilitation project on Interstate Highway 80 in California". In: vol. 394, pp. 620–630 (cit. on pp. 74, 89).

Macdonald, J.I. and P.E. Davies (2007). "Improving the upstream passage of two galaxiid fish species through a pipe culvert". In: *Fisheries Management and Ecology* 14.3, pp. 221–230 (cit. on pp. 3, 5, 32–34, 72, 97, 102, 103, 105).

Macpherson, L.M. et al. (2012). "Effects of culverts on stream fish assemblages in the alberta foothills". In: *North American Journal of Fisheries Management* 32.3, pp. 480–490 (cit. on p. 3).

Makrakis, S. et al. (2012). "Culverts in paved roads as suitable passages for Neotropical fish species". In: *Neotropical Ichthyology* 10.4 (cit. on p. 71).

Mangin, S.F. (2010). "Development of an equation Independent of Manning's Coefficient n for Depth Prediction in Partially Filled Circular Culverts". MA thesis. Youngstown State University (cit. on pp. 27, 64).

Mangin, S.F. et al. (2010). "Reducing the error associated with Manning's roughness in culvert design for improved fish passage". In: pp. 1540–1553 (cit. on p. 5).

Morris, H.M. (1955). "A new concept of flow in rough conduits". In: *ASCE Transactions* 120, pp. 373–410 (cit. on pp. 47, 49, 83, 84, 104).

Morrison, R.R. et al. (2008). "Turbulence characteristics of flow in a spiral corrugated culvert fitted with sloped- and slotted-weir baffles". In: vol. 316 (cit. on pp. 17–19).

Norman, J. et al. (2001). *Hydraulic design of highway culverts*. Tech. rep. FHWANHI01020HDS5. US Departement of Transportation (cit. on pp. 35–37, 87).

Olsen, A. (2011). "Fish Passage Through Rehabilitated Culverts Laboratory Study". Paper 1082. MA thesis. http://digitalcommons.usu.edu/etd/1082: Utah State University (cit. on pp. 5, 18, 20, 42).

Olsen, A.H. and B.P. Tullis (2013). "Laboratory study of fish passage and discharge capacity in slip-lined baffled culverts". In: *Journal of Hydraulic Engineering* 139.4, pp. 424–432 (cit. on pp. 5, 12, 49, 50, 57, 71, 75, 84).

Poplar-Jeffers, I.O. et al. (2009). “Culvert replacement and stream habitat restoration: Implications from Brook trout management in an Appalachian Watershed, U.S.A”. In: *Restoration Ecology* 17.3, pp. 404–413 (cit. on p. 11).

Rajaratnam, N. and C. Katopodis (1990). “Hydraulics of culvert fishways III. Weir baffle culvert fishways”. In: *Canadian journal of civil engineering* 17.4, pp. 558–568 (cit. on pp. 12, 14, 28, 30–32, 42–44, 72).

Rajaratnam, N. et al. (1988). “Hydraulics of offset baffle culvert fishways”. In: *Canadian Journal of Civil Engineering* 15.6, pp. 1043–1051 (cit. on pp. 28, 30).

Rajaratnam, N. et al. (1989). “Hydraulics of culvert fishways II: slotted-weir culvert fishways”. In: *Canadian Journal of Civil Engineering* 16.3, pp. 375–383 (cit. on pp. 12, 28, 30, 31, 42, 44, 72).

Rajaratnam, N. et al. (1991). “Hydraulics of culvert fishways IV. Spoiler baffle culvert fishways”. In: *Canadian journal of civil engineering* 18.1, pp. 76–82 (cit. on pp. 28, 34, 72).

Rayamajhi, B. et al. (2012). “Should fish passage through culverts be a concern for midwest engineers and planners: Determining the percentage of culverts that act as barriers to fish passage in NE Ohio”. In: pp. 1624–1634 (cit. on p. 71).

Richmond, M.C. et al. (2007). “Mean flow and turbulence characteristics of a full-scale spiral corrugated culvert with implications for fish passage”. In: *Ecological Engineering* 30.4, pp. 333–340 (cit. on pp. 17, 22, 57, 63).

Savoie, R. and D. Haché (2002). *Design Criteria for Fish Passage in New or Retrofit Culverts in the Maritime Provinces.* Moncton, NB, CA: Fisheries and Oceans (cit. on p. 20).

Stevenson, S. et al. (2008). *Culvert Barrel Design to Facilitate the Upstream Passage of Small Fish*. Tech. rep. TP366. Auckland Regional Council (cit. on p. 32).

Straub, L.G. and H.M. Morris (1951). *Hydraulic Tests on Corrugated Metal Culvert Pipes*. Tech. rep. Technical Paper No. 5, Series B. University of Minnesota, St. Anthony Falls Hydraulic Laboratory (cit. on pp. 22, 49, 84, 85).

Syachrani, S. et al. (2010). “A risk management approach to safety assessment of trenchless technologies for culvert rehabilitation”. In: *Tunnelling and Underground Space Technology* 25.6, pp. 681–688 (cit. on p. 71).

Thomas, R. (1990). *Polyethylene liner pipe*. Tech. rep. Indiana Department of Transportation, pp. 37, 39, 42 (cit. on p. 71).

Tritico, Hans M. (2009). “The effects of turbulence on habitat selection and swimming kinematics of fishes”. MA thesis. University of Michigan (cit. on p. 16).

Tritico, H.M. and A.J. Cotel (2010). “The effects of turbulent eddies on the stability and critical swimming speed of creek chub (Semotilus atromaculatus)”. In: *Journal of Experimental Biology* 213.13, pp. 2284–2293 (cit. on p. 17).

Tullis, B.P. and D.S. Anderson (2010). “Slip-lined culvert inlet end treatment hydraulics”. In: *Journal of Irrigation and Drainage Engineering* 136.1, pp. 31–36 (cit. on pp. 44, 45).

Tullis, B.P. et al. (2008). “Entrance loss coefficients and inlet control head-discharge relationships for buried-invert culverts”. In: *Journal of Irrigation and Drainage Engineering* 134.6, pp. 831–839 (cit. on pp. 5, 45–47, 71, 74).

Warren, M.L. and M.G. Pardew (1998). “Road crossings as barriers to small-stream fish movement”. In: *Transactions of the American Fisheries Society* 127.4, pp. 637–644 (cit. on p. 3).

Webb, J.R. and R.H. Hotchkiss (2009). “Culvert retrofit and fish passage: An update”. In: vol. 342, pp. 3222–3233 (cit. on pp. 5, 71).

Webb, P.W. and A.J. Cotel (2010). “Turbulence: Does vorticity affect the structure and shape of body and fin propulsors”. In: *Integrative and Comparative Biology* 50.6, pp. 1155–1166 (cit. on p. 16).

White, Frank M. (2009). *Fluid Mechanics*. 7th. New York, USA: Mcgraw-Hill (cit. on p. 104).